STUDIES IN THE AETIOLOGY, INVESTIGATION AND TREATMENT OF PERIANAL FISTULA

JAMES BOYD HADDOW

MAY 2017

Thesis submitted in partial fulfilment of the requirements of
the Degree of Doctor of Medicine by Research, MD(Res)

National Bowel Research Centre
Centre for Digestive Diseases
Blizard Institute
Barts and The London School of Medicine and Dentistry
Queen Mary University of London

STATEMENT OF ORIGINALITY

I, James Boyd Haddow, confirm that the research included within this thesis is my own work or that where it has been carried out in collaboration with, or supported by others, that this is duly acknowledged below and my contribution indicated. Previously published material is also acknowledged below.

I attest that I have exercised reasonable care to ensure that the work is original, and does not to the best of my knowledge break any UK law, infringe any third party's copyright or other Intellectual Property Right, or contain any confidential material.

I accept that the College has the right to use plagiarism detection software to check the electronic version of the thesis.

I confirm that this thesis has not been previously submitted for the award of a degree by this or any other university.

The copyright of this thesis rests with the author and no quotation from it or information derived from it may be published without the prior written consent of the author.

Signature: 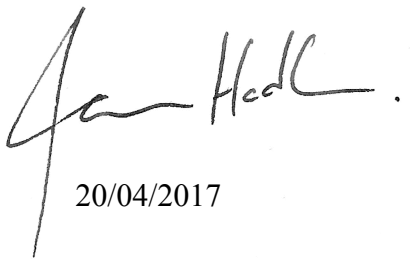

Date: 20/04/2017

ACKNOWLEDGEMENTS

I am indebted to all the brilliant people who helped me along the way in my research. The success of this project has very much depended on the co-operation and kindness of many people. There are a few notable people I wish to mention below, but there are countless others who were equally kind, and apologies for not being able to list everyone.

My sincere gratitude to Omar Musbahi for doing all of the data entry into the database and also doing a few of the tissue cultures when I couldn't be in two places at the same time. Thank you to Ellie McAlees for help with screening, tracking, recruiting and following up participants when I couldn't. And thank you to Amira Shamsiddinova for re-entering the participant identification numbers and biopsy sites for the phosphoprotein quantification experiments data.

Thank you so much to Prof Charles Knowles for his dedicated support, mentoring, encouragement, guidance and championing. Thank you also to everyone else at the National Bowel Research Centre for their motivational chats and cups of tea. Thank you to Prof Tom Macdonald for his knowledge and guidance, and his trust in me. Many thanks also to his other researchers, Anna Vossenkamper, Nadia Ahmad and Paolo Biancheri who gave me support, guidance and tuition in the laboratory. I am also grateful for Bob Hardcastle from Merck Millipore, who trained me on the expert use of the MagPix machine. Thank you to consultant gastrointestinal radiologist, Arman Parsai, who provided essential guidance and support for DCE-MRI study. Thank you also to Payal Julka and her team of MRI technicians for expertly running the DCE-MRI protocols on our participants. And thank you to the trustees at Bowel & Cancer Research charity, whose funding made it all possible. Thank you for taking a chance with me.

Lastly, and above all, I wish to thank my amazing wife, Swapna and my loving son, Phoenix, who have kept me going with love and laughter and a work desk on wheels when I found it toughest.

ABSTRACT

Background: Perianal fistulae are common and cause significant symptoms and psychosocial morbidity. Current theory suggests two distinct types: idiopathic (no established cause) and secondary, which usually arise from Crohn's disease. Research to date has assumed that idiopathic and Crohn's perianal fistulae differ in their pathogenesis and pathophysiology. This fundamental hypothesis has not yet been adequately tested. We therefore aimed to test the broad hypothesis that idiopathic and Crohn's perianal fistulae differ in their pathogenesis and pathophysiology.

Methods: We prospectively recruited a cohort of 61 participants (48 idiopathic, 13 Crohn's disease) and phenotyped them in detail using clinical assessment, Perineal Disease Activity Index, EQ-5D-5L, dynamic contrast-enhanced magnetic resonance imaging (DCE-MRI), operative assessment, biopsy, and clinical follow-up. We interrogated the biopsy samples in the laboratory to characterize their profiles for 30 cytokines and 39 phosphoproteins. Over 12,000 clinical and 23,500 laboratory measurements were made.

Results: We found no clear differences in the clinical characteristics or the overall cytokine or phosphoprotein profiles between idiopathic and Crohn's perianal fistulae. We also found no differences in the DCE-MRI measurements between the groups.

Conclusions: We did not find good evidence to support our hypothesis. The alternative hypothesis offers a shift in the current research paradigm: idiopathic and Crohn's perianal fistulae are the same pathology on a spectrum across which the pathogenic and pathophysiological features are distributed in a skewed manner. This may be the key to unravelling our understanding of the disease's aetiology. It would also be a construct within which trials of biological therapy, such as infliximab, could be justified for idiopathic disease.

Visual Abstract

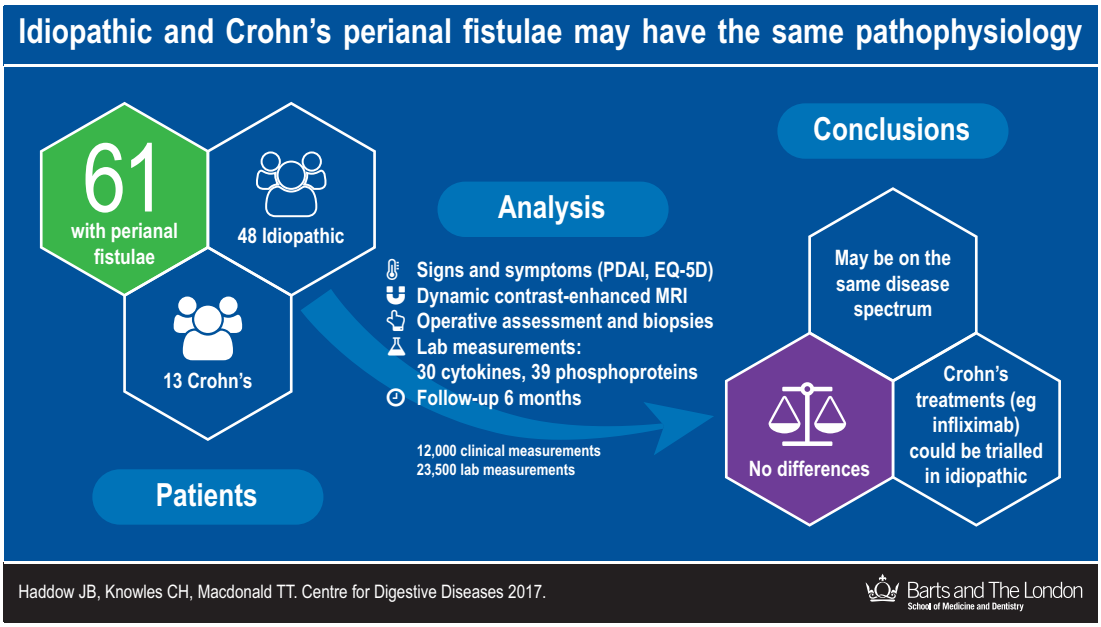

CONTENTS

TABLES AND FIGURES

Tables

Figures

1. BACKGROUND

1.1 History of Perianal Fistula Disease

A perianal fistula is an abnormal tract that communicates between an internal opening in the anal canal and an external opening on the perianal skin. This tract penetrates through intervening structures, which importantly include the anal sphincters. It is a condition that has troubled Mankind for millennia. Indeed, in 400 BC, Hippocrates described two strategies for treating perianal fistula:

"Taking a very slender thread of raw lint, and uniting it into five folds of the length of a span, and wrapping them round with a horse hair; then having made a director (specillum) of tin, with an eye at its extremity, and having passed through it the end of raw lint wrapped round as above described, introduce the director into the fistula, and, at the same time, introduce the index finger of the left hand per anum; and when the director touches the finger, bring it out with the finger, bending the extremity of the director and the end of the threads in it, and the director is to be withdrawn, but the ends of the threads are to be knotted twice or thrice, and the rest of the raw threads is to be twisted around and fastened into a knot…

"When the fistula does not get eaten through, having first examined it with a sound, cut down as far as it passes, and sprinkle with the flos aeris, and let it remain for five days…But it does not heal unless it be cut open." (Hippocrates 400 BC)

Despite intervening millennia with advances in knowledge and technology, these two operations remain essentially unchanged and are still the mainstay of modern-day perianal fistula management: the insertion of a seton* and the fistulotomy. This fact is testament to the incredible insight of Hippocrates, the father of modern medicine.

---

* Apparently from Latin *seta* meaning 'bristle' (Pearsall 1998, p.1702)

It is also an indictment of our collective failure to discover better alternative treatments.

In 1376, the English surgeon John Arderne (1307–1390) wrote systematically and in depth on the subject in Treatises of Fistula in Ano, Haemmorhoids, and Clysters (Arderne and Power 1910) and is credited for describing the modern fistulotomy for the first time. In 1686, Louis XIV developed a perianal fistula. This was treated by fistulotomy by barber-surgeon Charles-François Felix, who took six months (and several unethical trials on prisoners and peasants, many of whom died) to prepare for the operation. In his preparatory experiments he also invented an anal retractor and a curved scalpel to use (Figure 1). The operation was a success and many of the king's subjects took to wearing swathes of bandages around their buttocks, known as *le royale*, in homage to his bandaged bottom (Littman 2014).

Figure 1 Anal retractor (left) and curved scalpel invented by Charles-François Felix in 1686.

Much of our current knowledge and theories on perianal fistula disease is owed to several prominent surgeons at the turn of the 20th century. Goodsall and Miles, Milligan and Morgan, Thompson, and Lockhart-Mummery all contributed to theories on pathogenesis and classification, and standardized surgical treatment. Later in the 1960s and 70s, Parks, a consultant surgeon at the Royal London and St Mark's Hospitals, contributed a large body of work to improving our ideas around pathogenesis and classification.

However, despite the weight of history, which even includes the establishment in 1835 of a whole hospital devoted to the study and treatment of fistula-in-ano namely

St Mark's Hospital, the aetiology of perianal fistulae is still not clear, and for many patients, a cure has not yet been found.

1.2 Anatomy

A detailed knowledge of the pelvic floor, anal sphincters and perineum is essential to understanding the nature of perianal fistula disease. It is useful to think of the anal canal as the terminal part of the intestine, with all its layers present: mucosa, muscularis mucosae, circular muscle, and longitudinal muscle (Figure 2). As the rectal tube descends in the pelvis it encounters the pelvic floor, which is a bowl-shaped sheet of muscle, comprising the levator ani and puborectalis, slung across the pelvic outlet. Below the pelvic floor is ischioanal fat and perineal skin. The rectal tube penetrates the pelvic floor and in doing so carries some of the pelvic floor muscle with it, traversing down through the ischioanal fat to the perineum. Thus a 2–5 cm cylinder of muscle encircles the tract from the pelvic floor to the anal verge. This is defined as the surgical anal canal.

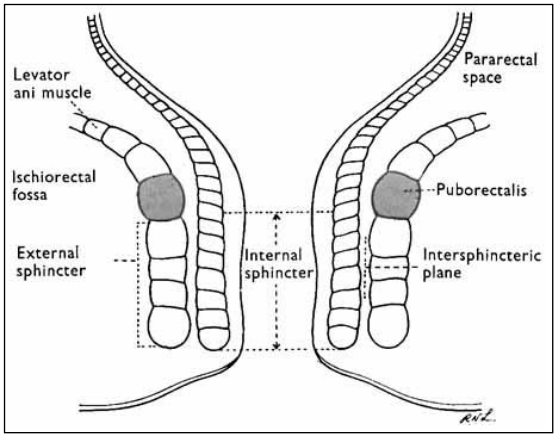

Figure 2 Coronal section of the pelvic floor, demonstrating the origin of the anal canal as a continuation of the rectum above and its relationship with the pelvic floor and external sphincter, with the inter-sphincteric plane existing between these two embryologically separate entities. For simplification, the longitudinal layer has been omitted. Source: Parks *et al.* 1976.

The circular muscle in the anal canal is hypertrophied and is called the internal sphincter. It comprises involuntary smooth muscle and exerts a constant pressure to maintain continence. The longitudinal muscle surrounding this is in most cases a thin layer of smooth muscle. The cylindrical projection of pelvic floor muscle that

encircles the anal canal is called the external sphincter. It comprises striated muscle also exerts a pressure to support continence, and provides reflex and voluntary sphincter control. The inter-sphincteric plane separates the longitudinal muscle and the external sphincter. It is a potential space that acts as a conduit, allowing pus to track cranially, caudally and circum-anally, and explains why we observe a wide variation in the anatomical configurations of perianal fistulae. This pathophysiology is detailed later on.

The anal canal mucosa contains longitudinal folds. These give rise to ridges and grooves called the columns of Morgagni and the anal crypts respectively. The lower border of this mucosal feature appears as a scalloped white line called the dentate line.

The mucosa within the anal canal contains the fusion of the endoderm-derived simple columnar epithelium of the gut above with the ectoderm-derived stratified squamous epithelium of the perineal skin below. Descriptions of the structure of the epithelium within the anal canal vary in textbooks. Most anatomists are of the opinion that there is an intervening transition zone that consists of either transitional epithelium, stratified columnar, or cuboidal epithelium, and that the dentate line represents the embryological site of transition. However, a recent study involving intact parts of the rectum and anus from 13 patients who underwent resection for carcinoma elegantly demonstrated the true histology of the anal canal using scanning electron microscopy. Tanaka *et al*. (2012) found that the anal canal epithelium starts at the anorectal line, which can be seen macroscopically and lies below the level of the pelvic floor (the anorectal ring), and terminates at the same level as the termination of the internal sphincter (the anal inter-sphincteric groove). Above the anorectal line, the epithelium is clearly continuous with the simple columnar epithelium of the rectum. Below the anal inter-sphincteric groove, the epithelium contains skin appendages such as hair follicles. Between these two landmarks exists the anatomical anal canal. Tanaka *et al.* did not demonstrate a transition zone. Rather they clearly showed stratified squamous epithelium devoid of appendages, with islands of stratified columnar epithelium surrounding the anal crypts (Figure 3).

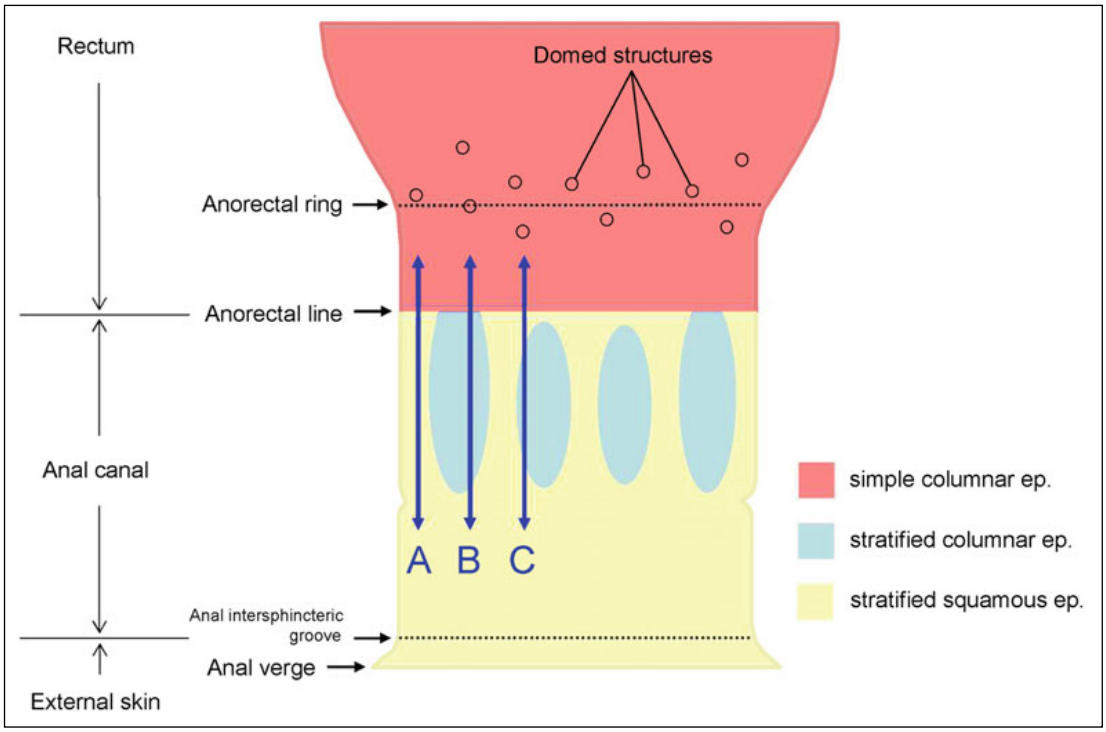

Figure 3 Coronal section of the anal canal and rectum, showing the distribution of the different types of epithelium found. Source: Tanaka *et al.* 2012.

Parks (1961) used light microscopy to study the structure of the anal glands in 44 operative specimens retrieved after resection for various nearby diseases that did not involve the anus (e.g. radical excision for carcinoma of the rectum). He found between 6–10 anal glands within the internal sphincter around the anal circumference. Each gland was lined by stratified columnar epithelium and discharged into an anal crypt, also lined by stratified columnar epithelium. The glands also branched immediately into a racemose structure of widely ramifying ducts. These branches could extend into the internal sphincter and sometimes through it into the longitudinal layer.

1.3 Classification

Parks' Classification

Again it fell to Parks to devise the classification of perianal fistulae that we use today. Prior to this, classification focused on the relationship of the tract to the puborectalis muscle. However this was ill defined and ambiguous. Parks *et al.* (1976)

embarked on a large cohort study involving 400 consecutive patients with perianal fistulae. His previous work brought the understanding that the primary focus of the disease starts in the anal glands and therefore at the level of the dentate line. With this in mind, he carefully documented in each patient the relationship of the primary tract to the external sphincter. He found that all fistulae could be classified into four main types: inter-sphincteric, trans-sphincteric, supra-sphincteric and extra-sphincteric (Figure 4). Superficial fistulae were excluded as he thought they did not arise from the anal gland.

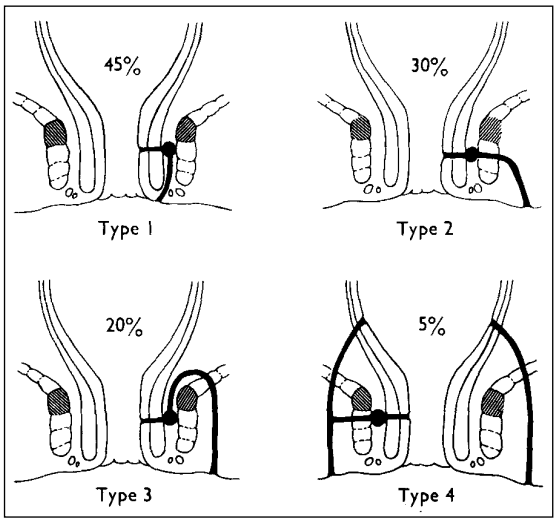

Figure 4 Four main anatomical types of perianal fistula with their prevalence (%). Type 1, Inter-sphincteric; type 2, trans-sphincteric; type 3, supra-sphincteric; type 4, extra-sphincteric. Source: Parks et al. 1976.

Inter-sphincteric. This was the commonest type (45%). An inter-sphincteric fistula traverses the internal sphincter only. It does not extend outside the inter-sphincteric plane. In most patients the tract descends straight downwards in the inter-sphincteric plane to the anal verge. However there is considerable variation in its course: it can extend upwards towards the rectum and the para-rectal space, or it can horseshoe around in a circum-anal direction, or it can branch to give rise to secondary tracts.

Trans-sphincteric. This was the second commonest type (30%). Here the primary tract crosses both sphincters. The level where the tract crosses the internal sphincter is relatively constant (i.e. the dentate line) because it arises from the anal gland and its duct. However, once the tract is in the inter-sphincteric plane it courses in any

direction (up, down or around). Thus the level where the tract perforates the external sphincter is variable. Most commonly this is at a low level but it can also be as high as the proximal external sphincter, just below the puborectalis. Again secondary tracts can branch off in the inter-sphincteric plane, giving rise to inter-sphincteric tracts, para-rectal tracts and secondary external openings anywhere on the anal verge. Secondary tracts can also branch off after the fistula has traversed the external sphincter, which result in ischio-rectal abscesses, infra-levator tracts, trans-levator tracts and secondary external openings anywhere on the perineum, including the scrotum or labia.

Supra-sphincteric. These accounted for 20% of fistulae. Supra-sphincteric fistula similarly start by crossing the internal sphincter at the level of the dentate line. Upon reaching the inter-sphincteric plane, they course upwards above the level of the puborectalis. This part of the fistula may form a horseshoe around the rectum before perforating the levator plate and descending down through the ischio-rectal fossa to exit on the perineum. Again secondary tracts can ramify from the primary tract in the inter-sphincteric plane, para-rectal space and ischio-rectal fossa.

Extra-sphincteric. These were the least common fistulae (5%). In affected patients, a trans-sphincteric fistula gives rise to a secondary tract in the ischio-rectal fossa, which then courses upwards, perforating the levator ani and the rectal wall to re-enter the intestinal lumen. However, iatrogenic trauma can also give rise to this morphology, whereby the operating surgeon probes a trans-sphincteric fistula with a high secondary extension, and mistakenly forces a false passage upwards into the rectum. Caution also needs to be given to the extra-sphincteric fistula that arises from a primary ischio-rectal or para-rectal abscess e.g. as a consequence of perforated diverticular disease or tumour. These are considered a separate entity because the anal glands are not implicated.

Subsequent case series have largely agreed with the prevalence of the four main types (Table 1).

Table 1 Prevalence of the different anatomical types of perianal fistulae.

	Parks et al. 1976	Marks and Ritchie 1977	Vasilevsky and Gordon 1985
N	400	666	160
Inter-sphincteric	45%	66%	42%
Trans-sphincteric	30%	26%	52%
Supra-sphincteric	20%	4%	1%
Extra-sphincteric	5%	4%	0%

Low versus High

Surgeons often describe perianal fistulae as high or low based on the nature of the primary track. There are, however, no accepted definitions for this classification. It is used to convey the relative risk of incontinence from lay open, i.e. a low fistula carries an acceptably low risk of incontinence if laid open, with the converse being the case for high fistulae.

The St Mark's Hospital group define a low perianal fistula as subcutaneous, inter-sphincteric or trans-sphincteric involving no more than 1 cm of external anal sphincter (Atkin *et al.* 2011). Göttgens *et al.*(2015) in their case series of 537 patients defined a low perianal fistula as one traversing the lower one third of the anal sphincter complex or a superficial fistula not involving the striated sphincter complex. Jordán *et al.* (2010) defined a high fistula as one crossing more than 50% of the external sphincter.

1.4 Grading

There is no accepted grading system for perianal fistulae. Previous authors have arbitrarily graded fistulae as simple or complex based on their morphology according to the Parks classification. Marks and Richie (1977) found that two-thirds of the patients they treated had simple fistulae. The vast majority of these responded adequately to surgery. The most common type of complex fistula they treated was

trans-sphincteric with an ischio-rectal extension. These patients were more likely to have had previous operations, particularly drainage of an abscess. The majority of these were treated in stages and stayed in hospital for 4 weeks – a 'major undertaking for both the surgeon and the patient.'

Jordán *et al.* (2010) defined a complex fistula as a tract crossing more than 50% of the external sphincter, presence of secondary tracks or chronic abscess cavities, or pre-existing faecal incontinence. Presence of a complex fistula was associated with a higher recurrence rate (16% *versus* 1.3% in simple fistulae; $p < 0.001$). Simpson *et al.* (2012) included complexity of management in their grading. Thus, their definition of complex fistulae included those with secondary tracks and cavities that extend above the levator muscles, supra-levator or supra-sphincteric extensions, horseshoe extensions, and a history of Crohn's disease, cancer, previous surgery or radiotherapy, and pre-existing impairment of continence. In a recent prospective study, Sileri *et al.* (2011) defined fistulae as complex if any of the following conditions were present: tract crossing more than 30% of the external sphincter, anterior fistula in a woman, recurrent fistula, or pre-existing incontinence.

The St James's University Hospital Classification was developed to grade fistulae using conventional magnetic resonance imaging (MRI) (Morris *et al.* 2000). This system arranges fistulae into five grades of increasing severity: *grade 1*, simple linear inter-sphincteric fistula; *grade 2*, inter-sphincteric with abscess or secondary tract; *grade 3*, trans-sphincteric; *grade 4*, trans-sphincteric with abscess or secondary tract in ischio-rectal or ischio-anal fossa; and *grade 5*, supra-levator and trans-levator. Spencer *et al.* (1998) studied outcome according to these grades. They considered grades 1 and 2 as simple, and grades 3 to 5 as complex, and showed that complex fistulae were associated with an unsatisfactory surgical outcome, meaning that further intervention was necessary.

1.5 Clinical Features

Epidemiology

Perianal fistulae occur in 1.84 per 10,000 people per annum in England (Zanotti *et al.* 2007), are commoner in males up to a ratio of 2:1 and usually present in mid-life. However, despite being a relatively uncommon disease, a perianal fistula carries significant physical and psychosocial morbidity, with an average of three operations being necessary to achieve cure or palliation.

Aetiology

Primary perianal fistulae, otherwise known as idiopathic, account for 90% of cases (Sainio 1984). Other perianal fistulae occur secondary to Crohn's disease (1.3%), ulcerative colitis (1.5%), tuberculosis (TB, 0.2%), perianal operations or trauma (3.3%), anal fissure (3.3%). Human immunodeficiency virus (HIV) infection has also been implicated in previous cases (Rivera *et al.* 2009).

Symptoms

Common complaints include perianal pain, swelling, discharge and or bleeding from the perineum or anus, skin excoriation or pruritus and a perineal external opening or subcutaneous lump. These can lead to a psychosocial restriction of lifestyle and sexual activity.

A thorough history includes a documentation of the symptomatology, the resultant psychosocial morbidity, and also questions on current sphincter function. This allows the clinician to estimate of the total burden of disease and the risk of sphincter disturbance from surgery, which is important in weighing up the benefits and risks of treatment.

Signs

Clinical examination gives valuable diagnostic and prognostic information. Inspection of the perineum and careful palpation with lubrication usually reveals the site of the external opening and the path of a subcutaneous tract. If the external opening is medial to the border of the pigmented perianal skin (the border of the external sphincter), it is likely that the primary tract is inter-sphincteric. The converse indicates a trans-sphincteric tract. Absence of an external opening is an indication for imaging. An impalpable subcutaneous tract suggests that the tract descends more vertically to the perineum either through the inter-sphincteric plane or the ischio-anal fossa. In these cases the fistula is more likely to be high. Digital rectal examination where only the tip of the finger is admitted into the anal canal can demonstrate the internal opening, which is a subtle sensation of a 'grain of rice' against the otherwise silky smooth anal mucosa. The height of the internal opening in relation to the anorectal junction is best estimated in the awake patient, when anal tone is not altered by anaesthesia. This estimation is important in judging the length and function of the uninvolved sphincter that would remain behind if a lay open were performed. Deeper palpation of the anorectal junction and the pelvic floor from within the rectum can demonstrate areas of high sepsis, which is felt as 'woodiness' instead of the usual soft springy musculature. However, it is impossible to differentiate whether the underlying sepsis is either in an infra- or supra-levator location.

1.6 Imaging

The role of imaging in perianal fistula disease is to reach a diagnosis when the clinical features are atypical, map out the full pathoanatomy to direct surgical treatment and monitor progress following treatment. The best modalities in common use today are anal endo-ultrasonography (ultrasound) and MRI, which have now superseded fistulography and computed tomography (Williams *et al.* 2007). Buchannan *et al.* (2004) compared ultrasound with digital rectal examination and MRI in 108 perianal fistulae. They found that classification of the fistula was correct

after digital rectal examination in 61%, ultrasound in 81%, and MRI in 90%, when compared against an outcome-derived outcome standard (which was determined post hoc by considering the findings of all the modalities with the clinical course after surgery).

Ultrasound is well tolerated and is able to demonstrate the internal opening, the primary tract traversing the sphincters and any associated collections or secondary tracts. However, insufficient penetration means that the ischio-anal fossa and supra-levator space are not demonstrated clearly, and extensions into these areas may be missed. In recurrent disease, scars of previous surgery pose a problem as they have the same appearance as active fistula tracts. In addition, the technique is operator dependent and therefore studies have reported both superiority (Orsoni *et al.* 1999) and inferiority (Chew *et al.* 2003) to MRI.

MRI is now the gold standard modality for imaging perianal fistula disease. A meta-analysis comparing ultrasound with MRI in 481 fistulae found that their sensitivity was similar (87%), but that MRI had a higher specificity (69% *versus* 43%) (Siddiqui *et al.* 2012).

MRI provides accurate morphology of the disease entities and their exact anatomical relationship with the perianal structures in multiple planes. It is also well tolerated, being non-invasive (unless an endo-anal coil is inserted, which is not common) and non-ionising. The technician should first perform an overview scan to plan the sequences. Crucially these sequences need to be orientated to the axis of the anal canal, which is approximately 45° in the sagittal plane. Both T1 and T2 weighted fast spin-echo (FSE) sequences are important. Fat-suppressed T2-weighted sequences such as short tau inversion-recovery (STIR) or frequency-selective fat-saturated T2-weighted FSE, are also valuable in demonstrating the fluid-filled tracts, and gadolinium-enhanced fat-suppressed T1 images are good at demonstrating the tracts and active granulation tissue (Criado *et al.* 2012).

1.7 Treatment

The ultimate goal of treatment of perianal fistulae is cure. However, this gives rise to a paradox as curative surgery can come at the cost of impaired continence. The more radical the surgery, the higher the chance of cure, but also higher the chance of life-changing faecal incontinence. Thus one set of chronic symptoms may be replaced by another, and the net benefit to the patient's quality of life may not be favourable. Therefore, treatment needs to be tailored to the patient, balancing the desire for fistula eradication against the need to preserve continence (Figure 5).

The general strategy for treating perianal fistulae involves (1) draining, controlling or resolving any acute sepsis; and (2) controlling or eradicating the primary tract, which includes the offending anal glands. If these principles are followed, secondary tracts usually resolve without direct intervention.

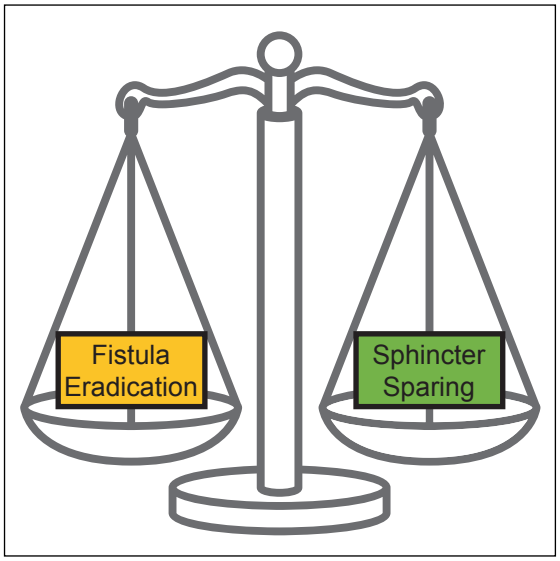

Figure 5 Balance of priorities when selecting treatment for a perianal fistula.

Fistulotomy

The most effective surgical treatment is fistulotomy, which involves laying open the fistula tract from the internal to the external opening. The intervening skin, fat and sphincter are divided, meaning that only the sphincter above the level of the fistula remains intact and functional.

Fistulotomy can achieve success in about 95% of patients (Vasilevsky and Gordon 1984). In a retrospective study involving 461 patients with simple perianal fistulae, 6.5% developed recurrent fistulae within a mean follow-up of 34 months (Sangwan *et al.* 1994). Van Tets and Kuijpers (1994) retrospectively surveyed 281 patients who had had fistulotomy and reported minor continence disorders in 26%. Garcia-Aguilar *et al.* (1996) retrospectively surveyed 375 patients. Mean follow-up was 29 months. Procedures included fistulotomy ($N = 300$), seton placement (63), endo-rectal advancement flap (3), and other (9). Fistula recurrence occurred in 8% and post-operative incontinence was experienced by 45% of patients. Westerterp *et al.* (2003) surveyed 60 patients who underwent fistulotomy for inter-sphincteric and trans-sphincteric fistulae. Within the follow-up of 1–4 years, none experienced a recurrence; 50% had impaired incontinence. Jordán *et al.* (2010) analysed 132 patients who had undergone fistulotomy. Minimum follow-up was 1 year. Recurrence occurred in 1.5% at a median of 4 months post-operatively and post-operative faecal incontinence in 10% of patients.

However, most studies struggled to accurately measure post-operative faecal incontinence and perhaps more importantly, its impact on quality of life. In an attempt to address this, Cavanaugh *et al.* (2002) measured the Faecal Incontinence Severity Index (FISI) in 110 patients after fistulotomy. Some degree of incontinence was reported in 64% and the use of a pad, lifestyle restriction, depression, and embarrassment after fistulotomy were unusual occurrences. No patient reported a severe restriction in lifestyle or severe depression as a result of fistulotomy, but one did report severe embarrassment.

Loose Seton

The purpose of a loose seton is to allow drainage of the fistula. This relies on the premise that acute symptoms are related to superficial closure of the fistula opening causing build up of transudate or exudate within the tract and abscess formation. A seton is a fibre (usually now a synthetic suture material such as non-absorbable braided Ethibond) that is passed into the external opening of the fistula, along the

primary tract, through the internal opening and drawn down out of the anus and tied upon itself to form a loop that remains *in situ*. It therefore allows drainage along the fibre by means of wicking, and prevents the openings from closing over.

A loose seton is often used as a bridge to definitive surgery. In these situations, the seton is deployed to drain the primary tract, resolve the acute sepsis and heal the secondary tracts prior to a fistulotomy (or other surgical approach). In a retrospective case series, the outcomes of 41 consecutive patients with high trans-sphincteric, supra-sphincteric, or extra-sphincteric perianal Crohn's fistulae were reported (Faucheron *et al.* 1996). Seven had a secondary fistulotomy and none experienced a recurrence. The authors concluded that this strategy was effective in treating sepsis and preserving anal sphincter function.

A hybrid operation involving a loose seton can achieve a cure with a lower risk of incontinence compared with fistulotomy. In several small studies, all retrospective, surgeons performed a partial internal sphincterotomy, or a core fistulectomy without sphincteric division and then deployed a loose seton across the tract. Within the follow-up, which ranged from 16 to 142 months, recurrence or persistence occurred in 10–79%, minor incontinence in 0–58% and major incontinence in 0–8% of patients (Thomson and Ross 1989; Kennedy and Zegarra 1990; Williams *et al.* 1991; Lentner and Wienert 1996; Balogh 1999; Joy and Williams 2002; G. N. Buchanan *et al.* 2004).

However, in approximately 50% of patients, fistulotomy is not feasible (Dudukgian and Abcarian 2011), because the risk of causing significant faecal incontinence is unacceptable. In these circumstances, a loose seton can be employed as a long-term non-curative strategy. In eleven patients with a mean follow-up of 75 weeks, a seton achieved resolution of septic episodes in eight (Joy and Williams 2002).

Other Operations

A cutting seton can treat trans-sphincteric fistulae (Williams *et al.* 2007). This method involves tying the seton tight in the fistula tract causing it to slowly cut-out

through the intervening sphincter. In theory the sphincter muscle is slowly divided and heals behind the seton without the muscle edges retracting apart. Recurrence is typically no more than 8% (Graf *et al.* 1995; Hämäläinen and Sainio 1997). However, authors have reported major incontinence as high as 20% after its use in low trans-sphincteric fistulae (Joy and Williams 2002). The cutting seton is also uncomfortable or even painful for patients.

An advancement flap may also achieve a cure. The surgeon raises a flap of mucosa or skin, advances it and secures it over the internal opening. This avoids sphincter division. Several techniques including trans-anal rectal mucosal advancements and cutaneous flaps exist. However, authors have reported recurrence rates of 36% (Sonoda *et al.* 2002).

Rojanasakul *et al.* (2007) first described ligation of the inter-sphincteric fistula tract (LIFT), another sphincter-sparing technique. Eighteen patients underwent the procedure, with only one (6%) recurrence reported. However, other groups in retrospective studies have since reported higher recurrence rates ranging from 8% (Mushaya *et al.* 2012) to 43% (Bleier *et al.* 2010). In a recent randomised controlled trial, 35 patients underwent LIFT for high trans-sphincteric fistulae (Madbouly *et al.* 2014); recurrence at one year was 26%.

Injecting fibrin glue into the fistula tract met with initial enthusiasm. Unfortunately subsequent authors reported disappointing long-term results, with recurrence rates of up to 100% (Hammond *et al.* 2004). This therapy has therefore evolved into placing a plug within the fistula tract. In a case series of 45 patients, the fistula plug achieved complete healing in 44% (Thekkinkattil *et al.* 2009). A large ($N = 500$) UK randomised controlled trial, the Fistula–In–Ano Trial (FIAT) is currently underway to establish the efficacy of this treatment (University of Birmingham 2015).

Other emerging techniques include fistula laser closure (FilaC) and video-assisted anal fistula treatment (VAAFT) with recurrence/failure rates of 29% and 26% respectively (Giamundo *et al.* 2014; Meinero and Mori 2011). Finally, researchers

are also exploring novel biomaterials such as adipose derived stem cells, human acellular dermal matrix and platelet rich plasma (Narang *et al.* 2016). See Table 2 for a comparison of these treatments.

Table 2 Comparison of surgical treatments with curative intent for perianal fistulae. VAAFT, video-assisted anal fistula treatment; LIFT, ligation of inter-sphincteric fistula tract; FiLaC, Fistula Laser Closure; ADM, acellular dermal matrix.

	Failure/recurrence rate	Comments
Fistulotomy	5%	Incontinence 26–64%
Cutting seton	8%	Painful, incontinence 20%
VAAFT	13%	Single series, special equipment
Platelet rich plasma	10-17%	Limited data
LIFT	26%	
FiLaC	18–29%	Limited data, special equipment
Advancement flaps	36%	
ADM	46%	Single series
Stem cells	29–48%	
Fistula plug	66%	
Fibrin glue	100%	

Crohn's Perianal Fistulae

The initial surgical strategy for treating Crohn's perianal fistulae is the same as in idiopathic fistulae, namely drainage and control of the acute sepsis. The longer-term surgical strategy generally favours long-term drainage (seton) rather than fistulotomy or other potentially curative procedures due to issues of wound healing and also need for future operations that may cumulatively result in incontinence. In response to this, several pharmacological agents as primary treatments for fistulating Crohn's disease have emerged. Long-term closure of Crohn's fistulae is rare in patients receiving therapies such as 5-aminosalicylates, corticosteroids, antibiotics,

methotrexate and cyclosporin (Klag *et al.* 2015). In a landmark randomised controlled trial, 94 adults with abdominal or perianal Crohn's fistulae received placebo or the chimeric anti-TNF-α (tumour necrosis factor alpha) antibody, infliximab (Present *et al.* 1999). The primary endpoint was a reduction of at least 50% in the number of draining fistulae. Sixty-eight per cent of the patients who received 5 mg/kg of infliximab and 56% of those who received 10 mg/kg achieved the primary endpoint, as compared with 26% of the patients in the placebo group ($p = 0.002$ and $p = 0.02$, respectively; Figure 6). A second trial then studied the efficacy of infliximab to maintain remission of fistulising disease in 306 patients with abdominal or perianal Crohn's fistulae (Sands et al. 2004). This multicentre, double-blind, randomized, placebo-controlled trial found that time to loss of response was significantly longer for patients who received infliximab maintenance therapy than for those who received placebo maintenance (more than 40 weeks *versus* 14 weeks, $p < 0.001$). Unfortunately, results for the perianal fistulae were not reported separately in either trial.

Infliximab therapy however carries significant risk of adverse effects, which include hypersensitivity reactions, infections, demyelinating disorders, lymphoma and death. Infliximab is also immunogenic meaning that long holidays between infusions can give rise to antibodies that cause infusion reactions and loss of efficacy. Another fully-human anti-TNF-α antibody, adalimumab, has since been developed. In three randomized controlled trials, it showed similar efficacy to infliximab in the treatment of Crohn's disease, but was less immunogenic (Hanauer *et al.* 2006; Colombel *et al.* 2007; Jilani and Akobeng 2008).

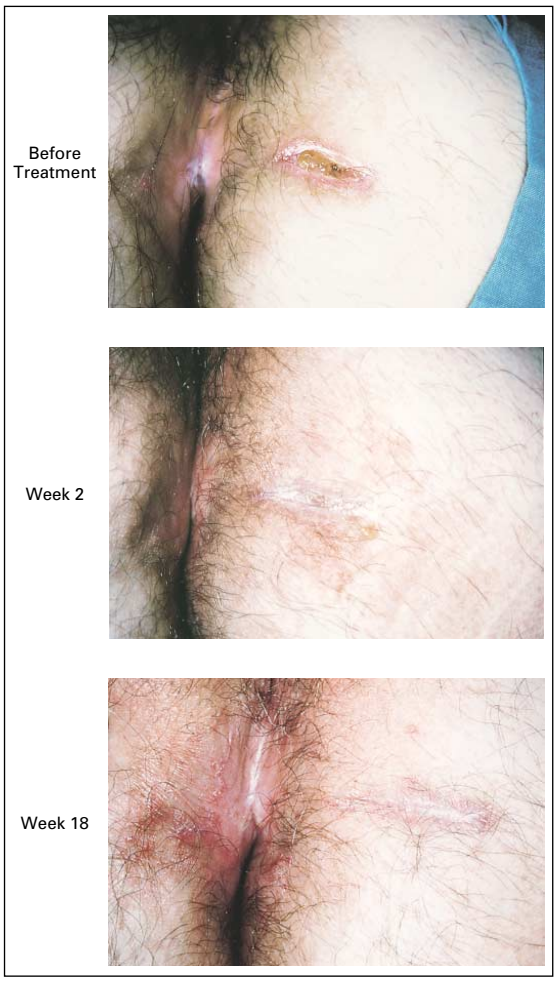

Figure 6 Results from treating a Crohn's perianal fistula with infliximab. Source: Present et al. (1999)

1.8 Pathogenesis of Crohn's Disease

Before discussing the pathogenesis of perianal fistulae, a brief summary of the pathogenesis of Crohn's disease in general is warranted.

Crohn's disease is a systemic inflammatory condition in which gastrointestinal manifestations predominate. The clinical picture is characterised by relapses of focal, asymmetric, transmural chronic inflammation involving any part of the gastrointestinal tract from the mouth to the anus. The commonest area involved is the terminal ileum, and perianal involvement is found in up to one third of patients.

The aetiology of Crohn's disease is unknown. Current research suggests that it arises in genetically susceptible individuals when environmental factors trigger a disturbed

innate and acquired immune response towards an altered gastrointestinal microbiome (Baumgart and Sandborn 2012). There is 35% concordance in monozygotic twins and siblings of affected individuals have a 30-fold increase in incidence. Genome wide association studies have identified 174 susceptibility loci for Crohn's disease so far (Bianco *et al.* 2015). Key factors include mutations in NOD2 (nucleotide-binding oligomerization domain-containing protein 2), which codes for an intracellular sensor of bacterial molecules (see below), the autophagy genes ATG16L1 (autophagy related 16-like 1) and IRGM (immunity-related GTP-ase M-protein), and IL-23 (interlukin 23) receptor gene. However, many mutations that confer susceptibility are also found in healthy individuals, highlighting the complexity of the disease's aetiology.

Differences in incidence across age, time, and geographic region suggest that environmental factors significantly modify the expression of Crohn's disease (Loftus 2004). Smokers are twice as likely to develop the disease. Other putative risk factors include oral contraceptives, high sugar diet, high fat diet and early childhood infections.

In contrast to nearly all other tissues, the mucosa of the small and large intestine has continuous, low-grade (physiologic) inflammation, most likely because the intestine is exposed to a great antigenic load from luminal bacteria and a large variety of Toll-like receptor (TLR) ligands (MacDonald *et al.* 2011). Crohn's disease seems to be a disorder of this symbiosis (Baumgart and Sandborn 2012). A detailed review of the immunopathology is outside the scope of this thesis. In summary, the main mechanisms are:

1. Diminished bacterial diversity
2. Impaired mucosal barrier that increases permeability to bacterial antigens
3. Stimulation of host pattern recognition receptors such as TLRs on the cell surface and intracellular NOD2 receptors
4. Disordered activation of the acquired immune system, which perpetuates the intestinal inflammation

5. Imbalance of effector T cells (predominantly Th1 and Th17), which secrete IFN-γ (interferon-gamma), TNF-α, IL-17 and IL-22, and regulatory T cells, which secrete IL-10, TGF-β (transforming growth factor-beta) and IL-35
6. Stimulation of macrophages to secrete pro-inflammatory cytokines such as TNF-α, IL-1 and IL-6 in large quantities
7. Increased adhesion molecule expression on the intestinal vascular endothelium, recruitment of leucocytes, and tissue damage

1.9 Pathogenesis of Perianal Fistulae

Until Parks' studies, the common pathogenic theory was that infection penetrated the mucosal surface through a fissure or other wound, creating a suppurative tract through the anal canal wall. Faecal contents entering the internal orifice then perpetuated the tract. Parks (1961) observed that the anatomical distribution of the anal glands and perianal fistulae was similar and thus hypothesized that the anal glands provide free channels for infection to pass from the anal lumen deep into the sphincter muscles: since termed the 'cryptoglandular theory'. In 30 consecutive patients with idiopathic perianal fistulae, he excised the internal part of the fistula tract and examined them using light microscopy. In all but two, the fistula tracts were lined by stratified columnar epithelium, the same epithelium that was present within normal anal glands. The other commonly observed features were a gross cystic dilatation of the anal gland (with two also containing vegetable matter) and an inter-sphincteric abscess lined by anal-gland epithelium. Parks concluded that infected anal glands caused the perianal fistulae in 28 (90%) patients.

The cryptoglandular theory is now widely accepted for idiopathic disease. However, subsequent work to support and explain the theory has been sparse. Challenge came from Golligher *et al.* (1967) who found evidence of inter-sphincteric sepsis or tracts in only 14 of 32 patients with perianal fistula. However, critics argue that the inclusion of superficial fistulae, which have a separate aetiology, led to this lower rate.

Fundamental questions remain unanswered (Gosselink *et al.* 2015): why do perianal fistulae occur more commonly in males in the third decade of life? Why do only a minority of perianal abscesses progress to a fistula? Why do they more commonly arise in the posterior quadrant of the anal canal? What drives fistulae to persist and to recur?

In Crohn's perianal fistulae, the cryptoglandular theory may also apply. If this is the case then it follows that idiopathic and Crohn's perianal fistula may share a common initial pathological process, which gives rise to further fundamental questions: is there an undescribed inflammatory disease or disease process similar to Crohn's disease that underpins idiopathic perianal fistula pathogenesis? Do both idiopathic and Crohn's perianal fistulae share risk factors that promote the initiation and progression of anal gland infection into a persistent perianal fistula?

Unfortunately, Parks' study excluded perianal fistulae secondary to Crohn's disease and no one has published a similar study in Crohn's perianal fistulae. Hughes (1978) offered an alternative pathogenic mechanism based on observations made during approximately 400 consecutive cases of perianal Crohn's disease. He suggested that faeces become trapped within an anal fissure and then forced into the submucosal tissues by the pressure of defecation. However, no data were presented to support this theory and there were no follow-up studies.

A third theory, again offered on the basis of weak evidence, proposed that the inflammatory tissue destruction observed in luminal Crohn's disease occurs in the anal canal and leads to a transmural tissue-overarching defect in the gut wall. Wound healing does not take place. Instead, these fissure-like tissue defects are characterized by epithelialization as an alternative healing mechanism of the intestinal barrier (Klag *et al*. 2015).

Working from these theories of pathogenesis, researchers have investigated genetic, microbiological and immunological factors implicated in the pathophysiology of perianal fistulae (Tozer *et al.* 2009).

1.10 Genetics

Studies of the genetic factors contributing to the pathogenesis of perianal fistulae are predominantly in Crohn's disease. As mentioned previously, Crohn's disease has a strong genetic basis and genome wide association studies have identified 174 susceptibility loci so far (Bianco *et al.* 2015). Some notable examples are highlighted.

NOD2 (nucleotide-binding oligomerization domain-containing protein 2)

Mutations in NOD2 account for approximately 15% of cases of Crohn's disease. The gene is located on chromosome 16 (16q12) and codes for an intracellular receptor for muramyl dipeptide, a bacterial molecule (peptidoglycan). Mutations confer loss of function, although exactly how these mutations cause Crohn's disease is still unknown (Hugot *et al.* 2001). In Crohn's disease, NOD2 mutations do not appear to be associated with risk of developing perianal fistulae (Freire *et al.* 2011; Karban *et al.* 2007). However, they do seem to be associated with perianal disease severity. When treated with ciprofloxacin, complete fistula response was observed in 13 of 39 patients with NOD2 wild-type (33%) compared with none in patients carrying NOD2 variants (0%, $p = 0.02$; Angelberger et al. 2008). In a study of 203 consecutive patients, response of perianal fistulas to antibiotics (metronidazole alone or combined with ciprofloxacin) was significantly higher in patients without NOD2 mutations (7.7% *versus* 41%, $p = 0.04$; Freire et al. 2011). Carriers of the G908R variant of NOD2 need fistula surgery more frequently (32% *versus* 4.8%; $p < 0.01$; Barreiro *et al.* 2005).

Yazdanyar and Nordestgaard (2010) extended the study of NOD2 polymorphisms to other common gastrointestinal diseases. Around 44,000 individuals from the Danish general population were genotyped. The age and sex adjusted hazard ratio for anal fissure, fistula and abscess amongst compound heterozygotes was 3.2 (95% CI 1.3–7.8, $p = 0.003$) compared with non-carriers. This suggests that NOD2 mutations may be pathogenic non-Crohn's perianal fistulae.

ATG16L1 (autophagy related 16-like 1) and IRGM (immunity-related GTP-ase M-protein)

Autophagy is a crucial defence mechanism against bacteria. Paneth cells found in the intestinal epithelium are crucial effectors of autophagy. They mediate host-microbe interactions, maintain a homeostatic balance with colonizing microbiota, provide innate immune protection from enteric pathogens and also modulate epithelial renewal (Clevers and Bevins 2013). NOD2 interacts with and recruits ATG16L1 to the plasma membrane to initiate autophagy of bacteria (Travassos *et al.* 2010). ATG16L1-deficient Paneth cells exhibit striking abnormalities in the granule exocytosis pathway (Cadwell *et al.* 2008).

IRGM also interacts importantly within this axis (Chauhan *et al.* 2015). Polymorphisms of IRGM are associated with Crohn's disease (Massey and Parkes 2007) and in particular, fistulising disease (Latiano *et al.* 2009). This explains how polymorphisms altering expression or function of any of the three factors individually can affect the same process and are thus all implicated as risk factors for Crohn's disease.

1.11 Microbiology

Anorectal Abscess

An acute clinical presentation with anorectal abscess is associated with the immediate or delayed finding of a perianal fistula in 26–41% of cases (Grace *et al.* 1982; Henrichsen and Christiansen 1986).

Culture of pus from anorectal abscesses shows that the infection is polymicrobial. In a retrospective study of 144 patients in a single hospital in the US, the commonest culture result from anorectal abscesses was mixed a growth of aerobic and anaerobic microorganisms (72%) with an average of three isolates per case (Brook and Frazier 1997). Most of the organisms isolated from the perirectal abscesses were of enteric (*Bacteriodes fragilis* and *Escherichia coli*) and skin (*Staphylococcus aureus* and

some *Streptococcus* spp.) flora origin. However, the complete list of identified species is extensive and varies between patients. Other retrospective studies have confirmed this general picture (de San Ildefonso Pereira *et al.* 2002; Ulug *et al.* 2010; Liu *et al.* 2011). In a retrospective study of 235 patients in a district general hospital in the UK, Coliforms or *Bacteroides* were found in 45%, mixed growth in 20%, skin flora including *Staphylococcus aureus* in 12%, and no growth in 7% (Leung *et al.* 2009).

Grace *et al.* (1982) studied 165 patients presenting with an anorectal abscess. A perianal fistula featured in 68 patients. Fistulae were absent in all patients whose abscess pus grew either *Staphylococcus aureus* or other skin-derived microorganisms. Likewise, Henrichsen and Christiansen (1986) found prospectively in 50 consecutive patients that when culture from the abscess revealed only skin flora, fistulae were absent. Lunniss and Phillips (1994) similarly reported this prospectively in 22 patients. They also concluded that culture of gut organisms was a good predictor of an underlying fistula. However, two later studies with similar sample sizes found no significant relationship between the type of bacteria and the subsequent development of a perianal fistula (de San Ildefonso Pereira *et al.* 2002; Leung *et al.* 2009). The relationship between routine microbiological culture results and fistula development must at best be considered uncertain.

Fistula Tract

Although bacterial infection is the primary feature of an anorectal abscess and generally accepted as the index pathogenic event, the role of microorganisms in the development and perpetuation of a perianal fistula is unclear.

In a prospective study of 25 patients, Seow-Choen *et al.* (1992) found that the microbiology of non-acute perianal fistula tracts was similar to anorectal abscesses. However, there was a paucity of cultured organisms, even when most were incubated in enriched culture. This difference could have resulted from the fact that fistula tract cultures were performed on tissue whereas anorectal abscess cultures were

performed on pus. However, the authors concluded that the chronic inflammation in perianal fistulae does not seem to be maintained by either excessive numbers of organisms or organisms of an unusual type. Further work from the same group correlated culture results with fistula tract histology in eight patients (Lunniss *et al.* 1993). Culture growth was again scanty. Histology revealed a pattern of active chronic inflammatory changes characterized by large numbers of plasma cells, scattered multinucleate foreign-body giant cells and prominent vascular proliferation, but no organisms were seen.

Recently, gram staining, fluorescent *in situ* hybridization and scanning electron microscopy were used in 18 patients with idiopathic fistulae and 14 patients with Crohn's perianal fistulae (Tozer *et al.* 2015). The six rRNA (ribosomal ribonucleic acid) probes targeted all bacteria, *Bifidobacterium*, the *Clostridium coccoides–Eubacterium rectale* cluster, the *Bacteroides–Prevotella* cluster, *Faecalibacterium prausnitzii*, and *Escherichia coli.* Bacteria were only barely found in the fistula tract of one patient from the idiopathic group.

While surgeons may find this counter-intuitive (on the basis that pus can be expressed from many fistula tracts), the above studies suggest that bacteria are not a feature of perianal fistulae and do not contribute to their persistence. However, it is possible that a putative organism has simply not yet been identified by the methods used to date. It is well known that many microorganisms are not detectable through traditional cultures. Recently developed gene amplification and sequencing techniques have led to the discovery of new pathogens as agents of disease. Researchers have not yet applied this to perianal fistulae, and so this remains a potential new area to be studied.

Even if bacteria might not contribute directly to perianal fistula persistence, there is evidence that they may exert and indirect effect. Van Onkelen *et al.* (2013) examined tissue samples from the peri-sphincteric portion of the fistula tract in 10 patients using conventional microbiological culture, 16S small-RNA sequencing and immunohistochemistry to identify the presence of peptidoglycan, a polymer that

forms the cell wall of Gram positive bacteria. They found a paucity of bacteria, consistent with the studies previously mentioned. However, macrophages, neutrophils and dendritic cells containing peptidoglycan were abundant in the fistula tracts of 9 of the patients. And a host inflammatory response to peptidoglycan, demonstrated by expression of peptidoglycan recognition proteins was found in 6 patients. The authors suggested that peptidoglycan stimulates the secretion of IL-1β and other inflammatory mediators in perianal fistulae.

Effects of Antibiotics and Faecal Diversion

The effect of antibiotics on perianal fistula has only been studied in relation to Crohn's disease fistulation. No study has yet shown sustained fistula healing with antibiotics alone. However, there appears to be a noticeable short-term response, suggesting that bacteria have a role in fistula pathophysiology, at least in Crohn's disease.

Three small cohort studies totalling 55 patients investigated the effect of metronidazole. Clinical improvement can occur in 6–8 weeks (Bernstein *et al.* 1980) and 50% of patients can achieve fistula closure (Jakobovits and Schuster 1984). However, when the metronidazole is stopped, 80% of patients at four months experience recurrence (Brandt *et al.* 1982). If the metronidazole is continued, side-effects are significant: a metallic taste in the mouth, dyspepsia, and risk of peripheral neuropathy.

Ciprofloxacin is also used routinely in perianal Crohn's disease. One pilot randomized controlled trial compared ciprofloxacin, metronidazole and placebo (Thia *et al.* 2009). In this study, 4 of 10 patients on ciprofloxacin, 1 of 7 patients on metronidazole, and 1 of 8 patients on placebo achieved a response at 10 weeks (defined as closure of at least half of fistulae that were draining at baseline).

Faecal diversion, by either defunctioning ileostomy or colostomy, is an option for patients with Crohn's disease whose perianal fistulae are refractory to all other treatments, save proctectomy. It is rarely employed in idiopathic disease. Its use

assumes that the absence of the faecal stream past the internal opening of the fistula, and reduction in luminal bacterial load have a therapeutic effect.

In a retrospective analysis spanning 27 years, 31 patients with perianal Crohn's disease underwent faecal diversion (Yamamoto *et al.* 2000). Although 25 (81%) showed an initial response, complete remission (defined as alleviation of the perianal disease with resolution of sepsis and active fistulas and objective improvement in the patient's condition) only occurred in 8 patients (26%).

A recent meta-analysis to evaluate the effectiveness, long-term outcomes and factors associated with success of temporary faecal diversion for perianal Crohn's disease included 16 cohort studies and 556 patients (Singh *et al.* 2015). Almost two thirds (64%) of patients had early clinical response after faecal diversion. Restoration of bowel continuity was attempted in 35% of patients, but was successful in only 17%.

In summary, the evidence, albeit weak, suggests that modifying the microbiological environment of perianal fistulae or the gastrointestinal lumen above them, either by antibiotic therapy or faecal diversion, has at best only a short-term effect. This is consistent with the assertion (section above) that bacteria do not play a direct role in fistula tract persistence, but may still have an indirect influence in fistula tract pathophysiology.

1.12 Immunopathology

Few studies have specifically focussed on the immunopathology of perianal fistula and most of these have been in relation to patients with Crohn's disease.

Morphology

Bataille *et al.* (2004) compared the morphology of enterocutaneous and perianal fistulae from 84 patients with Crohn's disease to 13 patients without inflammatory bowel disease. They showed that all fistulae, regardless of aetiology or site, appeared to have common features of a central fissure that penetrated the lamina propria and muscularis mucosae deep into the underlying tissue with a lining of granulation

tissue containing histiocytes and capillaries, and a lumen filled with nuclear debris, neutrophils and lymphocytes, thus indicating non-specific acute or chronic inflammation. Based on electron microscopy data from a small subset, the they concluded that the pathogenesis of fistulae involved myofibroblast-like cells, so-called transition cells, that respond to tissue injury and become organised by development of gap junctions and the formation of a basement membrane between the transition cells and the granulation tissue.

Bataille *et al.* also found differences between the groups. Crohn's fistulae presented with a central infiltration by CD45R0 (cluster of differentiation 45 receptor 0) positive T cells, followed by a small band of CD68 positive macrophages and dense accumulation of CD20 positive B cells. In contrast, in the idiopathic group, there was dense infiltrate of CD68 positive macrophages with only few CD20 positive B cells and CD45R0 positive T cells. However, in this study, the majority of Crohn's fistulae were enterocutaneous whereas the majority of the idiopathic fistulae were perianal, and subgroup analysis for perianal fistulae was not presented. Therefore, an alternative interpretation is that these were differences seen between enterocutaneous and perianal fistulae.

Colonic Lamina Propria Fibroblasts (CLPF)

Fibroblasts synthesize and degrade the extracellular matrix and play an important role in wound healing. Following tissue injury, migration of fibroblasts during the early stages of wound healing appears to be fundamental to wound contraction (Badid *et al.* 2000). Leeb *et al.* (2003) showed that fibroblasts from colonic mucosa of patients with inflammatory bowel disease displayed reduced migration compared to normal colonic mucosa. A follow-up study from the same group demonstrated that inflamed Crohn's colonic mucosa had reduced expression of extra domain A and B isoforms of fibronectin, an extracellular glycoprotein important in inducing migration of CLPF (Brenmoehl *et al.* 2007). Expression of extra domain A and B isoforms in Crohn's fistulae was virtually absent. A further study showed that

expression of galectin-3 in Crohn's fistulae, a carbohydrate-binding protein that activates CLPF, was also reduced in Crohn's fistulae (Lippert *et al.* 2008).

These data, if correct, imply that in Crohn's fistulae pathogenesis, CLPF functions are critically impaired, necessitating the activation of alternative pathological healing pathways, such as migration of intestinal epithelial cells. However, it must be noted that these findings pertain to enterocutaneous fistulae. Studies of CLPF function specifically in Crohn's perianal fistulae are lacking, as are those on idiopathic fistulae.

Epithelial to Mesenchymal Transition (EMT)

EMT is a normal feature of tissue remodelling and wound healing. It is also associated with an increased migratory and invasive potential of epithelial cells in different tissues (Kalluri and Neilson 2003). A study of both Crohn's disease and non-Crohn's fistulae, which included intestinal fistulae, showed that around two-thirds of Crohn's fistulae were lined not by epithelium, but by a thin basement membrane layer of myofibroblast-like transitional cells (Bataille *et al.* 2004). Unfortunately, the study was not clear on the findings in the non-Crohn's fistulae. In a follow-up study of 23 fistulae that included 18 Crohn's and two non-Crohn's perianal fistulae, Bataille *et al.* (2008) found that the distribution of markers in the transitional cell lining of the fistula tracts was typical of EMT. The findings in the Crohn's fistulae were very similar to the two non-Crohn's fistulae.

Further evidence for the role of EMT was provided by Scharl *et al.* (2011). They demonstrated that the nuclei of the transitional cells lining the fistula tracts showed an increased expression of SNAIL1 transcription factors. SNAIL1 normally promotes the repression of the adhesion molecule E-cadherin to regulate EMT in embryonic development. They also found that TGF-β and integrin-αvβ6 were also highly expressed (2013). Interestingly, integrin-αvβ6 in colon cancer regulates cell migration and secretion and activation of proteases capable of degrading matrix barriers (Agrez *et al.* 1999), and the TGF-β family of growth factors can initiate and

maintain EMT by activating major signalling pathways and transcriptional regulators (Zavadil and Böttinger 2005). One such downstream effect is the secretion of IL-13 from CLPF, which was demonstrated in patients with perianal Crohn's disease compared with patients with non-perianal Crohn's disease and healthy volunteers (Scharl *et al.* 2013). This pathway has not yet been studied in idiopathic perianal fistulae.

TNF-α is also present in the transitional cell lining of perianal fistula tracts from both Crohn's and non-Crohn's disease patients (Scharl *et al.* 2011). It is also expressed in peri-fistula immune cells. TNF-α induces the expression of factors associated with EMT and invasion in intestinal epithelial cells and Crohn's perianal fistula CLPF (Frei, Pesch, *et al.* 2013). This is blocked when anti-TNF-α antibody is administered *in vitro*. Furthermore, anti-TNF-α therapy is now a routine treatment for perianal Crohn's disease following a trial that showed that it could achieve fistula closure in 55% of patients (Present *et al.* 1999).

Muramyl-dipeptide (MDP) is a bacterial wall component. MDP is a ligand for NOD2, an important gene conferring susceptibility to Crohn's disease (see above). Together with TNF-α, it induces expression of factors associated with EMT and invasion in intestinal epithelial cells and Crohn's perianal fistula CLPF (Frei, Pesch, *et al.* 2013). MDP has not yet been studied in idiopathic perianal fistula.

Matrix Metalloproteinases (MMPs)

Matrix metalloproteinases (MMPs) are a family of neutral proteases with the ability to degrade all components of extracellular matrix. MMPs are now recognised as key regulators of cell function through their ability to cleave a vast range of cytokines, chemokines, receptors, proteases, and adhesion molecules to alter their function (O'Sullivan *et al.* 2015). Pender *et al.* (1997) first demonstrated the role of MMPs in T cell injury in the gut. Baugh *et al.* (1999) then showed that MMP expression is significantly higher in the affected and non-affected mucosa of Crohn's disease patients compared with healthy controls. With several subsequent studies providing

evidence, MMPs are now strongly implicated in the pathogenesis of inflammatory bowel disease (Pender and MacDonald 2004).

MMP expression has also been studied in fistulae. Kirkegaard *et al.* (2004) obtained fistula specimens from patients with Crohn's disease (n = 11), other diseases (n = 9) and normal colon (n = 5). Fistulae were mainly perianal, with a minority being enterocutaneous in both disease groups. Using single and double-labelled immunohistochemistry and *in situ* hybridisation, they found marked MMP-3 and MMP-9 upregulation in both Crohn's and non-Crohn's fistulae. Later in a small study that included Crohn's and non-Crohn's perianal fistulae specimens (n = 5), Frei *et al.* (2013) found MMP-9 and MMP-13 to be specifically expressed in cells lining the fistula tracts.

Putting it All Together

Recently Scharl and Rogler (2014) summarised the immunological evidence for the pathogenesis of fistulae (of all types) in Crohn's disease. In their proposed mechanism (Figure 7), an epithelial defect caused by inflammation or injury allows pathogen-associated patterns to gain entry and induce various pathways mediated by TNF-α, TGF-β, IL-13, MMPs and integrin-αvβ6. These drive EMT, which allows cell invasion and migration, resulting in a penetrating fistula tract lined by transitional cells. Unfortunately, this theory is mainly based on the study of fistulae in patients with Crohn's disease. It is therefore difficult to say if this theory is applicable to idiopathic fistula disease.

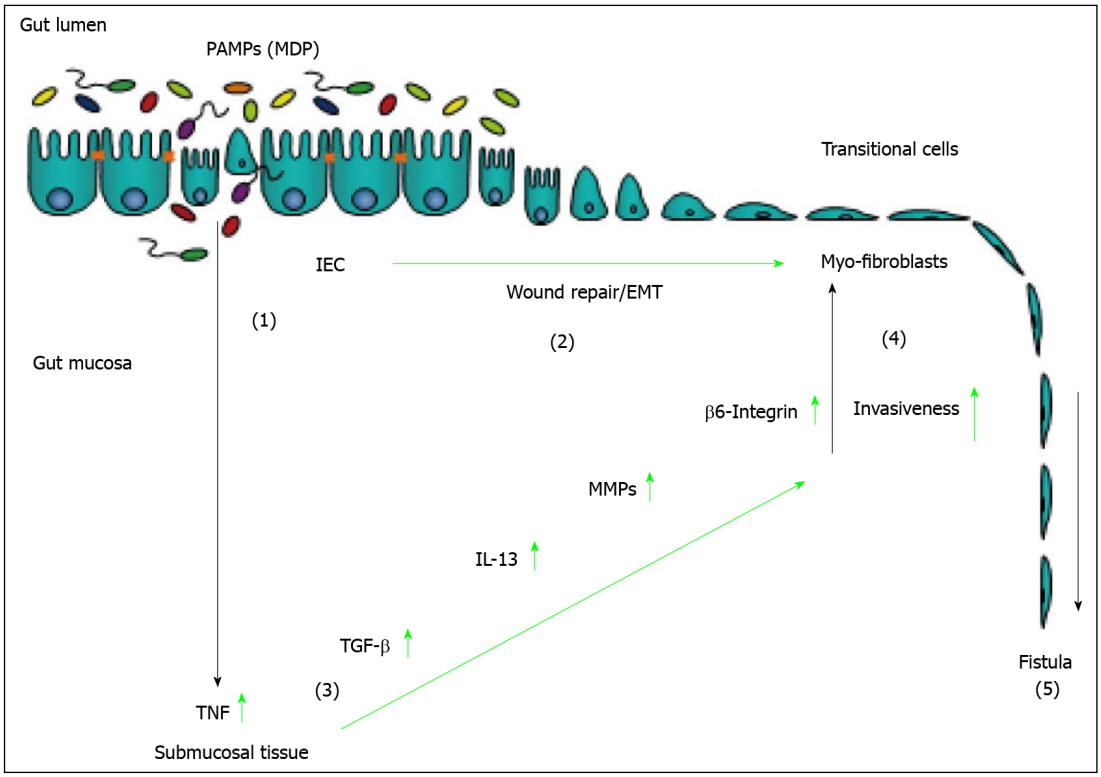

Figure 7 Pathogenesis of Crohn's disease-associated fistulae as proposed by Scharl and Rogler (2014). An epithelial barrier defect favours the invasion of pathogen-associated patterns (PAMPs) into the gut mucosa (1). On the one hand, for wound healing purposes, intestinal epithelial cells (IEC) undergo epithelial-to-mesenchymal transition (EMT) (2). On the other hand, the presence of PAMPs induce an inflammatory reaction resulting in increased secretion of tumour necrosis factor alpha (TNF-α) (3). TNF-α is able to induce secretion of transforming growth factor beta (TGF-β) as well as to induce EMT and expression of molecules associated with cell invasiveness, such as integrin-αvβ6 (aka β6-integrin). TGF-β-induced IL-13 and elevated activation of matrix remodelling matrix metalloproteinases (MMPs) critically contribute to invasive cell growth (4). Finally, EMT, MMP over-activation and elevated expression of invasive molecules contribute to the development of fistulae (5).

1.13 Hypothesis

The majority of perianal fistula research to date has been conducted within the same paradigm built upon the assumption that idiopathic and Crohn's perianal fistulae differ in their pathogenesis and pathophysiology. As previously discussed, the original theories of pathogenesis in these two disease groups were developed in parallel but separately and arose at different conclusions. Subsequent research has perpetuated this paradigm by continuing to study idiopathic and Crohn's perianal fistulae in isolation from each other (Table 3).

Only a handful of studies have attempted to compare the characteristics of perianal fistulae from each group. All these studies assumed there is a difference as the idiopathic group each time was used as the quasi-control group. These studies have indeed highlighted some differences between the groups. However, the above careful review of the literature through a neutral construct has revealed that there just as many similarities as there are differences between idiopathic and Crohn's perianal fistula disease. As such, this fundamental hypothesis has not yet been adequately tested.

The core hypothesis of this study is that idiopathic and Crohn's perianal fistulae differ in their pathogenesis and pathophysiology.

Table 3 The focus of previous studies of perianal fistulae.

Idiopathic only	Crohn's disease only	Idiopathic *v.* Crohn's disease
Parks (1961) Marks and Ritchie (1977) Grace *et al.* (1982) Seow-Cheon *et al.* (1992) Sangwan *et al.* (1984) Graf *et al.* (1995) de San Ildefonso Pereira *et al.* (2002) van Onkelen *et al.* (2013, 2016)	Hughes (1978) Bernstein *et al.* (1980) Present *et al.* (1980, 1999) Marks *et al.* (1981) Brandt *et al.* (1982) Allan *et al.* (1982) Jacobovits and Schuster (1984) Irvine (1995) Bell at al. (2003) West *et al.* (2005) Roffolo *et al.* (2008) Maggie *et al.* (2013)	Bataille *et al.* (2004, 2008) Kirkegaard *et al.* (2004) Tozer *et al.* (2011)

1.14 Aim and Objectives

The aim of this thesis was to compare idiopathic and Crohn's perianal fistula disease. The objectives were to phenotypically compare:

1. Clinical data,
2. Cytokine profiles,
3. Phosphoprotein profiles, and
4. Dynamic contrast-enhanced (DCE) MRI data.

The specific rationales for each of these approaches are discussed within their respective chapters below.

2. METHODS

2.1 Study Design

We conducted these observational studies within the basic construct of a prospective cohort study. This design appropriately balanced the potential for systematic high-quality data collection across a range of outcomes (and covariates of outcome) against risk. We refrained from introducing any deviation from routine standard of care to minimise the latter.

Nevertheless, we accepted that our design still carried limitations. One was the limitation of patient follow-up. This was constrained by the student's tenure, which meant that the longest possible follow-up length was six months. We judged this to be adequate because clinical failures, such as recurrence of the fistula after surgery, usually occur within the first three to six months (Marks and Ritchie 1977).

A possible alternative was a case-control study. Patients with Crohn's perianal fistulae would have been selected consecutively as the cases and matched to idiopathic controls. This would have required fewer patients to be recruited but would have taken too long to achieve an adequate overall total.

2.2 Controls

The study of perianal fistulae is frustrated by the absence of an established control to compare it to. For instance, when studying colitis, we can compare affected colons with the colons of healthy individuals. However, perianal fistulae are non-existent in health. Therefore, like previous studies (Table 3 above), we chose to compare idiopathic with Crohn's perianal fistulae, with the former acting as a quasi-control group.

If we assume Park's cryptogenic theory to be correct for both idiopathic and Crohn's perianal fistulae, then the true control might be the healthy anal gland and its duct. Obtaining such tissue from healthy volunteers would cause unacceptable morbidity.

Such tissue could be available from abdominoperineal resection specimens. However, this option was not feasible for this study due to the generally low incidence of this operation and the fact that most are undertaken after neoadjuvant chemoradiotherapy, which has profound effects on the mucosa and submucosa.

We also chose to biopsy the rectum in our participants (see Section 2.10). To provide a control for this, we also sampled the rectum in adults undergoing lower gastrointestinal endoscopy for non-inflammatory conditions. Further details on these participants are given in Chapter 4.

2.3 Inclusion and Exclusion Criteria

This study included all adults with an idiopathic or Crohn's perianal fistula requiring surgical intervention. Studies that can be easily recruited to are able to maintain their momentum and achieve their target recruitment. Therefore, the inclusion criteria were intentionally broad to facilitate steady recruitment of a sample that was sufficiently generalizable. Adults without the capacity to give their informed consent were excluded. We did not include children because of the additional ethical barriers, the lower incidence and the possibility of a different pathogenesis.

We excluded rectal, intestinal and subcutaneous fistulae because their pathogenesis is different. Rectal fistulae usually occur as a complication of previous surgery: improper probing of the external fistula tract can create a false tract and perforate the rectum. Intestinal fistulae can arise from intestinal pouches after a restorative proctocolectomy due to either anastomotic dehiscence or as a consequence of penetrating inflammatory bowel disease. Subcutaneous perianal fistulae may arise when an anal fissure heals over (Parks *et al.* 1976).

To avoid undue heterogeneity, we excluded perianal fistulae secondary to diseases other than Crohn's disease, such as tuberculosis and trauma.

2.4 Study Site

The sole study site was Bart's Health NHS Trust. It is the largest NHS Trust in the UK and serves a population of 2.5 million in the east of London and beyond (Barts Health NHS Trust 2015). It comprises five hospitals, three of which provide colorectal surgery services.

The Royal London Hospital is the main centre within the Trust, and was the focus for the study. It is a secondary care centre and accepts referrals concerning patients with perianal fistulae from the surrounding community. A significant number of patients also initially present to the hospital's urgent care centre and emergency department before being referred to the colorectal team, as either an inpatient admission or an outpatient appointment. The hospital is also a tertiary referral centre for patients with perianal fistula disease. Hospitals in north, central and east London, Essex and Kent, as well as the other four hospitals within the Trust, regularly refer patients who have not achieved clinical satisfaction with their treatment so far, which can range from none to multiple surgical attempts to eradicate the disease. The department also works closely with the co-located gastroenterology department, which itself is a tertiary referral centre for inflammatory bowel disease. As such, many patients with Crohn's disease come as internal tertiary referrals.

Whipps Cross University Hospital is also part of Barts Health and a secondary referral centre for perianal fistula disease. We included it as a recruitment centre, but we did not include Newham General Hospital, the third colorectal centre within the Trust, because resources were not available.

2.5 Sample Size

A formal sample size calculation was not relevant because this study was observational and there were no prior relevant data. We estimated that a reasonable degree of saturation would be provided by a minimum of 60 participants.

2.6 Study Scheme Diagram

The overall study scheme is depicted in Figure 8. An explanation is given in the following paragraphs.

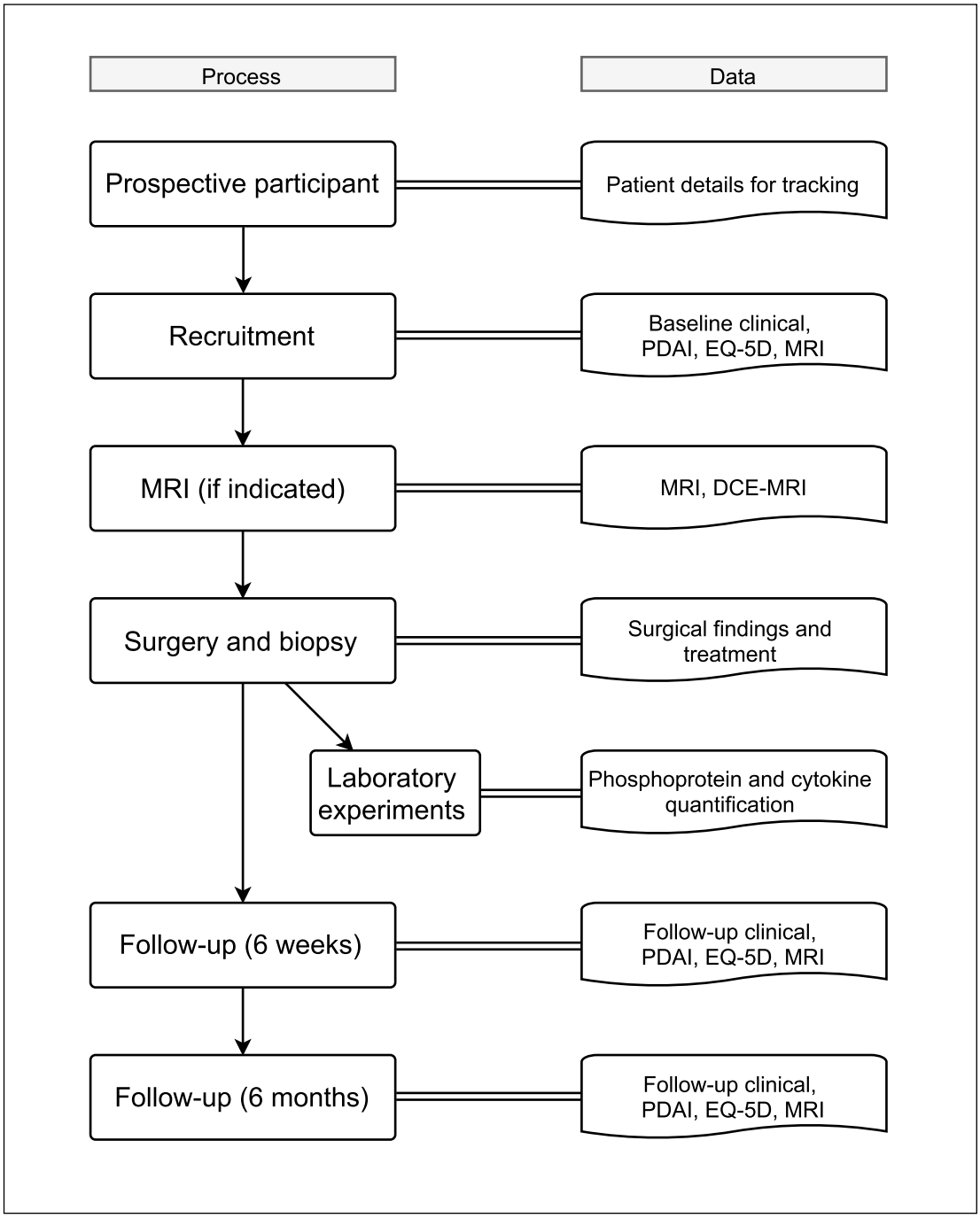

Figure 8 Study scheme diagram. DCE, dynamic contrast enhanced; MRI, magnetic resonance imaging; PDAI, perineal disease activity index.

2.7 Participant Identification

We identified potential participants at several points in their NHS care pathway, and then tracked them by recording their identifiers and upcoming hospital episodes in the research database. This then allowed the student to plan in advance whom to approach where and when, and minimised the number of potential participants missed.

Referral Vetting

The department agreed to channel all new referrals of patients with perianal disease to Professor Charles Knowles This common source allowed potential recruits to be tracked and approached by the student when they next visited the hospital.

Outpatient Clinic

All surgeons seeing patients with perianal fistula disease in the outpatient clinics were also asked to identify patients who met the inclusion criteria and notify the student or refer the patient on to Professor Knowles' clinic. To maintain the profile of the study and thus encourage continued participant identification, the student maintained rapport through regular face-to-face contact with the surgeons. The student also saw patients in clinic on a regular basis and identified patients through this.

Surgical Waiting Lists

The student scanned the theatre schedules for potential participants each week, and regularly contacted the admissions team to ensure that ad hoc sessions outside the regular slots were included.

Multidisciplinary Meeting

We also identified potential participants at a weekly meeting where surgeons, gastroenterologists and radiologists discussed patients with inflammatory bowel disease.

Inpatients

Surgeons who accepted acute admissions were asked to identify patients who met the inclusion criteria and notify the student. In many cases, their care was also transferred to Professor Knowles.

Whipps Cross University Hospital

Two consultant surgeons at Whipps Cross identified patients from their outpatient clinics and surgical waiting list. They explained the research and arranged for their operation on a dedicated list.

2.8 Recruitment

Eligible patients were approached in person by the student or, in some cases the research nurse, who explained the research, gave an information sheet, checked against the exclusion criteria and obtained written consent (Appendix 1).

2.9 Baseline Evaluation

Following recruitment, the student interviewed the participants to gather structured clinical information. In most cases, the student also examined the patient, except when a complete examination had recently been performed and documented by a senior surgeon. The student recorded the data on a bespoke paper case report form (CRF, Appendix 3), which included age, gender, ethnic origin, previous fistula disease and recurrence, presence of inflammatory bowel disease, previous medical and surgical treatment and response, current fistula disease duration and presence of seton, presence of stoma and smoking status. He also completed baseline Perineal

Disease Activity Index (PDAI, Irvine 1995) and EQ-5D-5L (Herdman *et al.* 2011) questionnaires with the participants.

If after recruitment, participants required an MRI scan on a basis of clinical need (i.e. those who not had an MRI in the last year and had recurrent disease, suspected complex anatomy or an absent external fistula opening), it was arranged with the addition of a supplementary DCE protocol. Gathering DCE-MRI data from all participants would have been ideal. However this was not possible due to funding constraints and the observational nature of the design. Where only conventional MRI data were available, quantitative analysis was omitted.

2.10 Surgery and Biopsies

Participants underwent surgery as part of their clinical care. The student attended the operation and recorded the intraoperative findings on a bespoke CRF (Appendix 3). This included the number of fistulae and presence of branching, Parks' classification, level of internal opening within the anal canal, position of the secondary tracts in relation to the levator ani, presence of horseshoe extensions, presence of associated collections (cavities > 3 mm diameter), rectal wall involvement, presence of hidradenitis suppurativa, and the surgical treatment given. If two or more separate fistulae were present, details of the most severe fistulae were recorded.

During the procedure, biopsy samples were taken from 4 different sites:

a. The fistula tract wall as far proximal as possible;
b. The granulation tissue within the tract (if present);
c. Mucosa from the internal opening (if present); and
d. Mucosa from the distal rectum away from the internal opening.

When the procedure was a lay-open, fistulectomy, LIFT or seton insertion (when an incision in the perineum at the external opening was initially necessary), it allowed adequate access to sample the fistula tract. To reduce the amount of cell damage and resultant artificial release of intracellular proteins, the surgeon used scissors and

scalpel and limited the use of diathermy until sampling was complete. When placement of a seton did not require an incision, they passed an endoscopic biopsy forceps into the external opening, advanced it to the proximal tract and used it to obtain the specimens. For the other biopsies, the surgeon sampled the granulation tissue with a blunt curette through the external opening, the internal opening with forceps and scissors through the anal canal, and the rectum with endoscopic cold biopsy forceps.

The student immediately placed the samples in labelled containers with normal saline at 4°C, and then completed a specimen form (Appendix 3) and the specimen logbook. When all samples for an operating session had been obtained, the student transported them to the laboratory for immediate processing. The maximum time between taking the biopsies and delivery to the laboratory was 4 hours.

2.11 Tissue Preparation and Storage

In the laboratory, the student examined each specimen in a sterile petri dish under a microscope at room temperature, before trimming off faecal debris, blood clots, extraneous and damaged tissues using forceps and scissors. He then divided each specimen into equal samples approximately 2–3 mm^3 in size. One sample was kept aside for immediate tissue culture. The remaining samples were transferred to cryotubes, labelled with participant ID and biopsy site, snap-frozen on dry ice for five minutes and then stored in a freezer at -80°C. Specific laboratory methods are discussed in the relevant chapters below.

2.12 Clinical Follow-up

We assessed participants in the outpatients' clinic at six weeks and six months after their surgery. When this was not possible, the student reviewed the case notes and telephoned the participant. We recorded signs and symptoms suspicious for Crohn's disease, investigations for Crohn's disease (colonoscopy, barium meal and follow-through, abdominal MRI, faecal calprotectin, intestinal biopsies), presence of confounding aetiology (HIV, TB), medical treatment received since recruitment,

overall response to treatment, management plan, microbiology results from surgery, PDAI and EQ-5D on a bespoke CRF (Appendix 3).

2.13 Definitions and Classifications

After considering the various grading definitions (see Section 1.4) together with our personal experience, we defined complex disease as a trans-sphincteric fistula with secondary tract or abscess or worse; or a recurrent or non-healing fistula after surgery with curative intent; or a fistula that only had a transient response or no response to seton insertion. We adopted the St Mark's Hospital group's definition of a low perianal fistula, which is an inter-sphincteric or trans-sphincteric fistula involving no more than 1 cm of external anal sphincter (Atkin *et al.* 2011). We classified patients as Crohn's disease if they had received a formal diagnosis of Crohn's disease from a specialist either before or during the study period.

We classified the treatment intent as 'symptom control' when the procedure performed was none, curettage or seton insertion, and 'cure' when the procedure performed was lay open, fistulectomy or LIFT. For those whose treatment intent was symptom control, a satisfactory outcome was when symptoms were controlled or had resolved. For those whose treatment intent was cure, a satisfactory outcome was when symptoms had resolved.

2.14 Study Database

The student programmed a bespoke coded database using Access 2010 (Microsoft, Redmond WA). There were several features to minimise data entry errors. They were automatic assignment of a study identification number for each participant; automatic lookup to ensure data was recorded against the correctly registered participant; warnings for duplicate CRFs being entered; using codes with the corresponding label showing in a drop-down menu to allow quick visual checks; data validation and formatting rules; the on-screen layout corresponding to the paper CRF layout; and flagging of incomplete CRFs. The database also contained queries to derive calculated variables, which were length of follow-up in weeks, Van Assche

score, PDAI score, EQ-5D-5L health value, study group (idiopathic or Crohn's disease), and treatment outcome subgroup. The database was validated before use by checking each table and query with dummy data.

To facilitate effective case management, the database included a participant tracker, which listed upcoming events such as surgery, MRI and clinic visits, in chronological order along with the next action such as recruit, or follow up; a data tracker, which showed the complete and incomplete CRFs and when follow-up was due for each participant; and a recruitment tracker, which tabulated recruitment by group. Using these functions, the student periodically audited to identify missed appointments and missed follow-up. This allowed these anomalies to be corrected or mitigated in a timely manner.

We determined data accuracy by selecting a random 10% sample of each CRF type and re-entering the data from the paper CRFs. This double-entered data was crosschecked against the originally entered data and mismatches were counted. One thousand four hundred and thirty-one data items across the six different CRFs were crosschecked. This revealed only nine (0.6%) mismatches.

2.15 Statistical Analysis

Once data collection was complete, the student extracted pseudo-anonymised data from the study database and imported it into SPSS Statistics version 22 (IBM, Armonk, NY). A standard process using SPSS syntax was used to ensure the data were handled appropriately with a full audit trail (Appendix 4). This process included reviewing and rectifying import errors; programming the data dictionary to set variable formats, variable labels, value labels, variable levels and user-missing values; programming filters to allow various analyses; inspecting the data for missing values, obvious mistakes and implausible values (uncertainties were resolved by consulting the original paper CRFs); and reviewing the histogram charts and Shapiro-Wilk tests of normality. Mean, standard deviation and parametric tests (e.g. independent samples t-test) were used for normal data, and median, interquartile

range and non-parametric tests (e.g. Kruskal-Wallis test) were used for non-normal data. We considered $p \leq 0.05$ to be statistically significant, or $p \leq 0.01$ where multiple comparisons were made (an established alternative to methods of 'correction').

3. CLINICAL DATA

3.1 Introduction

As detailed in Chapter 1, perianal fistulae present with a broad range of clinical phenotypes: simple and complex, low and high, primary and recurrent, and idiopathic and secondary. Their morphology also varies, resulting in four main patho-anatomical types under the generally accepted Parks' classification: inter-sphincteric, trans-sphincteric, supra-sphincteric and extra-sphincteric (Parks *et al.* 1976). The main symptoms are generally pain or discomfort and discharge, which can be present at varying levels of severity and fluctuate from week to week. In addition, the psychosocial impact upon the patient can range from none, to a prolonged period of unhappiness, sexual inhibition and poor work performance.

Many colorectal surgeons believe that Crohn's perianal fistulae tend to be more severe than idiopathic fistulae (Tozer *et al.* 2015). Crohn's fistula morphology appears more commonly to be complex, with high fistulae, secondary tracts, horseshoe extensions and collections. They appear to exhibit a greater degree of inflammation and as such inflict a greater symptomatic burden upon the patient. Attempts to lay open and eradicate Crohn's fistulae more commonly fail or end with recurrence. However, the literature lacks any direct comparison of the clinical phenotypes between these two groups.

The clinical assessment of perianal fistulae is largely subjective, relying on the clinician to take a detailed history from the patient and perform a careful clinical examination. Methods of objectively measuring perianal fistula disease activity have only been developed in Crohn's disease. These include that in Present *et al.* (1980), the Anal Disease Activity Index (Allan *et al.* 1992), the Perianal Disease Activity Index (PDAI, Irvine 1995), the Fistula Drainage Assessment (Present *et al.* 1999) and Pikarsky's Perianal Crohn's Disease Activity Index (Pikarsky *et al.* 2002). The Fistula Drainage Assessment measures the number of open draining fistulae (including enterocutaneous) on clinical examination, with criteria to describe either

improvement or remission, and was used as the primary endpoint in a seminal trial showing the efficacy of infliximab in treating Crohn's fistulae (Present *et al.* 1999). The PDAI, which scores five domains on a Likert scale, has also been used in clinical trials (Present *et al.* 1999). Although it has not generally been adopted into routine clinical practice, it is considered the current gold standard for assessing perianal Crohn's disease (Sostegni *et al.* 2003).

There are currently no validated objective methods described for assessing the activity of idiopathic perianal fistulae. Of those described in perianal Crohn's disease, the PDAI is most applicable, as it does not attempt to measure features that are generally only present in Crohn's disease, e.g. concomitant intestinal disease, which is included in Pikarsky's Perianal Crohn's Disease Activity Index.

Quality of life is also another important consideration. The commonest instrument used in trials concerning Crohn's disease is the Inflammatory Bowel Disease Questionnaire (IBDQ, Guyatt *et al.* 1989). However the IBDQ has not been validated in patients with primarily fistulating Crohn's disease. Similarly, quality of life data for patients with idiopathic perianal fistulae are scarce. Sailer *et al.* studied the Gastrointestinal Quality of Life Index (GIQLI) in patients with benign anorectal disorders, which included 22 patients with perianal fistula (Sailer *et al.* 1998). In subgroup analysis, the GIQLI did not discriminate between patients with perianal fistulae and the controls.

In summary, the current literature contains little data on the clinical phenotypes that are present in both idiopathic and Crohn's perianal fistula disease. This study aimed to describe and compare the clinical features of this disease in these groups.

3.2 Methods

The methodology for recruitment, data measurement, follow-up and analysis of the study cohort is described in Chapter 2. Two patient-reported outcome measures were chosen to augment the clinical assessment at baseline and follow-up: one to measure disease activity, and one to measure quality of life.

The PDAI was chosen as the measure of disease activity. It was judged to be the gold standard in Crohn's perianal fistula and most easily applicable to the idiopathic group for the reasons discussed above. However, it is noted that the PDAI is only validated in Crohn's perianal fistula. The instrument comprises five domains (Table 4). Each domain of discharge, pain, restriction of sexual activity, type of perianal disease and degree of induration is estimated between patient and clinician on a Likert scale from zero to four. The final index score is the sum total of the scores in each domain, with a score greater than four suggesting active disease requiring medical or surgical treatment (Losco *et al.* 2009).

General quality of life data was captured using the 5L version of the EQ-5D questionnaire (Herdman *et al.* 2011). It is a well-validated tool and one of the most widely used generic measures of health status. It comprises five questions that allow five levels of severity in their answers (Table 5). Concatenation of the numerical answers produces a five-digit health state. These health states are then mapped using published country-specific value sets (EuroQol 2015) to an index value on a scale anchored at one (full health) to zero (dead), which reflect the preferences of the general public. The questionnaire also has an additional item that asks the subject to grade their current overall health on a visual-analogue scale (VAS) ranging from zero to 100.

Other measures were considered. The GIQLI, mentioned earlier, comprises 36 multidimensional items covering symptoms, and physical, emotional and social dysfunction related to gastrointestinal diseases or their treatments. Each item scores between zero and four points. The overall score is the sum of all item scores where zero represents the worst and 144 represents the best possible results. The SF-36 is another widely-used generic health survey which gives an eight-scale profile of functional health and well-being scores as well as psychometrically-based physical and mental health summary measures and a preference-based health utility index (Ware 2002). Although these instruments may have provided greater granularity, many of the questions would have seemed irrelevant to the participants and the length of the questionnaire onerous.

Table 4 Perianal Crohn's Disease Activity Index (PDAI).

Discharge: 0 No discharge 1 Minimal mucous discharge 2 Moderate mucous or purulent discharge 3 Substantial discharge 4 Gross faecal soiling	Type of perianal disease: 0 No perianal disease / skin tags 1 Anal fissure or mucosal tear 2 < 3 Perianal fistulae 3 ≥ 3 Perianal fistulae 4 Anal sphincter ulceration or fistulae with significant undermining of skin
Pain / restriction of activities: 0 No activity restriction 1 Mild discomfort, no restriction 2 Mod. Discomfort, some limitation activities 3 Marked discomfort marked limitation 4 Severe pain, severe limitation	Degree of induration: 0 No induration 1 Minimal induration 2 Moderate induration 3 Substantial induration 4 Gross fluctuance / abscess
Restriction of sexual activity: 0 No restriction sexual activity 1 Slight restriction sexual activity 2 Mod. Limitation sexual activity 3 Marked limitation sexual activity 4 Unable to engage in sexual activity	PDAI = total score

Table 5 EQ-5D-5L questionnaire.

Mobility: 1 I have no problems in walking about 2 I have slight problems in walking about 3 I have moderate problems in walking about 4 I have severe problems in walking about 5 I am unable to walk about Self-Care: 1 I have no problems washing or dressing myself 2 I have slight problems washing or dressing myself 3 I have moderate problems washing or dressing myself 4 I have severe problems washing or dressing myself 5 I am unable to wash or dress myself Usual Activities: 1 I have no problems doing my usual activities 2 I have slight problems doing my usual activities 3 I have moderate problems doing my usual activities 4 I have severe problems doing my usual activities 5 I am unable to do my usual activities Pain/discomfort: 1 I have no pain or discomfort 2 I have slight pain or discomfort 3 I have moderate pain or discomfort 4 I have severe pain or discomfort 5 I have extreme pain or discomfort Anxiety/depression: 1 I am not anxious or depressed 2 I am slightly anxious or depressed 3 I am moderately anxious or depressed 4 I am severely anxious or depressed 5 I am extremely anxious or depressed EQ VAS (question accompanied by linear graduated scale from 0 to 100) We would like to know how good or bad your health is today. This scale is numbered from 0 to 100. 100 means the best health you can imagine. 0 means the worst health you can imagine. Mark an X on the scale to indicate how your health is TODAY. Now, please write the number you marked on the scale in the box below.

3.3 Results

Participants

Between March 2014 and April 2015, 130 consecutive patients were identified as potential participants. Figure 9 details the participant flow during the study. A total of 61 were included and followed-up, of whom 48 (79%) had idiopathic disease and 13 (11%) had Crohn's disease There was a preponderance of males (3:1) and the mean age was 40.0 years (SD = 13.3), in keeping with the general epidemiology of perianal fistula disease. The majority were of Asian ethnicity, reflecting the local population demographics.

The median duration when the fistula had been present at recruitment was 36 months (IQR = 14–60) and the median number of previous operations was one (IQR = 0–4), demonstrating the chronicity and persistence of the disease (and perhaps referral practice). Ten (16%) had previously had surgery with curative intent. Further baseline characteristics are detailed in Table 6. Both idiopathic and Crohn's disease groups had similar distributions of these characteristics, except for the number previously receiving antibiotics: this was higher in the idiopathic group (81% *versus* 23%).

None of the participants had a stoma. HIV infection was excluded by blood test in 28 (46%) and clinically in 33 (54%). TB infection was excluded by TB culture in 49 (80%) and clinically in 12 (20%).

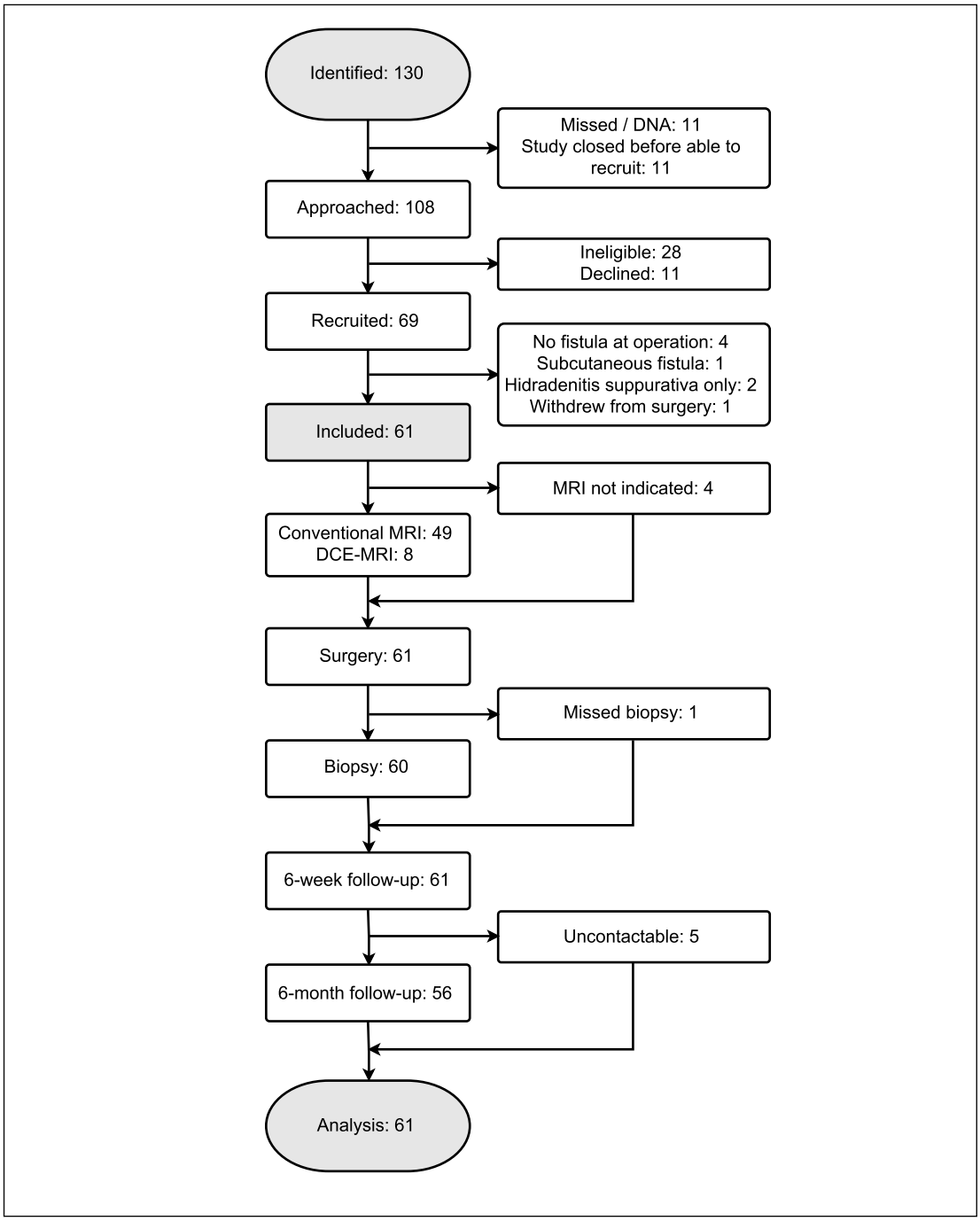

Figure 9 Participant flow diagram.

Table 6 Participant characteristics. SD, standard deviation; IQR, interquartile range.

	Idiopathic	Crohn's Disease	All
n	48	13	61
Male	38 (79%)	8 (62%)	46 (75%)
Mean age (SD), years	41.1 (11.6)	36.1 (18.5)	40.0 (13.3)
Ethnic origin:			
White	11 (23%)	5 (38%)	16 (26%)
Asian	26 (54%)	4 (31%)	30 (49%)
Black	3 (6%)	1 (8%)	4 (7%)
Other	7 (15%)	3 (23%)	10 (16%)
Unanswered	1 (2%)	0	1 (2%)
Median fistula duration (IQR), months	35 (14–60)	48 (17–66)	36 (14–60)
Previously received antibiotics	39 (81%)	3 (23%)	42 (69%)
Median previous operations (IQR)	1 (0–4)	0 (0–4)	1 (0–4)
Previously had surgery with curative intent	9 (19%)	1 (8%)	10 (16%)
Current smoker	22 (46%)	4 (31%)	26 (43%)

Of the 13 participants who had Crohn's disease, six had previous abdominal fistulae, six had previous abdominal surgery, and two were diagnosed with Crohn's disease during the study. At the time of recruitment, five participants were currently receiving and one had previously received anti-TNF-α antibody therapy (Table 7). All Crohn's disease participants had imaging features that were consistent with Crohn's disease; 12 had histological features consistent with Crohn's disease and six of these featured granulomas (Figure 10). Imaging included diagnostic signs on colonoscopy, MRI abdomen or barium small bowel follow-through, or a combination thereof.

In the 48 participants who had idiopathic disease, 32 participants underwent imaging, namely colonoscopy, MRI of the abdomen and/or barium small bowel follow-through, to exclude underlying Crohn's disease. This included one patient who had a single granuloma in a previous operative fistula specimen, but had subsequent

negative imaging and intestinal biopsy results. Of the other 16, none had symptoms to suggest Crohn's disease. Reasons for not performing imaging in these participants were patient declined (n = 4) and not clinically indicated (12). Thus, no patient with abdominal symptoms suggestive of Crohn's disease went un-investigated. Additionally, out of these 16 patients, 12 had their fistula specimens examined histologically, and none showed signs of Crohn's disease.

Table 7 Characteristics of Crohn's disease participants.

n	13
Crohn's disease diagnosed during study	2 (21%)
Highest order therapy received:	
Steroids	1 (8%)
Mesalazine	1 (8%)
Azathioprine	2 (15%)
Anti-TNF-α	6 (46%)
Receiving anti-TNF-α at recruitment	5 (38%)
Previous abdominal fistulae	6 (46%)
Previous abdominal surgery	6 (46%)

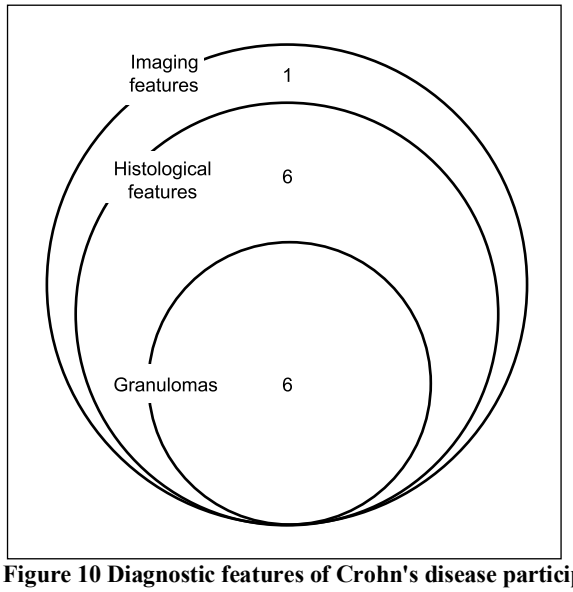

Figure 10 Diagnostic features of Crohn's disease participants. Imaging features includes diagnostic signs on colonoscopy, MRI abdomen, or barium small bowel follow-through, or a combination thereof.

Baseline Features

There were 44 participants with complex disease: 32 (67%) in the idiopathic group and 12 (92%) in the Crohn's disease group (Figure 11).

PDAI at baseline was measured in all but one participant. The mean scores for each PDAI domain were similar, except for induration, which was 0.61 and 2.29 in the idiopathic and Crohn's disease participants respectively (Table 8 and Figure 12). The PDAI was significantly higher in the Crohn's disease participants with a mean difference of 2.40 (95% CI = 0.52–4.28, p = 0.01).

EQ-5D-5L was measured at baseline in all but one participant (98%). We checked the original data for two outliers with very low EQ index values and confirmed they were correct. One participant who was wheelchair-bound due to a neurological condition returned an EQ-5D-5L health state that corresponded to a negative index value (-0.034). A negative health value represents a state considered 'worse than death', a concept supported by prior literature (Kind *et al.* 2006). The other patient, whose index value at baseline was 0.091, also had poor mobility.

Similar EQ-5D-5L levels were reported in the idiopathic and Crohn's disease participants in each dimension except usual activities, where a higher proportion of Crohn's disease participants reported higher levels (Table 9). The mean EQ VAS and EQ index values were also similar between the groups (Table 10 and Figure 13).

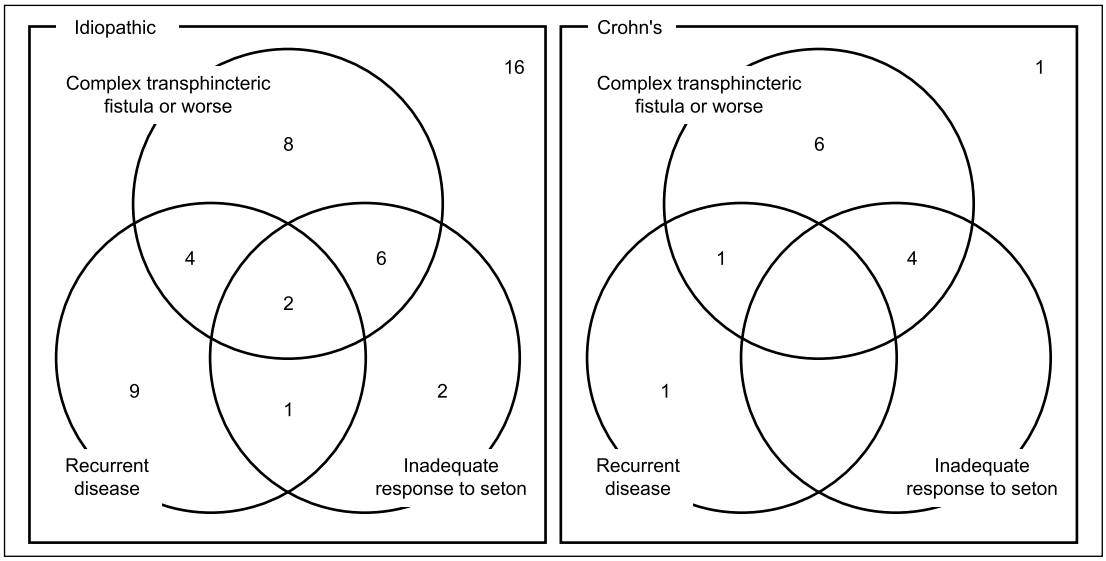

Figure 11 Comparison of clinical features. Complex trans-sphincteric: trans-sphincteric fistulae with secondary tract or abscess; recurrent disease: a recurrent or non-healing fistula after curative surgery; inadequate response to a seton: transient or no symptomatic response from a seton.

Table 8 PDAI at baseline. Mean (standard deviation) shown. *N* = 60. Each domain range is 0–4, PDAI range is 0–20. *p* estimated using independent samples t-test.

	Idiopathic	Crohn's Disease	All
Discharge	1.37 (0.95)	1.86 (1.10)	1.48 (1.00)
Pain/restriction	1.09 (1.09)	1.50 (1.29)	1.18 (1.14)
Sexual function	0.59 (1.24)	0.43 (1.16)	0.55 (1.21)
Type	2.02 (0.15)	2.00 (0.78)	2.02 (0.39)
Induration	0.61 (0.74)	2.29 (1.27)	1.00 (1.13)
PDAI	5.67 (2.76)	8.07 (3.99)	6.23 (3.22)
	PDAI mean difference = 2.40 (95% CI = 0.52–4.28, p = 0.01)		

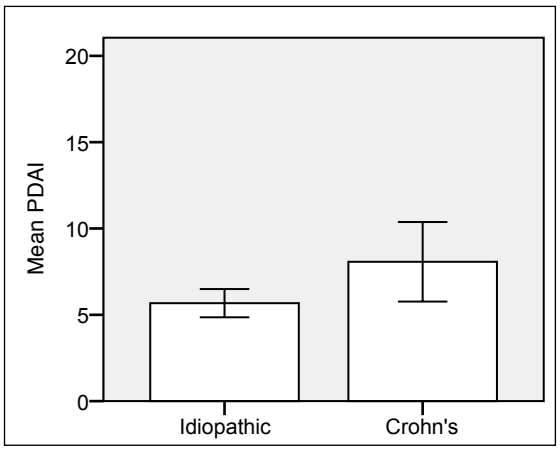

Figure 12 Mean PDAI at baseline. Range 0 to 20. Error bars show 95% confidence intervals.

Table 9 EQ-5D-5L dimensions at baseline. Percentage of participants reporting levels 1 to 5 (level 1 = no problems). *N* = 60.

		Idiopathic	Crohn's Disease	All
Mobility	Level 1	67%	57%	65%
	Level 2	20%	21%	20%
	Level 3	4%	21%	8%
	Level 4	7%	0%	5%
	Level 5	2%	0%	2%
Self-care	Level 1	89%	93%	90%
	Level 2	4%	7%	5%
	Level 3	7%	0%	5%
	Level 4	0%	0%	0%
	Level 5	0%	0%	0%
Usual activities	Level 1	70%	43%	63%
	Level 2	15%	14%	15%
	Level 3	2%	36%	10%
	Level 4	7%	0%	5%
	Level 5	7%	7%	7%
Pain/discomfort	Level 1	33%	29%	32%
	Level 2	37%	36%	37%
	Level 3	26%	21%	25%
	Level 4	2%	14%	5%
	Level 5	2%	0%	2%
Anxiety/depression	Level 1	63%	50%	60%
	Level 2	26%	36%	28%
	Level 3	4%	7%	5%
	Level 4	4%	7%	5%
	Level 5	2%	0%	2%

Table 10 EQ VAS and index values at baseline. Mean (standard deviation) shown. *N* = 60. *p* estimated using independent samples t-test.

	Idiopathic	Crohn's Disease	All
EQ VAS	71.2 (21.1)	63.4 (20.2)	69.4 (21.0)
		$p = 0.22$	
EQ index	0.734 (0.259)	0.715 (0.214)	0.730 (0.247)
		$p = 0.80$	

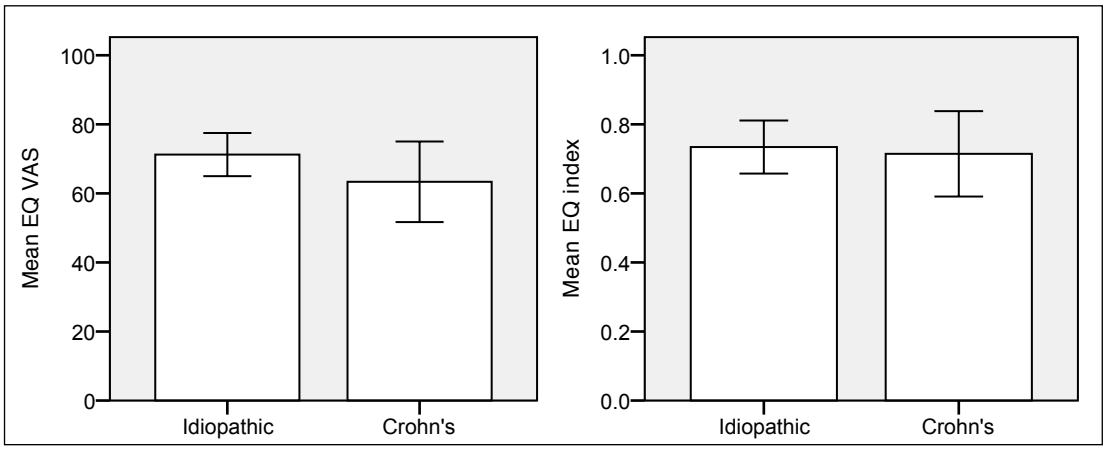

Figure 13 Mean EQ VAS and index at baseline. Error bars show 95% confidence intervals.

Operative Findings

Observations at operation revealed that 39% of patients had a seton *in situ*, reflecting that the fistulae were complex or refractory in a large proportion of this group (Table 11). Multiple fistulae were more prevalent in Crohn's disease participants as one would expect (23% *versus* 4%). The distribution of the different types of fistulae under the Parks' classification was the same between the groups, with trans-sphincteric being by far the commonest. Prevalence of a high primary tract and horseshoe extensions were also similar. However, supralevator extensions were statistically more common in Crohn's disease group (Fisher exact two-sided test $p = 0.02$). The prevalence of collections was significantly higher in the Crohn's group (92% *versus* 33%, $p < 0.001$). Rectal thickening was also significantly commoner in the Crohn's disease group (54% *versus* 2%), however this is expected given that proctitis is only a recognised feature of Crohn's disease.

Results of microbiological culture of intraoperative fistula specimens were available for 50 (82%) participants and yielded similar results for idiopathic and Crohn's disease participants (Table 12). The commonest were no growth, Coliforms, Enterococcus and Streptococcus species.

Table 11 Operative findings. *N* = 61. Fisher's Exact test is two-sided.

	Idiopathic	Crohn's Disease	All
Seton *in situ*	21 (44%)	3 (23%)	24 (39%)
Number of fistulae:			
Single unbranched	31 (65%)	3 (23%)	34 (56%)
Single branched	15 (31%)	7 (54%)	22 (36%)
Multiple	2 (4%)	3 (23%)	5 (8%)
		$p = 0.09$	
Parks' classification:			
Inter-sphincteric	7 (15%)	1 (8%)	8 (13%)
Trans-sphincteric	38 (79%)	10 (77%)	48 (79%)
Supra-sphincteric	3 (6%)	2 (15%)	5 (8%)
		$p = 0.54$	
High primary tract	15 (31%)	6 (46%)	21 (34%)
		$p = 0.34$	
Secondary tract(s):			
None	31 (65%)	4 (31%)	35 (57%)
Infralevator	14 (29%)	5 (38%)	19 (31%)
Supralevator	3 (6%)	4 (31%)	7 (11%)
		$p = 0.02$	
Horseshoe extension(s)	12 (25%)	5 (38%)	17 (38%)
		$p = 0.49$	
Collection(s)	16 (33%)	12 (92%)	28 (46%)
		$p < 0.001$	
Thickened rectum	1 (2%)	7 (54%)	8 (13%)
		$p < 0.001$	

Table 12 Bacterial isolates from culture of intraoperative fistula specimens. *N* = 50.

	Idiopathic	Crohn's Disease	All
No growth	18 (46%)	5 (45%)	23 (46%)
Coliforms	14 (36%)	4 (36%)	18 (36%)
Enterococcus	2 (5%)	1 (9%)	3 (6%)
Streptococcus	6 (15%)	1 (9%)	7 (14%)
Proteus	1 (3%)	0	1 (2%)
Morganella	0	1 (9%)	1 (2%)
Bacillus	0	1 (9%)	1 (2%)
Corneybacterium	0	1 (9%)	1 (2%)
Klebsiella	2 (5%)	0	2 (4%)
Staphylococcus	1 (3%)	0	1 (2%)
Actinomyces	1 (3%)	0	1 (2%)

Treatment Outcomes

The majority of patients (62%) had an operation aimed at symptom control only (curettage or seton insertion; Table 13). A curative procedure was only performed in one Crohn's disease participant, compared with 22 (45%) idiopathic disease participants. During the study, 30% received antibiotics. Almost half of the Crohn's disease participants received anti-TNF-α therapy. One patient with severe perianal hidradenitis suppurativa but without Crohn's disease also received anti-TNF-α therapy.

All participants completed the first follow-up at a median of 7 weeks (IQR = 6–11); 54 (89%) completed the second follow-up at a median of 29 weeks (25–37). By the end of the follow-up period only 12 (20%) had been discharged, 26 (43%) were being monitored or treated with drugs, while 23 (38%) were scheduled for further surgery. Proportionally less Crohn's disease patients were scheduled for further

surgery, reflecting the general strategy in this group, which favours adjuvant anti-TNF-α therapy. Of note, those scheduled for further surgery included those who had a seton inserted and required the next stage of their treatment, as well as those who had had an unsatisfactory outcome.

When stratified by treatment intent, 28 (73%) of those whose treatment intent was symptom control had control or resolution of their symptoms (Table 14). Treatment response was similar for idiopathic and Crohn's disease participants. For those whose treatment intent was cure, 13 (59%) had resolution of their symptoms. Comparisons between idiopathic and Crohn's disease groups for this treatment intent were not possible as only one Crohn's disease participant underwent a curative procedure.

When treatment intent and response were considered together, 41 (68%) had a satisfactory outcome by the end of the follow-up period (Table 15). Similar rates of satisfactory outcomes were observed between the idiopathic and Crohn's disease groups (see Section 2.13 for definitions).

Table 13 Clinical outcomes for participants after surgery. IQR, interquartile range; LIFT, ligation of inter-sphincteric fistula tract; 5-ASA, 5-aminosalicylic acid; TNF, tumour necrosis factor.

	Idiopathic	Crohn's Disease	All
Procedure performed:			
Curettage	4 (8%)	4 (31%)	8 (13%)
Seton	22 (46%)	8 (62%)	30 (49%)
Lay open	17 (35%)	1 (8%)	18 (30%)
Fistulectomy	3 (6%)	0	3 (5%)
LIFT	2 (4%)	0	2 (3%)
Medical treatment received (highest order):			
None	29 (62%)	2 (15%)	31 (52%)
Antibiotics	16 (34%)	2 (15%)	18 (30%)
5-ASA	0	1 (8%)	1 (2%)
Steroids	1 (2%)	0	1 (2%)
Immunosuppressants	0	2 (15%)	2 (3%)
Anti-TNF-α	1 (2%)	6 (46%)	7 (12%)
Management plan:			
Discharge	9 (19%)	3 (23%)	12 (20%)
Monitor	18 (38%)	2 (15%)	20 (33%)
Continue drugs	0	1 (8%)	1 (2%)
Escalate drugs	1 (2%)	4 (31%)	5 (8%)
Further surgery	20 (42%)	3 (23%)	23 (38%)

Table 14 Treatment response by treatment intent. Symptom control operations were curettage and seton insertion. Curative operations were lay open, fistulectomy and LIFT (ligation of inter-sphincteric fistula tract).

Treatment Intent and Response		Idiopathic	Crohn's Disease	All
Symptom control	None	1 (4%)	0	1 (3%)
	Inadequate	1 (4%)	1 (8%)	2 (5%)
	Transient	6 (23%)	1 (8%)	7 (18%)
	Controlled	17 (65%)	9 (75%)	26 (68%)
	Resolved	1 (4%)	1 (8%)	2 (5%)
	Total	26	12	38
Cure	None	0	0	0
	Inadequate	1 (5%)	0	1 (5%)
	Transient	4 (19%)	0	4 (18%)
	Controlled	3 (14%)	1 (100%)	4 (18%)
	Resolved	13 (62%)	0	13 (59%)
	Total	21	1	22

Table 15 Treatment outcomes with treatment intent taken into consideration. When symptom control was intended a treatment response of controlled or resolved was classified as satisfactory. When a cure was intended, a treatment response of resolved only was classified as satisfactory.

	Idiopathic	Crohn's Disease	All
Unsatisfactory	16 (34%)	3 (23%)	19 (32%)
Satisfactory	31 (66%)	10 (77%)	41 (68%)

Post-operative Perineal Disease Activity Index

We measured the PDAI at the first and second follow-up points in 57 (93%) and 48 (79%) participants respectively. Overall, the mean PDAI decreased from 6.23 (SD = 3.22) at baseline, to 5.00 (3.91) at first follow-up and to 5.56 (4.21) at second follow-up. Both groups had a similar post-operative decrease (Table 16 and Figure 14). In the idiopathic group, the 'type' domain showed the biggest change decreasing from 2.02 (0.15) to 1.34 (0.94). This is because many participants in this group had an uncomplicated lay open and thus went from having a fistula opening to a fissure or no perianal disease. Conversely, in the Crohn's disease group where insertion of a seton predominated, the 'type' domain showed little change. Rather in this group, there was a noticeable reduction in the discharge and induration domain scores. When divided by treatment outcome, the PDAI decreased in those who had a satisfactory outcome and increased in those who had an unsatisfactory outcome (Figure 14; Table 38 in Appendix 8).

Table 16 PDAI at baseline (t0), first follow-up 1 (t1) and second follow-up (t2). Mean (standard deviation) shown. Each domain range is 0–4, PDAI range is 0–20.

	Idiopathic			Crohn's Disease			All		
	t0	t1	t2	t0	t1	t2	t0	t1	t2
Discharge	1.37 (0.95)	1.18 (1.13)	1.32 (1.19)	1.86 (1.10)	1.71 (1.14)	1.17 (1.27)	1.48 (1.00)	1.31 (1.14)	1.28 (1.20)
Pain/restriction	1.09 (1.09)	0.81 (1.07)	0.86 (0.98)	1.50 (1.29)	1.64 (1.45)	1.36 (1.36)	1.18 (1.14)	1.02 (1.22)	0.98 (1.08)
Sexual function	0.59 (1.24)	0.58 (1.26)	0.70 (1.27)	0.43 (1.16)	0.86 (1.35)	0.91 (1.38)	0.55 (1.21)	0.65 (1.27)	0.75 (1.28)
Type	2.02 (0.15)	1.20 (0.93)	1.34 (0.94)	2.00 (0.78)	1.86 (0.66)	2.08 (0.90)	2.02 (0.39)	1.36 (0.91)	1.52 (0.97)
Induration	0.61 (0.74)	0.50 (0.76)	0.89 (1.20)	2.29 (1.27)	0.93 (1.27)	1.36 (1.21)	1.00 (1.13)	0.60 (0.92)	1.00 (1.21)
PDAI	5.67 (2.76)	4.35 (3.75)	5.14 (4.02)	8.07 (3.99)	7.00 (3.80)	7.00 (4.71)	6.23 (3.22)	5.00 (3.91)	5.56 (4.21)

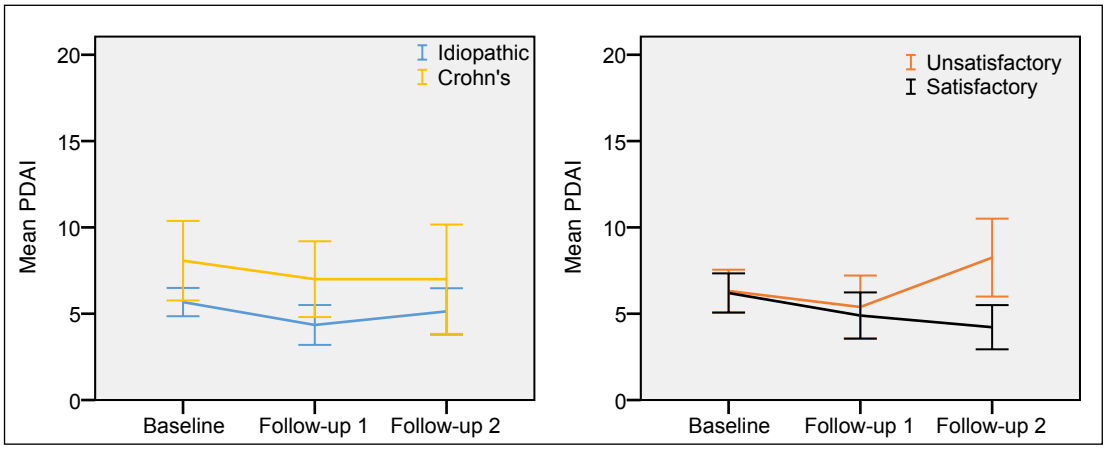

Figure 14 Mean PDAI from baseline to second follow-up by fistula type (left) and treatment outcome (right). Range 0 to 20. Error bars show 95% confidence interval.

Post-operative EQ-5D-5L

We measured the EQ-5D-5L at the first and second follow-up points in 56 (92%) and 48 (79%) participants respectively. The mean EQ VAS for both groups decreased between baseline and second follow-up. Both groups had a similar post-operative decrease (Table 17 and Figure 15). The mean EQ index for both groups also decreased between baseline and second follow-up.

We also observed changes in the individual EQ-5D-5L dimensions. Compared with baseline, there were increased levels for mobility at both follow-up points (Table 18). Mobility returned to baseline levels by the second follow-up for Crohn's disease but not idiopathic disease participants. Self-care levels worsened post-operatively, especially in the Crohn's disease participants, where the proportion reporting no restrictions (level 1) fell from 93% at baseline to 73% at follow-up. Difficulties in performing usual daily activities remained the same post-operatively in both groups. Pain and discomfort in the idiopathic disease group improved post-operatively but returned to baseline at the second follow-up. Conversely, in the Crohn's disease group, pain and discomfort increased post-operatively but then returned to baseline at the second follow-up. Anxiety and depression improved post-operatively in the idiopathic group, but increased in the Crohn's disease group.

When grouped by treatment outcome, the EQ VAS and EQ index improved in those who had a satisfactory outcome. In those who had an unsatisfactory outcome, these measures deteriorated (Figure 16; Table 39 and Table 40 in Appendix 8).

Table 17 EQ VAS and EQ index values at baseline (t0), follow-up 1 (t1) and follow-up 2 (t2). Mean (standard deviation) shown.

	Idiopathic			Crohn's Disease			All		
	t0	t1	t2	t0	t1	t2	t0	t1	t2
EQ VAS	71.2 (21.1)	70.0 (20.3)	68.2 (23.2)	63.4 (20.2)	61.1 (18.5)	62.3 (11.5)	69.4 (21.0)	67.8 (20.1)	66.8 (21.1)
EQ index	0.734 (0.259)	0.750 (0.295)	0.673 (0.268)	0.715 (0.214)	0.667 (0.241)	0.658 (0.261)	0.730 (0.247)	0.729 (0.283)	0.670 (0.264)

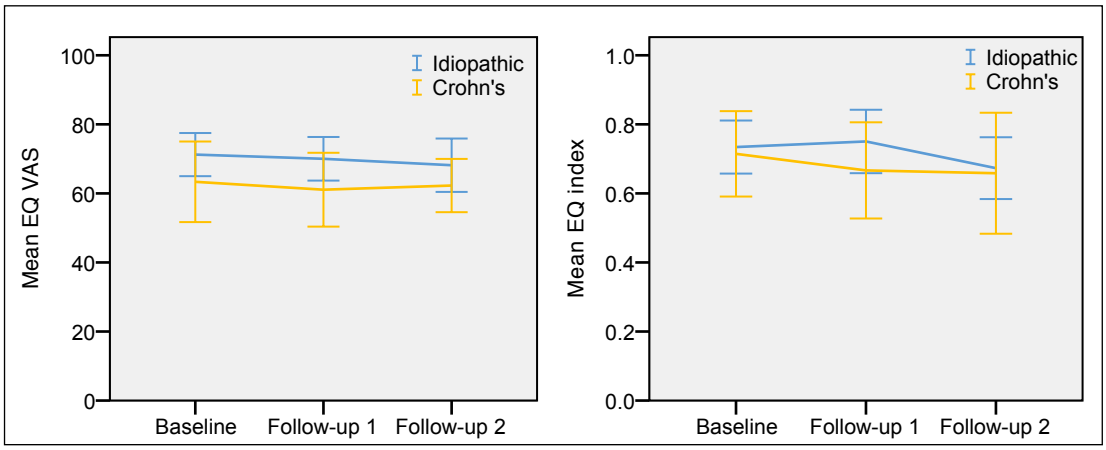

Figure 15 Mean EQ VAS and EQ index from baseline to second follow-up. Error bars show 95% confidence intervals.

Table 18 EQ-5D-5L dimensions at baseline (t0), first follow-up (t1) and second follow-up (t2). Percentage of participants reporting levels 1 to 5 (level 1 = no problems).

		Idiopathic			Crohn's Disease			All		
		t0	t1	t2	t0	t1	t2	t0	t1	t2
Mobility	Level 1	67%	69%	65%	57%	43%	55%	65%	63%	63%
	Level 2	20%	5%	11%	21%	14%	18%	20%	7%	13%
	Level 3	4%	14%	16%	21%	36%	18%	8%	20%	17%
	Level 4	7%	10%	8%	0%	7%	9%	5%	9%	8%
	Level 5	2%	2%	0%	0%	0%	0%	2%	2%	0%
Self-care	Level 1	89%	81%	89%	93%	71%	73%	90%	79%	85%
	Level 2	4%	12%	3%	7%	21%	18%	5%	14%	6%
	Level 3	7%	7%	3%	0%	7%	9%	5%	7%	4%
	Level 4	0%	0%	5%	0%	0%	0%	0%	0%	4%
	Level 5	0%	0%	0%	0%	0%	0%	0%	0%	0%
Usual activities	Level 1	70%	67%	73%	43%	50%	45%	63%	63%	67%
	Level 2	15%	5%	3%	14%	7%	9%	15%	5%	4%
	Level 3	2%	12%	14%	36%	29%	18%	10%	16%	15%
	Level 4	7%	12%	8%	0%	14%	18%	5%	13%	10%
	Level 5	7%	5%	3%	7%	0%	9%	7%	4%	4%
Pain/ discomfort	Level 1	33%	52%	30%	29%	14%	36%	32%	43%	31%
	Level 2	37%	17%	22%	36%	57%	9%	37%	27%	19%
	Level 3	26%	17%	19%	21%	29%	36%	25%	20%	23%
	Level 4	2%	14%	27%	14%	0%	18%	5%	11%	25%
	Level 5	2%	0%	3%	0%	0%	0%	2%	0%	2%
Anxiety/ depression	Level 1	63%	71%	70%	50%	43%	45%	60%	64%	65%
	Level 2	26%	7%	11%	36%	21%	0%	28%	11%	8%
	Level 3	4%	14%	5%	7%	21%	55%	5%	16%	17%
	Level 4	4%	7%	11%	7%	7%	0%	5%	7%	8%
	Level 5	2%	0%	3%	0%	7%	0%	2%	2%	2%

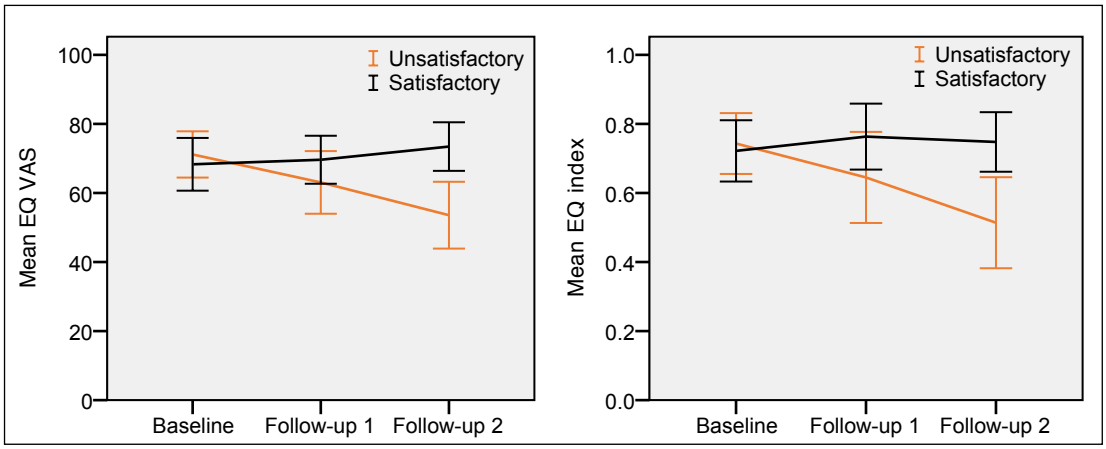

Figure 16 Mean EQ VAS and EQ index from baseline to second follow-up by treatment outcome. Error bars show 95% confidence intervals.

3.4 Discussion

We recruited a cohort of 61 consecutive participants with perianal fistula disease, carefully recording their clinical features at baseline and over a median follow-up period of 30 weeks. The age and sex distribution of the cohort was similar to previous studies (Marks and Ritchie 1977). All fistulae were chronic, with a median duration of disease prior to recruitment of 36 months. And at recruitment, participants were at varying stages of treatment, from those who had never had an operation, to those with a seton *in situ,* to those who had had up to four operations, including 10 (16%) who had previous surgery with curative intent. Simple and complex fistulae were also represented.

Overall, the cohort had a wide distribution of phenotypes including those with simple and complex, low and high, and primary and recurrent perianal fistula disease in both the idiopathic and Crohn's disease groups.

In contrast to many previous studies that focused on idiopathic or Crohn's disease fistulae separately (Table 3), we systematically recruited an adequate number of participants from both groups. The total of 61 recruited patients, including 13 with Crohn's disease, makes this the **largest study to date** to phenotype the disease across both groups in detail. A further strength of this study was that we thoroughly evaluated participants prospectively for signs of Crohn's disease. Thus, two

participants were diagnosed with Crohn's disease during the study period. Equally, we systematically excluded Crohn's disease in all participants in the idiopathic group. Participants in the Crohn's disease group were well characterized with all having imaging findings consistent with Crohn's disease, and all but one having histological features of Crohn's disease. The group showed a range of clinical phenotypes including those with and without abdominal complications and those who were and were not naive to anti-TNF-α treatment.

The PDAI was validated in a Crohn's perianal fistula population (Irvine 1995; Losco *et al.* 2009) but it has not yet been tested in an idiopathic group. The present study found that measurement of the PDAI in this group was feasible. At baseline, the PDAI was significantly higher in the Crohn's disease group, with a mean difference of 2.40 (95% CI = 0.52–4.28, $p = 0.01$). This may suggest that Crohn's perianal fistulae in general exhibit a higher degree of disease activity, which would fit with the commonly held clinical impression that Crohn's perianal fistulae are more severe than idiopathic.

In the post-operative follow-up, the PDAI decreased by a small amount. The mean difference between the idiopathic and Crohn's disease groups was maintained demonstrating stability of the index. When stratified by treatment outcome, the PDAI increased in those who had an unsatisfactory outcome, demonstrating the index's sensitivity to clinical changes. Furthermore, this deterioration was only evident at the second follow-up. This is consistent with clinical experience and probably reflects time to surgical healing.

The EQ-5D-5L is a generic measure of overall health and is commonly used in health economic evaluations. Data have been reported in many different diseases but not in perianal fistula disease. We found similar EQ index values in the idiopathic and Crohn's disease groups. Patients with Crohn's disease have a significant burden of disease. Whether their disease is active or quiescent, they have to cope with regular hospital appointments and investigations, blood tests, daily medication, dietary restrictions, and systemic symptoms. This commonly leads to a degree of

impairment of their lifestyle, aspirations and mood. The current results suggest (for the first time) that idiopathic fistula disease brings a burden of disease similar to Crohn's disease. Perianal fistulae cause chronic and unpredictable symptoms that precipitate multiple hospital visits and interventions. The symptoms are also socially embarrassing and impact upon the patient's confidence or ability to participate fully in day-to-day life and work. This was not previously appreciated.

The EQ VAS population norm in the UK for ages 35–44 years is 86.6 (Szende *et al.* 2014, pp.19–30). In our cohort, the EQ VAS at baseline was 71.2 (21.1) and 63.4 (20.2) for the idiopathic and Crohn's disease groups respectively. The EQ index population norm in England for ages 35–44 years is 0.891 (Szende *et al.* 2014, pp.19–30). In our cohort, the EQ index value at baseline was 0.734 (SD = 0.259) and 0.715 (SD = 0.214) for the idiopathic and Crohn's disease groups respectively. Other diseases which have a similar EQ index value include depression (0.732), ischaemic heart disease (0.738) and gastric ulcer (0.727) (Sullivan and Ghushchyan 2006).

A comparison of the bacterial isolates from culture of intraoperative fistula specimens has not been previously published. The present study found no growth in 46% of cases. The commonest isolates were both gut and skin-derived organisms: coliforms, enterococcus and streptococcus. Their distributions were similar between the groups.

Our findings between the idiopathic and Crohn's disease groups are summarised in Table 19. The baseline PDAI, a measure of disease activity (in perianal Crohn's disease), was significantly higher in the Crohn's disease group, mainly due to increased induration scores. At operation, there were more multiple fistulae, and significantly more supralevator extensions, collections and rectal thickening. To our knowledge, this is the first direct comparison that supports the current opinion that severe disease is more common in Crohn's perianal fistulae. However, severe disease was not exclusive to the Crohn's disease group. Both groups had fistulae on the full spectrum from simple to complex. We also observed many similarities between the groups. The baseline EQ VAS and EQ index scores, distribution of types by Park's

classification, prevalence of high fistulae and horseshoe extensions, post-operative PDAI, EQ VAS and EQ index trends were all similar. Therefore despite the evidence above that Crohn's perianal fistulae are often more severe than idiopathic fistulae, they are not phenotypically different.

Table 19 Summary of clinical data comparisons between idiopathic and Crohn's perianal fistulae. PDAI, perianal disease activity index; VAS, visual analogue score.

	Similarities	Differences
Baseline PDAI		Significantly higher PDAI in Crohn's disease
Baseline EQ-5D-5L	Similar EQ VAS and EQ index	
Morphology	Similar distribution of types by Parks' classification	More multiple fistulae in Crohn's disease
	Similar prevalence of high fistulae and horseshoe extensions	Significantly more supralevator extensions, collections and rectal thickening in Crohn's disease
Microbiological culture	Similar isolates	
Post-operative PDAI	Similar decrease in post-operative PDAI	
Post-operative EQ-5D-5L	Similar decrease in post-operative EQ VAS and EQ index	

Regarding the operations and outcomes, the majority of participants (38/61, 62%) received an operation aimed at symptom control only (curettage or seton insertion). This is consistent with current practice for complex fistulae where symptom control is paramount before operations with curative intent such as lay open are attempted. It also reflected the referral pattern to Professor Knowles' practice where many patients' fistulae were previously worsened by unsuccessful curative procedures. When the operation was with intent to control symptoms only, this was successful in the majority of participants (28/38, 73%). When the operation was with curative intent, this was successful in the majority (13/22, 59%). Thus overall, 41/61 (68%) had a satisfactory outcome, and this was similar between the idiopathic and Crohn's disease groups. Due to the heterogeneous distribution of the operative interventions

in this cohort, it is difficult to compare this outcome with other studies. However, the student recognises this to be in line with common clinical practice: it is frequent for a fistula operation to miss its therapeutic ambition and thus necessitate further intervention.

Limitations

We included patients from all stages of management, from those who were treatment-naïve, to those who had had multiple surgical procedures aimed at effecting a cure. This was to allow the study to recruit effectively within the time allowed. However this did increase the heterogeneity.

We only recruited patients who were planned for surgery for one reason or another. Therefore those with perianal fistula disease that was too mild to meet the threshold for surgery were excluded. This selection bias therefore limits the applicability of these data to this segment of the population. Furthermore, the threshold for surgery could have been different between the groups due to differing clinical strategies. If so, this selection bias may have introduced a difference between the groups.

The main study site was a tertiary referral centre. A more representative sample might have been achieved through multicentre recruitment. However, despite this, the recruited cohort of had participants with a wide distribution of disease phenotypes and an expected range of treatment outcomes. The sample size, although comparable to the majority of previous studies on the subject, was relatively small. This limited the capability of the statistical analysis.

Analysis of the outcomes following operative intervention was limited by the observational design. There was a varied mix of different interventions with either intention to control symptoms or cure, and only one patient in the Crohn's disease group underwent surgery with curative intent. The resultant heterogeneity made the clinical outcomes difficult to compare against contemporary data. Furthermore, the absence of observer blinding could have introduced a source of bias. However,

assessing the effect of operative intervention was not a primary objective of this study.

We only performed standard laboratory microscopy and cultures of intraoperative specimens. Although the results provide useful information, we acknowledge that there are more sophisticated methods of interrogating the microbiota in fistula tracts (see Tozer *et al.* 2015). However, a detailed investigation of perianal fistula microbiota was not a primary objective of this study.

3.5 Conclusions

This is the largest study to date to phenotype perianal fistula disease in detail in both idiopathic and Crohn's disease patients. Severe disease appears to be commoner in Crohn's perianal fistulae compared with idiopathic perianal fistulae. However, there were also many phenotypic similarities between the groups, and thus overall, the groups did not appear to be phenotypically distinct.

These data are also probably the most complete dataset to date using patient reported outcome measures, namely PDAI and EQ-5D, in these two groups. The PDAI appears to be a feasible, useful, stable and sensitive tool in measuring the disease activity in idiopathic as well as Crohn's perianal fistulae. Patients with idiopathic and Crohn's perianal fistulae have a similarly impaired quality of life, as measured by the EQ VAS and EQ index. Furthermore, the level of disease burden is akin to other significant chronic health conditions. Further validation studies are required and would lead to improved methodology in future perianal fistula disease research.

A comparison of the bacterial isolates from cultures of intraoperative specimens showed a wide range of organisms, which was similar in both groups.

4. CYTOKINE PROFILES

4.1 Introduction

Cytokines are a large group of proteins, peptides and glycoproteins that act as intercellular signalling molecules to regulate immunity and inflammation. They are produced by a broad range of immune and non-immune cells, and can act in an autocrine, paracrine and endocrine manner. They exert their actions by binding to cell-surface receptors, which in turn potentiate their action by the activation of various intracellular signalling pathways. These pathways may affect other cell-surface receptors and gene expression thereby stimulating or inhibiting cell behaviour and functions such as cell maturation, growth, adhesion and chemotaxis. There is much overlap and redundancy in the cytokine network.

Cytokine expression is a normal part of human physiology as the process of immunity and inflammation is necessary in both health and disease. In contrast to nearly all other tissues, the mucosa of the small and large intestine has continuous, low-grade (physiologic) inflammation, most likely because the intestine is exposed to a great antigenic load from luminal bacteria and a large variety of Toll-like receptor ligands (MacDonald *et al.* 2011).

Cytokine expression changes in response to an inflammatory or infectious stimulus. An appropriate response will handle and neutralise the threat in a proportionate manner before achieving resolution and restoring a normal state of health. However, cytokine expression can also be inappropriate or dysregulated, leading to diseases such as Crohn's disease. The precise aetiology of Crohn's disease is still unknown, but current theory suggests that it is the result of the interplay between three major factors – genetic susceptibility, intestinal microbiota and environmental factors – leading to a state of immune dysregulation (Kaser *et al.* 2010). Cytokines play a major part in this state of immune dysregulation, and many differences between Crohn's disease affected mucosa and healthy mucosa have been demonstrated. It is now generally accepted that there are significant differences in the expression of

many pro-inflammatory cytokines, such as IL-1, TNF-α, IL-6, IL-8, IL-12, IL-17 and IL-21, and anti-inflammatory cytokines, namely IL-10 and TGF-β (Műzes *et al.* 2012). These features of the cytokine network can be regarded as a molecular fingerprint that can be used as a way to identify the inflammatory phenotype of the affected tissue.

Little is known about the role of cytokines in perianal fistula disease. Kiehne *et al.* (2007) studied the perianal fistulae of 47 patients, excluding Crohn's disease. They obtained tissue from the fistula tract and, using immunohistochemistry, compared it to tissue from uninvolved perianal skin in the same patients and rectal mucosa in healthy control patients. IL-1β showed the most pronounced expression in the distal part of the fistula (8-fold increase compared with uninvolved perianal skin), while IL-8 was prominently expressed in the proximal part (63-fold increase). Expression of IL-6, IL-10 and TNF-α was low in the fistula. The perianal skin and rectal mucosa both showed very low levels of expression of all the analysed cytokines.

Ruffolo *et al.* (2007) studied cytokine concentrations in the blood of 12 patients with active perianal Crohn's disease and a low Crohn's disease activity index, 7 patients with indeterminate colitis after restorative panproctocolectomy with perianal complications, 7 patients with active intestinal Crohn's disease without perianal manifestations, and 19 healthy controls sex- and age-matched to the perianal Crohn's disease and the indeterminate colitis groups. Serum TNF-α and IL-6 concentrations were significantly higher in patients with perianal fistulas. Serum IL-1β and IL-12 concentrations were similar between the groups.

Following on from this, Ruffolo *et al.* (2008) studied the cytokine network in rectal mucosal biopsies, sampled endoscopically and mechanically homogenised, and serum samples. They included seventeen patients with perianal Crohn's disease, 7 patients with Crohn's disease without perianal involvement, and 7 healthy controls. Patients with idiopathic perianal fistula were not included. Mucosal and serum IL-6 concentrations were higher in the perianal Crohn's disease group, and the authors suggested that IL-6 contributes to the maintenance of perianal fistulae. Mucosal IL-

1β was also higher in perianal Crohn's disease and correlated with mucosal levels of TGF-β, TNF-α, and IL-6 and serum levels of TNF-α and IL-6. Mucosal TNF-α was the same among the three groups. The authors noted this was in contrast to previous studies, which showed an increase in mucosal TNF-α in Crohn's disease (Reimund *et al.* 1996), and could have been partially due to the patient sample. Mucosal IL-12 and TGF-β concentrations were the same among the three groups. Overall, IL-1β, IL-6 and TNF-α seemed to play an important role in perianal Crohn's disease. Van Onkelen *et al.* (2016) studied cytokine expression in 27 idiopathic perianal fistula tracts using immunohistochemistry. They also reported abundant expression of IL-1β. Expression of IL-8, IL-12p40 and TNF-α was also commonly observed.

In a cohort that included participants with idiopathic (n = 18) and Crohn's disease (n = 20) perianal fistulae, and healthy controls (n = 10), Tozer (2011) used multiplex methods to measure the concentrations of seven cytokines and chemokines in tissue culture supernatants: IL-2, IL-4, IL-6, IP-10 (interferon-gamma-inducible protein-10), TNF-α, IFN-γ and IL-17A. Biopsies from the fistula tract and rectum were studied. He found no significant differences in the concentrations of IL-2, IL-4, IL-6, IP-10, TNF-α and IFN-γ between the groups at either biopsy site. There was a difference between the healthy controls and Crohn's disease groups at the rectal biopsy site for IL-17A. The median concentration in the healthy controls was 3.01 pg/ml (IQR = 0.00–3.86) compared with 2.63 pg/ml (2.37–3.86) in the Crohn's disease group (p = 0.04, Mann-Whitney U test with Bonferonni correction). However, this result is of questionable significance because the investigators measured cytokines using the CBA Human Th1/Th2/Th17 Cytokine Kit (BD Biosciences, Europe), whose standard curve only reaches down to 20 pg/ml. Furthermore, the minimum detectable concentration for the IL-17A assay was 18.9 pg/ml. The reported concentrations of IL-17A were well below this level and as such were unlikely to be reliable and the subsequent hypothesis testing was therefore invalid. Accepting this important methodological consideration, Tozer did not find a difference in the cytokine concentrations between the three groups. In summary,

from these four studies, it appears that IL-1β, IL-6, IL-8, and TNF-α, may have an important role in perianal fistulae immunopathology.

As previously discussed in Section 0, it is believed that idiopathic and Crohn's disease fistulae differ in their pathogenesis and pathophysiology. Only one study by Tozer has tested this hypothesis with respect to a handful of cytokines, and no clear differences in the cytokine network were found. Building on this work, the current study aimed to more comprehensively describe the cytokine network in perianal fistula disease and compare the phenotypes between the idiopathic and Crohn's disease groups.

4.2 Methods

Participants and Biopsies

The methodology for recruitment of the study cohort and obtaining biopsy specimens (fistula tract, granulation tissue, internal opening and rectal mucosa) from participants is described in Chapter 2. In addition, we recruited further participants to serve as healthy controls for rectal biopsy tissue. The student screened consecutive patients from endoscopy lists for eligibility. We included adults undergoing lower gastrointestinal endoscopy for non-inflammatory conditions and excluded those who had a prior history, or upon endoscopy were suspected to have ileal, colonic or rectal inflammation, as well as those with a history of chemotherapy, radiotherapy, TB or HIV. The student approached potential participants asked for their consent to participate, which was recorded on a signed consent form, before obtaining a clinical history and recording the findings of the endoscopy. The endoscopist took three rectal biopsies using endoscopic cold biopsy forceps. The methods to collect, process and store these biopsies were identical to that described in Section 2.11 for all other samples.

Tissue Culture

All laboratory experiments were conducted in reference to a written protocol, to ensure the methods remained consistent (Appendix 4).

Working under a tissue culture hood at room temperature, the student arranged the samples reserved for tissue culture in a 24-well culture plate, covered each sample with 300 µl serum free HL-1 medium (Lonza, Cambridge, UK) containing 10 units/ml penicillin and streptokinase, 32 µg/ml gentamicin and 1 in 100 L-glutamine (Sigma-Aldrich, Gillingham, UK) using a filtered pipette (Figure 17), and then placed the covered culture plate in a controlled incubator at 37°C and 5% carbon dioxide for 24 hours. He then drew off the supernatants with a pipette and put them into mini Eppendorf tubes, labelled with participant ID and biopsy site, snap froze them on dry ice for 5 minutes and transferred them to -80°C freezer for storage. In a small number of cases where the tissue sample interfered with pipetting, the cell debris was removed by centrifugation at 12,000 rpm for 5 minutes.

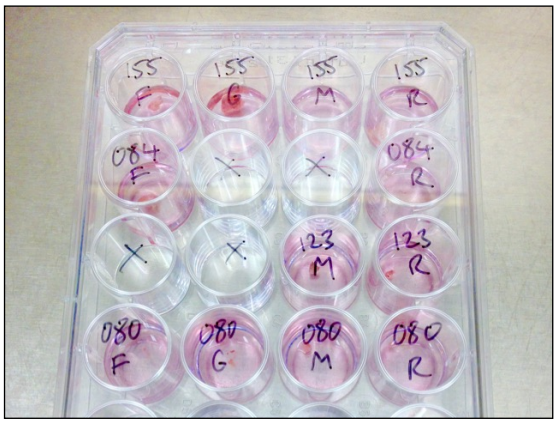

Figure 17 Tissue samples covered with culture medium in a 24-well culture plate.

Multi-analyte Panel

When all participant specimens had been processed and stored, the student performed quantification of the cytokine concentrations within the 24-hour tissue culture supernatant in batches using the 30-plex Milliplex MAP Human Cytokine/Chemokine Magnetic Bead Panel (EMD Millipore, Billerica, Massachusetts; Figure 18). This kit is based on the Luminex xMAP technology (see

Figure 19 for an explanation). We chose the Milliplex kit because there was excellent validation data that showed negligible cross-reactivity between the antibodies, high assay sensitivities, low intra- and inter-assay coefficients of variation (CV), and excellent spike recoveries (a measure of interference between the sample matrix and the assay).

The main advantage of using a multiplex system was that a large number of measurements could be made with the limited resources available. The main disadvantage of this approach was that super-sensitive assays could not be included in the multiplex because the standard curve needs to cover the same concentrations for all analytes and assay cross-reactivity can occur. We judged that multiplexing was best suited to the research objectives and chose a standard kit with 30 analytes to maximise the breadth of the cytokine profile being measured: EGF (epidermal growth factor), eotaxin, G-CSF (granulocyte-colony stimulating factor), GM-CSF (granulocyte-macrophage-CSF), IFN-α2, IFN-γ, IL-10, IL-12p40[†], IL-12p70, IL-13, IL-15, IL-17, IL-1RA (interlukin-1 receptor agonist), IL-1α, IL-1β, IL-2, IL-3, IL-4, IL-5, IL-6, IL-7, IL-8, IP-10, MCP-1 (monocyte chemoattractant protein-1), MIP-1α (macrophage inflammatory protein-1 alpha), MIP-1β, TNF-α, TNF-β, RANTES (regulated on activation normal T cell expressed and secreted), and VEGF (vascular endothelial growth factor).

[†] IL-12 is encoded by two separate genes. Protein synthesis results in an active heterodimer (p70), and a homodimer (p40).

Figure 18 Thirty-plex Milliplex MAP Human Cytokine/Chemokine Magnetic Bead Panel kit (EMD Millipore, Billerica, Massachusetts).

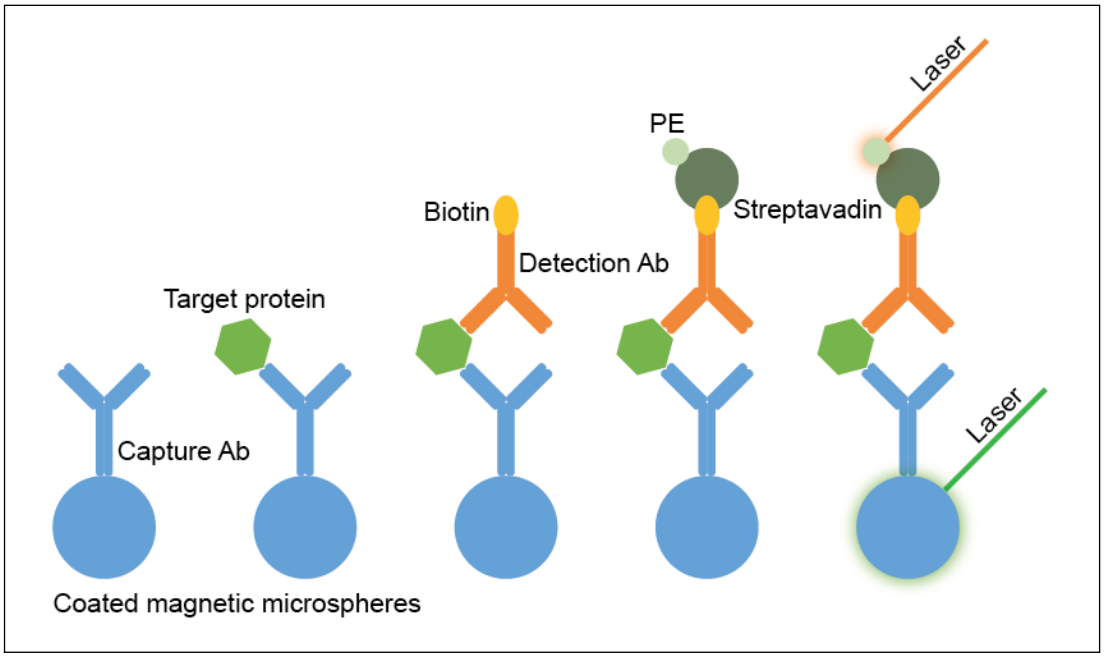

Figure 19 Principles of xMAP technology. Microspheres are colour-coded with two internal fluorescent dyes to create up to 100 distinct sets, each of which is coated by a specific capture antibody. Each bead captures its target protein in the test sample. Incubation with a biotinylated detection antibody, and a reporter molecule, streptavidin-phycoerythrin (PE) conjugate, completes the reaction. Within the automated analyser, the microspheres are passed through a laser, which excites the microsphere dyes. A second laser excites phycoerythrin, the fluorescent dye on the reporter molecule. Then, high-speed digital-signal processors identify each individual microsphere using its unique fluorescence code and then measure the fluorescence intensity of the reporter molecules. A standard curve is used to convert the fluorescence intensity is into an absolute concentration value.

The student thawed the tissue culture supernatant samples at room temperature and centrifuged them at 7,000 rpm for 5 minutes to remove any cell debris. After allowing the Milliplex kit to warm to room temperature, according to the instructions, he meticulously reconstituted the wash buffer, the two quality controls and the standards, using a one in five serial dilution to achieve decreasing concentrations (10,000, 2,000, 400, 80, 16 and 3.2 pg/ml). The background standard (0 pg/ml) comprised assay buffer only. He then sonicated, combined and vortexed the antibody-immobilized magnetic beads.

The student washed the 96-well plate according to the instructions and then laid it out with an automatic multi-pipette according to the plate plan (Table 20). Each well received 25 µl of either standard or control or sample, plus 25 µl of either the culture medium used previously (for standards and controls) or assay buffer (for samples), plus 25 µl of antibody-immobilized magnetic beads. Standards and controls were laid out in duplicate; samples were done in singlet. We considered running the samples in duplicate, however this was not possible due to limited funding. Furthermore, the intra-assay CV ranged between 1.5% and 3.4% with the exception of Eotaxin (7.2%, Appendix 6). We therefore judged that the level of variability from singlet testing was acceptable given the research objectives.

The student covered the completed plate with sealing tape and foil and incubated it overnight (16–18 hours) on a plate shaker at 500 rpm at 4°C. Then after allowing the plate to warm to room temperature for 30 minutes on the plate shaker at 500 rpm, he performed two manual wash cycles according to the instructions using wash buffer. During the decanting step of this process, a handheld plate magnet retained the magnetic beads within the wells. After this, the student added 25 µl of detection antibodies to each well in the plate, incubated it for 1 hour on a plate shaker at 500 rpm, then added 25 µl of streptavidin-phycoerythrin to each well before incubating for a further 30 minutes on a plate shaker at 500 rpm. After two more wash cycles, he resuspended the well contents in 100 µl of drive fluid and mixed them for 10 minutes on a plate shaker at 500 rpm. All these steps were performed at

room temperature. Sealing tape minimised evaporation during incubation and a foil cover prevented light degradation of the signal from the beads.

Table 20 Plate plan for Milliplex 96-well plate. QC, quality control.

	1	2	3	4	5	6	7	8	9	10	11	12
A	0 Standard	400 Standard	QC-2 Control	Sample	Sample	Sample	Sample	Sample	Sample	Sample	Sample	Sample
B	0 Standard	400 Standard	QC-2 Control	Sample	Sample	Sample	Sample	Sample	Sample	Sample	Sample	Sample
C	3.2 Standard	2,000 Standard	Sample	Sample	Sample	Sample	Sample	Sample	Sample	Sample	Sample	Sample
D	3.2 Standard	2,000 Standard	Sample	Sample	Sample	Sample	Sample	Sample	Sample	Sample	Sample	Sample
E	16 Standard	10,000 Standard	Sample	Sample	Sample	Sample	Sample	Sample	Sample	Sample	Sample	Sample
F	16 Standard	10,000 Standard	Sample	Sample	Sample	Sample	Sample	Sample	Sample	Sample	Sample	Sample
G	80 Standard	QC-1 Control	Sample	Sample	Sample	Sample	Sample	Sample	Sample	Sample	Sample	Sample
H	80 Standard	QC-1 Control	Sample	Sample	Sample	Sample	Sample	Sample	Sample	Sample	Sample	Sample

MAGPIX Measurement

The student prepared the MAGPIX multiplexing instrument (Luminex Corporation, Austin, TX) using the maintenance protocols on the xPONENT software. The probe was cleaned, checked for damage before calibrating its height. The system was cleaned by soaking it in 1M sodium hydroxide over the previous night. The instrument was then calibrated using the MAGPIX Calibration Kit (Luminex Corporation, Austin, Texas) and its performance was verified to within acceptable margins of error using the MAGPIX Performance Verification Kit (Luminex Corporation, Austin, Texas, Appendix 7).

The student programmed the xPONENT software to standardise plate processing and analysis. This specified the logistic 5P method to fit the standard curve to all the standards, a minimum required bead count of 50 per well, the analyte names and their bead regions, the known concentrations of the analytes in the standards and

controls, and participant identification numbers and biopsy sites for the sample wells. A second person double-checked all parameter entries.

After the above preparation, the MAGPIX system performed the programmed automated analysis. Halfway through the plate-reading, the system cleaned itself to reduce the build-up of protein and magnetic beads within the tubing and thus reduce the risk of encountering technical problems. The student reviewed the standard curves within the xPONENT software (Figure 20), and with each of the 30 analytes in turn, used the percentage recovery of the standards to determine the fit of each point to the standard curve. Points with a recovery less than 70% or greater than 130% were invalidated. Once all points lay within the acceptable percentage recovery range, the control results were reviewed to verify the standard curve fit.

For quality assurance, the student invalidated any analyte result that failed to reach a minimum bead count of 50. Protein or beads can adhere to the narrow channel within the instrument's probe and clog it causing low bead counts. Although a result is still obtainable, the reliability is lower. Therefore the MAGPIX system re-analysed the affected samples on the same plate to obtain the missing data.

Where the estimated concentration fell well outside the lower or upper limits of the standard curve, the xPONENT software returned a non-numerical value (e.g. < 3.2 pg/ml). To allow us to use these results with the rest of the continuous data, the student imputed either the minimum or the maximum result recorded for the affected analyte. For example, many results for EGF were "< 3.2 pg/ml". Imputation changed these values to 1.95 pg/ml, the lowest recorded EGF value. Results from all the plates were then imported into the study database.

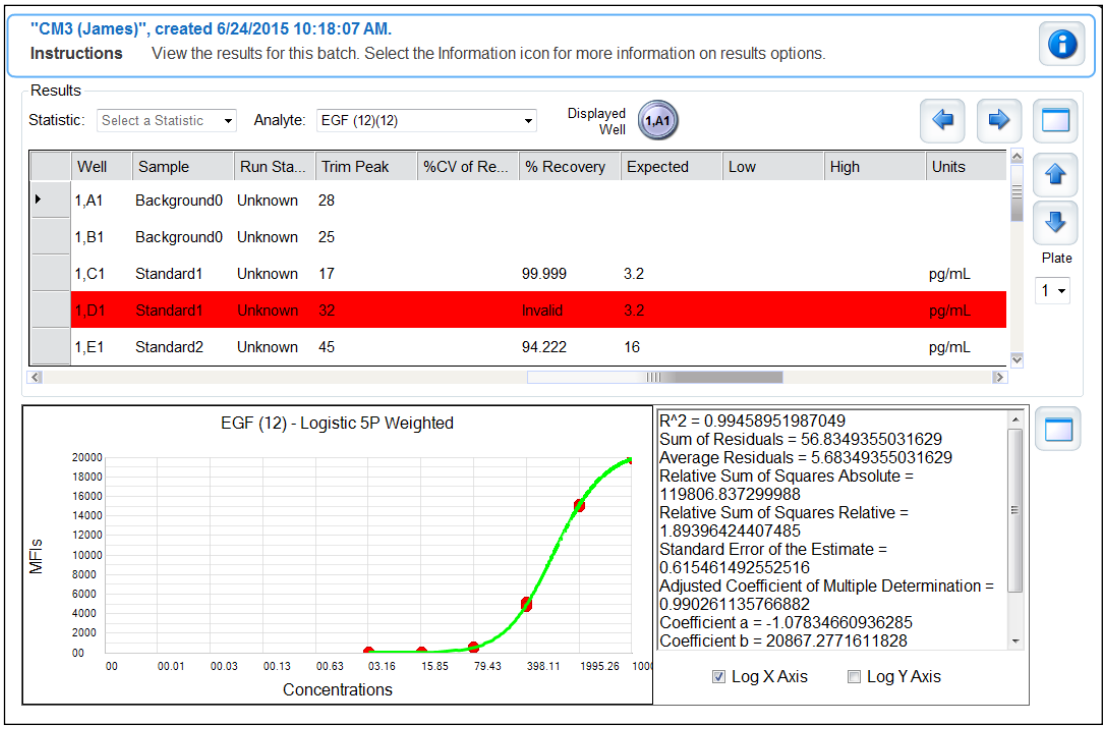

Figure 20 Adjusting the fit of the standard curve for EGF. The second Standard1 was invalidated because its result was outside the acceptable margin of error: the percentage recovery was > 130%. This process was repeated for each analyte.

4.3 Results

Specimens

Out of the 61 participants, one did not undergo biopsy due to unavailability of the student at the time. We approached nine healthy controls, however two declined and one was subsequently excluded due to ileal inflammation found during colonoscopy. Thus we recruited six healthy controls. Their characteristics are shown in Table 21. Five were female, and the mean age was 53.5 years (SD = 20.6).

Not all specimens were taken or analysed in each participant. Technical error caused the loss of four participants' specimens. Other problems were technical difficulty in taking the specimen, paucity of the tissue samples, and an absence of the tissue to be sampled (granulation tissue and internal opening sites only). A breakdown of the specimens analysed is shown in Table 22. Overall, a total of 202 specimens were available for cytokine quantification, specifically six control, 159 idiopathic and 37

Crohn's disease samples. With thirty cytokines measured per specimen, we made 6,060 measurements overall.

Table 21 Characteristics of healthy controls.

	Demographics	Indication	Endoscopic result
1	Female, 59 years	Survey for extra-mammary Paget's disease	Ileocolonoscopy revealed left sided diverticulosis only
2	Female, 71 years	Loose stools and bloating	Ileocolonoscopy revealed one small polyp only
3	Female, 30 years	Constipation	Normal flexible sigmoidoscopy
4	Male, 65 years	Anorectal bleeding	Normal flexible sigmoidoscopy
5	Female, 21 years	Constipation	Normal ileocolonoscopy
6	Female, 75 years	Iron deficiency anaemia	Normal colonoscopy

Table 22 Specimens processed for cytokine quantification. NA, not applicable.

	Healthy Control	Idiopathic	Crohn's Disease	All
Fistula Tract	NA	45	9	54
Granulation Tissue	NA	29	9	38
Internal Opening	NA	42	10	52
Rectal Mucosa	6	43	9	58
Total	6	159	37	202

Experiment Quality Control

All the specimens from the participants were processed using three Milliplex kits from the same batch, but due to manufacturing constraints, all the specimens from the healthy controls were processed using a different batch. We judged this to be acceptable as the inter-assay CVs were at most, 18% (Appendix 6).

We ran five plates, each with four quality controls for each of the 30 analytes. Thus there were 600 quality controls in total. The percentage recovery is the deviation of the measured analyte concentration from the expected concentration with 100% representing perfect agreement. As mentioned in the methods, a percentage recovery in the range 70–130% was acceptable. Eleven fell below this range and 22 fell above it. Thus 567 (95%) of the quality controls fell within the acceptable range. Over the 150 analytes (30 analytes by 5 plates), 17 had one out of four controls fail, eight had two out of four controls fail, and none had more than two controls fail.

Low bead counts affected 3.3% of results (N.B. in this context, result refers to a single concentration value, e.g. the EGF concentration for a fistula tract specimen from a single participant). After the student re-analysed the affected samples, only 0.03% of results remained invalidated.

The data comprised 3.78% of results returned as < 3.2 pg/ml, 0.06% as > 2,000 pg/ml, and 1.14% as > 10,000 pg/ml. Thus overall, 4.99% of results were non-numerical and required adjustment using the imputation rules described above. The cytokines that had > 5% of results imputed with the minimum value were eotaxin (14%), IL-3 (42%), and MIP-1α (6%). G-CSF had 35% of results imputed with the maximum value.

The data comprised 5.04% of results returned below the minimum detectable concentration for the assay. However, overall median concentrations only fell below the minimum detectable level for IL-3 (fistula tract-Crohn's disease, granulation tissue-idiopathic, rectal mucosa-all).

Cytokine Concentrations

All the four specimens (fistula tract, granulation tissue, internal opening and rectal mucosa) yielded significant levels of IL-1RA, IL-6, MCP-1, RANTES and VEGF, with very high levels of G-CSF and IL-8 (Table 23). Other cytokines were also moderately abundant in the granulation tissue, internal opening and rectal mucosa specimens: GM-CSF, IFN-α2, IP-10, MIP-1α and MIP-1β. The results also showed

that granulation tissue, compared to the other specimen sites, yielded higher concentration of G-CSF, IL-10, IL-1RA, and IL-1β.

We observed significant differences in just 2 instances. The IL-12p70 concentration at the internal opening specimen site was higher in the Crohn's disease group (Figure 21). The median concentration was 28.3 pg/ml (IQR = 7.4–50.1) compared with 7.4 pg/ml (4.6–12.7) in the idiopathic group. The median difference was 19.7 pg/ml (Hodges-Lehman, 99% CI = 0.2–40.4; Mann-Whitney U, $p = 0.008$).

The IL-1RA/IL-1β ratio was significantly lower in the Crohn's disease group at the internal opening specimen site (Figure 22; Table 45 in Appendix 8). The median ratio was 3.3 (1.8–7.6) compared with 19.0 (4.3–51.2) in the idiopathic group. The median difference was 15.0 (99% CI = 0.4–50.5, $p = 0.008$).

There were no significant differences in any of the other cytokine concentrations between the idiopathic and Crohn's disease groups at the four specimen sites (Figure 23; Table 41, Table 42, Table 43 and Table 44 in Appendix 8). There were also no significant differences in the cytokine concentrations between the rectal mucosa of healthy controls and Crohn's disease groups (Figure 24; Table 46 in Appendix 8).

Table 23 Median cytokine concentrations (pg/ml). HC, healthy controls; CD, Crohn's disease.
*** statistically significant difference $p < 0.01$.**
‡ result below the minimum detectable concentration for the assay.

	Fistula Tract		Granulation Tissue		Internal Opening		Rectal Mucosa		
	Idiopathic	CD	Idiopathic	CD	Idiopathic	CD	HC	Idiopathic	CD
EGF	14.7	17.4	34.8	28.7	20.5	28.2	20.7	22.7	20.8
Eotaxin	13.2	10.7	14.6	11	18	21.1	20.9	17.2	14.2
G-CSF	950.6	4693.6	22402.3	22402.3	7214.2	22402.3	2638.8	3139.5	1605.1
GM-CSF	14	30	69.3	128.5	34.5	203.6	32.1	31.2	30.2
IFN-α2	19.7	16.8	28.2	22.1	37.4	41.1	40.5	49.7	39
IFN-γ	4	5.7	12.3	28.9	7.4	12.6	11.6	8.4	9
IL-10	24.7	29.2	321.5	155.2	55.6	67.7	17.5	13.5	7.2
IL-12p40	12.4	8.8	24	21.7	19.2	29.1	33.3	37.2	28.7
IL-12p70	3.7	2.5	5.7	8.1	7.4*	28.3*	16.2	18.1	15.9
IL-13	3.9	5.2	6	6	8	7.5	5.9	6.9	4
IL-15	3.7	4.3	8.8	7.9	5	7.8	5.9	6.8	7.6
IL-17A	4.1	4.3	13.3	18.4	4.1	7.4	4.1	5.5	4
IL-1RA	31.8	244.5	741	541.7	516.1	128.3	79.6	72	84.9
IL-1α	10.5	24	140.5	51	24.3	17.4	10.8	11.4	13.7
IL-1β	4.4	4.3	302.2	263.3	20.2	58.3	22.7	20.6	15.5
IL-2	1.9	2.3	2.8	2.5	3.7	5.7	6.6	8.4	5.8
IL-3	1.15	0.32‡	0.04‡	0.88	1.20	1.09	0.32‡	0.04‡	0.04‡
IL-4	9.9	9.1	12.1	11.1	17.3	22.7	22.2	18.9	14.9
IL-5	1.1	2	2.5	2.3	2.1	3.2	2.8	2.7	1.9
IL-6	324.6	576.5	646.4	1010.2	6362.3	6181.2	580.6	638.3	427
IL-7	11	9.5	13.4	10.3	18.5	21	21.1	19.9	17.8
IL-8	8063.7	7996.7	8281.7	7863.6	10811.1	11902.6	6442.8	6002.3	4415.4
IP-10	16	22.8	30.3	116	26.6	33.4	23.9	30.5	29
MCP-1	540.7	709.8	744.1	678.6	1296.8	3390.3	1642.1	1089.2	741.4
MIP-1α	16.3	15.6	61.6	43.8	66.6	93.9	58.2	43	31.4
MIP-1β	9.9	14.9	34.6	32.5	23.4	36.8	22.5	26.9	17.9
RANTES	324.4	529.6	801.4	814.5	169.3	233.8	49	94.9	84.9
TNF-α	8.4	9.7	28.3	16.5	30.9	25	20.2	18.6	12.6
TNF-β	1.8	2.5	3.2	2.8	3.2	5.2	3.8	3.8	3.4
VEGF	82.2	107.1	124.4	104.5	173.5	284.3	230.7	225.8	159.4

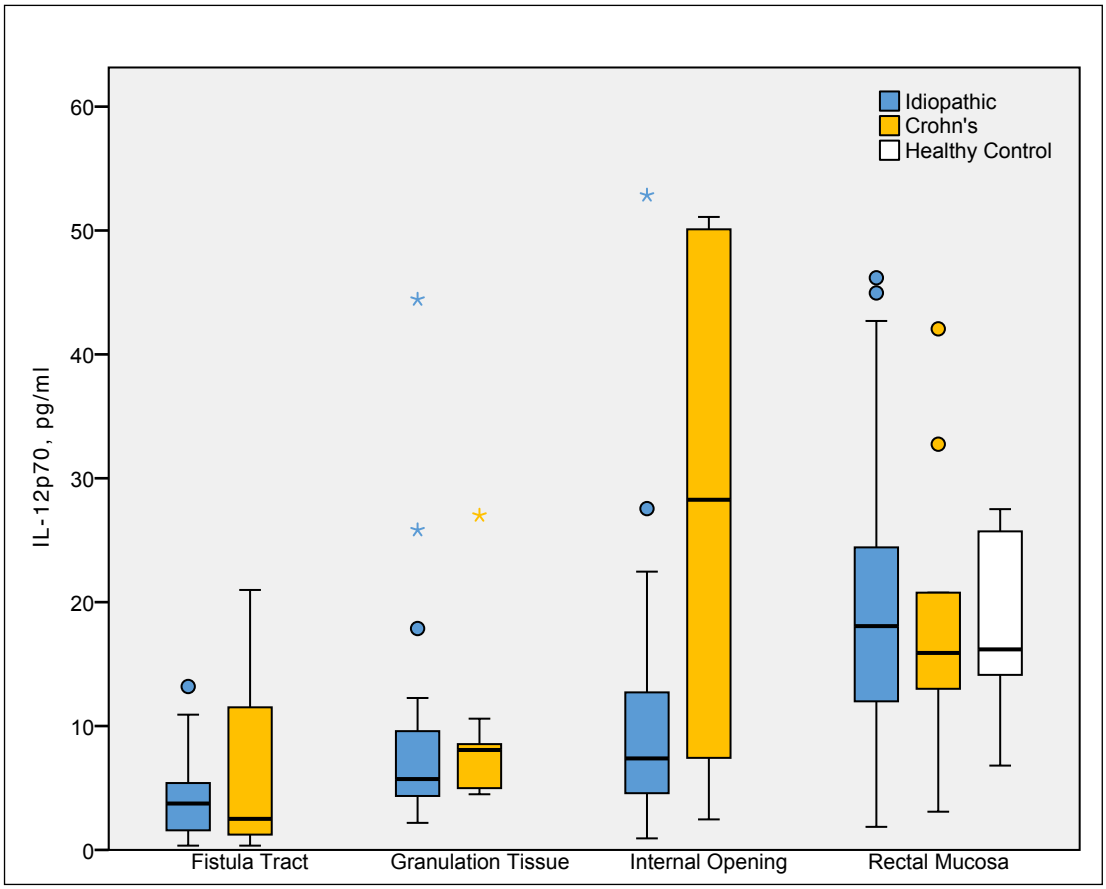

Figure 21 Boxplot for IL-12p70 concentrations. Median difference at the internal opening, 19.7 pg/ml (Hodges-Lehman, 99% CI = 0.2–40.4; Mann-Whitney U, $p = 0.008$). Circle marker, outlier within 1.5 x interquartile range (IQR); Star marker, outlier outwith 1.5 x IQR. One outlier not shown to limit y-axis scale.

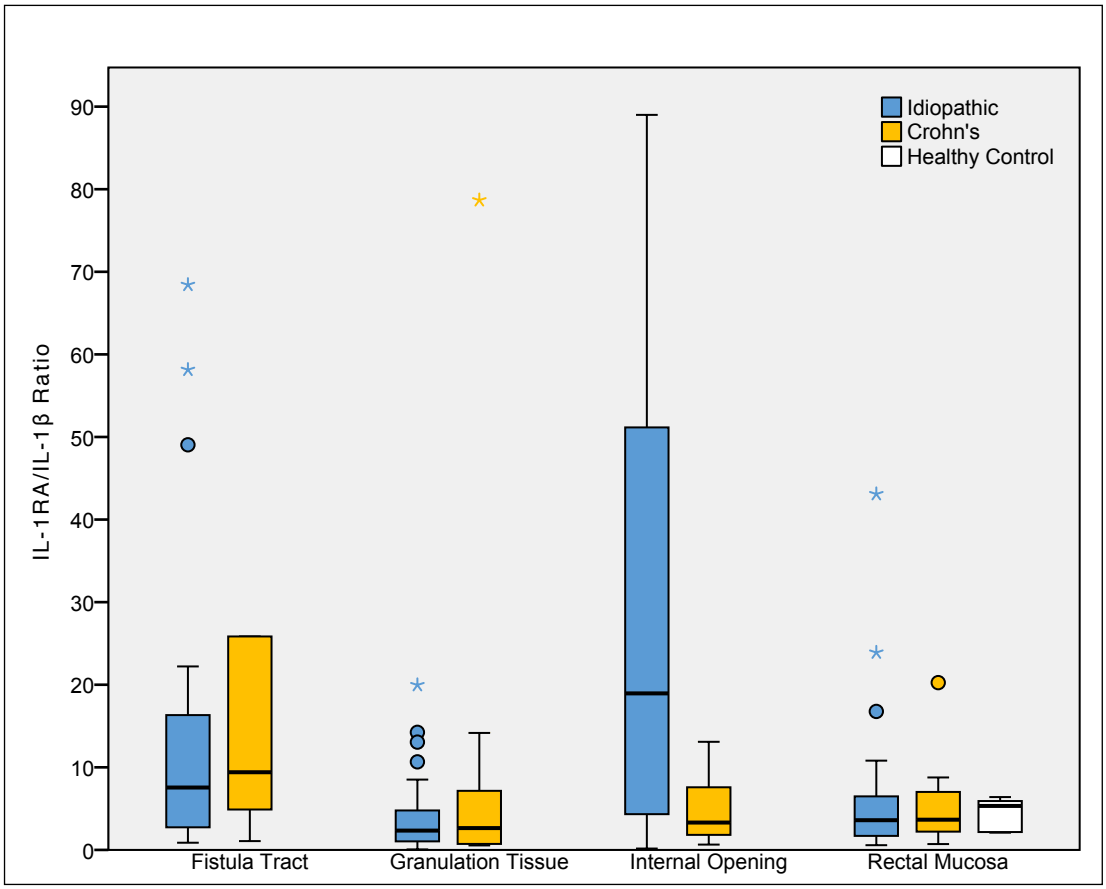

Figure 22 Boxplot for IL-1RA/IL-1β ratios. Median difference at the internal opening, 15.0 (Hodges-Lehman, 99% CI = 0.4–50.5; Mann-Whitney U, $p = 0.008$). Circle marker, outlier within 1.5 x interquartile range (IQR); Star marker, outlier outwith 1.5 x IQR. Fourteen outliers not shown to limit y-axis scale.

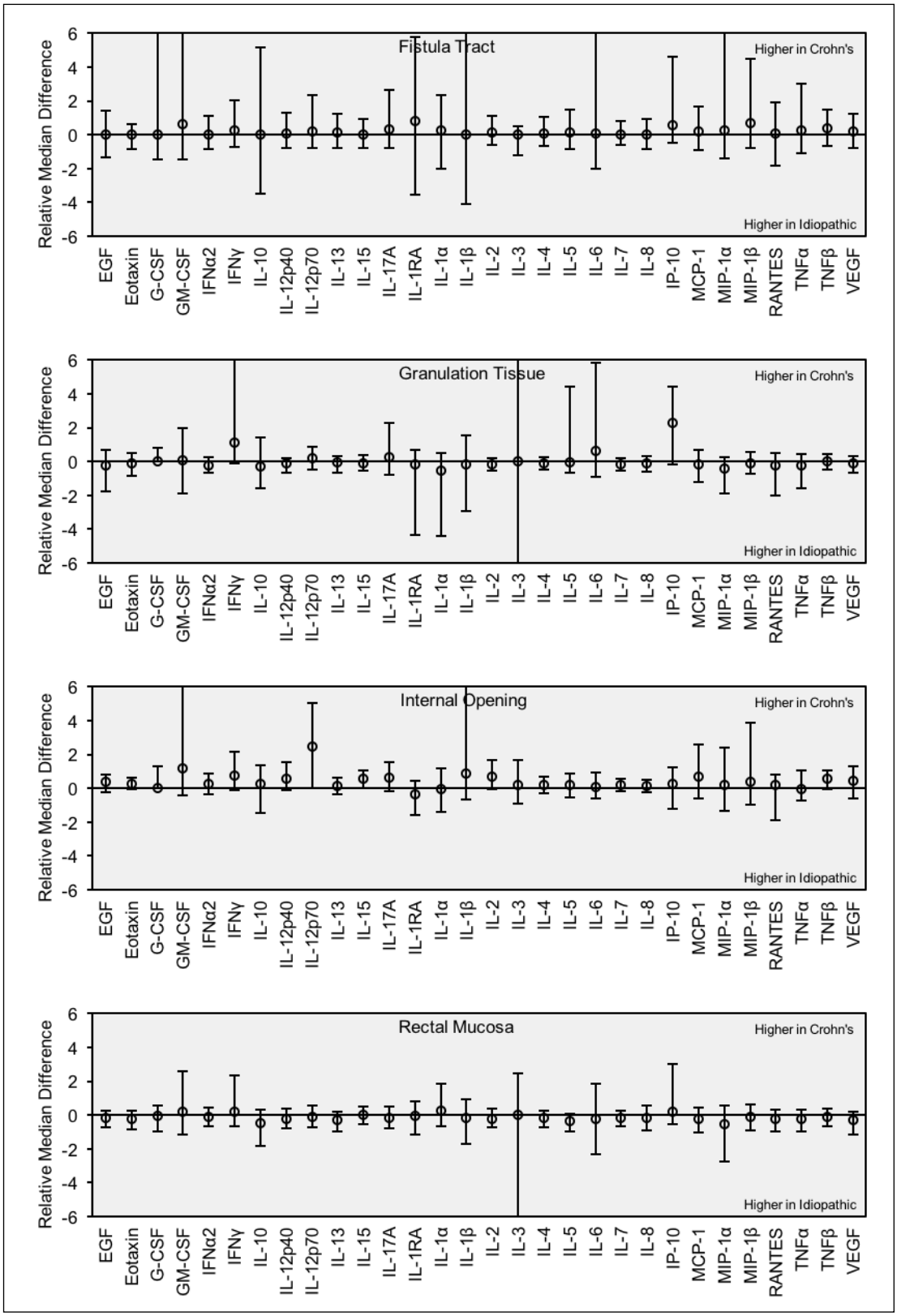

Figure 23 Relative median difference in cytokine concentrations between idiopathic and Crohn's disease groups. Error bars show 99% confidence intervals estimated using Hodges-Lehman method.

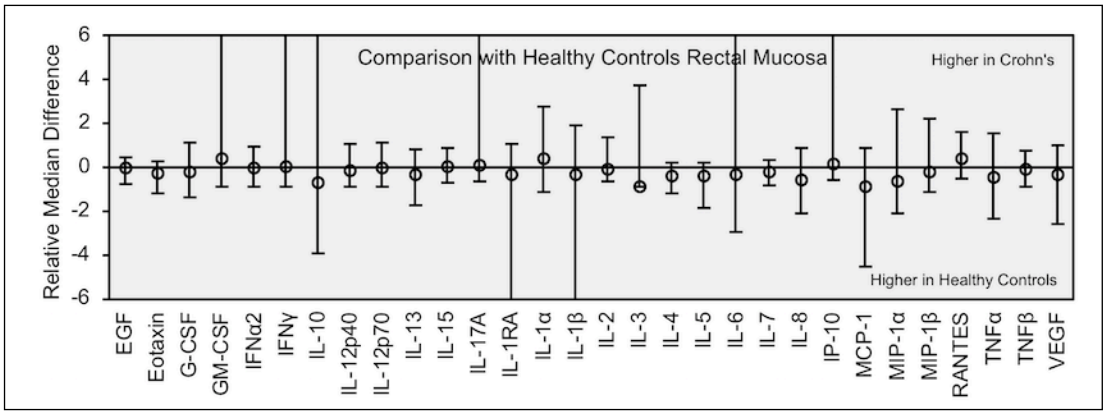

Figure 24 Comparison with healthy controls. Rectal mucosa relative median difference in cytokine concentrations between healthy controls and Crohn's disease groups. Error bars show 99% confidence intervals estimated using Hodges-Lehman method. See Appendix 8 for absolute values.

4.4 Discussion

This study aimed to describe the cytokine profile in perianal fistula disease and compare profiles between the idiopathic and Crohn's disease groups in order to test the hypothesis that perianal fistulae of these types differ in their pathophysiology, specifically immunopathology.

To reiterate the findings from Chapter 3, the cohort had a wide distribution of clinical and anatomical phenotypes including those with simple and complex, low and high, and primary and recurrent perianal fistula disease in both the idiopathic and Crohn's disease groups. Therefore these laboratory data can be considered to fairly encompass the breadth of the disease under study. They are also probably the most substantial to date in terms of breadth of cytokines measured for a cohort of participants with both idiopathic and Crohn's perianal fistula disease. We used a well-validated multiplex method to efficiently make thousands of accurate quantitative measurements. Several quality control features, such as data re-entry, experimental controls and calibration procedures, ensured the results were accurate and reliable. Analysis used medians and interquartile ranges to allow for skewed data in several of the analytes, 99% confidence intervals to allow for multiple hypothesis testing, and non-parametric methods to avoid problems with small subgroup numbers.

We systematically measured the concentrations of 30 cytokines (EGF, Eotaxin, G-CSF, GM-CSF, IFN-α2, IFN-γ, IL-10, IL-12P40, IL-12P70, IL-13, IL-15, IL-17, IL-1RA, IL-1α, IL-1β, IL-2, IL-3, IL-4, IL-5, IL-6, IL-7, IL-8, IP-10, MCP-1, MIP-1α, MIP-1β, TNF-α, TNF-β, RANTES, and VEGF) in the supernatant of a standard tissue culture of specimens. With 202 specimens analysed, this resulted in a total of 6,060 measurements. The median concentrations of each cytokine were compared between the disease groups for each of the four biopsy sites.

We observed significant differences between the groups in only two instances: IL-12p70 and the IL-1RA/IL-1β ratio, both at the internal opening specimen site. The relevance of these findings is discussed.

IL-12 is a proinflammatory cytokine produced by dendritic cells and macrophages. It comprises two subunits: IL-12p35 and IL-12p40. On its own, the p40 subunit acts as a natural antagonist.‡ The IL-12 receptor is found mainly on T cells and natural killer cells. In its combined form as IL-12p70, the cytokine induces the production of IFN-γ, promotes T helper 1 cell differentiation and forms a link between innate resistance and acquired immunity (Trinchieri 2003). IL-12 plays an important role in Crohn's disease pathogenesis. The expression of IL-12 is upregulated in Crohn's disease mucosa (Monteleone *et al.* 1997). The present study found significantly higher concentrations of IL-12p70 at the internal opening in the Crohn's disease group. This may suggest a similarly important role for IL-12 in Crohn's perianal fistula and may represent a difference in its pathophysiology compared with idiopathic perianal fistula disease. However, these data do need to be interpreted with caution, as the 99% CI came very close to zero. Further studies in the role of IL-12 in perianal fistula are therefore required.

---

‡ When measuring IL-12p40, it needs to be taken into account that the p40 subunit is shared with IL-23, another member of the IL-12 family (Oppmann *et al.* 2000).

The IL-1α and IL-1β mediate immune and inflammatory responses. They are primarily produced by tissue macrophages, monocytes, fibroblasts, and dendritic cells and enable transmigration of immune cells to the site of inflammation. Dionne *et al.* (1998) reported concentrations of IL-1 cytokines in colonic mucosa explant supernatants after 18 hours culture in healthy controls, Crohn's disease patients' inflamed mucosa, and Crohn's disease patients' uninflamed mucosa groups. IL-1β concentration was low in healthy controls and in uninflamed Crohn's disease, and increased in inflamed Crohn's disease. The present study also found low concentrations in the all groups at the fistula tract, internal opening and rectal mucosa sites, with no significant differences between the groups. This might suggest that Crohn's perianal fistula (and idiopathic for that matter) differ from inflamed Crohn's disease mucosa in their IL-1 mediated inflammatory response. For the receptor antagonist, IL-1RA, Dionne *et al.* (1998) did not find any significant difference in its culture supernatant concentration between the groups. This is also borne out by the present study's data.

However, when studying the IL-1RA/IL-1β ratio, Dionne *et al.* (1998) found the ratio was lower in the inflamed Crohn's disease group, compared to the healthy controls and uninflamed Crohn's disease groups. We made similar findings at the internal opening specimen site in that the ratio was significantly lower in the Crohn's disease group compared to the idiopathic group.

The current data also revealed that the concentrations of G-CSF, IL-10, IL-1RA, and IL-1β found at the granulation tissue sites were higher relative to the other three sites. This is likely to be a reflection of the acute on chronic inflammatory microenvironment of the fistula tract granulation tissue, which contains histiocytes and capillaries, neutrophils and lymphocytes (Bataille *et al.* 2004).

There were no significant differences between the groups for any of the other measurements. When the cytokine concentrations from the rectal mucosa of Crohn's disease participants were compared with the healthy controls, again no significant differences were found. The above comparisons are summarised in Table 24.

As discussed in Section 1, Crohn's disease is characterised by chronic inflammation. At the molecular level, in general, pro-inflammatory cytokines and chemokines are upregulated and anti-inflammatory cytokines and chemokines are suppressed. Within the currently accepted theory, idiopathic perianal fistulae do not have an underlying dysregulated inflammation. Therefore, we would expect this contrast to be evident in the cytokine and chemokine profiles. However, our data is striking in its lack of demonstrable differences between the two groups and therefore challenges the current thinking that they these groups are immunologically separate.

Table 24 Summary of cytokine profile data comparisons between idiopathic and Crohn's perianal fistulae.

	Similarities	Differences
Cytokine concentrations	Similar concentrations of 27 cytokines at all four biopsy sites (EGF, eotaxin, G-CSF, GM-CSF, IFN-α2, IFN-γ, IL-10, IL-12p40, IL-13, IL-15, IL-17, IL-1α, IL-2, IL-3, IL-4, IL-5, IL-6, IL-7, IL-8, IP-10, MCP-1, MIP-1α, MIP-1β, TNF-α, TNF-β, RANTES and VEGF)	Significantly higher IL-12p70 concentration at internal opening in Crohn's disease Significantly lower IL-1RA/IL-1β ratio concentration at internal opening in Crohn's disease

Comparison with Prior Data

Two previous studies described in the introduction provided comparable data. In comparison with Tozer's measurements, we found similar concentrations of the corresponding cytokines at the corresponding biopsy sites within the same study groups (Table 25).

A comparison with Ruffolo *et al.* (2008) is shown in Table 26. However this is interpreted cautiously as their laboratory methods differed to ours. Instead of analysing the supernatant from 24-hour tissue culture, they homogenized the fresh frozen biopsies before directly measuring the cytokine concentrations using enzyme-linked immunosorbent assays. Compared with Ruffolo *et al.,* we found lower absolute concentrations of rectal IL-12 in both healthy controls and Crohn's disease participants. However, like Ruffolo *et al.*, there was no statistically significant

difference between the Crohn's disease and healthy controls groups. For IL-1β, Ruffolo *et al.* found that concentrations were low in healthy rectal mucosa and significantly higher in Crohn's disease. Contrastingly, we found no significant difference. For IL-6, we measured much higher absolute concentrations in the rectal mucosa compared with Ruffolo *et al.* And for TNF-α, we found rectal mucosal concentrations lower than in Ruffolo *et al.* So overall, the results from this study differ from Ruffolo *et al.* but it is difficult to comment why as it could just be a reflection of the different laboratory methods used, especially considering that the present study's results are congruent with Tozer, as described above.

Table 25 Comparison of cytokine median concentrations, pg/ml (IQR) with Tozer (2011).

	Fistula Tract				Rectal Mucosa	
	Idiopathic		Crohn's Disease		Healthy Controls	
	This study	Tozer 2011	This study	Tozer 2011	This study	Tozer 2011
IL-2	1.9 (1.2–2.7)	1.9 (1.8–2.5)	2.3 (1.0–3.5)	2.0 (1.8–2.3)	6.6 (5.7–7.1)	2.3 (2.0–2.6)
IL-4	9.9 (5.1–12.8)	1.9 (1.9–2.1)	9.1 (5.8–18.0)	1.9 (1.8–2.0)	22.2 (17.2–27.4)	1.9 (1.5–2.1)
IL-6	325 (83–1977)	1201 (250–4692)	577 (29–2302)	334 (106–1345)	581 (497–1689)	350 (283–1213)
IP-10	16.0 (6.7–28.4)	2.8 (1.4–6.2)	22.8 (17.2–80.2)	1.9 (1.6–4.1)	23.9 (21.4–27.7)	2.0 (1.5–2.8)
TNF-α	8.4 (3.2–21.0)	2.9 (2.1–6.6)	9.8 (4.1–29.8)	1.6 (1.2–2.7)	20.2 (13.9–35.6)	2.2 (1.7–2.9)
IFN-γ	4.0 (1.6–7.3)	4.0 (1.7–7.5)	5.7 (1.1–10.9)	1.4 (1.2–1.7)	11.6 (8.2–12.0)	1.5 (1.4–2.5)
IL-17A	4.1 (2.0–6.3)	3.4 (3.1–4.6)	4.3 (1.1–12.7)	2.6 (2.4–3.9)	4.1 (3.3–4.5)	3.0 (0.0–3.9)

Table 26 Comparison of cytokine median concentrations, pg/ml (IQR) with Ruffolo (2008). Note that Ruffolo used a different method of cytokine quantification.

	Rectal Mucosa			
	Healthy Controls		Crohn's Disease	
	This Study	Ruffolo 2008	This Study	Ruffolo 2008
IL-12	16.2 (14.1–25.7)	40 (16–82)	15.9 (13–20.8)	40 (13–140)
IL-1β	22.7 (11.9–74.7)	0.4 (5–64.4)	15.5 (9.7–35.7)	46.3 (3.4–641)
IL-6	580.6 (496.9–1689.3)	2 (2–10.9)	427 (161.7–1314.6)	2.2 (2–58.8)
TNF-α	20.2 (13.9–35.6)	32.2 (28.4–264)	12.6 (11–16.5)	33.3 (26.7–1000)

Comparison with Current Theory

Across all specimens and groups, we found significant levels of G-CSF, IL-6, IL-8, MCP-1, RANTES and VEGF.

G-CSF is produced by macrophages, endothelium and other immune cells. It is an important pro-inflammatory mediator, mediating the proliferation and maturation of neutrophils in the bone marrow, and survival, adhesion and phagocytosis of mature neutrophils in the blood. Expression of the G-CSF receptor has been demonstrated on a wide variety of haemopoetic cells, including monocytes and lymphocytes. G-CSF in perianal fistula disease has not been previously reported. Considering the chronic inflammatory nature of all perianal fistulae, which have been shown to contain T cells, macrophages, B cells and monocytes (Bataille *et al.* 2004), our findings regarding G-CSF are consistent.

In our data, IL-6 concentrations were high. Atreya *et al.* (2000) demonstrated that IL-6 is a principle cytokine produced by macrophages in the lamina propria of the gut wall. Production of IL-6 and expression of the IL-6 receptor is increased in

inflammatory bowel disease. Stimulation of the IL-6 receptor in T cells causes activation of the STAT-3 pathway, preventing apoptosis. Thus IL-6 promotes a pro-inflammatory phenotype. Serum IL-6 is higher in Crohn's disease patients with perianal fistulae compared with Crohn's disease patients without perianal fistulae and healthy controls (Ruffolo *et al.* 2007). Anti-IL-6 therapy for Crohn's disease can cause remission and also perianal fistula closure (Ito *et al.* 2004). We found tissue from the internal opening yielded the highest IL-6 concentrations with no statistically significant differences in between the groups. The importance of this is unclear. It could suggest that the inflammatory phenotype is similar in perianal fistulae of both types. Further clarity could come from comparing against normal anal mucosa. However obtaining such tissue could be ethically challenging.

IL-8 is another pro-inflammatory cytokine. It is released by many cell types in response to inflammatory stimuli and attracts neutrophils, basophils and T cells, but not monocytes into tissues. It also is involved in neutrophil activation (Hornbeck *et al.* 2015). Il-8 concentrations are increased in colitic mucosa, compared with healthy controls (Rodríguez-Perálvarez *et al.* 2012). Interestingly, IL-8 expression is increased in idiopathic perianal fistula tracts, especially proximally, compared with rectal mucosa and perianal skin (Kiehne *et al.* 2007). We also found substantial concentrations of IL-8 in all specimens, with the highest found at the internal opening. This is consistent with the above, and further supports the case for IL-8 as an important mediator of inflammation in both idiopathic and Crohn's perianal fistulae.

MCP-1 is a chemotactic factor that attracts monocytes and basophils but not neutrophils or eosinophils. Compared with normal colonic mucosa from health controls, the epithelium, inflammatory cells, and stromal cells from endoscopic biopsies from Crohn's disease affected colon show significantly higher expression of MCP-1 (Banks *et al.* 2003). We found substantial concentrations of MCP-1, especially at the internal opening, although there were no significant differences between the groups. MCP-1 has not been reported before in perianal fistula disease.

RANTES is a chemotactic factor for monocytes, memory T helper cells and eosinophils. It has not been implicated in Crohn's disease pathogenesis (Moriyama *et al.* 2005). We demonstrated RANTES was present at all the specimen sites in all the groups. Concentrations were higher at the fistula tract, granulation tissue and internal opening sites compared with the rectal mucosa. This may just be a reflection of a higher degree of inflammation in these specimens. It could, however also be a clue to the pathophysiology of perianal fistulae.

VEGF is a growth factor active in angiogenesis, vasculogenesis and endothelial cell growth. IL-4 reduces VEGF production in peripheral blood mononuclear cells from patients with inflammatory bowel disease to normal levels. The known defective immunosuppressive effect of IL-4 in inflammatory bowel disease may contribute to the pathogenic cascade leading to inflammation mediated by VEGF (Griga *et al.* 2000). We found significant concentrations of VEGF at all specimen sites. VEGF in perianal fistulae has not been studied before.

Limitations

Our cohort included a broad range of clinical phenotypes, representing the full spectrum of perianal fistula disease. However, this introduced heterogeneity. As the sample size, although comparable to the vast majority of previous studies on perianal fistula, was relatively small, differences may not have been apparent within the heterogeneity.

Collection of tissue specimens followed a protocol, and in most cases were performed by the same two surgeons (JBH, CHK) to standardise the method as much as possible. However, patient and operative factors influenced the size, depth and position of the specimens taken relative to the internal opening, and these differences in theory may have impacted on the results obtained.

This study analysed fresh biopsy specimens cultured *ex vivo*. Therefore the validity of the results is based upon the assumption that these tissues function within culture in a way that is similar or at least relevant to their natural *in vivo* environment.

We only examined certain cytokines. Their selection was influenced by what was possible to be co-measured using a commercial multiplex assay. A key cytokine not measured was TGF-β, which together with IL-13 might play a synergistic role in the pathogenesis of Crohn's disease fistulae (Scharl *et al.* 2013). By examining a broad panel of cytokines, a deeper interrogation of the role of each cytokine and how they interact in perianal fistula disease was not feasible. Only a cautious comparison and triangulation of these data with current knowledge was therefore possible.

Almost half of the Crohn's disease group had received anti-TNF-α prior to or at recruitment. This could have attenuated the cytokine concentrations in the Crohn's disease group and masked any differences with the idiopathic group. However the same could also be said for those in the idiopathic group who had prior treatment, such as a lay open or seton. A future ideal study should study treatment-naïve patients from the time of their index presentation.

There is no accepted healthy control for perianal fistulae and was therefore not included in this study (see Section 2.2 for discussion). This limited the interpretation of the data.

4.5 Conclusions

The concentrations of 30 cytokines at 4 specimen sites in 60 participants with idiopathic and Crohn's perianal fistulae were examined. We found no clear differences in the overall cytokine profiles between the groups. Furthermore, when comparing the rectal mucosa of healthy controls to the participants with Crohn's perianal fistulae, no differences were observed.

Only two significant differences in individual cytokines were found. At the internal opening specimen site, IL-12p70 was higher, and IL-1RA/IL-1β ratio was lower in the Crohn's disease group. These findings are consistent with current knowledge on the general pathophysiology of Crohn's disease. However, given that multiple hypothesis tests were performed, these results should be treated with caution and

further focussed research is needed. Immunocytochemistry, using normal anal mucosa as the control, for example, would offer further interrogation.

These data agree with and add considerably to what Tozer (2011) found using similar techniques. Significant levels of G-CSF, IL-6, IL-8, MCP-1, RANTES and VEGF were found across all specimens and groups. These findings are broadly consistent with current theories on inflammation, and may point towards further research opportunities in perianal fistulae.

Previous studies suggested that IL-1β, IL-6, IL-8, and TNF-α, may have an important role in perianal fistulae immunopathology (Kiehne *et al.* 2007; Ruffolo *et al.* 2007; Ruffolo *et al.* 2008; Tozer 2011). These data also suggest IL-1β, IL-6 and IL-8 may be important. However, results regarding TNF-α were unremarkable.

5. PHOSPHOPROTEIN PROFILES

5.1 Introduction

Receptor tyrosine kinases (RTKs) and intracellular signalling pathways control and regulate cell behaviour (Gilbert 2000). Activation of RTKs usually involves the binding of a ligand to the extracellular component of the receptor. This causes dimerization of the receptor, which allows autophosphorylation of the intracellular component. Often the signal will not exert its effect directly, but will be transduced along intracellular signalling pathways. Thus the next phase involves the recruitment and activation of a host of downstream signalling molecules. As RTKs have multiple phosphotyrosines that can involve numerous docking proteins, they can thus recruit and influence many different signalling molecules. Therefore an activated RTK and the downstream signalling molecules can be thought of nodes within a complex signalling network that transmit information from outside to inside the cell. The end effect, which may be up- or downregulation of gene transcription, cell function or apoptosis, is influenced at each level by receptor downregulation, the activation states of the other signalling pathways within the cell, and positive and negative feedback mechanisms. The outcome is regulation of critical cellular processes, such as proliferation and differentiation, cell survival and metabolism, cell migration and cell cycle control.

Humans have 58 known RTKs, which fall into twenty subfamilies (Lemmon and Schlessinger 2010). Abnormalities in RTK structure and function have been linked to several diseases such as cancers, diabetes, bone disorders, arteriosclerosis and inflammation. The role of RTKs and signalling molecules in gut homeostasis and inflammation have been studied individually for the EphRs (ephrin receptors), Axl (AXL receptor tyrosine kinase), Tie 1 (tyrosine kinase with immunoglobulin like and epidermal growth factor like domains 1), VEGFRs (vascular endothelial growth factor receptors), TrkA/NTRK1 (neurotrophic receptor tyrosine kinase 1), Ron/MST1R (macrophage stimulating 1 receptor), InsR (insulin receptor), Jak/Stat

(Janus kinase/signal transducers and activators of transcription), MAPK (mitogen-activated protein kinases), and Akt/PKB/Rac (protein kinase B) subfamilies amongst others (Frey and Polk 2014; Rothlin *et al.* 2014; Linares *et al.* 2014; Linares and Gisbert 2011; Steinkamp *et al.* 2012; Gorlatova *et al.* 2011; Zhao *et al.* 2011; Coskun *et al.* 2013; Setia *et al.* 2014).

Vossenkämper *et al.* (2014) studied the molecular signature of healthy and inflamed colon. They measured the phosphorylation status of 39 RTKs and signalling molecules in freshly isolated colonic mucosa of healthy subjects and patients with inflammatory bowel disease using a phosphorylation-specific protein array. Healthy colon showed very few phosphorylation events. In contrast, colonic mucosa from patients in the Crohn's disease and ulcerative colitis groups showed higher relative intensities in the majority of the analysed phosphoproteins. When otelixizumab, a monoclonal immunoglobulin against human CD3, was added to the explants from the disease groups, the phosphorylation of the majority of the kinases was strongly reduced.

As previously discussed in Section 0, it is believed that idiopathic and Crohn's disease fistulae differ in their pathogenesis and pathophysiology. The phosphorylation status of the RTKs and signalling molecules gives an insight into disease processes in the tissue, and have not been analysed in perianal fistulae. We therefore aimed to describe the phosphorylation profile in this cohort and compare between the idiopathic and Crohn's disease groups.

5.2 Methods

Participants and Biopsies

The methodology for recruitment of the study cohort and obtaining biopsy specimens (fistula tract, granulation tissue, internal opening and rectal mucosa) from participants is described in Chapter 2. Recruitment of participants to serve as healthy controls is described in Chapter 4.

Cell Lysis

The student thawed the fresh-frozen tissue samples at room temperature. Working on ice, he added 100 µl of radioimmunoprecipitation assay buffer containing one microlitre of Phosphatase Inhibitor Cocktail 2 and one microlitre of Protease Inhibitor in dimethyl sulfoxide (Sigma-Aldrich, Gillingham, UK) to each sample (Figure 25), and lysed the cells with a manual ultrasonic cell disruptor. Restricting sonication to short bursts prevented excessive warming of the samples. After 10 minutes of incubation, with mixing every one minute, centrifugation at 16,250 *g* for 5 minutes at 4°C separated off the cell debris. The cell lysate supernatant was drawn off with a pipette into labelled Eppendorf tubes and either used immediately or stored at -80°C.

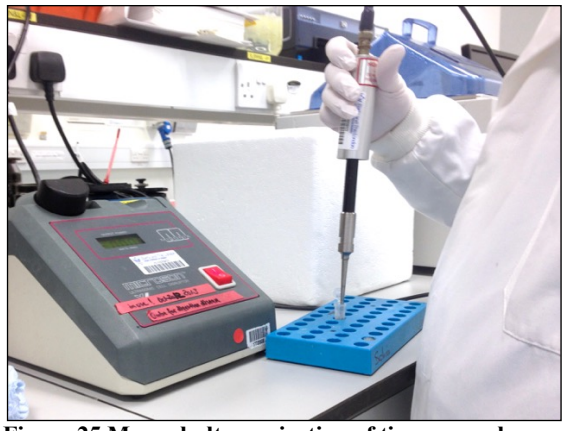

Figure 25 Manual ultrasonication of tissue sample.

Bradford Assay

The student prepared the standards using a one-in-two serial dilution of 40 µl of 2 mg/ml Bovine Gamma Globulin (Bio-Rad Laboratories Inc., Hercules, California) in 40 µl of distilled water to achieve concentrations of 1.0, 0.5, 0.25, 0.125, 0.063, 0.031, 0.016 mg/ml and then placed 10 µl of each standard and diluted lysate (1 in 100 concentration in distilled water) in duplicate into a 96-well plate. Fifty microlitres of 1X QuickStart Bradford Dye Reagent (Bio-Rad Laboratories Inc., Hercules, California) added to each well produced a colour change. A visual check determined if any lysates fell outside the standard range. For these lysates, alternative

dilutions were also prepared (e.g. 1 in 50 or 1 in 200) and added to the 96-well plate with dye reagent. An ELx800 plate reader and Gen5 2.00.18 software (Biotek Instruments Ltd., Winooski VT) measured the optical density of each well at 595 nm. Using Excel 2010 (Microsoft, Redmond, WA), the results from the standards generated a quadratic polynomial equation, which estimated the protein concentration of each cell lysate (Figure 26).

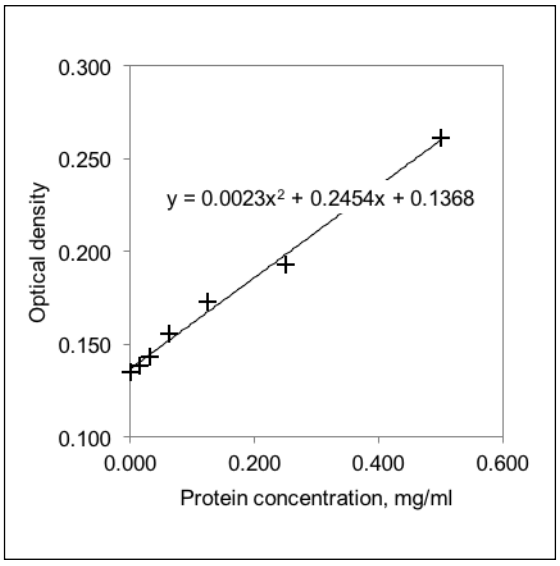

Figure 26 Bradford assay standard curve example, showing quadratic polynomial curve used to estimate the protein concentrations.

Antibody Array

The PathScan RTK Signaling Antibody Array, Chemiluminescent Readout (Cell Signaling Technology, Danvers, Massachusetts) was used to quantify the phosphorylation status of receptor tyrosine kinases in the cell lysates (Figure 27). It is a slide-based antibody array founded upon the sandwich immunoassay principle (Cell Signaling Technology 2015). It measures the relative levels of 28 RTKs and 11 signalling nodes, when phosphorylated at tyrosine or other residues. Each nitrocellulose-coated glass slide holds target-specific capture antibody microdots arranged in duplicate in eight arrays, which after processing yields chemiluminescent signals at variable intensities from each spot (see Figure 28 for an explanation).

Figure 27 PathScan RTK Signaling Antibody Array kit, Chemiluminescent Readout (Cell Signaling Technology, Danvers, Massachusetts).

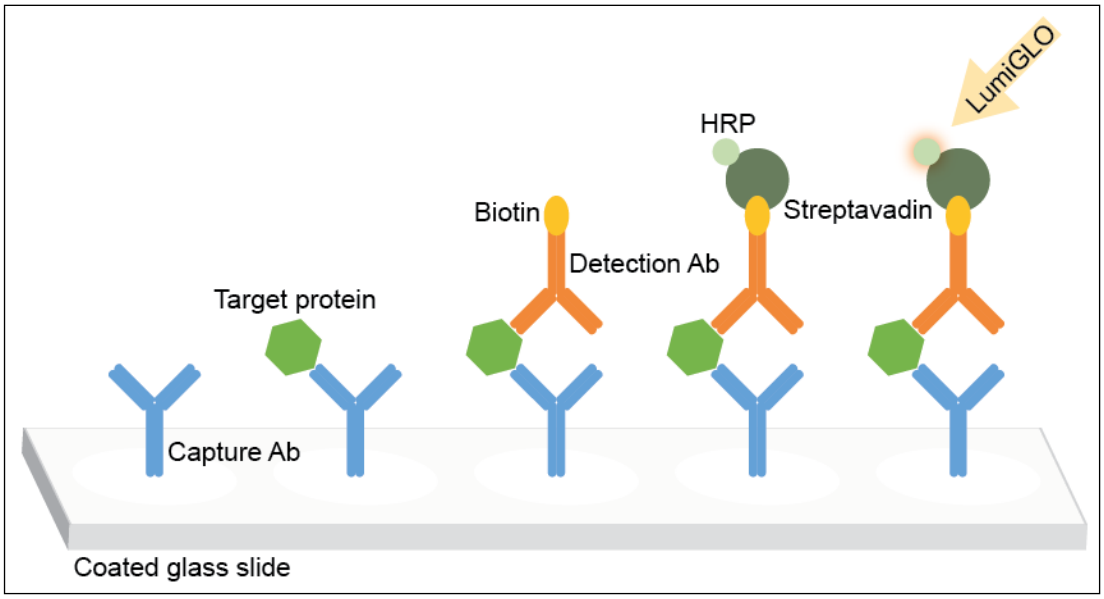

Figure 28 Sandwich immunoassay principle. In this established technique, the capture antibody is bound to the slide. The target protein in the sample binds to the capture antibody. Detection antibody then binds to the target protein so that it is 'sandwiched' between the two antibodies. The amount of detection antibody on the slide is directly proportional to the concentration of the analyte. In the PathScan RTK Signaling Antibody Array, the detection antibody is biotinylated, allowing it to avidly bind the reporter molecule, streptavidin-conjugated horseradish peroxidase (HRP). LumiGLO reagent activates it to produce a chemiluminescent signal whose intensity varies in proportion to the concentration. The signal is captured on radiographic film.

Working at room temperature, the student assembled the slide into an eight-well cassette, added 150 µl of Array Blocking Buffer to each well and incubated it on a rocker at 12 rpm for 15 minutes. Using the results from the Bradford assay, an individually calculated volume of Array Diluent Buffer added to each cell lysate achieved a consistent protein concentration of 0.75 mg/ml. Each well received 150 µl of each diluted cell lysate. The cassette was then covered with sealing tape and incubated at 4°C overnight (16–20 hours).

The student then washed the cassette was according to the instructions, added 150 µl of Biotinylated Detection Antibody Cocktail to each well, covered the cassette and incubated it on a rocker for 1 hour. Following further washing, he added 150 µl of Streptavidin-conjugated Horseradish Peroxidase to each well, covered the cassette and incubated it on a rocker for 30 minutes. After further washing the cassette was then dismantled and covered evenly with LumiGLO-peroxide reagent. An even coverage ensured no air bubbles and reduced the risk of image artefact. Exposure to Amersham Hyperfilm ECL (GE Healthcare Life Sciences, Buckinghamshire, UK) in a dark room at varying exposures between 20 and 50 seconds captured the image of the slide. An automatic film developer (Amersham Pharmacia Biotech, Amersham, UK) processed the film, which was then labelled and checked for quality.

Image Digitisation

The student developed a bespoke method of digitising the image. Previously in the laboratory, a flatbed scanner (HP LaserJet 100 Colour MFP M175nw, Hewlett Packard, Palo Alto, California) was used to scan the developed film into a digital image (Vossenkämper *et al.* 2014). However, this method yielded images with poor contrast because of the following reason. Flatbed scanners have their CCD camera on the same side as the light source, which means they capture reflected light. This is suitable when scanning opaque media as reflectivity is high. However, chemiluminescent film is transparent and has low reflectivity. The highest contrast can only be achieved by having the light source behind the transparency. Flatbed

scanners can be used to reliably digitise radiographs, but only when used with a slide kit for scanning transparencies (Chen and Hollender 1995).

To address this limitation, the student set up a light box and digital camera held within a rig (Figure 29a). The closest possible distance from the film to the camera (Nikon D70 digital camera with a Nikon 18–70 mm 1:3.5–4.5G DX lens, Nikon Corporation, Tokyo, Japan) was used and kept constant at 51.5 cm. The light box is illuminated by fluorescent light tubes, which due to their physical properties flicker at 100 to 120 Hz. This results in fluctuations in light intensity and colour temperature. Using a slow shutter speed of 1/10 second with an ISO of 200 captured enough cycles to achieve a smooth, consistent picture. Different apertures from f22 to f16 allowed adjustment of the exposure. The digital image was stored in raw format to allow greatest fidelity. The full settings are listed in Appendix 4.

The student captured each film at different exposures and reviewed their pixel histograms on the camera display. These histograms plot the frequency of pixels within the image against their brightness value ranging from zero (black) to 255 (white). If the histogram is clipped at the left, then the image may be underexposed and consequently differentiation between pixels of a low brightness are lost, e.g. an underexposed image may not show a difference between black and dark grey as all those pixels have been stored with a brightness value of zero. If the histogram is clipped at the right, then the image may be overexposed and consequently differentiation between pixels of a high brightness is lost. For the images of the antibody array, the information of interest mainly existed in the pixels with a low brightness value (i.e. blacks and greys). Therefore the optimum exposure chosen was one where the histogram was never clipped on the left and just touching the right-hand edge of the graph (Figure 29).

After checking the images in Zoner Photo Studio 17 (Zoner Inc., Kennesaw GA), to ensure that overexposed areas did not encroach onto the slide, the student converted them to 8-bit grayscale TIFF format without compression.

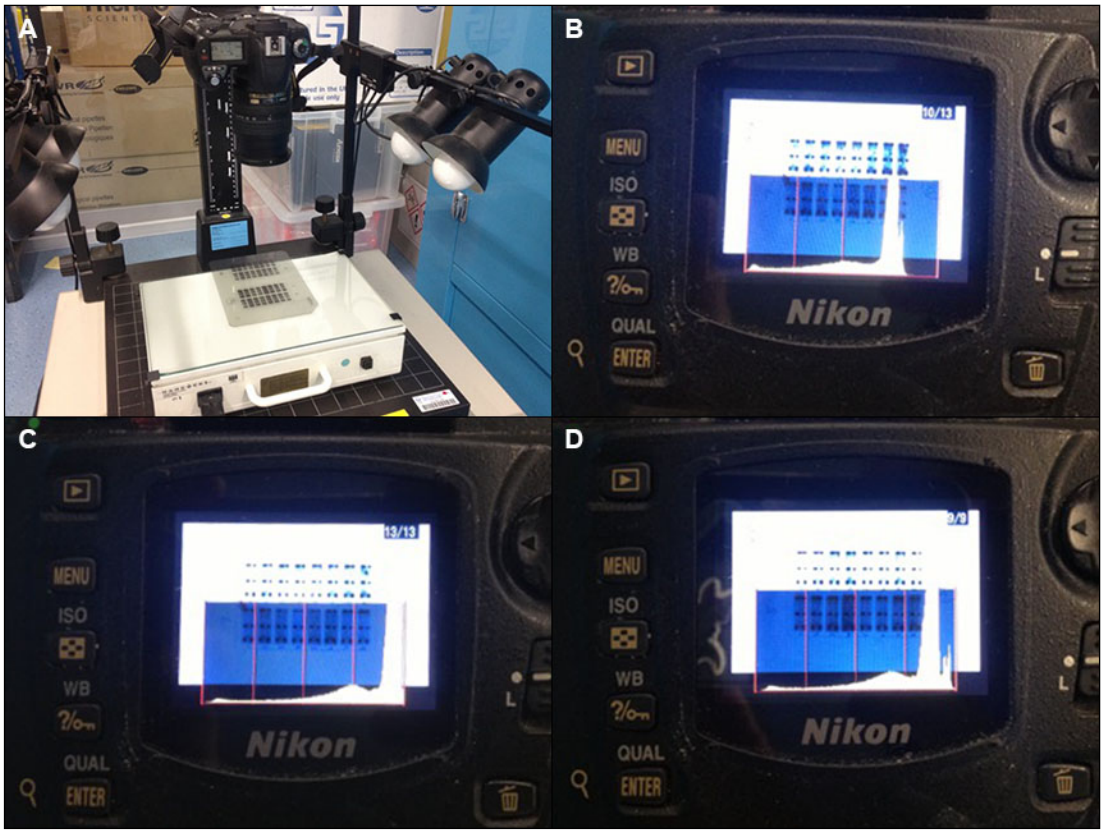

Figure 29 (A) Light box setup with digital camera clamped into rig above. (B) Histogram showing an absence of pixels towards the right of the graph indicating underexposure. (C) Histogram showing truncation of the graph on the right indicating overexposure. (D) Histogram showing the graph just touching the right-hand limit and no truncation of the graph on the left (optimum exposure).

Comparison of Image Digitization Methods

To validate the new method of image digitization, the student processed the same film from the first experiment (eight arrays) using both the flatbed scanner and the digital camera (Figure 30). A visual inspection revealed that the digital camera produced images with a better contrast between the background and the spots. An analysis of the pixel histograms in ImageJ (Schneider *et al.* 2012) confirmed that the digital camera produced a digital image with greater dynamic range: the range of pixel brightness was 188 compared to 160. The intensities of the 720 spots were then quantified using ImageQuant TL 2005 (GE Healthcare Life Sciences, Pittsburg PA) using the method described below. The mean background absolute pixel intensity was lower in the digital camera image: 12,108 (SD = 993) *versus* 69,141 (6,823). A lower background signal means less noise obscuring the signal from the spots. The

histograms of the absolute pixel intensities showed that there was a clearer bimodal distribution of pixel intensities measured from the digital camera image. A bimodal distribution is expected as most spots are light, giving the high peak towards the left, and the positive controls, which feature less frequently, are dark giving the smaller peak towards the right.

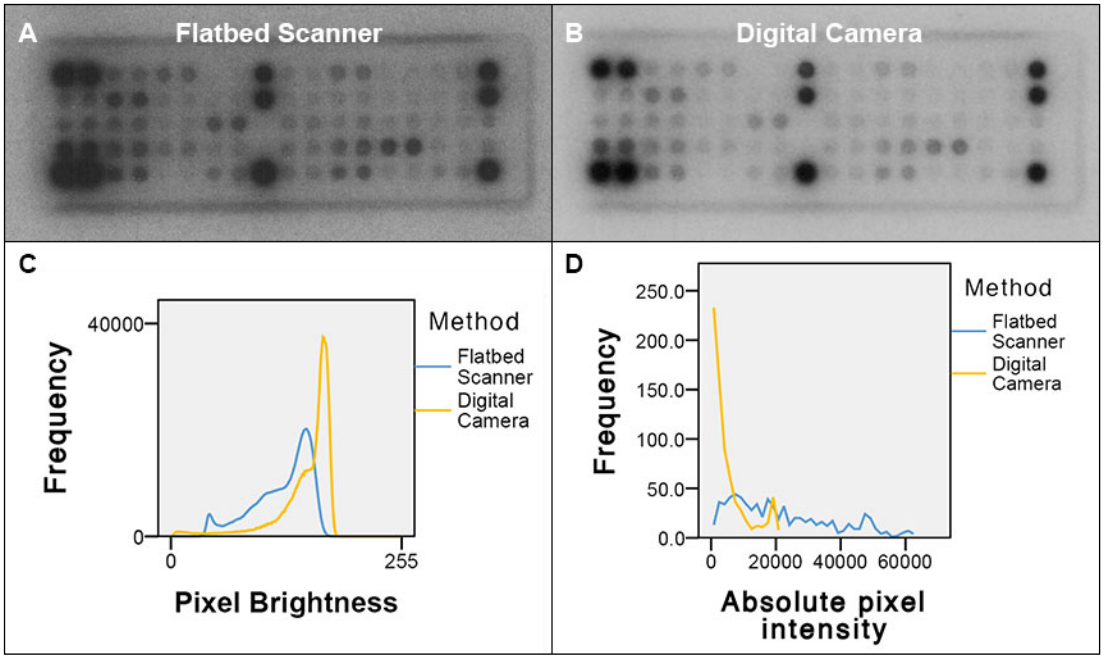

Figure 30 (A) One array digitized using flatbed scanner. (B) The same array digitized using digital camera, showing better contrast between the background and the spots. (C) Pixel histograms from the digitized images of eight arrays (one experiment), showing a wider dynamic range acquired by the digital camera. (D) Histograms from the results of the analysed images of those eight arrays, showing a clearer bimodal distribution of pixel intensities measured from the digital camera image.

Spot Intensity Quantification

The student analysed the digital images in ImageQuant TL 2005 (GE Healthcare Life Sciences, Pittsburg PA), using a standard spot grid pre-programmed with the manufacturer's target map and key (Figure 31, Figure 32 and Table 27). The edge of the slide where it appeared lightest specified the background pixel intensity. The mean pixel intensity of the positive controls defined 100% against which the analyte pixel intensity values were normalised. The data were imported into the study database. AS then double-entered the corresponding participant identification numbers and biopsy sites to ensure accuracy.

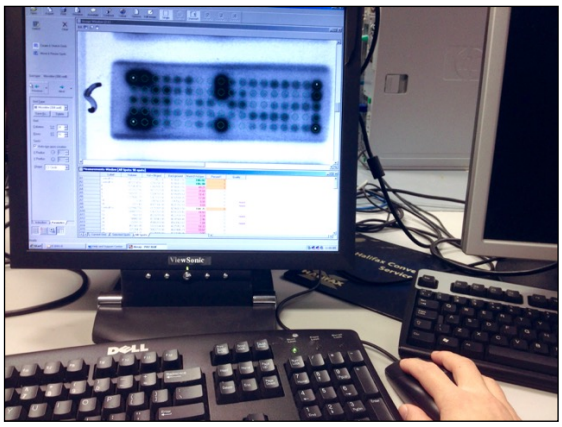

Figure 31 Spot intensity quantification using ImageQuant software.

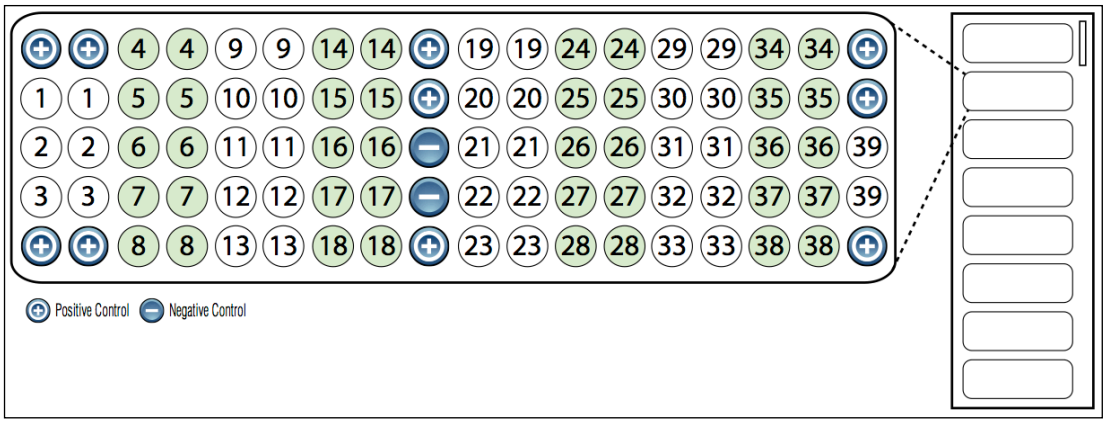

Figure 32 Target map of one array in the PathScan® RTK Signaling Antibody Array Kit (Chemiluminescent Readout).

Table 27 Key to target map listing the 28 receptor tyrosine kinases and 11 signalling nodes.

Label	Protein (phosphorylation site)	Name
Receptor tyrosine kinases		
1	EGFR/ErbB1	Epidermal growth factor receptor
2	HER2/ErbB2	Human epidermal growth factor receptor 2
3	HER3/ErbB3	Human epidermal growth factor receptor 3
4	FGFR1	Fibroblast growth factor receptor 1
5	FGFR3	Fibroblast growth factor receptor 3
6	FGFR4	Fibroblast growth factor receptor 4
7	InsR	Insulin receptor
8	IGF-IR	Insulin-like growth factor receptor 1
9	TrkA/NTRK1	Tyrosine kinase receptor A
10	TrkB/NTRK2	Tyrosine kinase receptor B
11	Met/HGFR	Hepatocyte growth factor receptor
12	Ron/MST1R	Macrophage stimulating 1 receptor
13	Ret	Ret proto-oncogene receptor tyrosine kinase
14	ALK	Anaplastic lymphoma kinase
15	PDGFR	Platelet-derived growth factor receptor
16	c-Kit/SCFR	Stem cell growth factor receptor
17	FLT3/Flk2	Foetal liver kinase 2
18	M-CSFR/CSF-1R	Macrophage colony-stimulating factor 1 receptor
19	EphA1	Ephrin type-A receptor 1
20	EphA2	Ephrin type-A receptor 2
21	EphA3	Ephrin type-A receptor 3
22	EphB1	Ephrin type-B receptor 1
23	EphB3	Ephrin type-B receptor 3
24	EphB4	Ephrin type-B receptor 4
25	Tyro3/Dtk	Tyro3 tyrosine-protein kinase
26	Axl	AXL receptor tyrosine kinase
27	Tie2/TEK	Tunica interna endothelial cell kinase
28	VEGFR2/KDR	Vascular endothelial growth factor receptor 2
Signalling Nodes		
29	Akt/PKB/Rac (Thr308)	Proto-oncogene c-Akt / protein kinase B
30	Akt/PKB/Rac (Ser473)	Proto-oncogene c-Akt / protein kinase B
31	p44/42 MAPK	Mitogen-activated protein kinase isoform p44
32	S6 Ribosomal Protein	S6 Ribosomal Protein
33	c-Abl	Abelson murine leukaemia viral oncogene homolog 1
34	IRS-1	Insulin receptor substrate 1
35	Zap-70	70 kDa zeta-associated protein
36	Src	Rous sarcoma
37	Lck	Lymphocyte cell-specific protein-tyrosine kinase
38	Stat1	Signal transducer and activator of transcription 1
39	Stat3	Signal transducer and activator of transcription 3

Choice of Spot Result Value

The target-specific capture antibody microdots are arranged in duplicate (Figure 32), and the mean of each pair is usually used as the result value. However, visual inspection of the films revealed that the positive control spots, even at very short exposure times, gave an intense signal that encroached asymmetrically on adjacent analyte spots (Figure 33).

To assess the effect of this signal overlap, the student calculated the difference in the normalised pixel intensity, the pixel intensity range, between each spot pair for 8,892 spot pairs. For the spots that did not suffer encroachment from adjacent positive control spots, the mean pixel intensity range was small, 3.19 (SD = 3.56). This demonstrated that variability between spot pairs when there was no encroachment was low, and that the performance of the array was consistent enough to justify a result based on a single spot instead of the mean of the pair. For the spots that did suffer from encroachment, the mean pixel intensity range was larger, 11.73 (SD = 10.17). This showed that the signal from the affected spots was significantly amplified. To control for this, the minimum pixel intensity from each spot pair was used as the result value.

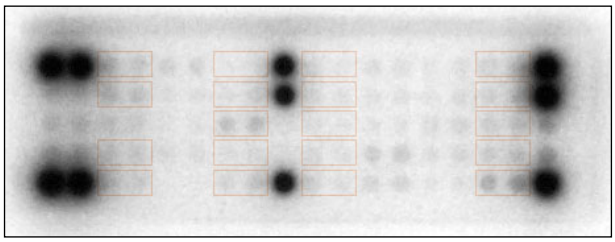

Figure 33 One array from the PathScan RTK Signaling Antibody Array, showing asymmetrical encroachment of the signal from the positive control microdots on the adjacent microdots (highlighted).

5.3 Results

Specimens

Out of the 61 participants, one did not undergo biopsy due to unavailability of the student at the time. Additionally, as described in Section 4.3, six healthy controls underwent biopsy of their rectal mucosa only.

Not all specimens were taken or analysed in each participant. Reasons were: technical difficulty in taking the specimen, inadequate specimen, and an absence of the tissue to be sampled (granulation tissue and internal opening sites only). A breakdown of the specimens analysed is shown in Table 28. Overall, a total of 224 specimens were available for phosphoprotein quantification, specifically six control, 171 idiopathic, and 47 Crohn's disease samples. With 39 phosphoproteins measured per specimen, we made 17,472 measurements overall.

Experiment Quality Controls

Each array contained positive and negative control spots. The median pixel intensities for the negative control spots for each specimen site were below 20% (Figure 34 and Table 47 in Appendix 8). The positive control spots served as a reference for 100%, thus their median pixel intensities were 100%. Two negative control samples were run: one array containing lysis buffer and one containing distilled water. The majority of the spots produced no signal. EGFR/ErbB1, HER2/ErbB2, HER3/ErbB3, FGR1, FGR4 and Stat3 produced a pixel intensity below 20%. Thus we subsequently considered a result above 20% pixel intensity to be positive.

Table 28 Specimens processed for phosphoprotein quantification. NA, not applicable.

	Healthy Control	Idiopathic	Crohn's Disease	All
Fistula Tract	NA	46	12	58
Granulation Tissue	NA	33	11	44
Internal Opening	NA	45	12	57
Rectal Mucosa	6	47	12	65
Total	6	171	47	224

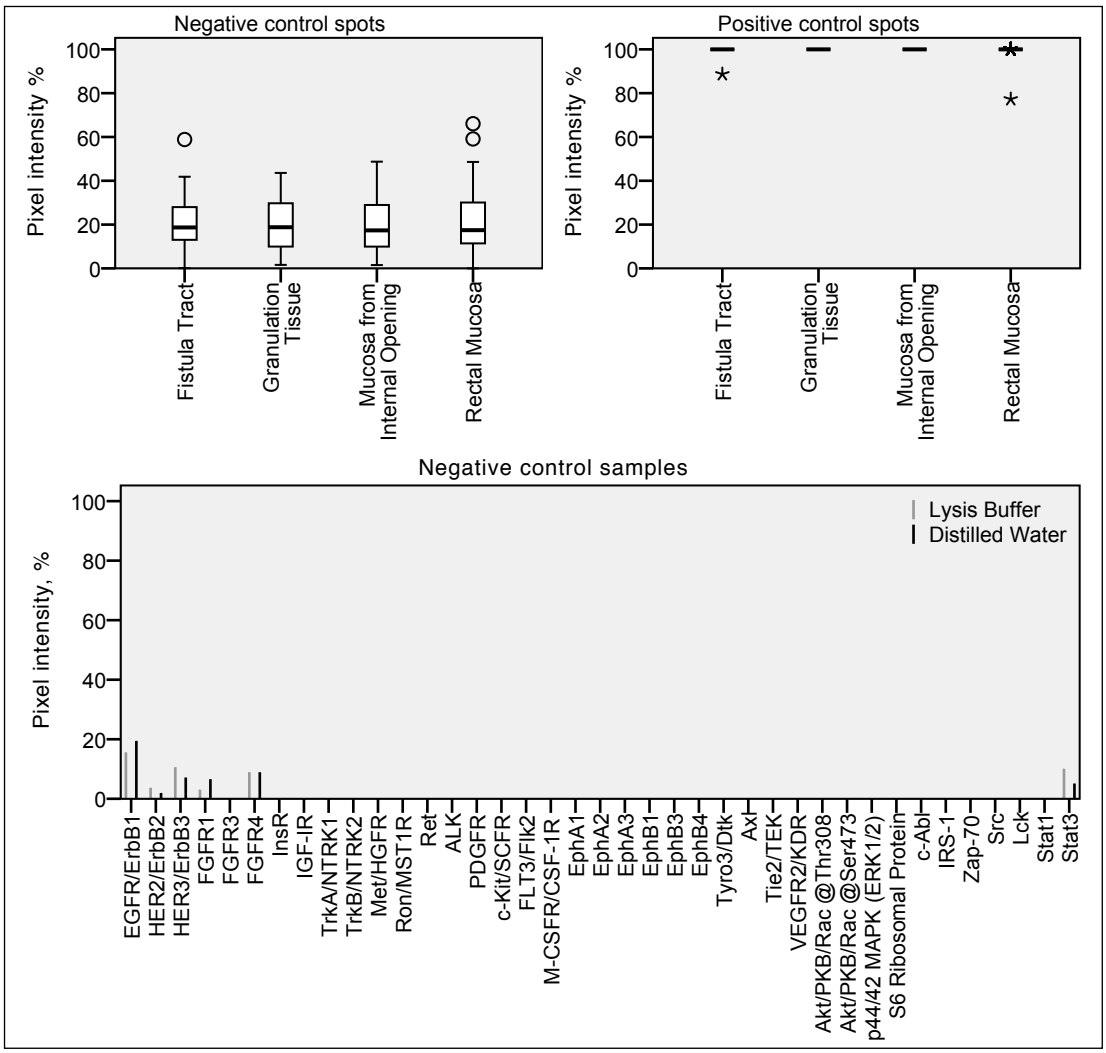

Figure 34 Control results. Boxplots of results from negative and positive control spots from each array and bar chart showing pixel intensities from the negative control samples: one array containing lysis buffer only, and one array containing distilled water only.

Phosphoprotein Profiles

All the four specimens (fistula tract, granulation tissue, internal opening and rectal mucosa) yielded consistently positive results across both disease groups for EGFR/ErbB1, HER2/ErbB2 HER3/ErbB3, FGFR1, FGFR3, FGFR4, Stat1, and Stat3. In the rectal mucosa, positive levels for InsR, IGF-1R, c-Kit/SCFR, Tie2/TEK, Akt/PKB/Rac at phosphorylation site Thr308, S6 Ribosomal Protein, IRS-1 and Src were also seen in both disease groups and the healthy controls (Table 29).

There were no significant differences in the phosphoprotein levels between the idiopathic and Crohn's disease groups at the four specimen sites (Figure 35; Table 48, Table 49, Table 50 and Table 51 in Appendix 8). Example microarray images are shown in Figure 36. When comparing the healthy controls and the Crohn's disease groups at the rectal mucosa specimen site, the levels of six phosphoproteins were significantly higher in the healthy controls: EphA1, EphA2, EphB1, EphB4, Tyro3/Dtk and VEGFR2/KDR (Figure 37; Table 52 in Appendix 8). Example microarray images are shown in Figure 38.

Table 29 Median pixel intensities (%) of phosphoproteins. Id, idiopathic; CD, Crohn's disease; HC, healthy controls.
*** statistically significant difference compared with Crohn's disease, p <0.01.**

	Fistula Tract		Granulation Tissue		Internal Opening		Rectal Mucosa		
	Id	CD	Id	CD	Id	CD	HC	Id	CD
EGFR/ErbB1	26.7	41.1	26.0	37.3	35.0	43.8	30.5	48.2	45.4
HER2/ErbB2	18.1	26.6	17.1	24.2	23.4	22.4	59.2	37.3	36.3
HER3/ErbB3	37.4	49.4	37.5	41.0	50.7	47.2	81.0	63.2	75.0
FGFR1	24.1	29.7	23.1	22.5	28.6	36.3	56.8	40.9	43.7
FGFR3	21.8	22.6	33.8	26.6	43.5	36.3	71.0	60.1	68.4
FGFR4	27.4	30.1	23.0	28.6	33.2	33.2	51.6	42.7	46.4
InsR	10.4	16.3	9.3	19.4	17.8	20.2	67.7	35.9	42.6
IGF-1R	7.3	10.5	7.0	13.1	13.6	16.1	58.0	29.0	42.1
TrkA/NTRK1	8.2	6.7	5.6	10.4	12.6	12.2	62.6	22.6	28.9
TrkB/NTRK2	10.0	6.5	6.9	7.2	12.7	9.1	41.2	17.0	17.9
Met/HGFR	1.4	1.3	0.8	2.2	0.8	0.0	16.7	7.7	8.2
Ron/MST1R	4.3	2.3	2.9	8.2	5.7	3.7	34.2	15.2	21.7
Ret	1.6	0.1	1.0	2.9	1.5	0.4	9.7	0.5	1.9
ALK	1.0	0.1	0.1	0.2	0.1	0.0	3.3	0.5	0.1
PDGFR	5.3	2.4	1.7	6.2	4.5	1.2	17.5	5.5	6.8
c-Kit/SCFR	10.7	15.1	8.9	14.8	14.0	9.3	55.5	30.6	33.8
FLT3/Flk2	3.8	4.0	3.3	6.3	4.8	2.2	12.8	6.9	4.8
M-CSFR/CSF-1R	6.4	5.8	5.0	7.8	11.3	6.7	39.1	20.6	15.9
EphA1	1.5	1.2	2.0	5.1	3.3	0.3	42.2	13.7	10.3
EphA2	3.3	4.1	4.0	4.0	5.0	0.8	27.1	10.0	7.6
EphA3	3.8	3.1	3.5	6.0	11.1	3.0	32.7	10.3	9.6
EphB1	2.8	1.2	4.2	3.6	3.2	1.1	46.9	7.9	5.9
EphB3	0.2	0.0	0.2	0.6	0.1	0.0	22.7	0.1	0.0
EphB4	2.3	2.5	1.5	0.0	6.9	0.1	68.3	23.2	17.1
Tyro3/Dtk	0.0	0.1	0.7	0.0	0.9	0.0	35.8	9.4	3.7
Axl	0.3	1.4	0.9	0.0	1.3	0.0	36.1	10.9	6.1
Tie2/TEK	9.2	13.1	13.5	10.6	22.8	17.1	70.6	41.6	38.4
VEGFR2/KDR	0.7	0.9	3.6	2.1	8.2	0.9	81.1	14.1	15.5
Akt/PKB/Rac @Thr308	9.2	12.8	8.4	5.8	37.4	11.9	31.1	41.4	34.1
Akt/PKB/Rac @Ser473	0.6	1.2	0.7	0.0	4.2	0.0	32.5	11.5	7.2
p44/42 MAPK (ERK1/2)	4.6	3.6	0.4	0.0	12.2	3.9	24.3	23.9	10.7
S6 Ribosomal Protein	1.3	0.2	2.6	0.2	14.5	1.0	62.6	24.9	23.1
c-Abl	0.2	0.0	0.9	0.1	5.6	0.0	30.8	9.5	5.3
IRS-1	13.1	13.3	20.9	16.4	26.1	7.3	73.7	40.9	25.0
Zap-70	9.1	9.1	13.0	7.0	11.5	0.1	28.1	18.7	6.8
Src	17.4	13.9	18.2	10.1	35.1	7.5	29.4	35.7	23.3
Lck	4.7	4.2	9.3	4.5	10.9	0.8	27.2	14.4	5.6
Stat1	16.6	37.0	27.8	40.6	49.3	33.9	50.9	40.8	35.8
Stat3	48.7	57.7	62.7	64.7	74.0	59.8	40.3	62.4	53.6

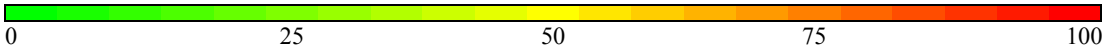

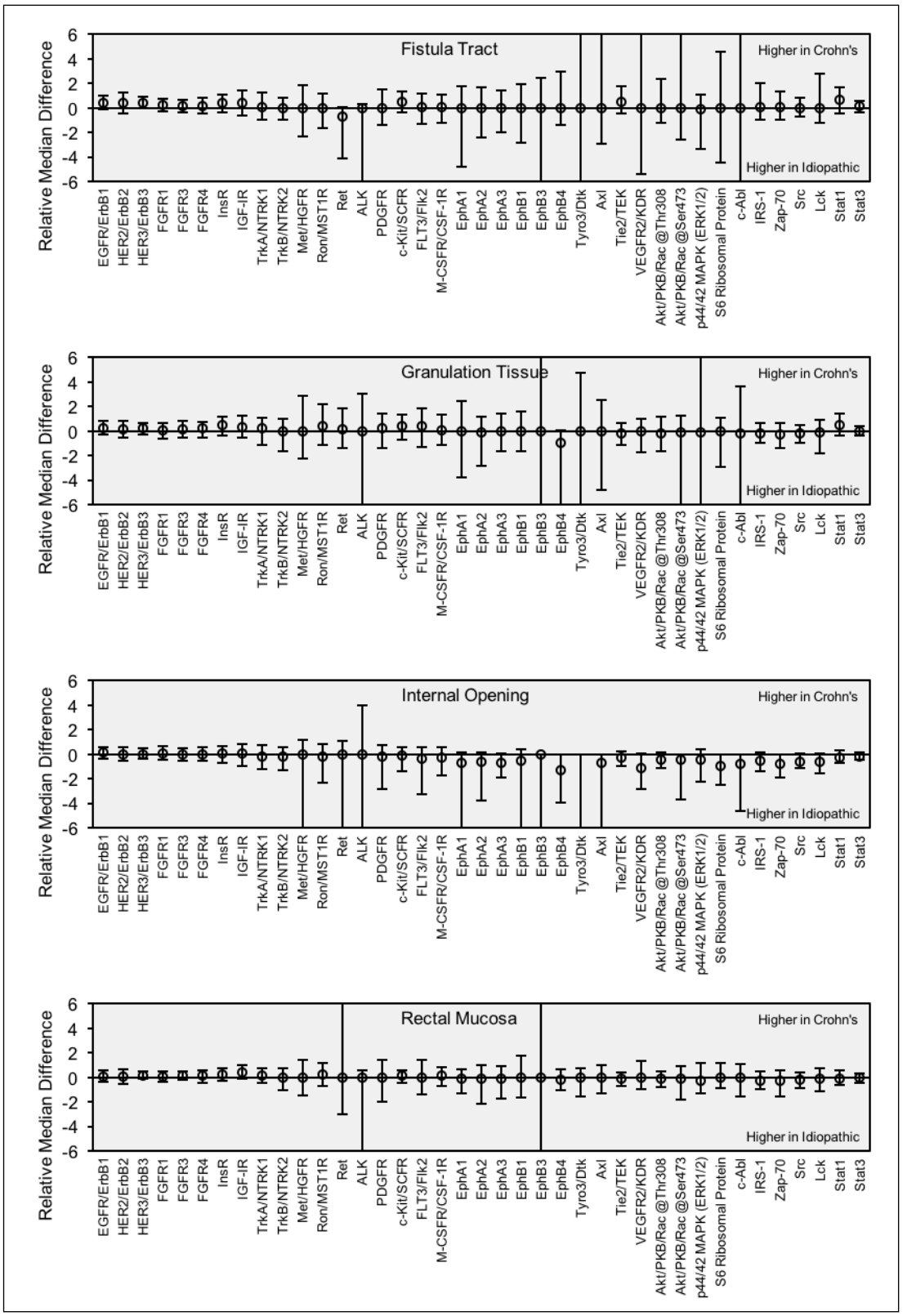

Figure 35 Relative median difference in phosphoprotein pixel intensities between idiopathic and Crohn's disease groups. Error bars show 99% confidence intervals estimated using Hodges-Lehman method.

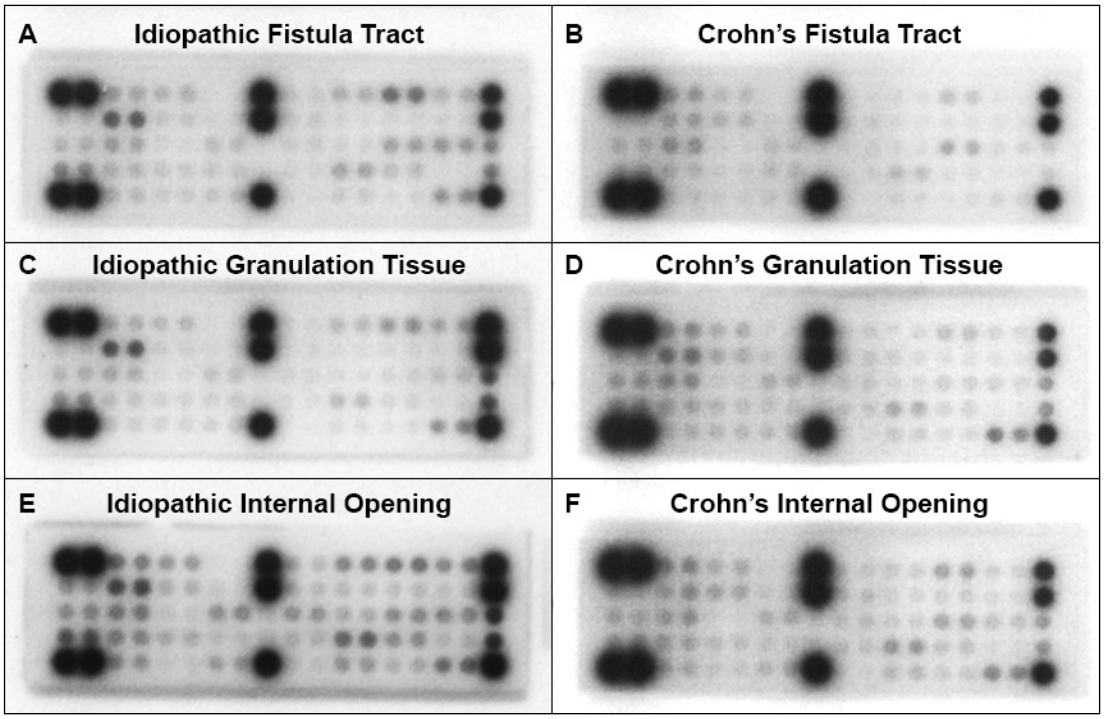

Figure 36 Example microarray images. Fistula tract samples from (A) idiopathic and (B) Crohn's disease participants. Granulation tissue samples from (C) idiopathic and (D) Crohn's disease participants. Internal opening samples from (E) idiopathic and (F) Crohn's disease participants.

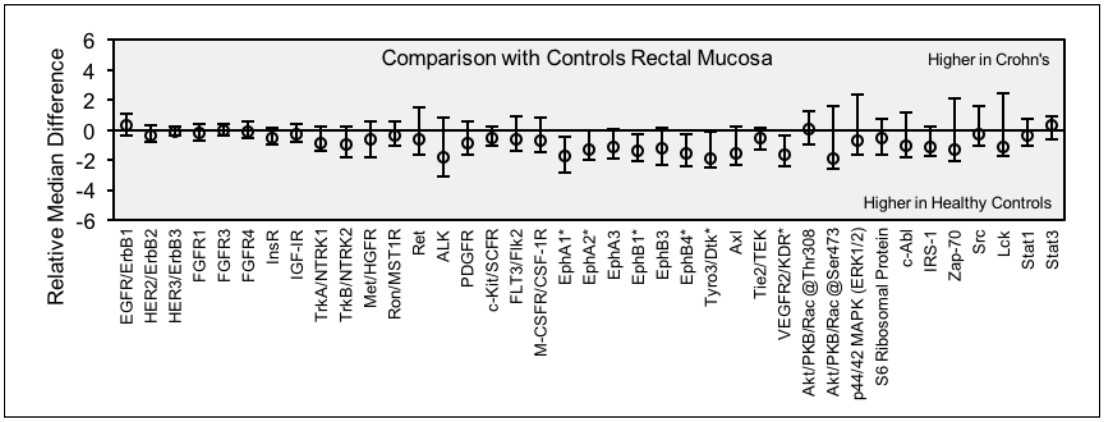

Figure 37 Comparison with healthy controls rectal mucosa. Relative median difference in phosphoprotein pixel intensities between healthy controls and Crohn's disease groups. Error bars show 99% confidence intervals estimated using Hodges-Lehman method. See Appendix 8 for absolute values.
*** statistically significant, p <0.01.**

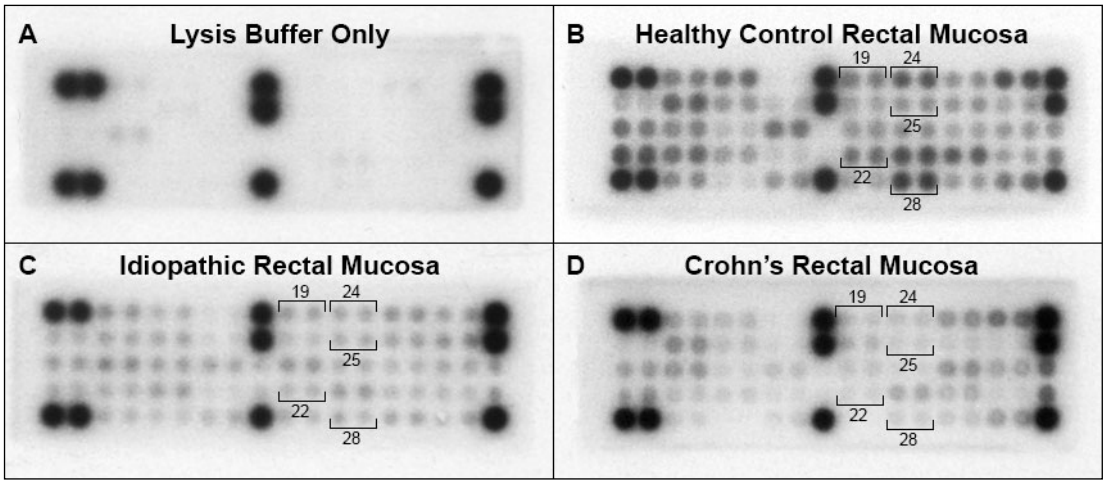

Figure 38 Example microarray images. (A) Negative control array containing lysis buffer only, showing an absent signal from all spots, except the positive control spots. (B) Healthy control rectal mucosa showing positive signal from numerous spots including EphA1 (19), EphB1 (22), EphB4 (24), Tyro3/Dtk (25) and VEGFR (28). (C) Idiopathic rectal mucosa showing significantly lower signal from the same highlighted spots. (D) Crohn's disease rectal mucosa, again showing significantly lower signal from the same highlighted spots.

5.4 Discussion

We aimed to describe the phosphorylation profile in this cohort and compare between the idiopathic and Crohn's disease groups in order to test the hypothesis that perianal fistulae of these types differ in their pathophysiology. The relative concentrations, measured as pixel intensities, of 28 receptor tyrosine kinases and 11 signalling nodes, when phosphorylated at tyrosine or other residues, in fresh tissue homogenates taken from the study cohort were systematically measured.

To reiterate the findings from Chapter 3, the cohort had a wide distribution of phenotypes including those with simple and complex, low and high, and primary and recurrent perianal fistula disease in both the idiopathic and Crohn's disease groups. Therefore these laboratory data encompass the breadth of the disease under study. We used a well-validated multiplex method efficiently make thousands of accurate quantitative measurements. Our laboratory had prior experience in these techniques and showed them capable of demonstrating differences in mucosa from inflammatory bowel disease patients compared with healthy volunteers (Vossenkämper *et al.* 2014). We employed several quality control features, such as data re-entry and experimental controls to ensure the results were accurate and

reliable. Analysis used medians and interquartile ranges to allow for skewed data, 99% confidence intervals to allow for multiple hypothesis testing, and non-parametric methods to avoid problems with small subgroup numbers.

With 61 participants, 4 biopsy sites (fistula tract, granulation tissue, internal opening and rectal mucosa) and 39 analytes (EGFR/ErbB1, HER2/ErbB2, HER3/ErbB3, FGFR1, FGFR3, FGFR4, InsR, IGF-IR, TrkA/NTRK1, TrkB/NTRK2, Met/HGFR, Ron/MST1R, Ret, ALK, PDGFR, c-Kit/SCFR, FLT3/Flk2, M-CSFR/CSF-1R, EphA1, EphA2, EphA3, EphB1, EphB3, EphB4, Tyro3/Dtk, Axl, Tie2/TEK, VEGFR2/KDR, Akt/PKB/Rac (at Thr308), Akt/PKB/Rac (at Ser473), p44/42 MAPK, S6 Ribosomal Protein, c-Abl, IRS-1, Zap-70, Src, Lck, Stat1 and Stat3), a total of 17,472 measurements were made. Despite this extensive approach, there were no significant differences in the median pixel intensities of each phosphoprotein between the disease groups for each of the four biopsy sites (Table 30).

When comparing the phosphoprotein levels from the rectal mucosa of Crohn's disease participants with the healthy controls, we found significantly higher levels in the healthy controls for six phosphoproteins: EphA1, EphA2, EphB1, EphB4, Tyro3/Dtk and VEGFR2/KDR. The first four are RTKs from the Ephrin subfamily. They are membrane-bound cell surface receptors and are mainly activated through direct cell-cell interaction with membrane-bound ephrin ligands. Ephrin receptor and ephrin signalling is important in controlling cellular proliferation in the crypts and differentiation of enterocytes on the villi. Loss of ephrin receptor and ephrin signalling appears to contribute to wound healing defects, as in inflammatory bowel disease, and tumorigenesis (Perez White and Getsios 2014). Thus, the present study suggests that suppression of ephrin receptor expression in the rectal mucosa may be a pathological feature in patients with both idiopathic and Crohn's perianal fistulae. The consequence of this conclusion is potentially important for two reasons: (1) it suggests that idiopathic and Crohn's perianal fistulae may be similar in their immunopathology with regards to ephrin signalling, and (2) it suggests that abnormalities in those with idiopathic perianal fistulae are not confined to the peri-fistula tissue, a notion that has not previously been reported.

Tyro3 is a RTK that, along with Axl and Mertk (c-Mer proto-oncogene tyrosine kinase), and their ligands Gas6 (Growth arrest-specific protein 6) and Protein S, makes up the TAM (Tyro3, Axl, Mertk) signalling pathway. This pathway is involved in the negative regulation of inflammation, removal of apoptotic cells and potential induction of the tissue repair response. In inflammatory bowel disease, TAM signalling is suppressed, which, in the presence of intestinal mucosal injury, leads to an accumulation of apoptotic neutrophils and a failure of intestinal macrophages to acquire an alternative activation state (Rothlin *et al.* 2014). The present study with respect to the rectal mucosa in the Crohn's disease group is consistent with this. However, it also suggests that suppression of Tyro3 may also occur in the rectal mucosa of those with idiopathic perianal fistulae, further supporting the notions described at the end of the previous paragraph.

VEGFR2 is the principle RTK that transmits VEGF signals in the vascular endothelium. The principle effect of VEGFR2 activation is angiogenesis, which is a feature of both health and disease. Algaba *et al.* (2013) measured the concentrations of angiogenic and lymphangiogenic factors, including VEGFR2, in colonic mucosa culture supernatants in patients with endoscopically active and quiescent Crohn's disease, compared with healthy controls. They concluded the concentration of these factors correlated with disease activity. However, closer inspection of the data shows that VEGFR2 was higher in the active compared with quiescent Crohn's disease groups, but not significantly different to the healthy control group. The lowest concentration of VGEFR2 was found in the quiescent Crohn's disease group. It could therefore be the case that VEGFR2 is suppressed in those with quiescent Crohn's disease. We found that VEGFR2 levels in the fresh colonic mucosa homogenates were lower in patients both with idiopathic and Crohn's perianal fistulae, compared with healthy controls. This could suggest that expression of this RTK is suppressed in these diseases. This may also correlate with results presented in the previous chapter, where significant concentrations of VEGF were seen in each group at all specimen sites. There were no significant differences between the groups, but in the rectal mucosa there was a trend to higher expression in the healthy controls.

Table 30 Summary of phosphoprotein profile data comparisons between idiopathic and Crohn's perianal fistulae.

	Similarities	Differences
Phosphoprotein concentrations	Similar levels of 39 phosphoproteins at the four specimen sites (EGFR/ErbB1, HER2/ErbB2, HER3/ErbB3, FGFR1, FGFR3, FGFR4, InsR, IGF-IR, TrkA/NTRK1, TrkB/NTRK2, Met/HGFR, Ron/MST1R, Ret, ALK, PDGFR, c-Kit/SCFR, FLT3/Flk2, M-CSFR/CSF-1R, EphA1, EphA2, EphA3, EphB1, EphB3, EphB4, Tyro3/Dtk, Axl, Tie2/TEK, VEGFR2/KDR, Akt/PKB/Rac (at Thr308), Akt/PKB/Rac (at Ser473), p44/42 MAPK, S6 Ribosomal Protein, c-Abl, IRS-1, Zap-70, Src, Lck, Stat1 and Stat3)	None

Comparison with Current Theory

All the four specimens (fistula tract, granulation tissue, internal opening and rectal mucosa) yielded consistently positive results across both disease groups for phosphorylated EGFR/ErbB1, HER2/ErbB2 and HER3/ErbB3. The first three are receptor tyrosine kinases (RTKs) from the ErbB family and are involved in epithelial cell growth and survival. Activation leads to phosphorylation and subsequent intracellular signalling. Intracellular signal transduction utilises several pathways, including Akt and MAPK (Gerbin 2010). ErbB activation in colonic epithelial cells appears to be protective during inflammation. For example, activation of EGFR/ErbB1 by EGF stimulates proliferation, reduction in cytokine-induced apoptosis, and migration/wound healing, both *in vitro* and *in vivo* (Frey and Polk 2014). Mice that are deficient in EGFR or the ligand TGF-α develop more severe experimental colitis (Dubé *et al.* 2012; Egger *et al.* 1997). Our results for phosphorylated ErbB receptors are therefore consistent with this current knowledge. Looking at the rectal mucosa, although there were no statistically significant

differences between the groups, there was a consistent trend of higher levels of phosphorylated ErbB in the healthy controls compared with both disease groups. Suppression of ErbB would be expected in Crohn's disease mucosa, but suppression also in the idiopathic group is an interesting possibility, as it would also support the ideas that idiopathic and Crohn's perianal fistulae have a similar immunopathology and that immunopathological changes are not confined to the peri-fistula tissue in idiopathic disease. We raise this idea cautiously as the results presented in the previous chapter do not seem to fit: there were no trends in the EGF concentrations across the groups.

The four sample sites also yielded consistently positive results across both disease groups for phosphorylated FGFR1, FGFR3, FGFR4, Stat1, and Stat3. The FGFR family of RTKs is also involved in cellular proliferation, migration, survival, angiogenesis and wound healing. When ligands bind to the extracellular component, phosphorylation of the cytoplasmic kinase domain induces Akt, MAPK, and Jak/Stat intracellular signalling pathways. Numerous FGFR gene mutations have been found in many different cancers, however its role in gut homeostasis and inflammation has not been reported. One could speculate that its role in gut health and disease is similar to ErbB, given its similar functions in cell behaviour, which would then lead to similar conclusions regarding the present study's results.

Limitations

The cohort included a broad range of clinical phenotypes, representing the full spectrum of perianal fistula disease. However, this meant that the data were naturally heterogeneous. As our sample size, although comparable to the vast majority of previous studies on perianal fistula, was relatively small, differences may not have been apparent within the heterogeneity.

Collection of tissue specimens followed a protocol and in most cases performed by the same two surgeons (JH, CHK) to standardise the methods as much as possible. However, patient and operative factors influenced the size, depth and position of the

specimens taken, relative to the internal opening, and these differences in theory may have impacted on the results obtained.

By examining a broad panel of phosphoproteins, a deeper interrogation of the role of each one and how they interact in perianal fistula disease was not feasible. Only a cautious comparison and triangulation of these data with current knowledge was therefore possible.

A healthy control for specimens taken from the fistula tract, granulation tissue and internal opening was not included in this study for reasons discussed in Section 2.2.

5.5 Conclusions

After examining the relative concentrations of 28 receptor tyrosine kinases and 11 signalling nodes, when phosphorylated at tyrosine or other residues, in fresh tissue homogenates taken at four specimen sites in 60 participants with idiopathic and Crohn's perianal fistula disease, there was no clear difference in the overall phosphoprotein profile between idiopathic and Crohn's perianal fistulae.

When we compared the rectal mucosa of healthy controls against the participants with Crohn's perianal fistulae, differences were seen in six phosphoproteins: EphA1, EphA2, EphB1, EphB4, Tyro3/Dtk and VEGFR2/KDR. Considering what is already known about the role of these receptors in gut health and disease, this pattern raises the possibility that idiopathic and Crohn's perianal fistulae have similar immunopathology that is not confined to the peri-fistula tissue.

6. DYNAMIC CONTRAST-ENHANCED MRI

6.1 Introduction

MRI for perianal fistulae was first described by Lunniss *et al.* (1992) and has since emerged as the technique of choice for preoperative evaluation of perianal fistulae to improve patient outcome (Criado *et al.* 2012). It is superior to computed tomography in terms of demonstrating the soft tissue structures of interest, namely the internal and external anal sphincters and their relationship to the fistula disease; and it is superior to anal endo-ultrasonography, which can fail to demonstrate fistula tracts that are outside the close imaging field.

The use of MRI to evaluate perianal fistulae is now standard practice and is indicated in recurrent disease, suspected complex disease, non-idiopathic aetiology, and when clinical examination fails to demonstrate an external opening. Fat-suppressed T2-weighted sequences such as short tau inversion recovery (STIR) or frequency-selective fat-saturated T2-weighted fast spin-echo (FSE) usually provide the necessary information to accurately understand the course of the primary tract, the presence and anatomy of any secondary tracts and abscesses, and the anatomy of the anal canal and its relationship with the tracts. This information is useful as it can help the clinician evaluate how much of the anal sphincters are spared, and therefore the likely risks of incontinence from laying open of the fistula. The information can also aid the operative strategy as it allows the surgeon to target clinically occult disease and thus reduce recurrence. In a study of 71 patients with recurrent perianal fistula, Buchanan *et al.* found that surgery guided by MRI reduced further recurrence by 75% (Buchanan *et al.* 2002).

Interpretation of conventional MRI is usually subjective and qualitative. In an attempt to quantify the severity of disease, two image grading systems were developed. In Crohn's disease, the severity of disease can be graded using the Van Assche score (Van Assche *et al.* 2003), which consists of both anatomic variables and variables indicative of active inflammation and ranges from 0 to 22, with higher

scores indicating more severe disease. For all perianal fistulae, the St James's University Hospital Classification can be applied. This anatomical grading system arranges fistulae into five grades of increasing severity: grade 1, simple linear inter-sphincteric fistula; grade 2, inter-sphincteric with abscess or secondary tract; grade 3, trans-sphincteric; grade 4, trans-sphincteric with abscess or secondary tract in ischiorectal or ischioanal fossa; grade 5, supralevator and translevator. These grades demonstrate significant correlation with outcome (Spencer *et al.* 1998).

However, both these grading systems are still subjective, as they require a certain degree of judgement by the radiologist reviewing the images. Objective quantitative information from MRI can be obtained using dynamic contrast-enhanced (DCE) protocols. In DCE-MRI, images are acquired serially during the delivery of an intravenous contrast material to obtain volumes in four dimensions: three spatial and one temporal. The dynamic tissue enhancement of a region of interest can be seen and measured over time to produce a time-intensity curve (TIC). Local tissue characteristics such as inflammation or tumour affect the inflow of blood into the tissue of interest and subsequent distribution in the extravascular space. Thus these tissue characteristics are reflected in differences in the TIC.

DCE-MRI is now established as a clinical tool in a number of diseases including breast cancer, where quantitative data before and after treatment are used to assess response (Wang *et al.* 2014). Three methods of analysis of DCE-MRI data have been reported: TIC shape analysis, parametric analysis and pharmacokinetic modelling (Lavini *et al.* 2013). TIC shape analysis categorizes the shape of the curve against known types. Parametric analysis involves the generation of parameters describing the TIC, such as maximum enhancement, wash in rate, wash out rate and area under the TIC. Pharmacokinetic modelling permits the extraction of physiologically relevant quantities that reflect intrinsic properties of the tissue, such as micro-vascularity permeability, tissue perfusion and cellular density.

The use of DCE-MRI in perianal fistula is not established. Horsthuis *et al.* (2009) was the first to report on the use of DCE-MRI in perianal fistulae. Only Crohn's

disease patients were included in their cohort of 33. They concluded from TIC shape and parametric analysis that DCE-MRI could be used to determine disease activity in perianal Crohn's disease, and might be helpful in selecting a subpopulation of patients who should be monitored more closely for development of more extensive disease. The same institution then applied DCE-MRI with pharmacokinetic modelling in a pilot study of 16 consecutive patients with perianal Crohn's disease. A second DCE-MRI examination was also performed in six patients six weeks after starting treatment with anti-TNF-α. They concluded that maximum enhancement and wash in rate correlate with disease activity in perianal Crohn's disease, and K^{trans} (the forward transfer coefficient of gadolinium between plasma and the extracellular extravascular space) may be an indicator of the effect of therapy on patients starting anti-TNF-α. The use of DCE-MRI has not been reported in idiopathic perianal fistula disease.

The aims of this study were to: demonstrate the feasibility of DCE-MRI in both idiopathic and Crohn's perianal fistulae; provide, for the first time, reference DCE-MRI data in idiopathic disease; and compare the DCE-MRI characteristics between idiopathic and Crohn's disease groups in order to test the hypothesis that perianal fistulae of these types differ.

6.2 Methods

Participants

We selected a subgroup of participants from the whole cohort in this study. Eligibility was based on the requirement for pelvic MRI scan as part of their routine clinical evaluation. This limitation was due to the excess costs involved in performing de novo MRIs for the purposes of this research. Indications for MRI included recurrent disease or persistence of symptoms after surgery with curative intent (e.g. lay open), deterioration of symptoms after surgery with symptomatic control intent (e.g. seton), absence of an external opening and/or presence of supralevator sepsis on examination.

Prior to the recruitment of the main cohort, we recruited consecutive patients from the MRI waiting list into a pilot cohort, the purpose of which was to determine feasibility. The same inclusion and exclusion criteria as the main cohort were applied. Following DCE-MRI acquisition, the pilot subjects only underwent clinical follow-up by their direct care team. We recorded outcomes from these follow-up episodes, but did not perform PDAI and EQ-5D-5L measurements.

MRI Acquisition

Firstly, conventional MRI series were acquired. A survey sequence delineated the anatomy. A STIR sagittal sequence then followed. STIR is a Short TI Inversion Recovery technique that suppresses the signal from fat and thus improves the contrast and appearance of the fistula (white) against the surrounding ischioanal fat (black). We then acquired STIR sequences parallel (coronal oblique) and perpendicular (axial oblique) to the axis of the anal canal. This was followed by an e-THRIVE sequence in the axial oblique plane. e-THRIVE is a T1-weighted High Resolution Isotropic Volume Examination designed for DCE studies using SPAIR (SPectral Attenuated Inversion Recovery) fat suppression: a hybrid technique that offers an even homogenous fat suppression.

The dynamic MRI series was then acquired. An automated injection pump delivered a bolus of 10 ml gadolinium contrast agent followed by 30 ml normal saline at a rate of 4 ml/s into an antecubital intravenous cannula. Image acquisition started simultaneously. PJ identified the most prominent part of the fistula, and therefore the presumed site of maximum inflammation, on the previous e-THRIVE series. Centred on this area, an e-THRIVE technique acquired a six-section axial oblique volume 10 consecutive times with a temporal resolution of 4.2 seconds. A post-contrast e-THRIVE sequence was then also acquired.

A senior MRI technician (PJ) and experienced consultant gastrointestinal radiologist (AP) adapted this protocol from a standard commercial protocol for DCE-MRI of the prostate (Philips, Amsterdam, Netherlands). They chose a high temporal resolution

because previous studies have shown that most perianal fistulae show early enhancement, which is likely due to their high vascularization (Horsthuis *et al.* 2009; Ziech *et al.* 2013).

We took care to ensure these DCE-MRI studies were performed in a consistent manner: the same 3T MRI scanner (Philips, Amsterdam, Netherlands) at St Bartholomew's Hospital was used for all participants, with the same six-channel torso phased-array body coil applied around the pelvic area in the supine position; the same senior MRI technician conducted the scans using the same protocol stored on the scanner's software; the same contrast agent, injection pump, syringe, tubing and intravenous cannula diameter were used to achieve the same image enhancement conditions.

Qualitative Analysis

A departmental gastrointestinal radiologist reported the conventional series as part of routine NHS care. The student, who had been trained to interpret these images, reviewed the report and the images, and gathered data on a bespoke CRF (Appendix 3), which included the number of fistulae and presence of branching, Parks' classification, level of internal opening within the anal canal, position of the secondary tracts in relation to the levator ani, presence of horseshoe extensions, presence of associated collections (cavities > 3 mm diameter), rectal wall involvement, T2 hyperintensity, and the Van Assche Score.

Van Assche Score

We graded the severity of perianal fistula from the conventional MRI series using the Van Assche score (also known as the MRI-based score). It comprises six dimensions covering criteria of local extension of fistulas: complexity, supralevator extension, relation to the sphincters; and criteria of active inflammation: T2 hyperintensity, presence of cavities/abscesses, and rectal wall involvement. Van Assche *et al.* (2003) devised and developed the score using the MRI data from 18 patients with Crohn's disease. The scoring system demonstrated good inter-observer concordance, with κ

values ranging from 0.79 to 1.00, and overall significant correlation with $p < 0.001$. The score was also sensitive to change: patients who had a clinical response infliximab treatment showed a reduction in the MRI-based score at 6 and 46 weeks after commencement. Subsequent studies also showed a reduction in the Van Assche score with a decrease in the clinical severity of the disease (Karmiris *et al.* 2011; Kulkarni *et al.* 2014). One study did not show this concordance, although it was limited by the small number of patients ($N = 16$) included in the analysis (Horsthuis *et al.* 2011).

The current study did not include T2-weighted images. In the Van Assche score, the most important measure of local inflammation is T2 hyperintensity. However, gadolinium-enhanced T1-weighted images are better indicators of fistula activity (Semelka *et al.* 1997). On gadolinium-enhanced T1-weighted images, a marked increase in signal intensity of inflammatory tissue can be seen because of increased tissue perfusion (Weinmann *et al.* 1984). Therefore, as a proxy in this study, we estimated fistula hyperintensity from the post-contrast e-THRIVE series.

Quantitative Analysis

The student analysed the dynamic series using the Extended MR Workspace (version 2.6.3.5, Philips, Amsterdam, Netherlands). Within the six sections dynamic volume, the section with the most extensive and most hyperintense lesion was used for analysis. The student, aided by AP, manually drew a single oval-shaped region of interest around the fistula on the last dynamic image of the chosen section, corresponding to 42 seconds after injection (Figure 39). For each region of interest, the software calculated the maximum enhancement, maximum relative enhancement, wash in rate, wash out rate, area under the curve and plotted a time-intensity curve (TIC). The student classified the shape of the TIC by comparing it against a standard chart taken from Lavini *et al.* (2007; Figure 40).

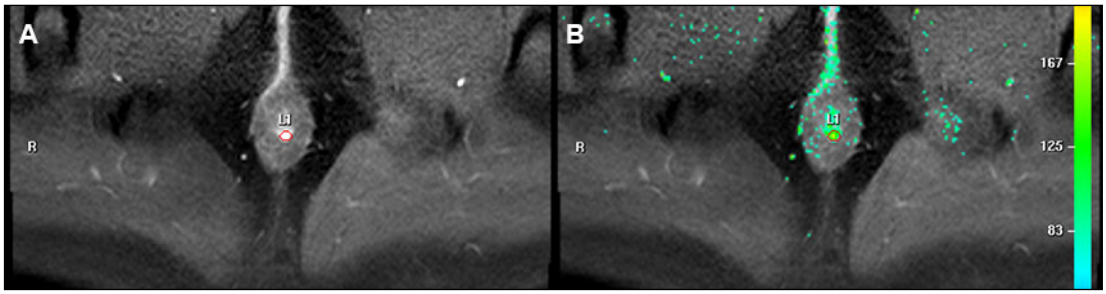

Figure 39 DCE-MRI. (A) Region of interest drawn around the fistula where it is most prominent. (B) Perfusion heat map overlaid.

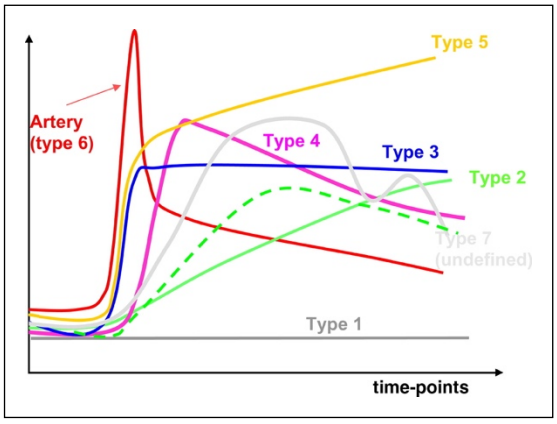

Figure 40 Standard chart used to classify time-intensity curves (Lavini *et al.* 2007). Type 1 (gray), no enhancement; Type 2 (green), slow enhancement, maximum of the curve is reached after half scan; Type 3 (blue), quick enhancement, followed by a signal plateau; Type 4 (magenta), fast enhancement and quick washout; Type 5 (yellow), quick enhancement, followed by a slow constant enhancement; Type 6 (red), artery; Type 7 (white/light gray), all others.

6.3 Results

Participant Characteristics

Eight participants from the main cohort and 16 from the pilot (March to September 2013) underwent DCE-MRI. Thus a total of 24 participants were included in this study, including 15 participants with idiopathic and nine with Crohn's perianal fistulae. There was a male preponderance (2:1) and the mean age was 36.2 years (SD = 14.5) in keeping with the general epidemiology of perianal fistula disease. The majority were of Asian ethnicity, reflecting the local population demographics.

The median time since fistula development at recruitment was eight months (IQR = 4–26) and the median number of previous operations was one (0–2). Four (17%) had

previously had surgery with curative intent. Further baseline characteristics are detailed in Table 31.

In the Crohn's disease group, participants had a moderately lower median age and the majority had received anti-TNF-α therapy. The mean PDAI (measured only in the main cohort) was 12.0 (SD = 2.6). Follow up was for a median of 30 months (IQR = 21–50).

Conventional MRI Characteristics

Most of the fistulae were single (n = 22, 92%) and trans-sphincteric (19, 79%). Five (21%) were high, 14 (58%) had secondary tracts, eight (33%) had horseshoe extensions, 10 (42%) had associated collections and four (17%) had a thickened rectum (Table 32). The mean Van Assche score was 11.4 (SD = 5.2). Fistulae morphology ranged through all described types. The majority of the participants had complex fistula morphologies with a Van Assche score indicating significant disease activity. The distribution of the characteristics between the groups was similar, apart from thickened rectum, which was only seen in the Crohn's disease group.

Dynamic Contrast-Enhanced MRI Parametric Analysis

DCE-MRI measurements were consistently obtained from all participants. The mean maximum enhancement, maximum relative enhancement, wash in rate, wash out rate and area under the TIC measurements are presented in Table 33.

There were no differences in any of the DCE-MRI measurements between the idiopathic and Crohn's disease groups. There were also no significant differences when sub-grouped by fistula disease duration (<12 *versus* ≥ 12 months; Table 53 and Table 54 in Appendix 8). When sub-grouped by Parks' classification (inter-sphincteric *versus* trans- or supra-sphincteric), the mean maximum enhancement (p = 0.04) and mean maximum relative enhancement (p = 0.03) were both significantly higher in trans- or supra-sphincteric fistulae (Figure 41; Table 55 in

Appendix 8). The mean area under TIC was also higher but this trend did not reach statistical significance ($p = 0.06$).

Table 31 Participant characteristics in DCE-MRI study. SD, standard deviation; IQR, interquartile range.

	Idiopathic	Crohn's Disease	All
n	15	9	24
Male	10 (67%)	6 (67%)	16 (67%)
Mean age (SD), years	40.5 (14.9)	29.0 (11.2)	36.2 (14.5)
Ethnic origin:			
White	2 (13%)	5 (56%)	7 (29%)
Asian	7 (47%)	4 (44%)	11 (46%)
Black	2 (13%)	0	2 (8%)
Other	4 (27%)	0	4 (17%)
Median fistula duration (IQR), months	10 (4–18)	8 (4–40)	8 (4–26)
Previously received antibiotics	6 (40%)	0	6 (25%)
Previously received anti-TNF-α	0	8 (89%)	8 (33%)
Median previous operations (IQR)	0 (0–2)	1 (0–1)	1 (0–2)
Previously had surgery with curative intent	1 (7%)	3 (33%)	4 (17%)
Current smoker	4 (27%)	0	4 (17%)

Table 32 Conventional MRI characteristics. SD, standard deviation.

	Idiopathic	Crohn's Disease	All
Number of fistulae:			
Single unbranched	7 (47%)	3 (33%)	10 (42%)
Single branched	8 (53%)	4 (44%)	12 (50%)
Multiple	0	2 (22%)	2 (8%)
Parks' classification:			
Inter-sphincteric	3 (20%)	1 (11%)	4 (17%)
Trans-sphincteric	12 (80%)	7 (78%)	19 (79%)
Supra-sphincteric	0	1 (11%)	1 (4%)
High fistula on MRI at baseline	3 (20%)	2 (22%)	5 (21%)
Secondary tract(s):			
None	6 (40%)	4 (44%)	10 (42%)
Infralevator	8 (53%)	4 (44%)	12 (50%)
Supralevator	1 (7%)	1 (11%)	2 (8%)
Horseshoe extension(s)	6 (40%)	2 (22%)	8 (33%)
Collection(s)	5 (33%)	5 (56%)	10 (42%)
Thickened rectum	0	4 (44%)	4 (17%)
Fistula hyperintensity:			
Absent	2 (13%)	0	2 (8%)
Mild	8 (53%)	5 (56%)	13 (54%)
Pronounced	5 (33%)	4 (44%)	9 (38%)
Mean Van Assche score (SD)	10.1 (5.0)	13.4 (5.2)	11.4 (5.2)

Table 33 DCE-MRI characteristics. Hypotheses tested using T test (significance level 0.05). SD, standard deviation; CI, confidence interval; TIC, time-intensity curve. NB these measurements have no units.

	Idiopathic	Crohn's Disease	All	Mean difference	*p*
Mean max enhancement (SD, 95% CI)	688 (431)	723 (352)	701 (395)	35 (-318–388)	0.84
Mean max relative enhancement (SD, 95% CI)	0.862 (0.417)	0.965 (0.514)	0.900 (0.448)	0.103 (-0.295–0.501)	0.60
Mean wash in rate (SD, 95% CI)	73.2 (48.8)	74.3 (37.6)	73.6 (44)	1.1 (-38.3–40.5)	0.95
Mean wash out rate (SD, 95% CI)	20.8 (26.4)	4.7 (3.3)	13.7 (20.6)	-16.2 (-48.0–15.7)	0.27
Mean area under TIC (SD, 95% CI)	11516 (10741)	13376 (7660)	12213 (9564)	1860 (-6652–10372)	0.66

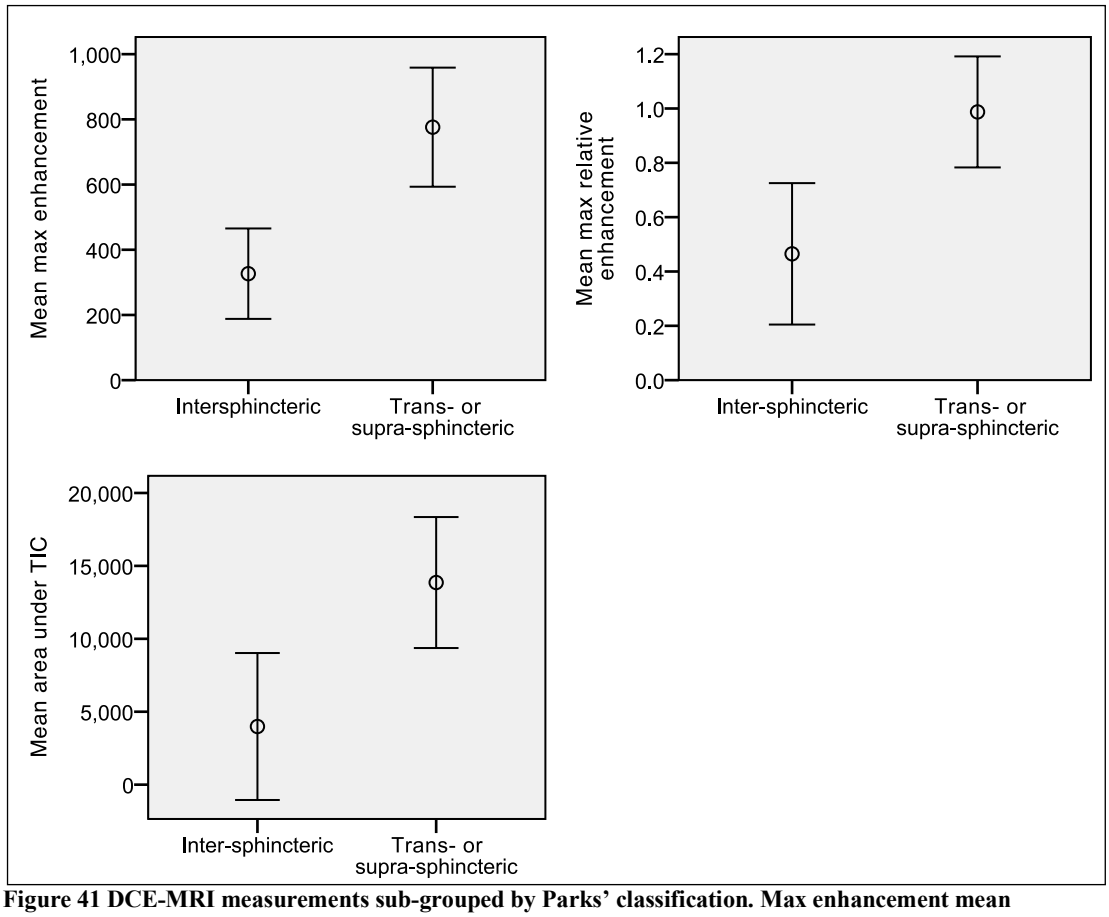

Figure 41 DCE-MRI measurements sub-grouped by Parks' classification. Max enhancement mean difference 449 (95% CI = 36–863; *p* = 0.04), max relative enhancement mean difference 0.522 (0.056–0.988; *p* = 0.03), area under TIC mean difference 9872 (-343–20087; *p* = 0.06). TIC, time intensity curve.

Time Intensity Curve Shape Analysis

TIC types 2, 3, 4 and 5 were observed. Examples are shown in Figure 42. The commonest was type 3 (Table 34), and overall, 21 (87%) had a TIC with a quick enhancement phase (type 3–5). There was no difference in the distribution of TIC types between the idiopathic and Crohn's disease groups ($p = 0.37$ Fisher's Exact Test).

There were no significant differences in the distribution of Parks' classification (inter- *versus* trans- or supra-sphincteric), fistula disease duration (<12 *versus* ≥ 12 months) and treatment outcome when sub-grouped into quick enhancement TIC, types 3–5, *versus* slow enhancement TIC, type 2 (Table 56 in Appendix 8).

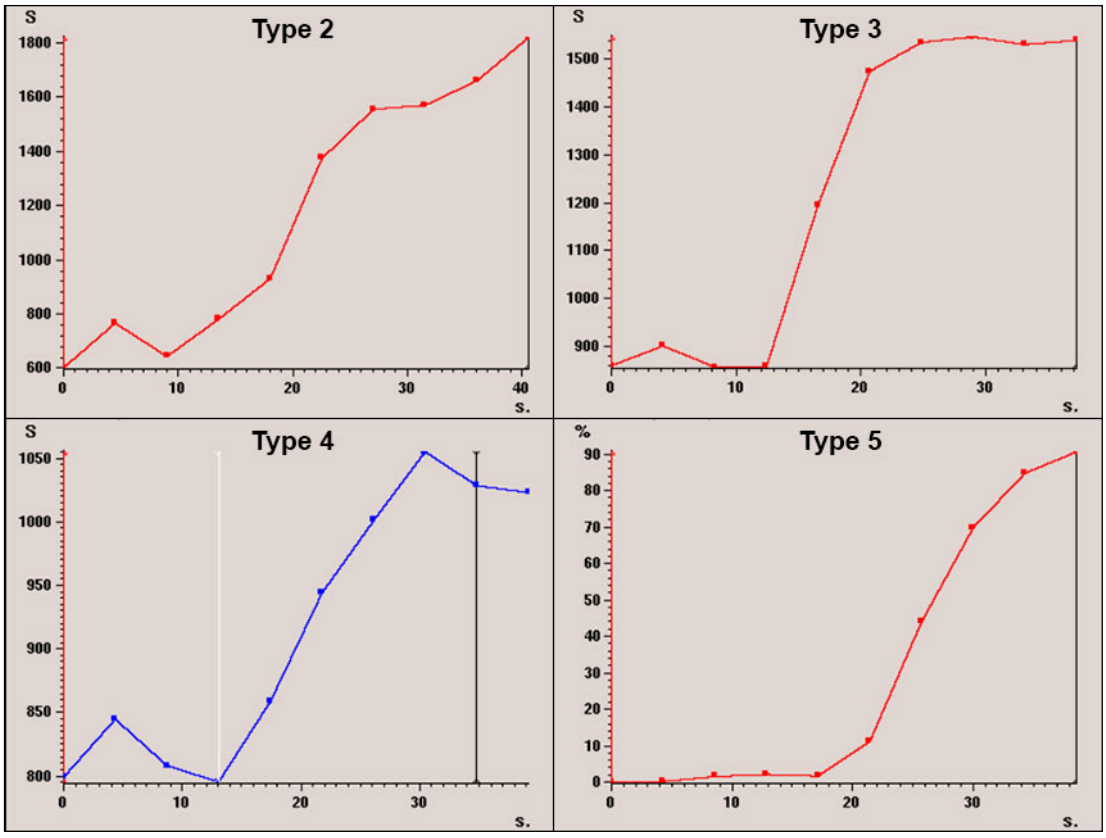

Figure 42 Examples of the time-intensity curve types.

Table 34 Time intensity curve (TIC) types. No significant differences found between the groups ($p = 0.37$ Fisher's Exact Test).

TIC type	Idiopathic	Crohn's Disease	All
2	1 (7%)	2 (22%)	3 (13%)
3	7 (47%)	5 (56%)	12 (50%)
4	1 (7%)	1 (11%)	2 (8%)
5	6 (40%)	1 (11%)	7 (29%)

6.4 Discussion

We aimed to demonstrate the feasibility of DCE-MRI in both idiopathic and Crohn's perianal fistulae; to provide for the first time reference DCE-MRI data in idiopathic disease; and to compare the DCE-MRI characteristics between idiopathic and Crohn's disease groups in order to test the hypothesis that perianal fistulae of these types differ perhaps reflecting differences in pathophysiology.

Twenty-four participants were included consisting 16 participants from the pilot study and 8 participants from the main study. The gender and age distributions were in keeping with the general epidemiology. The cohort had a wide distribution of clinical phenotypes: number of fistulae, Parks' classification, high and low fistulae, secondary tracts, horseshoe extensions, collections and rectal thickening, thus being a fair representation of the population. These characteristics were also evenly distributed between the idiopathic and Crohn's disease groups, except for previous anti-TNF-α therapy: almost all participants in the Crohn's disease group had received or were currently receiving anti-TNF-α therapy, compared with none in the idiopathic group.

Obtaining DCE-MRI measurements was feasible. The methods did not fail in any participant. These techniques were previously reported in exclusively Crohn's perianal fistulae cohorts (Horsthuis *et al.* 2009; Villa *et al.* 2012; Ziech *et al.* 2013). Although idiopathic fistulae are generally less thick and prominent on MRI, which

makes drawing a region of interest around them more difficult, we demonstrated that DCE-MRI measurements are also feasible in idiopathic disease.

There were no differences in any of the DCE-MRI measurements between the idiopathic and Crohn's disease groups. As these measurements are an indirect measure of tissue vascularity and permeability, they are thus an indicator of local tissue inflammation. These data suggest there is no obvious difference in the degree of inflammation associated with idiopathic and Crohn's perianal fistulae. It is however possible that a larger sample size is needed to find small differences.

Further sub-group analysis suggested that DCE-MRI measurements also do not correlate with fistula disease duration or treatment outcome. However significant differences were found when sub-grouped by Parks' classification. We found higher mean maximum enhancement and maximum relative enhancement in those with trans- or supra-sphincteric fistulae. This may suggest those with more pathoanatomically advanced disease have a greater degree of peri-fistula inflammation.

The majority of the perianal fistulae had a TIC with a quick enhancement phase (types 3–5). TIC shape reflects tissue viability and permeability to the contrast agent from the capillary to the extravascular space, from which the agent is later reabsorbed by the blood pool, resulting eventually in a signal decrease (Lavini *et al.* 2013). Areas of high perfusion and permeability, such as acutely inflamed tissue, typically show a quick enhancement; areas of low perfusion and permeability, such as fibrotic tissue tend to enhance in a much slower fashion, and the signal does not decrease until after the end of the DCE-MRI scan (TIC type 2).

TIC shape analysis, which is established and standardised in breast imaging, is still evolving in other diseases such as perianal fistulae. Horsthuis *et al.* (2009) used a modified method to analyse the TIC shapes. Instead of obtaining a single averaged TIC from a region of interest, the authors measured the frequency of the different TIC types on a pixel-by-pixel basis within the region of interest. They found that

significantly higher numbers of quickly enhancing pixels were seen in patients who then developed new perianal abscesses and needed medication changes during follow-up. Ziech *et al.* (2013) also used the same method but only reported that total pixel counts of individual TIC types had moderate to strong correlation with the Van Assche score.

We found no differences in the distribution of the TIC types between the idiopathic and Crohn's disease groups. This may be further evidence for a similar inflammatory phenotype between the two groups, although as the significance of TIC types in perianal fistula disease in general is still unknown, further study is required before this conclusion can be made. The above comparisons are summarised in Table 35.

Table 35 Summary of DCE-MRI data comparisons between idiopathic and Crohn's disease perianal fistulae. DCE-MRI, dynamic contrast-enhanced-magnetic resonance imaging; TIC, time-intensity curve.

	Similarities	Differences
DCE-MRI	Similar mean maximum enhancement, maximum relative enhancement, wash in rate, wash out rate, area under the TIC and TIC types	None

Limitations

Participants were selected based on their clinical indication for MRI. We therefore excluded many patients such as those with simple primary fistulae, and those who had been recently imaged before recruitment. The cohort was also heterogeneous (primary and recurrent disease, treatment-naïve and previously operated). Future studies would need to consider performing DCE-MRI in all participants at the same point in the natural history of their perianal fistula disease, and reducing the heterogeneity of the cohort.

Because almost all participants in the Crohn's disease group were subjected to anti-TNF-α, the results in this group could have been attenuated: anti-TNF-α may have reduced peri-fistula inflammation and thus disease severity, resulting in any

difference between the groups being nullified. This arose due to the study's pragmatic design: inclusion was not restricted to those who were treatment-naïve.

PDAI was used as a clinical measure of disease severity. However it was only measured in the main cohort. It is likely that the PDAI distribution in the pilot cohort is similar to the main cohort, given that the fistula characteristics and indications for performing the MRI were the same. Nevertheless, this limited analysis of this variable.

Distribution of the PDAI was confined to the middle of the index's scale. Due to the indications for MRI and the inclusion criteria, there were no participants with PDAI of ≤ 4, the cut-off above which active disease requiring medical or surgical treatment is suggested. There were also no participants with PDAI towards the top of the scale. It might be the case that a wider range of disease severity is needed before differences in these DCE-MRI data are seen.

Parametric analysis of DCE-MRI signal intensity is vulnerable to variability across participants in clinical studies as the parameters used in the T1-weighted MRI sequence significantly affect the relationship between the amount of contrast agent in the tissue and the signal intensity change (Evelhoch 1999). This inter-participant variability was minimised by keeping all parameters and methods the same for all participants: the MRI machine, the contrast injector, the contrast agent, the MRI sequence protocol, the MRI technician running the sequences, and the post-hoc analysis software remained consistent throughout the study. More accurate quantitative analysis using pharmacokinetic models have been described in the literature (Tofts *et al.* 1999). These techniques have the advantage of extracting physiologically relevant quantities that reflect the intrinsic properties of the tissue. However, its complex implementation was beyond the expertise available to the study.

Due to limited resources, it was not possible conduct this study in a way that enabled analysis of the intra- and inter-observer variability. This would have provided a

degree of confidence in the reliability of the measurements, as although the majority of the DCE analysis is quantitative and objective, defining the region of interest requires a degree of subjective human judgement.

6.5 Conclusions

We examined the DCE-MRI characteristics of perianal fistulae in 24 participants with idiopathic and Crohn's disease. The feasibility of this modality in idiopathic disease was demonstrated for the first time. Data for this cohort is now available and will serve as a useful reference for future studies.

We found no differences in the DCE-MRI measurements and the TIC types between the idiopathic and Crohn's disease groups. However, secondary sub-group analysis revealed the mean maximum enhancement and maximum relative enhancement were significantly higher in participants with a more advanced pathoanatomy (trans- or supra-sphincteric fistulae). Further study into this area needs to consider performing *de novo* MRI in all participants, a more homogenous cohort, and including inter-observer variability assessment.

7. CONCLUSION

7.1 Summary

This research aimed to test the broad hypothesis that idiopathic and Crohn's perianal fistulae differ in their pathogenesis and pathophysiology. We prospectively recruited a cohort of 61 participants and phenotyped them in detail using clinical assessment, MRI, operative assessment, biopsy, and clinical follow-up. We interrogated the biopsy samples in the laboratory to characterize their profiles for 30 cytokines and 39 phosphoproteins. Over 12,000 clinical and 23,500 laboratory measurements were made.

Chapter 3: Clinical Data

- This is the largest study to date to phenotype perianal fistula disease in detail in both idiopathic and Crohn's disease patients. Severe disease appears to be commoner in Crohn's perianal fistulae compared with idiopathic perianal fistulae. However, there were also many phenotypic similarities between the groups, and thus overall, the groups did not appear to be phenotypically distinct.

- These data are also probably the most complete dataset to date using patient reported outcome measures, namely PDAI and EQ-5D, in these two groups. The PDAI appears to be a feasible, useful, stable and sensitive tool in measuring the disease activity in idiopathic as well as Crohn's perianal fistulae. Patients with idiopathic and Crohn's perianal fistulae have a similarly impaired quality of life, as measured by the EQ VAS and EQ index. Furthermore, the level of disease burden is akin to other significant chronic health conditions. Further validation studies are required and would lead to improved methodology in future perianal fistula disease research.

- A comparison of the bacterial isolates from cultures of intraoperative specimens showed a wide range of organisms, which was similar in both groups.

Chapter 4: Cytokine Profiles

- The concentrations of 30 cytokines at 4 specimen sites in 60 participants with idiopathic and Crohn's perianal fistulae were examined. We found no clear differences in the overall cytokine profiles between the groups. Furthermore, when comparing the rectal mucosa of healthy controls to the participants with Crohn's perianal fistulae, no differences were observed.

- Only two significant differences in individual cytokines were found. At the internal opening specimen site, IL-12p70 was higher, and IL-1RA/IL-1β ratio was lower in the Crohn's disease group. These findings are consistent with current knowledge on the general pathophysiology of Crohn's disease. However, given that multiple hypothesis tests were performed, these results should be treated with caution and further focussed research is needed. Immunocytochemistry, using normal anal mucosa as the control, for example, would offer further interrogation.

- These data agree with and add considerably to what Tozer (2011) found using similar techniques. Significant levels of G-CSF, IL-6, IL-8, MCP-1, RANTES and VEGF were found across all specimens and groups. These findings are broadly consistent with current theories on inflammation, and may point towards further research opportunities in perianal fistulae.

- Previous studies suggested that IL-1β, IL-6, IL-8, and TNF-α, may have an important role in perianal fistulae immunopathology (Kiehne et al. 2007; Ruffolo et al. 2007; Ruffolo et al. 2008; Tozer 2011). These data also suggest IL-1β, IL-6 and IL-8 may be important. However, results regarding TNF-α were unremarkable.

Chapter 5: Phosphoprotein Profiles

- After examining the relative concentrations of 28 receptor tyrosine kinases and 11 signalling nodes, when phosphorylated at tyrosine or other residues, in fresh tissue homogenates taken at four specimen sites in 60 participants with idiopathic and

Crohn's perianal fistula disease, there was no clear difference in the overall phosphoprotein profile between idiopathic and Crohn's perianal fistulae.

- When we compared the rectal mucosa of healthy controls against the participants with Crohn's perianal fistulae, differences were seen in six phosphoproteins: EphA1, EphA2, EphB1, EphB4, Tyro3/Dtk and VEGFR2/KDR. Considering what is already known about the role of these receptors in gut health and disease, this pattern raises the possibility that idiopathic and Crohn's perianal fistulae have similar immunopathology that is not confined to the peri-fistula tissue.

Chapter 6: Dynamic Contrast-Enhanced MRI

- We examined the DCE-MRI characteristics of perianal fistulae in 24 participants with idiopathic and Crohn's disease. The feasibility of this modality in idiopathic disease was demonstrated for the first time. Data for this cohort is now available and will serve as a useful reference for future studies.

- We found no differences in the DCE-MRI measurements and the TIC types between the idiopathic and Crohn's disease groups. However, secondary sub-group analysis revealed the mean maximum enhancement and maximum relative enhancement were significantly higher in participants with a more advanced pathoanatomy (trans- or supra-sphincteric fistulae). Further study into this area needs to consider performing *de novo* MRI in all participants, a more homogenous cohort, and including inter-observer variability assessment.

Limitations

The pragmatic study design brought certain limitations. We included patients from all stages of management, from those who were treatment-naïve, to those who had had multiple surgical procedures aimed at achieving a cure. This allowed effective recruitment within a reasonable timeframe. However this did increase participant heterogeneity.

We only recruited patients who were planned for surgery for one reason or another. Therefore those with perianal fistula disease that was too mild to meet the threshold for surgery were excluded. This selection bias limits the applicability of these data to a non-operated population. Furthermore, the threshold for surgery could have been different between the groups due to differing clinical strategies. If so, this selection bias may have introduced a difference between the groups.

The main study site was a tertiary referral centre. A more representative sample might have been achieved through multicentre recruitment. However, despite this, the recruited cohort had participants with a wide distribution of disease phenotypes and an expected range of treatment outcomes.

We did not perform a formal sample size calculation, as there were no prior relevant data. However this is the largest study to date to phenotype the disease across both groups in detail.

Further limitations specific to each results section were discussed within their respective chapters.

7.2 Overall Conclusions

In summary, over 200 variables were measured in each participant within this cohort, and only a handful showed possible differences between idiopathic and Crohn's disease groups (Table 36). Further research is required to look deeper into these particular differences. Certainly, these data do not give clear support to the study hypothesis that idiopathic and Crohn's perianal fistulae differ in their pathogenesis and pathophysiology.

As argued in Chapter 1, the majority of perianal fistula research to date has been conducted within the same paradigm built upon the assumption that idiopathic and Crohn's perianal fistulae differ in their pathogenesis and pathophysiology. Only a handful of studies have attempted to compare the characteristics of perianal fistulae from each group. All these studies have assumed there is a difference as the

idiopathic group each time has been used as a quasi-control group against which the Crohn's disease group is compared. These studies have indeed highlighted some differences between the groups.

However, the careful review of the literature in Chapter 1 through a neutral construct revealed that there just as many similarities as there are differences between idiopathic and Crohn's perianal fistula disease. The present study is commensurate with this.

It may be that further research to test the hypothesis that idiopathic and Crohn's perianal fistulae differ in their pathogenesis and pathophysiology is required before it is proven. An alternative explanation may be that the chronic fistula is a common pathway for both idiopathic and Crohn's perianal fistulae, but the initial pathogenesis or mechanism of susceptibility is separate. Countering this is the argument that if the two diseases begin separately, then differences between each type should be seen throughout the full course of the disease.

However, it may also be time to consider approaching perianal fistula research from the antithesis. From this stance, the underlying assumption would be that idiopathic and Crohn's perianal fistulae are the same pathology on a spectrum across which the pathogenic and pathophysiological features are distributed in a skewed manner. This notion is analogous to clinical practice. Surgeons often observe that some patients with complex idiopathic perianal fistulae have a disease that behaves like perianal Crohn's disease, except all subsequent investigations to diagnose Crohn's disease prove negative. Within this new research paradigm, the idiopathic group would no longer be a valid quasi-control and instead, other control groups would have to be employed. This may be the key to unravelling our understanding of the disease's aetiology. It would also be a construct within which trials of biological therapy, such as infliximab, could be justified for idiopathic disease.

Table 36 Summary of data comparisons between idiopathic and Crohn's disease perianal fistulae. DCE-MRI, dynamic contrast-enhanced-magnetic resonance imaging; PDAI, perianal disease activity index; TIC, time-intensity curve; VAS, visual analogue score.

	Similarities	Differences
Baseline PDAI		Significantly higher PDAI in Crohn's disease
Baseline EQ-5D-5L	Similar EQ VAS and EQ index	
Morphology	Similar distribution of types by Parks' classification	More multiple fistulae in Crohn's disease
	Similar prevalence of high fistulae and horseshoe extensions	Significantly more supralevator extensions, collections and rectal thickening in Crohn's disease
Microbiological culture	Similar isolates	
Post-operative PDAI	Similar decrease in post-operative PDAI	
Post-operative EQ-5D-5L	Similar decrease in post-operative EQ VAS and EQ index	
Cytokine concentrations	Similar concentrations of 27 cytokines at all four biopsy sites (EGF, eotaxin, G-CSF, GM-CSF, IFN-α2, IFN-γ, IL-10, IL-12p40, IL-13, IL-15, IL-17, IL-1α, IL-2, IL-3, IL-4, IL-5, IL-6, IL-7, IL-8, IP-10, MCP-1, MIP-1α, MIP-1β, TNF-α, TNF-β, RANTES and VEGF)	Significantly higher IL-12p70 concentration at internal opening in Crohn's disease
		Significantly lower IL-1RA/IL-1β ratio concentration at internal opening in Crohn's disease
Phosphoprotein concentrations	Similar levels of 39 phosphoproteins at the four specimen sites (EGFR/ErbB1, HER2/ErbB2, HER3/ErbB3, FGFR1, FGFR3, FGFR4, InsR, IGF-IR, TrkA/NTRK1, TrkB/NTRK2, Met/HGFR, Ron/MST1R, Ret, ALK, PDGFR, c-Kit/SCFR, FLT3/Flk2, M-CSFR/CSF-1R, EphA1, EphA2, EphA3, EphB1, EphB3, EphB4, Tyro3/Dtk, Axl, Tie2/TEK, VEGFR2/KDR, Akt/PKB/Rac (at Thr308), Akt/PKB/Rac (at Ser473), p44/42 MAPK, S6 Ribosomal Protein, c-Abl, IRS-1, Zap-70, Src, Lck, Stat1 and Stat3)	
DCE-MRI	Similar mean maximum enhancement, maximum relative enhancement, wash in rate, wash out rate, area under the TIC and TIC types	

7.3 Future Research

This study has identified some worthwhile targets for future basic science research: the role of IL-12p70, and the IL-1RA/IL-1β ratio at the internal opening; the role of EphA1, EphA2, EphB1, EphB4, Tyro3/Dtk and VEGFR2/KDR in the rectal mucosa. And further clinical research into the validity of PDAI in non-Crohn's perianal fistula disease and the utility of DCE-MRI in all types of perianal fistulae is also warranted.[§]

However, greater advances may ultimately come from studies working from the paradigm that idiopathic and Crohn's perianal fistulae are the same disease entity. Thus, they would be aimed at finding pathophysiological mechanisms in idiopathic perianal fistula disease that are already known to be of importance in Crohn's perianal fistulae. This would lead to greater insights into the disease across both these groups. The long-term goal of such research would be to support the hypothesis that idiopathic and Crohn's perianal fistulae share the same pathogenesis and pathophysiology. This would then be translatable into clinical trials of infliximab and other biological agents in idiopathic perianal fistulae. With curative outcome in idiopathic perianal fistulae having essentially not improved significantly since Hippocrates, such trials would hold the promise of a step change in its management.

[§] The Bowel Disease Research Foundation's on-going ENIGMA project, developed alongside the Association of Coloproctology of Great Britain and Ireland and the British Society of Gastroenterology, includes the development of patient reported outcomes in perianal fistula disease.

8. DECLARATIONS

Ethics

This research was reviewed and approved by Queen's Square Research Ethics Committee in March 2014 (reference number 14/LO/0071).

Funding

This work was supported by the Bowel & Cancer Research charity in 2014–16, grant number MMBG1J3R, to cover laboratory consumables, the student's university tuition fees and costs for attending one conference.

The student's salary was provided in part by NIHR Enteric HTC and in part by the National Centre for Bowel Research, Queen Mary University of London.

Conflicts of Interest

Professor Knowles is a trustee of the Bowel & Cancer Research charity, but was excluded from discussions and decisions regarding the funding of this project. He is also the co-director of NIHR Enteric HTC and the National Centre for Bowel Research. However, decisions regarding employment of the student were subjected to committee approval and the University's due process.

The student has no conflicts of interest.

9. BIBLIOGRAPHY

Agrez, M. *et al.* (1999). The alpha v beta 6 integrin induces gelatinase B secretion in colon cancer cells. *International Journal of Cancer*, 81(1), pp.90–97.

Algaba, A. *et al.* (2013). Relationship between levels of angiogenic and lymphangiogenic factors and the endoscopic, histological and clinical activity, and acute-phase reactants in patients with inflammatory bowel disease. *Journal of Crohn's & Colitis*, 7(11), pp.e569-579.

Allan, A. *et al.* (1992). Clinical index to quantitate symptoms of perianal Crohn's disease. *Diseases of the Colon and Rectum*, 35(7), pp.656–661.

Angelberger, S. *et al.* (2008). NOD2/CARD15 gene variants are linked to failure of antibiotic treatment in perianal fistulating Crohn's disease. *The American journal of gastroenterology*, 103(5), pp.1197–1202.

Arderne, J. and Power, D. (1910). *Treatises of fistula in ano, haemorrhoids and clysters*. London : Published for the Early English Text Society by Kegan Paul, Trench, Trübner. [online]. Available from: http://archive.org/details/treatisesoffistu00ardeuoft [Accessed November 26, 2015].

Atkin, G.K. *et al.* (2011). For many high anal fistulas, lay open is still a good option. *Techniques in Coloproctology*, 15(2), pp.143–150.

Atreya, R. *et al.* (2000). Blockade of interleukin 6 trans signaling suppresses T-cell resistance against apoptosis in chronic intestinal inflammation: evidence in crohn disease and experimental colitis in vivo. *Nature Medicine*, 6(5), pp.583–588.

Badid, C. *et al.* (2000). Role of myofibroblasts during normal tissue repair and excessive scarring: interest of their assessment in nephropathies. *Histology and Histopathology*, 15(1), pp.269–280.

Balogh, G. (1999). Tube loop (seton) drainage treatment of recurrent extrasphincteric perianal fistulae. *American Journal of Surgery*, 177(2), pp.147–149.

Banks, C. *et al.* (2003). Chemokine expression in IBD. Mucosal chemokine expression is unselectively increased in both ulcerative colitis and Crohn's disease. *The Journal of Pathology*, 199(1), pp.28–35.

Barreiro, M. *et al.* (2005). Association of NOD2/CARD15 mutations with previous surgical procedures in Crohn's disease. *Revista Española De Enfermedades Digestivas: Organo Oficial De La Sociedad Española De Patología Digestiva*, 97(8), pp.547–553.

Barts Health NHS Trust. (2015). About Barts Health NHS Trust. *Barts Health NHS Trust*. [online]. Available from: http://www.bartshealth.nhs.uk/about-us/ [Accessed August 3, 2015].

Bataille, F. *et al.* (2008). Evidence for a role of epithelial mesenchymal transition during pathogenesis of fistulae in Crohn's disease. *Inflammatory bowel diseases*, 14(11), pp.1514–1527.

Bataille, F. *et al.* (2004). Morphological characterisation of Crohn's disease fistulae. *Gut*, 53(9), pp.1314–1321.

Baugh, M.D. *et al.* (1999). Matrix metalloproteinase levels are elevated in inflammatory bowel disease. *Gastroenterology*, 117(4), pp.814–822.

Baumgart, D.C. and Sandborn, W.J. (2012). Crohn's disease. *The Lancet*, 380(9853), pp.1590–1605.

Bernstein, L.H. *et al.* (1980). Healing of perineal Crohn's disease with metronidazole. *Gastroenterology*, 79(2), pp.357–365.

Bianco, A.M., Girardelli, M. and Tommasini, A. (2015). Genetics of inflammatory bowel disease from multifactorial to monogenic forms. *World Journal of Gastroenterology*, 21(43), pp.12296–12310.

Bleier, J.I.S., Moloo, H. and Goldberg, S.M. (2010). Ligation of the intersphincteric fistula tract: an effective new technique for complex fistulas. *Diseases of the Colon and Rectum*, 53(1), pp.43–46.

Brandt, L.J. *et al.* (1982). Metronidazole therapy for perineal Crohn's disease: a follow-up study. *Gastroenterology*, 83(2), pp.383–387.

Brenmoehl, J. *et al.* (2007). Evidence for a differential expression of fibronectin splice forms ED-A and ED-B in Crohn's disease (CD) mucosa. *International Journal of Colorectal Disease*, 22(6), pp.611–623.

Brook, I. and Frazier, E.H. (1997). The aerobic and anaerobic bacteriology of perirectal abscesses. *Journal of Clinical Microbiology*, 35(11), pp.2974–2976.

Buchanan, G. *et al.* (2002). Effect of MRI on clinical outcome of recurrent fistula-in-ano. *Lancet*, 360(9346), p.1661.

Buchanan, G.N. *et al.* (2004). Clinical examination, endosonography, and MR imaging in preoperative assessment of fistula in ano: comparison with outcome-based reference standard. *Radiology*, 233(3), pp.674–681.

Buchanan, G.N. *et al.* (2004). Long-term outcome following loose-seton technique for external sphincter preservation in complex anal fistula. *The British Journal of Surgery*, 91(4), pp.476–480.

Cadwell, K. *et al.* (2008). A unique role for autophagy and Atg16L1 in Paneth cells in murine and human intestine. *Nature*, 456(7219), pp.259–263.

Cavanaugh, M., Hyman, N. and Osler, T. (2002). Fecal Incontinence Severity Index After Fistulotomy. *Diseases of the Colon & Rectum*, 45(3), pp.349–353.

Cell Signaling Technology. (2015). PathScan® RTK Signaling Antibody Array Kit (Chemiluminescent Readout) #7982. [online]. Available from: http://www.cellsignal.com/products/antibody-arrays/pathscan-rtk-signaling-antibody-array-kit-chemiluminescent-readout/7982.

Chauhan, S., Mandell, M.A. and Deretic, V. (2015). Mechanism of action of the tuberculosis and Crohn disease risk factor IRGM in autophagy. *Autophagy*, p.0.

Chen, S.K. and Hollender, L. (1995). Digitizing of radiographs with a flatbed scanner. *Journal of Dentistry*, 23(4), pp.205–208.

Chew, S.S.B. *et al.* (2003). Anal fistula: Levovist-enhanced endoanal ultrasound: a pilot study. *Diseases of the Colon and Rectum*, 46(3), pp.377–384.

Clevers, H.C. and Bevins, C.L. (2013). Paneth cells: maestros of the small intestinal crypts. *Annual Review of Physiology*, 75, pp.289–311.

Colombel, J. *et al.* (2007). Adalimumab for Maintenance of Clinical Response and Remission in Patients With Crohn's Disease: The CHARM Trial. *Gastroenterology*, 132(1), pp.52–65.

Coskun, M. *et al.* (2013). Involvement of JAK/STAT signaling in the pathogenesis of inflammatory bowel disease. *Pharmacological Research*, 76, pp.1–8.

Criado, J. de M. *et al.* (2012). MR Imaging Evaluation of Perianal Fistulas: Spectrum of Imaging Features. *Radiographics*, 32(1), pp.175–194.

Dionne, S. *et al.* (1998). Colonic explant production of IL-1 and its receptor antagonist is imbalanced in inflammatory bowel disease (IBD). *Clinical and Experimental Immunology*, 112(3), pp.435–442.

Dubé, P.E. *et al.* (2012). Epidermal growth factor receptor inhibits colitis-associated cancer in mice. *The Journal of Clinical Investigation*, 122(8), pp.2780–2792.

Dudukgian, H. and Abcarian, H. (2011). Why do we have so much trouble treating anal fistula? *World Journal of Gastroenterology : WJG*, 17(28), pp.3292–3296.

Egger, B. *et al.* (1997). Mice lacking transforming growth factor alpha have an increased susceptibility to dextran sulfate-induced colitis. *Gastroenterology*, 113(3), pp.825–832.

EuroQol. (2015). EQ-5D-5L Value sets. [online]. Available from: http://www.euroqol.org/about-eq-5d/valuation-of-eq-5d/eq-5d-5l-value-sets.html [Accessed August 5, 2015].

Evelhoch, J.L. (1999). Key factors in the acquisition of contrast kinetic data for oncology. *Journal of magnetic resonance imaging: JMRI*, 10(3), pp.254–259.

Faucheron, J.L. *et al.* (1996). Long-term seton drainage for high anal fistulas in Crohn's disease--a sphincter-saving operation? *Diseases of the Colon and Rectum*, 39(2), pp.208–211.

Frei, S.M., Pesch, T., *et al.* (2013). A role for tumor necrosis factor and bacterial antigens in the pathogenesis of Crohn's disease-associated fistulae. *Inflammatory Bowel Diseases*, 19(13), pp.2878–2887.

Frei, S.M., Jehle, E.C., *et al.* (2013). Expression of Interleukins 22 and 33, Matrix Metalloproteinases 9 and 13, Mast Cell Markers and Hypoxia-Inducible Factor 1α in Crohn's Disease Associated Fistulae. *Gastroenterology*, 144(5, Supplement 1), pp.S441–S442.

Freire, P. *et al.* (2011). CARD15 mutations and perianal fistulating Crohn's disease: correlation and predictive value of antibiotic response. *Digestive Diseases and Sciences*, 56(3), pp.853–859.

Frey, M.R. and Polk, D.B. (2014). ErbB receptors and their growth factor ligands in pediatric intestinal inflammation. *Pediatric research*, 75(0), pp.127–132.

Garcia-Aguilar, J. *et al.* (1996). Anal fistula surgery. Factors associated with recurrence and incontinence. *Diseases of the Colon and Rectum*, 39(7), pp.723–729.

Gerbin, C.S. (2010). Activation of ERBB Receptors. *Nature Education*, 3(9), p.35.

Giamundo, P. *et al.* (2014). Closure of fistula-in-ano with laser--FiLaC™: an effective novel sphincter-saving procedure for complex disease. *Colorectal Disease: The Official Journal of the Association of Coloproctology of Great Britain and Ireland*, 16(2), pp.110–115.

Gilbert, S.F. (2000). Cell Surface Receptors and Their Signal Transduction Pathways. [online]. Available from: http://www.ncbi.nlm.nih.gov/books/NBK10043/ [Accessed May 9, 2016].

Goligher, J.C., Ellis, M. and Pissidis, A.G. (1967). A critique of anal glandular infection in the aetiology and treatment of idiopathic anorectal abscesses and fistulas. *The British Journal of Surgery*, 54(12), pp.977–983.

Gorlatova, N. *et al.* (2011). Protein characterization of a candidate mechanism SNP for Crohn's disease: the macrophage stimulating protein R689C substitution. *PloS One*, 6(11), p.e27269.

Gosselink, M.P., van Onkelen, R.S. and Schouten, W.R. (2015). The cryptoglandular theory revisited. *Colorectal Disease: The Official Journal of the Association of Coloproctology of Great Britain and Ireland*, 17(12), pp.1041–1043.

Göttgens, K.W.A. *et al.* (2015). Long-term outcome of low perianal fistulas treated by fistulotomy: a multicenter study. *International Journal of Colorectal Disease*, 30(2), pp.213–219.

Grace, R.H., Harper, I.A. and Thompson, R.G. (1982). Anorectal sepsis: microbiology in relation to fistula-in-ano. *The British Journal of Surgery*, 69(7), pp.401–403.

Graf, W., Påhlman, L. and Ejerblad, S. (1995). Functional results after seton treatment of high transsphincteric anal fistulas. *The European Journal of Surgery = Acta Chirurgica*, 161(4), pp.289–291.

Griga, T. *et al.* (2000). Interleukin-4 inhibits the increased production of vascular endothelial growth factor by peripheral blood mononuclear cells in patients with inflammatory bowel disease. *Hepato-Gastroenterology*, 47(36), pp.1604–1607.

Guyatt, G. *et al.* (1989). A new measure of health status for clinical trials in inflammatory bowel disease. *Gastroenterology*, 96(3), pp.804–810.

Hämäläinen, K.P. and Sainio, A.P. (1997). Cutting seton for anal fistulas: high risk of minor control defects. *Diseases of the Colon and Rectum*, 40(12), p.1443–1446; discussion 1447.

Hammond, T.M., Grahn, M.F. and Lunniss, P.J. (2004). Fibrin glue in the management of anal fistulae. *Colorectal Disease: The Official Journal of the Association of Coloproctology of Great Britain and Ireland*, 6(5), pp.308–319.

Hanauer, S.B. *et al.* (2006). Human anti-tumor necrosis factor monoclonal antibody (adalimumab) in Crohn's disease: the CLASSIC-I trial. *Gastroenterology*, 130(2), p.323–333; quiz 591.

Henrichsen, S. and Christiansen, J. (1986). Incidence of fistula-in-ano complicating anorectal sepsis: a prospective study. *The British Journal of Surgery*, 73(5), pp.371–372.

Herdman, M. *et al.* (2011). Development and preliminary testing of the new five-level version of EQ-5D (EQ-5D-5L). *Quality of Life Research*, 20(10), pp.1727–1736.

Hippocrates. (400AD). *On Fistulae*. [online]. Available from: http://classics.mit.edu/Hippocrates/fistulae.mb.txt.

Hornbeck, P.V. *et al.* (2015). PhosphoSitePlus, 2014: mutations, PTMs and recalibrations. *Nucleic Acids Research*, 43(D1), pp.D512–D520.

Horsthuis, K. *et al.* (2011). Evaluation of an MRI-based score of disease activity in perianal fistulizing Crohn's disease. *Clinical Imaging*, 35(5), pp.360–365.

Horsthuis, K. *et al.* (2009). Perianal Crohn Disease: Evaluation of Dynamic Contrast-enhanced MR Imaging as an Indicator of Disease Activity. *Radiology*, 251(2), pp.380–387.

Hughes, L.E. (1978). Surgical pathology and management of anorectal Crohn's disease. *Journal of the Royal Society of Medicine*, 71(9), pp.644–651.

Hugot, J.P. *et al.* (2001). Association of NOD2 leucine-rich repeat variants with susceptibility to Crohn's disease. *Nature*, 411(6837), pp.599–603.

Irvine, E. (1995). Usual therapy improves perianal Crohn's disease as measured by a new disease activity index. McMaster IBD Study Group. *Journal of Clinical Gastroenterology*, 20(1), pp.27–32.

Ito, H. *et al.* (2004). A pilot randomized trial of a human anti-interleukin-6 receptor monoclonal antibody in active Crohn's disease. *Gastroenterology*, 126(4), p.989–996; discussion 947.

Jakobovits, J. and Schuster, M.M. (1984). Metronidazole therapy for Crohn's disease and associated fistulae. *The American Journal of Gastroenterology*, 79(7), pp.533–540.

Jilani, N.Z. and Akobeng, A.K. (2008). Adalimumab for maintenance of clinical response and remission in patients with Crohn's disease: the CHARM trial. Colombel JF, Sandborn WJ, Rutgeerts P et al. Gastroenterology 2007;132:52-65. *Journal of Pediatric Gastroenterology and Nutrition*, 46(2), pp.226–227.

Jordán, J. *et al.* (2010). Risk factors for recurrence and incontinence after anal fistula surgery. *Colorectal Disease*, 12(3), pp.254–260.

Joy, H.A. and Williams, J.G. (2002). The outcome of surgery for complex anal fistula. *Colorectal Disease*, 4(4), pp.254–261.

Kalluri, R. and Neilson, E.G. (2003). Epithelial-mesenchymal transition and its implications for fibrosis. *Journal of Clinical Investigation*, 112(12), pp.1776–1784.

Karban, A. *et al.* (2007). Risk factors for perianal Crohn's disease: the role of genotype, phenotype, and ethnicity. *The American Journal of Gastroenterology*, 102(8), pp.1702–1708.

Karmiris, K. *et al.* (2011). Long-Term Monitoring of Infliximab Therapy for Perianal Fistulizing Crohn's Disease by Using Magnetic Resonance Imaging. *Clinical Gastroenterology and Hepatology*, 9(2), pp.130-e1.

Kaser, A., Zeissig, S. and Blumberg, R.S. (2010). Inflammatory Bowel Disease. *Annual review of immunology*, 28, pp.573–621.

Kennedy, H.L. and Zegarra, J.P. (1990). Fistulotomy without external sphincter division for high anal fistulae. *The British Journal of Surgery*, 77(8), pp.898–901.

Kiehne, K. *et al.* (2007). Antimicrobial peptides in chronic anal fistula epithelium. *Scandinavian journal of gastroenterology*, 42(9), pp.1063–1069.

Kind, P., Brooks, R. and Rabin, R. (2006). *EQ-5D concepts and methods:: a developmental history*. Springer Science & Business Media.

Kirkegaard, T. *et al.* (2004). Expression and localisation of matrix metalloproteinases and their natural inhibitors in fistulae of patients with Crohn's disease. *Gut*, 53(5), pp.701–709.

Klag, T. *et al.* (2015). Medical Therapy of Perianal Crohn's Disease. *Viszeralmedizin*, 31(4), pp.265–272.

Kulkarni, S. *et al.* (2014). MRI-Based Score Helps in Assessing the Severity and in Follow-up of Pediatric Patients With Perianal Crohn Disease. *Journal of Pediatric Gastroenterology*, 58(2), pp.252–257.

Latiano, A. *et al.* (2009). Polymorphism of the IRGM gene might predispose to fistulizing behavior in Crohn's disease. *The American journal of gastroenterology*, 104(1), pp.110–116.

Lavini, C. *et al.* (2007). Pixel-by-pixel analysis of DCE MRI curve patterns and an illustration of its application to the imaging of the musculoskeletal system. *Magnetic Resonance Imaging*, 25(5), pp.604–612.

Lavini, C., Buiter and Maas. (2013). Use of dynamic contrast enhanced time intensity curve shape analysis in MRI: theory and practice. *Reports in Medical Imaging*, p.71.

Leeb, S.N. *et al.* (2003). Reduced migration of fibroblasts in inflammatory bowel disease: role of inflammatory mediators and focal adhesion kinase. *Gastroenterology*, 125(5), pp.1341–1354.

Lemmon, M.A. and Schlessinger, J. (2010). Cell signaling by receptor-tyrosine kinases. *Cell*, 141(7), pp.1117–1134.

Lentner, A. and Wienert, V. (1996). Long-term, indwelling setons for low transsphincteric and intersphincteric anal fistulas. Experience with 108 cases. *Diseases of the Colon and Rectum*, 39(10), pp.1097–1101.

Leung, E., McArdle, K. and Yazbek-Hanna, M. (2009). Pus swabs in incision and drainage of perianal abscesses: what is the point? *World Journal of Surgery*, 33(11), pp.2448–2451.

Linares, P.M., Chaparro, M. and Gisbert, J.P. (2014). Angiopoietins in inflammation and their implication in the development of inflammatory bowel disease. A review. *Journal of Crohn's & Colitis*, 8(3), pp.183–190.

Linares, P.M. and Gisbert, J.P. (2011). Role of growth factors in the development of lymphangiogenesis driven by inflammatory bowel disease: a review. *Inflammatory Bowel Diseases*, 17(8), pp.1814–1821.

Lippert, E. *et al.* (2008). Regulation of galectin-3 function in mucosal fibroblasts: potential role in mucosal inflammation. *Clinical and Experimental Immunology*, 152(2), pp.285–297.

Littman, G. (2014). The royal fistula that changed the face of surgery. *Bilan*. [online]. Available from: http://www.bilan.ch/garry-littman/english-room/royal-fistula-changed-face-surgery [Accessed November 26, 2015].

Liu, C.-K. *et al.* (2011). Clinical and microbiological analysis of adult perianal abscess. *Journal of Microbiology, Immunology, and Infection = Wei Mian Yu Gan Ran Za Zhi*, 44(3), pp.204–208.

Loftus, E.V. (2004). Clinical epidemiology of inflammatory bowel disease: incidence, prevalence, and environmental influences. *Gastroenterology*, 126(6), pp.1504–1517.

Losco, A. *et al.* (2009). Assessing the activity of perianal Crohn's disease: Comparison of clinical indices and computer-assisted anal ultrasound. *Inflammatory Bowel Diseases*, 15(5), pp.742–749.

Lunniss, P. *et al.* (1992). Magnetic resonance imaging of anal fistulae. *Lancet*, 340(8816), pp.394–6.

Lunniss, P.J. *et al.* (1993). Histological and microbiological assessment of the role of microorganisms in chronic anal fistula. *The British journal of surgery*, 80(8), p.1072.

Lunniss, P.J. and Phillips, R.K. (1994). Surgical assessment of acute anorectal sepsis is a better predictor of fistula than microbiological analysis. *The British Journal of Surgery*, 81(3), pp.368–369.

MacDonald, T.T. *et al.* (2011). Regulation of Homeostasis and Inflammation in the Intestine. *Gastroenterology*, 140(6), pp.1768–1775.

Madbouly, K.M. *et al.* (2014). Ligation of intersphincteric fistula tract versus mucosal advancement flap in patients with high transsphincteric fistula-in-ano: a prospective randomized trial. *Diseases of the Colon and Rectum*, 57(10), pp.1202–1208.

Marks, C.G. and Ritchie, J.K. (1977). Anal fistulas at St Mark's Hospital. *The British Journal of Surgery*, 64(2), pp.84–91.

Massey, D.C.O. and Parkes, M. (2007). Genome-wide association scanning highlights two autophagy genes, ATG16L1 and IRGM, as being significantly associated with Crohn's disease. *Autophagy*, 3(6), pp.649–651.

Meinero, P. and Mori, L. (2011). Video-assisted anal fistula treatment (VAAFT): a novel sphincter-saving procedure for treating complex anal fistulas. *Techniques in Coloproctology*, 15(4), pp.417–422.

Monteleone, G. *et al.* (1997). Interleukin 12 is expressed and actively released by Crohn's disease intestinal lamina propria mononuclear cells. *Gastroenterology*, 112(4), pp.1169–1178.

Moriyama, T. *et al.* (2005). Mucosal proinflammatory cytokine and chemokine expression of gastroduodenal lesions in Crohn's disease. *Alimentary Pharmacology & Therapeutics*, 21 Suppl 2, pp.85–91.

Morris, J., Spencer, J.A. and Ambrose, N.S. (2000). MR imaging classification of perianal fistulas and its implications for patient management. *Radiographics: A Review Publication of the Radiological Society of North America, Inc*, 20(3), pp.623-635; discussion 635-637.

Mushaya, C. *et al.* (2012). Ligation of intersphincteric fistula tract compared with advancement flap for complex anorectal fistulas requiring initial seton drainage. *American Journal of Surgery*, 204(3), pp.283–289.

Műzes, G. *et al.* (2012). Changes of the cytokine profile in inflammatory bowel diseases. *World Journal of Gastroenterology : WJG*, 18(41), pp.5848–5861.

Narang, S.K. *et al.* (2016). A systematic review of new treatments for cryptoglandular fistula in ano. *The Surgeon*, 0(0). [online]. Available from: http://www.thesurgeon.net/article/S1479-666X(16)00019-6/fulltext [Accessed November 18, 2016].

van Onkelen, R.S. *et al.* (2013). Assessment of microbiota and peptidoglycan in perianal fistulas. *Diagnostic Microbiology and Infectious Disease*, 75(1), pp.50–54.

van Onkelen, R.S. *et al.* (2016). Pro-inflammatory cytokines in cryptoglandular anal fistulas. *Techniques in Coloproctology*, 20(9), pp.619–625.

Oppmann, B. *et al.* (2000). Novel p19 protein engages IL-12p40 to form a cytokine, IL-23, with biological activities similar as well as distinct from IL-12. *Immunity*, 13(5), pp.715–725.

Orsoni, P. *et al.* (1999). Prospective comparison of endosonography, magnetic resonance imaging and surgical findings in anorectal fistula and abscess complicating Crohn's disease. *The British Journal of Surgery*, 86(3), pp.360–364.

O'Sullivan, S., Gilmer, J.F. and Medina, C. (2015). Matrix metalloproteinases in inflammatory bowel disease: an update. *Mediators of Inflammation*, 2015, p.964131.

Parks, A.G. (1961). Pathogenesis and Treatment of Fistula-in-Ano. *BMJ*, 1(5224), pp.463–460.

Parks, A.G., Gordon, P.H. and Hardcastle, J.D. (1976). A classification of fistula-in-ano. *The British journal of surgery*, 63(1), pp.1–12.

Pearsall, J. ed. (1998). *The New Oxford Dictionary of English*. Oxford University Press.

Pender, S.L. *et al.* (1997). A major role for matrix metalloproteinases in T cell injury in the gut. *Journal of Immunology (Baltimore, Md.: 1950)*, 158(4), pp.1582–1590.

Pender, S.L.F. and MacDonald, T.T. (2004). Matrix metalloproteinases and the gut - new roles for old enzymes. *Current Opinion in Pharmacology*, 4(6), pp.546–550.

Perez White, B.E. and Getsios, S. (2014). Eph receptor and ephrin function in breast, gut, and skin epithelia. *Cell Adhesion & Migration*, 8(4), pp.327–338.

Pikarsky, A.J., Gervaz, P. and Wexner, S.D. (2002). Perianal Crohn disease: a new scoring system to evaluate and predict outcome of surgical intervention. *Archives of Surgery (Chicago, Ill.: 1960)*, 137(7), p.774–777; discussion 778.

Present, D. *et al.* (1999). Infliximab for the treatment of fistulas in patients with Crohn's disease. *Journal of Medicine*, 340(18), pp.1398–405.

Present, D.H. *et al.* (1980). Treatment of Crohn's disease with 6-mercaptopurine. A long-term, randomized, double-blind study. *The New England Journal of Medicine*, 302(18), pp.981–987.

Reimund, J.M. *et al.* (1996). Increased production of tumour necrosis factor-alpha interleukin-1 beta, and interleukin-6 by morphologically normal intestinal biopsies from patients with Crohn's disease. *Gut*, 39(5), pp.684–689.

Rivera, M. *et al.* (2009). Perianal fistulas mimicking Crohn's disease in HIV-infected male patient. *The American Journal of Gastroenterology*, 104(3), pp.793–794.

Rodríguez-Perálvarez, M.L. *et al.* (2012). Role of serum cytokine profile in ulcerative colitis assessment. *Inflammatory Bowel Diseases*, 18(10), pp.1864–1871.

Rojanasakul, A. *et al.* (2007). Total anal sphincter saving technique for fistula-in-ano; the ligation of intersphincteric fistula tract. *Journal of the Medical Association of Thailand = Chotmaihet Thangphaet*, 90(3), pp.581–586.

Rothlin, C.V., Leighton, J.A. and Ghosh, S. (2014). Tyro3, Axl, and Mertk Receptor Signaling in Inflammatory Bowel Disease and Colitis-associated Cancer. *Inflammatory bowel diseases*, 20(8), pp.1472–1480.

Ruffolo, C. *et al.* (2007). Cytokine network in chronic perianal Crohn's disease and indeterminate colitis after colectomy. *Journal of Gastrointestinal Surgery: Official Journal of the Society for Surgery of the Alimentary Tract*, 11(1), pp.16–21.

Ruffolo, C. *et al.* (2008). Cytokine network in rectal mucosa in perianal Crohn's disease: relations with inflammatory parameters and need for surgery. *Inflammatory bowel diseases*, 14(10), pp.1406–1412.

Sailer, M. *et al.* (1998). Quality of life in patients with benign anorectal disorders. *British Journal of Surgery*, 85(12), pp.1716–1719.

Sainio, P. (1984). Fistula-in-ano in a defined population. Incidence and epidemiological aspects. *Annales Chirurgiae Et Gynaecologiae*, 73(4), pp.219–224.

de San Ildefonso Pereira, A. *et al.* (2002). Bacteriology of anal fistulae. *Revista Española De Enfermedades Digestivas: Organo Oficial De La Sociedad Española De Patología Digestiva*, 94(9), pp.533–536.

Sands, B.E. *et al.* (2004). Infliximab Maintenance Therapy for Fistulizing Crohn's Disease. *New England Journal of Medicine*, 350(9), pp.876–885.

Sangwan, Y.P. *et al.* (1994). Is simple fistula-in-ano simple? *Diseases of the Colon and Rectum*, 37(9), pp.885–889.

Scharl, M. *et al.* (2013). Interleukin-13 and transforming growth factor β synergise in the pathogenesis of human intestinal fistulae. *Gut*, 62(1), pp.63–72.

Scharl, M. *et al.* (2011). Potential role for SNAIL family transcription factors in the etiology of Crohn's disease-associated fistulae. *Inflammatory Bowel Diseases*, 17(9), pp.1907–1916.

Scharl, M. and Rogler, G. (2014). Pathophysiology of fistula formation in Crohn's disease. *World Journal of Gastrointestinal Pathophysiology*, 5(3), pp.205–212.

Schneider, C.A., Rasband, W.S. and Eliceiri, K.W. (2012). NIH Image to ImageJ: 25 years of image analysis. *Nature Methods*, 9(7), pp.671–675.

Semelka, R.C. *et al.* (1997). Pelvic fistulas: appearances on MR images. *Abdominal Imaging*, 22(1), pp.91–95.

Seow-Choen, F. *et al.* (1992). Bacteriology of anal fistulae. *The British journal of surgery*, 79(1), pp.27–28.

Setia, S., Nehru, B. and Sanyal, S.N. (2014). Upregulation of MAPK/Erk and PI3K/Akt pathways in ulcerative colitis-associated colon cancer. *Biomedicine & Pharmacotherapy = Biomédecine & Pharmacothérapie*, 68(8), pp.1023–1029.

Siddiqui, M.R.S. *et al.* (2012). A diagnostic accuracy meta-analysis of endoanal ultrasound and MRI for perianal fistula assessment. *Diseases of the Colon and Rectum*, 55(5), pp.576–585.

Sileri, P. *et al.* (2011). Ligation of the intersphincteric fistula tract (LIFT) to treat anal fistula: early results from a prospective observational study. *Techniques in Coloproctology*, 15(4), pp.413–416.

Simpson, J.A., Banerjea, A. and Scholefield, J.H. (2012). Management of anal fistula. *BMJ*, 345, p.e6705.

Singh, S. *et al.* (2015). Systematic review with meta-analysis: faecal diversion for management of perianal Crohn's disease. *Alimentary Pharmacology & Therapeutics*, 42(7), pp.783–792.

Sonoda, T. *et al.* (2002). Outcomes of primary repair of anorectal and rectovaginal fistulas using the endorectal advancement flap. *Diseases of the Colon and Rectum*, 45(12), pp.1622–1628.

Sostegni, R. *et al.* (2003). Crohn's disease: monitoring disease activity. *Alimentary Pharmacology & Therapeutics*, 17, pp.11–17.

Spencer, J.A. *et al.* (1998). Outcome after surgery for perianal fistula: predictive value of MR imaging. *American Journal of Roentgenology*, 171(2), pp.403–406.

Steinkamp, M. *et al.* (2012). Brain derived neurotrophic factor inhibits apoptosis in enteric glia during gut inflammation. *Medical Science Monitor: International Medical Journal of Experimental and Clinical Research*, 18(4), pp.BR117-122.

Sullivan, P.W. and Ghushchyan, V. (2006). Preference-Based EQ-5D Index Scores for Chronic Conditions in the United States. *Medical decision making : an international journal of the Society for Medical Decision Making*, 26(4), pp.410–420.

Szende, A., Janssen, B. and Cabases, J. (2014). *Self-Reported Population Health: An International Perspective*. Netherlands: Springer. [online]. Available from: http://www.springer.com/gb/book/9789400775954 [Accessed February 10, 2016].

Tanaka, E. *et al.* (2012). Morphology of the epithelium of the lower rectum and the anal canal in the adult human. *Medical Molecular Morphology*, 45(2), pp.72–79.

van Tets, W.F. and Kuijpers, H.C. (1994). Continence disorders after anal fistulotomy. *Diseases of the Colon and Rectum*, 37(12), pp.1194–1197.

Thekkinkattil, D.K. *et al.* (2009). Efficacy of the anal fistula plug in complex anorectal fistulae. *Colorectal Disease: The Official Journal of the Association of Coloproctology of Great Britain and Ireland*, 11(6), pp.584–587.

Thia, K.T. *et al.* (2009). Ciprofloxacin or metronidazole for the treatment of perianal fistulas in patients with Crohn's disease: a randomized, double-blind, placebo-controlled pilot study. *Inflammatory Bowel Diseases*, 15(1), pp.17–24.

Thomson, J.P. and Ross, A.H. (1989). Can the external anal sphincter be preserved in the treatment of trans-sphincteric fistula-in-ano? *International Journal of Colorectal Disease*, 4(4), pp.247–250.

Tofts, P.S. *et al.* (1999). Estimating kinetic parameters from dynamic contrast-enhanced T(1)-weighted MRI of a diffusable tracer: standardized quantities and symbols. *Journal of magnetic resonance imaging: JMRI*, 10(3), pp.223–232.

Tozer, P. (2011). *Clinical and experimental studies in idiopathic and Crohn's-related anal fistula*. MD(Res). London: Imperial College.

Tozer, P.J. *et al.* (2009). Etiology of perianal Crohn's disease: role of genetic, microbiological, and immunological factors. *Inflammatory Bowel Diseases*, 15(10), pp.1591–1598.

Tozer, P.J. *et al.* (2015). What role do bacteria play in persisting fistula formation in idiopathic and Crohn's anal fistula? *Colorectal Disease: The Official Journal of the Association of Coloproctology of Great Britain and Ireland*, 17(3), pp.235–241.

Travassos, L.H. *et al.* (2010). Nod1 and Nod2 direct autophagy by recruiting ATG16L1 to the plasma membrane at the site of bacterial entry. *Nature Immunology*, 11(1), pp.55–62.

Trinchieri, G. (2003). Interleukin-12 and the regulation of innate resistance and adaptive immunity. *Nature Reviews. Immunology*, 3(2), pp.133–146.

Ulug, M. *et al.* (2010). The evaluation of bacteriology in perianal abscesses of 81 adult patients. *The Brazilian Journal of Infectious Diseases: An Official Publication of the Brazilian Society of Infectious Diseases*, 14(3), pp.225–229.

University of Birmingham. (2015). Fistula-In-Ano trial (FIAT). *Birmingham Clinical Trials Unit*. [online]. Available from: http://www.birmingham.ac.uk/research/activity/mds/trials/bctu/trials/coloproctology/fiat/index.aspx [Accessed December 14, 2015].

Van Assche, G. *et al.* (2003). Magnetic resonance imaging of the effects of infliximab on perianal fistulizing Crohn's disease. *American Journal of Gastroenterology*, 98(2), pp.332–9.

Vasilevsky, C.A. and Gordon, P.H. (1985). Results of treatment of fistula-in-ano. *Diseases of the Colon and Rectum*, 28(4), pp.225–231.

Vasilevsky, C.A. and Gordon, P.H. (1984). The incidence of recurrent abscesses or fistula-in-ano following anorectal suppuration. *Diseases of the Colon and Rectum*, 27(2), pp.126–130.

Villa, C. *et al.* (2012). Role of magnetic resonance imaging in evaluation of the activity of perianal Crohn's disease. *European Journal of Radiology*, 81(4), pp.616–622.

Vossenkämper, A. *et al.* (2014). A CD3-Specific Antibody Reduces Cytokine Production and Alters Phosphoprotein Profiles in Intestinal Tissues From Patients With Inflammatory Bowel Disease. *Gastroenterology*, 147(1), pp.172–183.

Wang, C.-H. *et al.* (2014). Review of treatment assessment using DCE-MRI in breast cancer radiation therapy. *World Journal of Methodology*, 4(2), pp.46–58.

Ware, J.E. (2002). SF-36 Health Survey Update. *sf-36.org*. [online]. Available from: http://www.sf-36.org/tools/sf36.shtml#LIT [Accessed June 8, 2015].

Weinmann, H. *et al.* (1984). Characteristics of gadolinium-DTPA complex: a potential NMR contrast agent. *American Journal of Roentgenology*, 142(3), pp.619–624.

Westerterp, M. *et al.* (2003). Anal fistulotomy between Skylla and Charybdis. *Colorectal Disease: The Official Journal of the Association of Coloproctology of Great Britain and Ireland*, 5(6), pp.549–551.

Williams, J.G. *et al.* (1991). Seton treatment of high anal fistulae. *The British Journal of Surgery*, 78(10), pp.1159–1161.

Williams, J.G. *et al.* (2007). The Treatment of Anal Fistula: ACPGBI Position Statement. *Colorectal Disease*, 9, pp.18–50.

Yamamoto, T., Allan, R.N. and Keighley, M.R. (2000). Effect of fecal diversion alone on perianal Crohn's disease. *World journal of surgery*, 24(10), pp.1258-1262; discussion 1262-1263.

Yazdanyar, S. and Nordestgaard, B.G. (2010). NOD2/CARD15 genotype and common gastrointestinal diseases in 43,600 individuals. *Journal of Internal Medicine*, 267(2), pp.228–236.

Zanotti, C. *et al.* (2007). An assessment of the incidence of fistula-in-ano in four countries of the European Union. *International Journal of Colorectal Disease*, 22(12), pp.1459–1462.

Zavadil, J. and Böttinger, E.P. (2005). TGF-beta and epithelial-to-mesenchymal transitions. *Oncogene*, 24(37), pp.5764–5774.

Zhao, D. *et al.* (2011). Insulin-like growth factor-1 receptor transactivation modulates the inflammatory and proliferative responses of neurotensin in human colonic epithelial cells. *The Journal of Biological Chemistry*, 286(8), pp.6092–6099.

Ziech, M.L.W. *et al.* (2013). Dynamic Contrast-Enhanced MRI in Determining Disease Activity in Perianal Fistulizing Crohn Disease: A Pilot Study. *American Journal of Roentgenology*, 200(2), pp.W170–W177.

APPENDIX 1 PATIENT INFORMATION SHEET

Queen Mary University of London

Barts Health NHS NHS Trust

Participant Information Sheet

Research Study Title: Perianal Fistula Research
Researcher Name: Professor Charles Knowles

We would like to invite you to take part in a research study. Please take time to read the following information carefully. Talk to others about the study if you wish. We will give you at least a day to make your decision, but please take as much time as you like.

PART 1: About the research

What is the purpose of this study?

This research is looking into **perianal fistulas**, which are abnormal connections between the back passage and the nearby skin. We still do not know why many fistulas form and why they do not heal on their own. This research aims to understand more about the **biology of fistulas** and why some are more difficult to cure than others. This could lead to better treatments for some patients in the future.

We also do not have accurate ways of *measuring* the symptoms caused by perianal fistulas. Therefore this research will also aim to develop a **questionnaire tool** to measure these symptoms. In the future, this questionnaire will help us to assess how well certain treatments work.

Why have I been invited?

You have been asked to participate because you have attended this hospital for diagnosis and/or treatment of a **perianal fistula**.

Do I have to take part?

Participation is entirely **voluntary**. It is up to you to decide to join the study. We will describe the study and go through this information sheet. If you agree to take part, we will then ask you to sign a consent form. You are free to withdraw at any time, without giving a reason. This would not affect the standard of care you receive.

What will happen if I take part?

You will be asked to complete a 10-minute symptom questionnaire up to four times in total, before, during and after your care. This can be done by post or online or during one of your hospital visits. You may also be invited to a 60-minute interview, if convenient, to explore your symptoms in more depth. We may ask to audio tape this interview if you are happy with this.

If you need a MRI scan, it will routinely involve an injection of contrast agent into your veins via a plastic cannula. For the purposes of this research, we will use a special setting on the machine to take pictures that allows us to measure the blood flow in the fistula.

If you need surgery, whilst you are asleep under general anaesthetic, we will take four tiny biopsy samples from your fistula and the lining of your back passage. This would take us about 5 minutes to do.

During your follow-up we will examine you to record how successful your treatment has been. You may also be invited to a 20-minute interview, if convenient, to ask about

your views on this research. Your participation in the research will end when you are discharged from outpatient follow-up, which will be approximately within 6 to 12 months.

How will participating affect me?

We will give you a minimum of 24 hours to decide whether you wish to participate in the study or not.

There will be little that affects you other than giving your time as detailed above. Your tests and **treatment will not be different** and will proceed as planned with your clinical team. There will also be no delays to your treatment as a result of participating in this research.

For those having an MRI scan, the special setting we will use is already done routinely for some types of brain scans in the NHS. There are no known side effects to MRI scanning. If you need surgery, the tiny biopsy samples will be done whilst you are asleep under the same general anaesthetic. There is a small risk of pain, bleeding and infection afterwards.

Will my taking part in this study be kept confidential?

Yes. We will follow ethical and legal practice and all information about you will be handled in the **strictest confidence**. Electronic data and paper files containing details that could identify you, such as your name, date of birth and hospital number, and any audio tapings, will be destroyed 1 year after the study has ended. Data collected for the research will be stripped of your personal details so you cannot be identified. This anonymous data will be used for analysis and to report our findings. It will then be encrypted and kept secure for 10 years, and we may use it for other related research. Only members of the research team will have access to the data. The data will not be used or transferred to commercial organisations.

Will my biopsy samples be stored?

Your biopsy samples will be stored until the project ends in October 2016. They will be stored in a secure freezer at our research facilities and will be linked to the anonymous data, but not to your personal details. If we have made some discoveries that suggest further testing on these samples would be useful, we will apply for ethical approval for this further research to be done. If we don't apply by the end of the project, the samples will be destroyed safely.

PART 2: Information if you participate

What will happen if I don't want to carry on with the study?

You are free to drop out at any time. This would not affect your care. If you wish any unused specimens to be discarded please let us know.

What if there is a problem?

If you have a concern about any aspect of this study, you should ask to speak to the researchers who will do their best to answer your questions. The main research fellow, **Mr James Haddow**, can be contacted on 020 7882 8755 or jameshaddow@nhs.net. If you remain unhappy and wish to complain the normal NHS complaints mechanisms will be available to you through the hospital's **Patient Advice and Liaison Service (PALS)** on 020 3594 2040 or pals@bartshealth.nhs.uk.

We do not expect you to suffer any harm or injury as a result of this research. In the event that something does go wrong and you are harmed during the research and this is due to someone's negligence then you may have grounds for a legal action for compensation against the sponsor Queen Mary University of London, but you may have to pay your legal costs.

What will happen to the results of this study?

We aim to publish our work in scientific journals and present at meetings and conferences. Patient identifiable information **will not be divulged**.

How can I be kept informed?

As the information from this research will not be directly relevant to your treatment we will not be routinely feeding back this information to you. However it is possible for you to know more about the research and what has happened to any specimens collected:

- You are welcome to **visit** our research office and talk to us about our research
- We have a **web page** http://blizard.qmul.ac.uk/centres/digestive-diseases.html for information on our other research
- Mr Haddow maintains a **log of the specimens** and what has happened to them and this can been seen on request
- You can sign up to an **emailing list** by going to http://eepurl.com/Gxghn

Who is organising and funding this research?

We are a collaboration involving surgeons, gastroenterologists, immunologists, radiologists and nurses. There are both hospital and university staff from Bart's Health, North West London Hospitals, and Queen Mary University of London. The Sponsor, who is overall responsible for this research, is Queen Mary University of London.

We are funded by the NHS (through the National Institute for Health Research) and Department of Health (through the Healthcare Technology Co-operative, Enteric). If further funding is secured, this will be from charitable or commercial sources. At all times, our autonomy will be preserved, meaning that none of the funders will be able to influence the conduct, analysis or results of this research.

Who has reviewed this study?

All research in the NHS is looked at by an independent group of people, called a **Research Ethics Committee** to protect your safety, rights, wellbeing and dignity. This study has been reviewed and approved by Queen's Square Research Ethics Committee.

Further information and contact details

The research team is based at the National Centre for Bowel Research and Surgical Innovation, Blizard Institute, 1st Floor Abernethy Building, 2 Newark St, Whitechapel, London E1 2AT.

The chief investigator is **Professor Charles Knowles**. The hospital's research fellow is **Mr James Haddow** and can be contacted on 020 7882 8755 or jameshaddow@nhs.net

The office that oversees all research at Queen Mary University of London is the **Joint Research Management Office**, Queen Mary Innovation Centre, Lower Ground Floor 5 Walden St, London E1 2EF. The Director is Gerry Leonard and can be contacted on 020 7882 7250 or sponsorsrep@bartshealth.nhs.uk.

Page 4 of 5 is BLANK

APPENDIX 2 INFORMED CONSENT FORM

Queen Mary University of London

Barts Health NHS NHS Trust

Consent Form for Participation in Research

Research Study Title: Perianal Fistula Research
Name of Researcher: Professor Charles Knowles

Participant Details *(or please affix sticker)*

Surname | Hospital No

First name

Statement of Participant *Please initial each box*

I confirm that I have read and understood the **information sheet** (version 2.3). I have had the opportunity to consider the information ask questions and have had these answered satisfactorily. ☐

I understand that my **participation is voluntary** and that I am free to withdraw at any time without giving any reason, without my medical care or legal rights being affected. ☐

I understand that relevant sections of any of my medical notes and data collected during the study, may be looked at by responsible individuals from Queen Mary University of London, or from regulatory authorities, where it is relevant to my taking part in this research. I give permission for these individuals to have **access to my records**. ☐

I understand that the Sponsor research administrators at Queen Mary University of London may also access my data for **monitoring and audit** purposes. ☐

If I am invited to a 60-minute interview, I understand that this may be **audio taped** and transcribed. I am aware that I can decline this at the time. ☐

If I undergo surgery I give permission for **biopsy samples** to be taken, stored and used for research purposes and potential future studies that will be ethically approved. ☐

I agree to take part in this research. ☐

Name of participant | Signature | Date

Name of person taking consent | Signature | Date

When completed: 1 for participant; 1 for researcher site file; 1 (original) to be kept in medical notes.

APPENDIX 3 CASE REPORT FORMS

Fistula CRF-Registration

To be completed for each patient approached

Name

Hospital Number

Procedure

1. **Introduce self and research**
2. **Check eligbility**
   Include any adult (18+) with a perianal fistula
   Exclude rectal or intestinal fistulae; fistulae secondary to diseases other than Crohn's; positivity for blood-borne viruses (e.g. HIV, Hep B/C); lack capacity
3. **Give patient information sheet**
4. **Obtain written consent**

A1. Date patient approached

dd/mm/yyyy

A2. Registration Outcome

Ineligible	Declined	Recruited	
☐ 1	☐ 2	☐ 10	→ Continue

A3. Email

A4. Telephone

A5. Substudy Enrolment

PROM	☐	*All eligible*
DCE-MRI	☐	*Include those having MRI; exclude those who've had anti-TNF within last year*
Immunopathology	☐	*Include those having surgery; exclude those who've had anti-TNF within last year*

CONTINUED

Patient tracking

OPD Pending	☐	*dd/mm/yyyy*
MRI Pending	☐	*dd/mm/yyyy*
Colonoscopy Pending	☐	*dd/mm/yyyy*
Surgery Pending	☐	*dd/mm/yyyy*

Notes

END OF CRF

Fistula CRF-Baseline

To be completed before treatment

Hospital Number

B1. Date CRF done

dd/mm/yyyy

B2. Age

years

B3. Gender

Male ☐ 1 Female ☐ 10

B4. Ethnic Origin

White	☐ 10	Asian Indian	☐ 18
Mixed White and Black African	☐ 11	Asian Pakistani	☐ 19
Mixed White and Black Caribbean	☐ 12	Asian Bangladeshi	☐ 20
Mixed White and Asian	☐ 13	Asian Other	☐ 21
Mixed Other	☐ 14	Chinese	☐ 22
Black African	☐ 15	Arab	☐ 23
Black Caribbean	☐ 16		
Black Other	☐ 17	Other	☐ 24
		Not answered	☐ 0

B5. Previous Fistula

None ☐ 1 Single ☐ 10 Multifocal ☐ 11

B6. Previous Fistula Recurrence

No ☐ 1 Yes ☐ 10

CONTINUED

B7. IBD history

No IBD	UC	Indeterminate	Crohn's
☐ 1	☐ 2	☐ 10	☐ 11

B8. Previous medical treatment (highest order)

None	Antibiotics	Steroids	Immuno-suppressants	Anti-TNF	5-ASA
☐ 1	☐ 10	☐ 11	☐ 12	☐ 13	☐ 14

B9. Anti-TNF timing

>1 year ago	Within last year	Currently	Not applicable
☐ 1	☐ 10	☐ 11	☐ 0

B10. Previous number of operations

B11. Previous surgical treatment (highest order)

None	Curettage	Seton	Lay open	LIFT	Fistulectomy
☐ 1	☐ 10	☐ 11	☐ 12	☐ 13	☐ 14

B12. Treatment response (current situation)

None	Inadequate	Transient	Controlled	Resolved	Not applicable
☐ 1	☐ 2	☐ 3	☐ 4	☐ 10	☐ 0

B13. Total fistula disease duration

months

B14. Current Stoma

No	Yes
☐ 1	☐ 10

B15. Current Seton

No	Yes
☐ 1	☐ 10

B16. Smoking status

Never	Ex-smoker	Current Smoker
☐ 1	☐ 10	☐ 11

Notes

END OF CRF

Fistula CRF-PDAI

To be completed before treatment, 6 weeks post treatment; 6 months post treatment

Hospital Number

C1. Date CRF done

dd/mm/yyyy

C2. Time point

Baseline ☐1 6-weeks ☐10 6-months ☐11

C3. Discharge

- No discharge ☐1
- Minimal mucous discharge ☐2
- Moderate mucous or purulent discharge ☐3
- Substantial discharge ☐4
- Gross fecal soiling ☐5

C4. Pain/restriction of activities

- No activity restriction ☐1
- Mild discomfort, no restriction ☐2
- Moderate discomfort, some limitation activities ☐3
- Marked discomfort, marked limitation ☐4
- Severe pain, severe limitation ☐5

C5. Restriction of sexual activities

- No restriction sexual activity ☐1
- Slight restriction sexual activity ☐2
- Moderate limitation sexual activity ☐3
- Marked limitation sexual activity ☐4
- Unable to engage in sexual activity ☐5

C6. Type of perianal disease

- No perianal disease / skin tags ☐1
- Anal fissure or mucosal tear ☐2
- <3 perianal fistulae ☐3
- ≥3 perianal fistulae ☐4
- Anal spincter ulceration or fistulae with significant undermining of skin ☐5

C7. Degree of induration

- No induration ☐1
- Minimal induration ☐2
- Moderate induration ☐3
- Substantial induration ☐4
- Gross fluctuance/abscess ☐5

END OF CRF

Page 6 of 16 is BLANK

Fistula CRF-EQ5D

To be completed before treatment, 6 weeks post treatment; 6 months post treatment

Hospital Number *(office use)*

D1. **Date CRF done** *(office use)*

dd/mm/yyyy

D2. **Time point** *(office use)*

Baseline ☐ 1 6-weeks ☐ 10 6-months ☐ 11

Under each heading, please tick the ONE box that best describes your health TODAY:

D3. **Mobility**

- I have no problems in walking about ☐ 1
- I have slight problems in walking about ☐ 2
- I have moderate problems in walking about ☐ 3
- I have severe problems in walking about ☐ 4
- I am unable to walk about ☐ 5

D4. **Self-care**

- I have no problems with self-care ☐ 1
- I have slight problems washing or dressing ☐ 2
- I have moderate problems washing or dressing myself ☐ 3
- I have severe problems washing or dressing ☐ 4
- I am unable to wash or dress myself ☐ 5

D5. **Usual Activities** *(e.g. work, study, housework, family or leisure activities)*

- I have no problems with performing my usual activities ☐ 1
- I have slight problems with performing my usual activities ☐ 2
- I have moderate problems with performing my usual activities ☐ 3
- I have severe problems with performing my usual activities ☐ 4
- I am unable to do my usual activities ☐ 5

D6. **Pain / Discomfort**

- I have no pain or discomfort ☐ 1
- I have slight pain or discomfort ☐ 2
- I have moderate pain or discomfort ☐ 3
- I have severe pain or discomfort ☐ 4
- I have extreme pain or discomfort ☐ 5

D7. **Anxiety / Depression**

- I am not anxious or depressed ☐ 1
- I am slightly anxious or depressed ☐ 2
- I am moderately anxious or depressed ☐ 3
- I am severely anxious or depressed ☐ 4
- I am extremely anxious or depressed ☐ 5

CONTINUED

We would like to know how good or bad your health is TODAY.

- **This scale is numbered from 0 to 100.**
- **100 means the best health you can imagine. 0 means the worst health you can imagine.**
- **Mark an X on the scale to indicate how your health is TODAY.**
- **Now, please write the number you marked on the scale in the box below.**

D8. Your health score TODAY

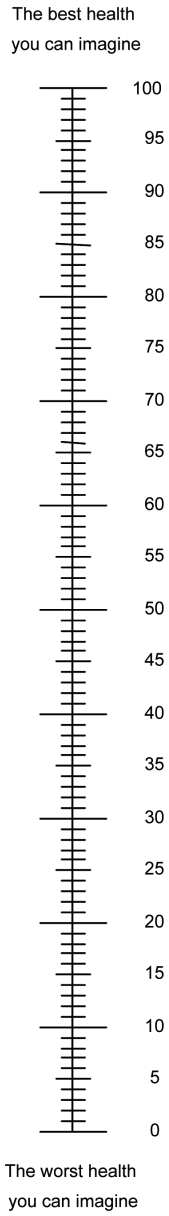

END OF CRF

Fistula CRF-MRI

To be completed for each MRI

Hospital Number

E1. Date MRI done

dd/mm/yyyy

E2. Timepoint

Baseline ☐ 1 | 6-weeks ☐ 10 | 6-months ☐ 11

E3. Number of fistula

Single unbranched ☐ 1 | Single branched ☐ 2 | Multiple ☐ 10 | None ☐ 0

E4. Park's Classification of most severe fistula

Subcutaneous ☐ 10

Inter-sphincteric ☐ 11

Trans-sphincteric ☐ 12

Supra-sphincteric ☐ 13

Extra-sphincteric ☐ 14

Not applicable ☐ 0

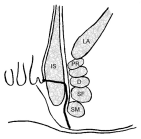

Intersphincteric Fistula

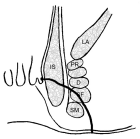

Transsphincteric Fistula

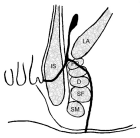

Suprasphincteric Fistula

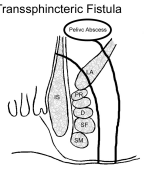

Extrasphincteric Fistula

E5. Fistula level of most severe fistula

Low ☐ 10 | High ☐ 11 | Not applicable ☐ 0

E6. Secondary tracts of most severe fistula

None ☐ 1 | Infralevator ☐ 10 | Supralevator ☐ 11 | Not applicable ☐ 0

E7. Horseshoe extension of most severe fistula

No ☐ 1 | Yes ☐ 10 | Not applicable ☐ 0

CONTINUED

E8. **Associated collections (cavities >3mm diameter)**

No	Yes	Not applicable
☐ 1	☐ 10	☐ 0

E9. **Rectal wall involvement**

Normal	Thickened	Not applicable
☐ 1	☐ 10	☐ 0

E10. **Hyperintensity on T2-weighted images**

Absent	Mild	Pronounced	Not applicable
☐ 1	☐ 10	☐ 11	☐ 0

E11. **MRI Based Score**

To be derived from above data

E18. **Perfusion data**

1. **Select the slice which shows the fistula with its maximum enhancement**
2. **Draw a region of interest around the whole fistula**
3. **Set the reference point to the lowest enhancement value**
4. **Store the images**
   Conventional MRI, perfusion map, quantitative data table, perfusion curve
5. **Append the data table and graph to this CRF**

E40. **TIC Type**

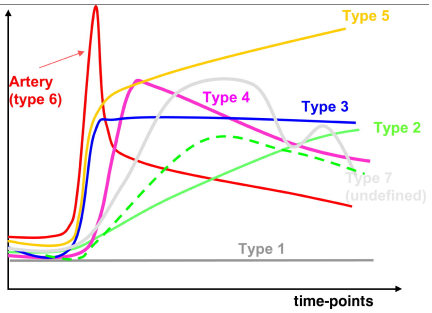

Notes

END OF CRF

Fistula CRF-Surgery

To be completed at surgery

Hospital Number

F1. Date of Surgery

dd/mm/yyyy

F2. Number of fistula

Single unbranched ☐ 1 | Single branched ☐ 2 | Multiple ☐ 10 | None ☐ 0

F3. Park's Classification of most severe fistula

Subcutaneous ☐ 10

Inter-sphincteric ☐ 11

Trans-sphincteric ☐ 12

Supra-sphincteric ☐ 13

Extra-sphincteric ☐ 14

Not applicable ☐ 0

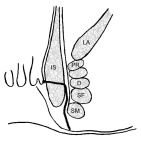

Intersphincteric Fistula

Transsphincteric Fistula

Suprasphincteric Fistula

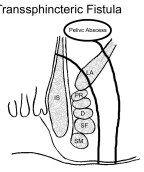

Extrasphincteric Fistula

F4. Fistula level of most severe fistula

Low ☐ 10 | High ☐ 11 | Not applicable ☐ 0

F5. Secondary tracts of most severe fistula

None ☐ 1 | Infralevator ☐ 10 | Supralevator ☐ 11 | Not applicable ☐ 0

F6. Horseshoe extension of most severe fistula

No ☐ 1 | Yes ☐ 10 | Not applicable ☐ 0

CONTINUED

F7. **Associated collections (cavities >3mm diameter)**

No	Yes	Not applicable
☐ 1	☐ 10	☐ 0

F8. **Rectal wall involvement**

Normal	Thickened	Not applicable
☐ 1	☐ 10	☐ 0

F9. **Surgical treatment given (highest order)**

None	Curettage	Seton	Lay open	LIFT	Fistulectomy
☐ 1	☐ 10	☐ 11	☐ 12	☐ 13	☐ 14

F10. **Tract epithelialized**

No	Yes	Unknown
☐ 1	☐ 10	☐ 0

F11. **Hydradenitis supprativa**

No	Yes	Unknown
☐ 1	☐ 10	☐ 0

Notes

END OF CRF

Fistula Biopsy Specimen Form

To be completed at surgery

Participant ID *(not hospital no)*

Procedure

Equipment required: curette, biopsy forceps, 4 specimen containers each containing 10ml Normal Saline (no formalin or additive).

1. **The surgeon takes each specimen when appropriate and places in a universal container with 10ml of Normal Saline**
2. **Store on ice**
3. **At the end of the session, the specimens are transported immediately to the lab for processing**

Take the following specimens and place in plain containers

	Not taken	Taken	Label
Microbiology biopsy or swab for MC&S and AAFB	☐ 1	☐ 10	For micro lab processing
Histopathology fistula biopsy	☐ 1	☐ 10	For histopath lab processing
F: Fistula tract	☐ 1	☐ 10	[Participant ID]-F
G: Granulation tissue from within the fistula tract	☐ 1	☐ 10	[Participant ID]-G
M: Mucosa adjacent to internal opening	☐ 1	☐ 10	[Participant ID]-M
R: Rectal mucosa	☐ 1	☐ 10	[Participant ID]-R

KEEP ON ICE AND TRANSPORT TO LABS

Page 14 of 16 is BLANK

Fistula CRF-Follow-up

To be completed 6 weeks post treatment; 6 months post treatment

Hospital Number

G1. Date CRF done

dd/mm/yyyy

G2. Timepoint

6-weeks ☐ 10 6-months ☐ 11

G3. Any symptoms suspicious of Crohn's to date

No ☐ 1 Yes ☐ 10

G4. Any abdominal fistula suspicious of Crohn's to date

No ☐ 1 Yes ☐ 10

G5. Any abdominal surgery for Crohn's to date

No ☐ 1 Yes ☐ 10

G6. Any colonoscopies to date

No IBD ☐ 1 UC ☐ 2 Declined ☐ 3 Indeterminate ☐ 10 Crohn's ☐ 11 Never had ☐ 0

G7. Any barium follow through / enemas to date

No IBD ☐ 1 UC ☐ 2 Declined ☐ 3 Indeterminate ☐ 10 Crohn's ☐ 11 Never had ☐ 0

G8. Any MRI Abdomen (not pelvis) to date

No IBD UC ☐ 2 Declined ☐ 3 Indeterminate ☐ 10 Crohn's ☐ 11 Never had ☐ 0

G9. Highest faecal calprotectin to date

µg/g *If none, leave blank*

CONTINUED

G10. Any histology to date

No IBD	UC	Indeterminate	Crohn's	Never had
☐ 1	☐ 2	☐ 10	☐ 11	☐ 0

G11. Any granulomas on histology to date

No	Yes	Not applicable
☐ 1	☐ 10	☐ 0

G12. Any HIV aetiology to date

Excluded	No clinical suspicion	Causing fistula	Not considered
☐ 1	☐ 2	☐ 10	☐ 0

G13. Any TB aetiology to date

Excluded	No clinical suspicion	Causing fistula	Not considered
☐ 1	☐ 2	☐ 10	☐ 0

G14. Medical treatment received since recruitment (highest order)

None	Antibiotics	Steroids	Immuno-suppressants	Anti-TNF	5-ASA
☐ 1	☐ 10	☐ 11	☐ 12	☐ 13	☐ 14

G15. Date medical treatment started since recruitment

dd/mm/yyyy *If not applicable, leave blank*

G16. Response (current situation)

None	Inadequate	Transient	Controlled	Resolved	Not applicable
☐ 1	☐ 2	☐ 3	☐ 4	☐ 10	☐ 0

G17. Treatment plan (current situation)

Discharge	Monitor	Continue drugs	Escalate drugs	Further surgery
☐ 1	☐ 2	☐ 3	☐ 10	☐ 11

G18. Fistula microbiology results (specify up to 2 microorganisms)

No growth	Coliforms	Enterococcus	Bacteroides	Mycobacterium	Mixed growth
☐ 1	☐ 10	☐ 11	☐ 12	☐ 13	☐ 15

Other please specify

Not done ☐ 0

G20. Histopathology lab number from surgery specimens

If none, leave blank

END OF CRF

APPENDIX 4 SPSS SYNTAX

Data Preparation

```
* OPEN DATA.
CD '/Users/james/Dropbox/Fistula Studies/Analysis/2015-10 Clinical'.

* FORMAT DATA.
FORMATS ParticipantID(F4.0).
VARIABLE LABELS ParticipantID "Participant ID".
VARIABLE LEVEL ParticipantID(Nominal).
FORMATS B02_Age(F4.1).
VARIABLE LABELS B02_Age "Age (years)".
VARIABLE LEVEL B02_Age(Scale).
FORMATS B03_Gender(F4.0).
VARIABLE LABELS B03_Gender "Gender".
VALUE LABELS B03_Gender 1 "Male" 10 "Female" .
VARIABLE LEVEL B03_Gender(Nominal).
FORMATS B04_EthnicOrigin(F4.0).
VARIABLE LABELS B04_EthnicOrigin "Ethinic origin".
VALUE LABELS B04_EthnicOrigin 0 "Not answered" 10 "White" 11 "Mixed
White and Black African"
12 "Mixed White and Black Caribbean" 13 "Mixed White and Asian" 14
"Mixed Other" 15 "Black African"
16 "Black Caribbean" 17 "Black Other" 18 "Asian Indian" 19 "Asian
Pakistani" 20 "Asian Bangladeshi"
21 "Asian Other" 22 "Chinese" 23 "Arab" 24 "Other" .
VARIABLE LEVEL B04_EthnicOrigin(Nominal).
MISSING VALUES B04_EthnicOrigin(0).
FORMATS B05_PrevFistula(F4.0).
VARIABLE LABELS B05_PrevFistula "Previous fistula".
VALUE LABELS B05_PrevFistula 1 "None" 10 "Single" 11 "Multifocal" .
VARIABLE LEVEL B05_PrevFistula(Ordinal).
FORMATS B06_PrevFistulaRecurrence(F4.0).
VARIABLE LABELS B06_PrevFistulaRecurrence "Previous fistula
recurrence".
VALUE LABELS B06_PrevFistulaRecurrence 1 "No" 10 "Yes" .
VARIABLE LEVEL B06_PrevFistulaRecurrence(Ordinal).
FORMATS B07_PrevIBD(F4.0).
VARIABLE LABELS B07_PrevIBD "IBD History".
VALUE LABELS B07_PrevIBD 1 "None" 2 "UC" 10 "Indeterminate Colitis"
11 "Crohn's" .
VARIABLE LEVEL B07_PrevIBD(Ordinal).
FORMATS B08_PrevRxMed(F4.0).
VARIABLE LABELS B08_PrevRxMed "Previous medical treatment (highest
order)".
VALUE LABELS B08_PrevRxMed 1 "None" 10 "Antibiotics" 11 "Steriods"
12 "Immunosuppressants" 13 "Anti-TNF" 14 "5-ASA" .
VARIABLE LEVEL B08_PrevRxMed(Ordinal).
FORMATS B09_PrevRxAntiTNF(F4.0).
VARIABLE LABELS B09_PrevRxAntiTNF "Anti-TNF timing".
VALUE LABELS B09_PrevRxAntiTNF 0 "NA" 1 ">1 year ago" 10 "Within
last year" 11 "Currently" .
VARIABLE LEVEL B09_PrevRxAntiTNF(Ordinal).
```

```
FORMATS B10_PrevRxSurgNo(F4.0).
VARIABLE LABELS B10_PrevRxSurgNo "Previous operations".
VARIABLE LEVEL B10_PrevRxSurgNo(Scale).
FORMATS B11_PrevRxSurg(F4.0).
VARIABLE LABELS B11_PrevRxSurg "Previous surgical treatment (highest
order)".
VALUE LABELS B11_PrevRxSurg 1 "None" 10 "Curettage" 11 "Seton" 12
"Lay open" 13 "LIFT" 14 "Fistulectomy" .
VARIABLE LEVEL B11_PrevRxSurg(Ordinal).
FORMATS B12_PrevRxResponse(F4.0).
VARIABLE LABELS B12_PrevRxResponse "Previous treatment response".
VALUE LABELS B12_PrevRxResponse 0 "NA" 1 "None" 2 "Inadequate" 3
"Transient" 4 "Controlled" 10 "Resolved" .
VARIABLE LEVEL B12_PrevRxResponse(Ordinal).
FORMATS B13_FistulaDuration(F4.0).
VARIABLE LABELS B13_FistulaDuration "Fistula disease duration
(months)".
VARIABLE LEVEL B13_FistulaDuration(Scale).
FORMATS B14_CurrentStoma(F4.0).
VARIABLE LABELS B14_CurrentStoma "Stoma".
VALUE LABELS B14_CurrentStoma 1 "No" 10 "Yes" .
VARIABLE LEVEL B14_CurrentStoma(Ordinal).
FORMATS B15_CurrentSeton(F4.0).
VARIABLE LABELS B15_CurrentSeton "Seton in situ at recruitment".
VALUE LABELS B15_CurrentSeton 1 "No" 10 "Yes" .
VARIABLE LEVEL B15_CurrentSeton(Ordinal).
FORMATS B16_Smoking(F4.0).
VARIABLE LABELS B16_Smoking "Smoking status".
VALUE LABELS B16_Smoking 1 "Never" 10 "Ex-smoker" 11 "Current
smoker" .
VARIABLE LEVEL B16_Smoking(Ordinal).
FORMATS MaxOfG03_CDClinical(F4.0).
VARIABLE LABELS MaxOfG03_CDClinical "Crohn's symptoms".
VALUE LABELS MaxOfG03_CDClinical 1 "No" 10 "Yes" .
VARIABLE LEVEL MaxOfG03_CDClinical(Ordinal).
FORMATS MaxOfG04_CDAbdoFistula(F4.0).
VARIABLE LABELS MaxOfG04_CDAbdoFistula "Abdominal Crohn's fistulae".
VALUE LABELS MaxOfG04_CDAbdoFistula 1 "No" 10 "Yes" .
VARIABLE LEVEL MaxOfG04_CDAbdoFistula(Ordinal).
FORMATS MaxOfG05_CDAbdoSurgery(F4.0).
VARIABLE LABELS MaxOfG05_CDAbdoSurgery "Abdominal surgery for
Crohn's".
VALUE LABELS MaxOfG05_CDAbdoSurgery 1 "No" 10 "Yes" .
VARIABLE LEVEL MaxOfG05_CDAbdoSurgery(Ordinal).
FORMATS MaxOfG06_CDColonoscopy(F4.0).
VARIABLE LABELS MaxOfG06_CDColonoscopy "Previous colonoscopies".
VALUE LABELS MaxOfG06_CDColonoscopy 0 "None" 1 "No IBD" 2 "UC" 3
"Declined" 10 "Indeterminate Colitis" 11 "Crohn's" .
VARIABLE LEVEL MaxOfG06_CDColonoscopy(Ordinal).
FORMATS MaxOfG07_CDBariumFT(F4.0).
VARIABLE LABELS MaxOfG07_CDBariumFT "Previous barium studies".
VALUE LABELS MaxOfG07_CDBariumFT 0 "None" 1 "No IBD" 2 "UC" 3
"Declined" 10 "Indeterminate Colitis" 11 "Crohn's" .
VARIABLE LEVEL MaxOfG07_CDBariumFT(Ordinal).
FORMATS MaxOfG08_CDMRIAbdo(F4.0).
VARIABLE LABELS MaxOfG08_CDMRIAbdo "Previous abdominal MRIs".
```

```
VALUE LABELS MaxOfG08_CDMRIAbdo 0 "None" 1 "No IBD" 2 "UC" 3
"Declined" 10 "Indeterminate Colitis" 11 "Crohn's" .
VARIABLE LEVEL MaxOfG08_CDMRIAbdo(Ordinal).
FORMATS MaxOfG09_CDCalprotectin(F4.1).
VARIABLE LABELS MaxOfG09_CDCalprotectin "Highest faecal
calprotectin".
VARIABLE LEVEL MaxOfG09_CDCalprotectin(Scale).
FORMATS MaxOfG10_CDHistoDiagnosis(F4.0).
VARIABLE LABELS MaxOfG10_CDHistoDiagnosis "Previous histology".
VALUE LABELS MaxOfG10_CDHistoDiagnosis 0 "None" 1 "No IBD" 2 "UC" 10
"Indeterminate Colitis" 11 "Crohn's" .
VARIABLE LEVEL MaxOfG10_CDHistoDiagnosis(Ordinal).
FORMATS MaxOfG11_CDHistoGranulomas(F4.0).
VARIABLE LABELS MaxOfG11_CDHistoGranulomas "Granulomas on
histology".
VALUE LABELS MaxOfG11_CDHistoGranulomas 0 "NA" 1 "No" 10 "Yes" .
VARIABLE LEVEL MaxOfG11_CDHistoGranulomas(Ordinal).
FORMATS MaxOfG12_HIVAetiology(F4.0).
VARIABLE LABELS MaxOfG12_HIVAetiology "HIV status".
VALUE LABELS MaxOfG12_HIVAetiology 0 "Unknown" 1 "Excluded" 2 "No
clinical suspicion" 10 "Positive" .
VARIABLE LEVEL MaxOfG12_HIVAetiology(Ordinal).
MISSING VALUES MaxOfG12_HIVAetiology(0).
FORMATS MaxOfG13_TBAetiology(F4.0).
VARIABLE LABELS MaxOfG13_TBAetiology "TB status".
VALUE LABELS MaxOfG13_TBAetiology 0 "Unknown" 1 "Excluded" 2 "No
clinical suspicion" 10 "Positive" .
VARIABLE LEVEL MaxOfG13_TBAetiology(Ordinal).
MISSING VALUES MaxOfG13_TBAetiology(0).
FORMATS WeeksSurgery(F4.1).
VARIABLE LABELS WeeksSurgery "Recruitment to surgery (weeks)".
VARIABLE LEVEL WeeksSurgery(Scale).
FORMATS F02_FistulaNo(F4.0).
VARIABLE LABELS F02_FistulaNo "Number of fistula at surgery".
VALUE LABELS F02_FistulaNo 0 "None" 1 "Single unbranched" 2 "Single
branched" 10 "Multiple" .
VARIABLE LEVEL F02_FistulaNo(Ordinal).
FORMATS F03_FistulaParks(F4.0).
VARIABLE LABELS F03_FistulaParks "Park's Classification at surgery".
VALUE LABELS F03_FistulaParks 0 "NA" 10 "Subcutaneous" 11 "Inter-
sphincteric" 12 "Trans-sphincteric" 13 "Supra-sphincteric" 14
"Extra-sphincteric" .
VARIABLE LEVEL F03_FistulaParks(Ordinal).
FORMATS F04_FistulaLevel(F4.0).
VARIABLE LABELS F04_FistulaLevel "Level of fistula at surgery".
VALUE LABELS F04_FistulaLevel 0 "NA" 10 "Low" 11 "High" .
VARIABLE LEVEL F04_FistulaLevel(Ordinal).
FORMATS F05_FistulaSecondaryTracts(F4.0).
VARIABLE LABELS F05_FistulaSecondaryTracts "Secondary tracts at
surgery".
VALUE LABELS F05_FistulaSecondaryTracts 0 "NA" 1 "None" 10
"Infralevator" 11 "Supralevator" .
VARIABLE LEVEL F05_FistulaSecondaryTracts(Ordinal).
FORMATS F06_FistulaHorseshoe(F4.0).
VARIABLE LABELS F06_FistulaHorseshoe "Horseshoe extension at
surgery".
VALUE LABELS F06_FistulaHorseshoe 0 "NA" 1 "No" 10 "Yes" .
```

```
VARIABLE LEVEL F06_FistulaHorseshoe(Ordinal).
FORMATS F07_FistulaCollections(F4.0).
VARIABLE LABELS F07_FistulaCollections "Collections at surgery".
VALUE LABELS F07_FistulaCollections 0 "NA" 1 "No" 10 "Yes" .
VARIABLE LEVEL F07_FistulaCollections(Ordinal).
FORMATS F08_FistulaRectalInvolvement(F4.0).
VARIABLE LABELS F08_FistulaRectalInvolvement "Rectal involvement at
surgery".
VALUE LABELS F08_FistulaRectalInvolvement 0 "NA" 1 "Normal" 10
"Thickened" .
VARIABLE LEVEL F08_FistulaRectalInvolvement(Ordinal).
FORMATS F09_RxSurg(F4.0).
VARIABLE LABELS F09_RxSurg "Surgery performed".
VALUE LABELS F09_RxSurg 1 "None" 10 "Curettage" 11 "Seton" 12 "Lay
open" 13 "LIFT" 14 "Fistulectomy" .
VARIABLE LEVEL F09_RxSurg(Ordinal).
FORMATS F10_FistulaEpithelialized(F4.0).
VARIABLE LABELS F10_FistulaEpithelialized "Epithelialization at
surgery".
VALUE LABELS F10_FistulaEpithelialized 0 "Unknown" 1 "No" 10 "Yes" .
VARIABLE LEVEL F10_FistulaEpithelialized(Ordinal).
MISSING VALUES F10_FistulaEpithelialized(0).
FORMATS MaxOfG14_RxMed(F4.0).
VARIABLE LABELS MaxOfG14_RxMed "Medical treatment since recruitment
(highest order)".
VALUE LABELS MaxOfG14_RxMed 1 "None" 10 "Antibiotics" 11 "Steriods"
12 "Immunosuppressants" 13 "Anti-TNF" 14 "5-ASA" .
VARIABLE LEVEL MaxOfG14_RxMed(Ordinal).
FORMATS LastOfG16_RxResponse(F4.0).
VARIABLE LABELS LastOfG16_RxResponse "Treatment response at follow-
up".
VALUE LABELS LastOfG16_RxResponse 0 "NA" 1 "None" 2 "Inadequate" 3
"Transient" 4 "Controlled" 10 "Resolved" .
VARIABLE LEVEL LastOfG16_RxResponse(Ordinal).
FORMATS MaxOfG17_RxPlan(F4.0).
VARIABLE LABELS MaxOfG17_RxPlan "Management plan at follow-up".
VALUE LABELS MaxOfG17_RxPlan 1 "Discharge" 2 "Monitor" 3 "Continue
drugs" 10 "Escalate drugs" 11 "Further surgery" .
VARIABLE LEVEL MaxOfG17_RxPlan(Ordinal).
FORMATS G18_FistulaMicro(F4.0).
VARIABLE LABELS G18_FistulaMicro "Fistula microbiology".
VALUE LABELS G18_FistulaMicro 0 "Unknown" 1 "No growth" 10
"Coliforms" 11 "Enterococcus" 12 "Bacteroides" 13 "Mycobacterium"
14 "Streptococcus" 15 "Mixed growth" 16 "Proteus" 17
"Bifidobacterium" 18 "Morganella" 19 "Bacillus" 20 "Corneybacterium"
21 "Klebsiella" 22 "Staphylococcus" 23 "Actinomyces" .
VARIABLE LEVEL G18_FistulaMicro(Ordinal).
MISSING VALUES G18_FistulaMicro(0).
FORMATS G19_FistulaMicro2(F4.0).
VARIABLE LABELS G19_FistulaMicro2 "Fistula microbiology 2".
VALUE LABELS G19_FistulaMicro2 0 "Unknown" 1 "No growth" 10
"Coliforms" 11 "Enterococcus" 12 "Bacteroides" 13 "Mycobacterium"
14 "Streptococcus" 15 "Mixed growth" 16 "Proteus" 17
"Bifidobacterium" 18 "Morganella" 19 "Bacillus" 20 "Corneybacterium"
21 "Klebsiella" 22 "Staphylococcus" 23 "Actinomyces" .
VARIABLE LEVEL G19_FistulaMicro2(Ordinal).
MISSING VALUES G19_FistulaMicro2(0).
```

```
FORMATS G21_WeeksFollowUp(F4.0).
VARIABLE LABELS G21_WeeksFollowUp "Length of follow-up (weeks)".
VARIABLE LEVEL G21_WeeksFollowUp(Scale).
FORMATS G22_WeeksMedsStart(F4.0).
VARIABLE LABELS G22_WeeksMedsStart "Recruitment to medical treatment
start (weeks)".
VARIABLE LEVEL G22_WeeksMedsStart(Scale).
FORMATS BasePDAIC03_PDAIDischarge(F4.0).
VARIABLE LABELS BasePDAIC03_PDAIDischarge "PDAI Discharge at
baseline".
VALUE LABELS BasePDAIC03_PDAIDischarge 1 "None" 2 "Minimal" 3
"Moderate" 4 "Substantial" 5 "Gross faeces" .
VARIABLE LEVEL BasePDAIC03_PDAIDischarge(Ordinal).
FORMATS BasePDAIC04_PDAIPain(F4.0).
VARIABLE LABELS BasePDAIC04_PDAIPain "PDAI Pain at baseline".
VALUE LABELS BasePDAIC04_PDAIPain 1 "None" 2 "Mild" 3 "Moderate" 4
"Marked" 5 "Severe" .
VARIABLE LEVEL BasePDAIC04_PDAIPain(Ordinal).
FORMATS BasePDAIC05_PDAISexual(F4.0).
VARIABLE LABELS BasePDAIC05_PDAISexual "PDAI Sexual Restriction at
baseline".
VALUE LABELS BasePDAIC05_PDAISexual 1 "None" 2 "Slight" 3 "Moderate"
4 "Marked" 5 "Total" .
VARIABLE LEVEL BasePDAIC05_PDAISexual(Ordinal).
FORMATS BasePDAIC06_PDAIDiseaseType(F4.0).
VARIABLE LABELS BasePDAIC06_PDAIDiseaseType "PDAI Disease Type at
baseline".
VALUE LABELS BasePDAIC06_PDAIDiseaseType 1 "No perianal disease" 2
"Anal fissure or mucosal tear" 3 "<3 perianal fistulae" 4 ">=
perianal fistulae" 5 "Sphincter ulceration" .
VARIABLE LEVEL BasePDAIC06_PDAIDiseaseType(Ordinal).
FORMATS BasePDAIC07_PDAIInduration(F4.0).
VARIABLE LABELS BasePDAIC07_PDAIInduration "PDAI Induration at
baseline".
VALUE LABELS BasePDAIC07_PDAIInduration 1 "None" 2 "Minimal" 3
"Moderate" 4 "Substantial" 5 "Abscess" .
VARIABLE LEVEL BasePDAIC07_PDAIInduration(Ordinal).
FORMATS BasePDAIC08_PDAI(F4.0).
VARIABLE LABELS BasePDAIC08_PDAI "PDAI Score at baseline".
VARIABLE LEVEL BasePDAIC08_PDAI(Scale).
FORMATS FUp1PDAIC03_PDAIDischarge(F4.0).
VARIABLE LABELS FUp1PDAIC03_PDAIDischarge "PDAI Discharge at follow-
up 1".
VALUE LABELS FUp1PDAIC03_PDAIDischarge 1 "None" 2 "Minimal" 3
"Moderate" 4 "Substantial" 5 "Gross faeces" .
VARIABLE LEVEL FUp1PDAIC03_PDAIDischarge(Ordinal).
FORMATS FUp1PDAIC04_PDAIPain(F4.0).
VARIABLE LABELS FUp1PDAIC04_PDAIPain "PDAI Pain at follow-up 1".
VALUE LABELS FUp1PDAIC04_PDAIPain 1 "None" 2 "Mild" 3 "Moderate" 4
"Marked" 5 "Severe" .
VARIABLE LEVEL FUp1PDAIC04_PDAIPain(Ordinal).
FORMATS FUp1PDAIC05_PDAISexual(F4.0).
VARIABLE LABELS FUp1PDAIC05_PDAISexual "PDAI Sexual Restriction at
follow-up 1".
VALUE LABELS FUp1PDAIC05_PDAISexual 1 "None" 2 "Slight" 3 "Moderate"
4 "Marked" 5 "Total" .
VARIABLE LEVEL FUp1PDAIC05_PDAISexual(Ordinal).
```

```
FORMATS FUp1PDAIC06_PDAIDiseaseType(F4.0).
VARIABLE LABELS FUp1PDAIC06_PDAIDiseaseType "PDAI Disease Type at
follow-up 1".
VALUE LABELS FUp1PDAIC06_PDAIDiseaseType 1 "No perianal disease" 2
"Anal fissure or mucosal tear" 3 "<3 perianal fistulae" 4 ">=
perianal fistulae" 5 "Sphincter ulceration" .
VARIABLE LEVEL FUp1PDAIC06_PDAIDiseaseType(Ordinal).
FORMATS FUp1PDAIC07_PDAIInduration(F4.0).
VARIABLE LABELS FUp1PDAIC07_PDAIInduration "PDAI Induration at
follow-up 1".
VALUE LABELS FUp1PDAIC07_PDAIInduration 1 "None" 2 "Minimal" 3
"Moderate" 4 "Substantial" 5 "Abscess" .
VARIABLE LEVEL FUp1PDAIC07_PDAIInduration(Ordinal).
FORMATS FUp1PDAIC08_PDAI(F4.0).
VARIABLE LABELS FUp1PDAIC08_PDAI "PDAI Score at follow-up 1".
VARIABLE LEVEL FUp1PDAIC08_PDAI(Scale).
FORMATS FUp2PDAIC03_PDAIDischarge(F4.0).
VARIABLE LABELS FUp2PDAIC03_PDAIDischarge "PDAI Discharge at follow-
up 2".
VALUE LABELS FUp2PDAIC03_PDAIDischarge 1 "None" 2 "Minimal" 3
"Moderate" 4 "Substantial" 5 "Gross faeces" .
VARIABLE LEVEL FUp2PDAIC03_PDAIDischarge(Ordinal).
FORMATS FUp2PDAIC04_PDAIPain(F4.0).
VARIABLE LABELS FUp2PDAIC04_PDAIPain "PDAI Pain at follow-up 2".
VALUE LABELS FUp2PDAIC04_PDAIPain 1 "None" 2 "Mild" 3 "Moderate" 4
"Marked" 5 "Severe" .
VARIABLE LEVEL FUp2PDAIC04_PDAIPain(Ordinal).
FORMATS FUp2PDAIC05_PDAISexual(F4.0).
VARIABLE LABELS FUp2PDAIC05_PDAISexual "PDAI Sexual Restriction at
follow-up 2".
VALUE LABELS FUp2PDAIC05_PDAISexual 1 "None" 2 "Slight" 3 "Moderate"
4 "Marked" 5 "Total" .
VARIABLE LEVEL FUp2PDAIC05_PDAISexual(Ordinal).
FORMATS FUp2PDAIC06_PDAIDiseaseType(F4.0).
VARIABLE LABELS FUp2PDAIC06_PDAIDiseaseType "PDAI Disease Type at
follow-up 2".
VALUE LABELS FUp2PDAIC06_PDAIDiseaseType 1 "No perianal disease" 2
"Anal fissure or mucosal tear" 3 "<3 perianal fistulae" 4 ">=
perianal fistulae" 5 "Sphincter ulceration" .
VARIABLE LEVEL FUp2PDAIC06_PDAIDiseaseType(Ordinal).
FORMATS FUp2PDAIC07_PDAIInduration(F4.0).
VARIABLE LABELS FUp2PDAIC07_PDAIInduration "PDAI Induration at
follow-up 2".
VALUE LABELS FUp2PDAIC07_PDAIInduration 1 "None" 2 "Minimal" 3
"Moderate" 4 "Substantial" 5 "Abscess" .
VARIABLE LEVEL FUp2PDAIC07_PDAIInduration(Ordinal).
FORMATS FUp2PDAIC08_PDAI(F4.0).
VARIABLE LABELS FUp2PDAIC08_PDAI "PDAI Score at follow-up 2".
VARIABLE LEVEL FUp2PDAIC08_PDAI(Scale).
FORMATS FUpLastPDAIC03_PDAIDischarge(F4.0).
VARIABLE LABELS FUpLastPDAIC03_PDAIDischarge "PDAI Discharge at
follow-up".
VALUE LABELS FUpLastPDAIC03_PDAIDischarge 1 "None" 2 "Minimal" 3
"Moderate" 4 "Substantial" 5 "Gross faeces" .
VARIABLE LEVEL FUpLastPDAIC03_PDAIDischarge(Ordinal).
FORMATS FUpLastPDAIC04_PDAIPain(F4.0).
VARIABLE LABELS FUpLastPDAIC04_PDAIPain "PDAI Pain at follow-up".
```

```
VALUE LABELS FUpLastPDAIC04_PDAIPain 1 "None" 2 "Mild" 3 "Moderate"
4 "Marked" 5 "Severe" .
VARIABLE LEVEL FUpLastPDAIC04_PDAIPain(Ordinal).
FORMATS FUpLastPDAIC05_PDAISexual(F4.0).
VARIABLE LABELS FUpLastPDAIC05_PDAISexual "PDAI Sexual Restriction
at follow-up".
VALUE LABELS FUpLastPDAIC05_PDAISexual 1 "None" 2 "Slight" 3
"Moderate" 4 "Marked" 5 "Total" .
VARIABLE LEVEL FUpLastPDAIC05_PDAISexual(Ordinal).
FORMATS FUpLastPDAIC06_PDAIDiseaseType(F4.0).
VARIABLE LABELS FUpLastPDAIC06_PDAIDiseaseType "PDAI Disease Type at
follow-up".
VALUE LABELS FUpLastPDAIC06_PDAIDiseaseType 1 "No perianal disease"
2 "Anal fissure or mucosal tear" 3 "<3 perianal fistulae" 4 ">=
perianal fistulae" 5 "Sphincter ulceration" .
VARIABLE LEVEL FUpLastPDAIC06_PDAIDiseaseType(Ordinal).
FORMATS FUpLastPDAIC07_PDAIInduration(F4.0).
VARIABLE LABELS FUpLastPDAIC07_PDAIInduration "PDAI Induration at
follow-up".
VALUE LABELS FUpLastPDAIC07_PDAIInduration 1 "None" 2 "Minimal" 3
"Moderate" 4 "Substantial" 5 "Abscess" .
VARIABLE LEVEL FUpLastPDAIC07_PDAIInduration(Ordinal).
FORMATS FUpLastPDAIC08_PDAI(F4.0).
VARIABLE LABELS FUpLastPDAIC08_PDAI "PDAI Score at follow-up".
VARIABLE LEVEL FUpLastPDAIC08_PDAI(Scale).
FORMATS PDAI_Change(F4.0).
VARIABLE LABELS PDAI_Change "PDAI Score change from baseline at
follow-up".
VARIABLE LEVEL PDAI_Change(Scale).
FORMATS BaseEQ5DValueSetsEQ5D_Health_UK(F4.3).
VARIABLE LABELS BaseEQ5DValueSetsEQ5D_Health_UK "EQ-5D health value
at baseline".
VARIABLE LEVEL BaseEQ5DValueSetsEQ5D_Health_UK(Scale).
FORMATS FUp1EQ5DValueSetsEQ5D_Health_UK(F4.3).
VARIABLE LABELS FUp1EQ5DValueSetsEQ5D_Health_UK "EQ-5D health value
at follow-up 1".
VARIABLE LEVEL FUp1EQ5DValueSetsEQ5D_Health_UK(Scale).
FORMATS FUp2EQ5DValueSetsEQ5D_Health_UK(F4.3).
VARIABLE LABELS FUp2EQ5DValueSetsEQ5D_Health_UK "EQ-5D health value
at follow-up 2".
VARIABLE LEVEL FUp2EQ5DValueSetsEQ5D_Health_UK(Scale).
FORMATS LastEQ5DValueSetsEQ5D_Health_UK(F4.3).
VARIABLE LABELS LastEQ5DValueSetsEQ5D_Health_UK "EQ-5D health value
at follow-up".
VARIABLE LEVEL LastEQ5DValueSetsEQ5D_Health_UK(Scale).
FORMATS EQ5D_Change(F4.3).
VARIABLE LABELS EQ5D_Change "EQ-5D health value change from baseline
at follow-up".
VARIABLE LEVEL EQ5D_Change(Scale).
FORMATS BaseEQ5DD08_EQVAS(F4.0).
VARIABLE LABELS BaseEQ5DD08_EQVAS "EQ-5D VAS at baseline".
VARIABLE LEVEL BaseEQ5DD08_EQVAS(Scale).
FORMATS FUp1EQ5DD08_EQVAS(F4.0).
VARIABLE LABELS FUp1EQ5DD08_EQVAS "EQ-5D VAS at follow-up 1".
VARIABLE LEVEL FUp1EQ5DD08_EQVAS(Scale).
FORMATS FUp2EQ5DD08_EQVAS(F4.0).
VARIABLE LABELS FUp2EQ5DD08_EQVAS "EQ-5D VAS at follow-up 2".
```

```
VARIABLE LEVEL FUp2EQ5DD08_EQVAS(Scale).
FORMATS FUpLastEQ5DD08_EQVAS(F4.0).
VARIABLE LABELS FUpLastEQ5DD08_EQVAS "EQ-5D VAS at follow-up".
VARIABLE LEVEL FUpLastEQ5DD08_EQVAS(Scale).
FORMATS EQVAS_Change(F4.0).
VARIABLE LABELS EQVAS_Change "EQ-5D VAS change from baseline at
follow-up".
VARIABLE LEVEL EQVAS_Change(Scale).
FORMATS WeeksMRIBase(F4.1).
VARIABLE LABELS WeeksMRIBase "Recruitment to baseline MRI (weeks)".
VARIABLE LEVEL WeeksMRIBase(Scale).
FORMATS BaseMRIE03_FistulaNo(F4.0).
VARIABLE LABELS BaseMRIE03_FistulaNo "Number of fistula on MRI at
baseline".
VALUE LABELS BaseMRIE03_FistulaNo 0 "None" 1 "Single unbranched" 2
"Single branched" 10 "Multiple" .
VARIABLE LEVEL BaseMRIE03_FistulaNo(Ordinal).
FORMATS BaseMRIE04_FistulaParks(F4.0).
VARIABLE LABELS BaseMRIE04_FistulaParks "Park's Classification on
MRI at baseline".
VALUE LABELS BaseMRIE04_FistulaParks 0 "NA" 10 "Subcutaneous" 11
"Inter-sphincteric" 12 "Trans-sphincteric" 13 "Supra-sphincteric" 14
"Extra-sphincteric" .
VARIABLE LEVEL BaseMRIE04_FistulaParks(Ordinal).
FORMATS BaseMRIE05_FistulaLevel(F4.0).
VARIABLE LABELS BaseMRIE05_FistulaLevel "Level of fistula on MRI at
baseline".
VALUE LABELS BaseMRIE05_FistulaLevel 0 "NA" 10 "Low" 11 "High" .
VARIABLE LEVEL BaseMRIE05_FistulaLevel(Ordinal).
FORMATS BaseMRIE06_SecondaryTracts(F4.0).
VARIABLE LABELS BaseMRIE06_SecondaryTracts "Secondary tracts on MRI
at baseline".
VALUE LABELS BaseMRIE06_SecondaryTracts 0 "NA" 1 "None" 10
"Infralevator" 11 "Supralevator" .
VARIABLE LEVEL BaseMRIE06_SecondaryTracts(Ordinal).
FORMATS BaseMRIE07_FistulaHorseshoe(F4.0).
VARIABLE LABELS BaseMRIE07_FistulaHorseshoe "Horseshoe extension on
MRI at baseline".
VALUE LABELS BaseMRIE07_FistulaHorseshoe 0 "NA" 1 "No" 10 "Yes" .
VARIABLE LEVEL BaseMRIE07_FistulaHorseshoe(Ordinal).
FORMATS BaseMRIE08_Collections(F4.0).
VARIABLE LABELS BaseMRIE08_Collections "Collections on MRI at
baseline".
VALUE LABELS BaseMRIE08_Collections 0 "NA" 1 "No" 10 "Yes" .
VARIABLE LEVEL BaseMRIE08_Collections(Ordinal).
FORMATS BaseMRIE09_RectalInvolvement(F4.0).
VARIABLE LABELS BaseMRIE09_RectalInvolvement "Rectal involvement on
MRI at baseline".
VALUE LABELS BaseMRIE09_RectalInvolvement 0 "NA" 1 "Normal" 10
"Thickened" .
VARIABLE LEVEL BaseMRIE09_RectalInvolvement(Ordinal).
FORMATS BaseMRIE10_FistulaHyperintensityT2(F4.0).
VARIABLE LABELS BaseMRIE10_FistulaHyperintensityT2 "Hyperintensity
on MRI at baseline".
VALUE LABELS BaseMRIE10_FistulaHyperintensityT2 0 "NA" 1 "Absent" 10
"Mild" 11 "Pronounced" .
VARIABLE LEVEL BaseMRIE10_FistulaHyperintensityT2(Ordinal).
```

```
FORMATS E11_MRIScoreFistulaNo(F4.0).
VARIABLE LABELS E11_MRIScoreFistulaNo "MRI score fistula number".
VARIABLE LEVEL E11_MRIScoreFistulaNo(Scale).
FORMATS E12_MRIScoreLocation(F4.0).
VARIABLE LABELS E12_MRIScoreLocation "MRI score location".
VARIABLE LEVEL E12_MRIScoreLocation(Scale).
FORMATS E13_MRIScoreExtension(F4.0).
VARIABLE LABELS E13_MRIScoreExtension "MRI score extension".
VARIABLE LEVEL E13_MRIScoreExtension(Scale).
FORMATS E14_MRIScoreCollections(F4.0).
VARIABLE LABELS E14_MRIScoreCollections "MRI score collections".
VARIABLE LEVEL E14_MRIScoreCollections(Scale).
FORMATS E15_MRIScoreRectum(F4.0).
VARIABLE LABELS E15_MRIScoreRectum "MRI score rectum".
VARIABLE LEVEL E15_MRIScoreRectum(Scale).
FORMATS E16_MRIScoreHyperintensity(F4.0).
VARIABLE LABELS E16_MRIScoreHyperintensity "MRI score
hyperintensity".
VARIABLE LEVEL E16_MRIScoreHyperintensity(Scale).
FORMATS BaseMRIE17_MRIScoreTotal(F4.0).
VARIABLE LABELS BaseMRIE17_MRIScoreTotal "MRI score at baseline".
VARIABLE LEVEL BaseMRIE17_MRIScoreTotal(Scale).
FORMATS E18_SliceNo(F4.0).
VARIABLE LABELS E18_SliceNo "Slice number".
VARIABLE LEVEL E18_SliceNo(Scale).
FORMATS E19_MaxEnhance(F6.0).
VARIABLE LABELS E19_MaxEnhance "Max enhancement".
VARIABLE LEVEL E19_MaxEnhance(Scale).
FORMATS E20_MaxRelEnhance(F4.3).
VARIABLE LABELS E20_MaxRelEnhance "Max relative enhancement".
VARIABLE LEVEL E20_MaxRelEnhance(Scale).
FORMATS E21_T0(F4.1).
VARIABLE LABELS E21_T0 "T0".
VARIABLE LEVEL E21_T0(Scale).
FORMATS E22_TPeak(F4.1).
VARIABLE LABELS E22_TPeak "Time to peak".
VARIABLE LEVEL E22_TPeak(Scale).
FORMATS E23_WashIn(F4.1).
VARIABLE LABELS E23_WashIn "Wash in rate".
VARIABLE LEVEL E23_WashIn(Scale).
FORMATS E24_WashOut(F4.1).
VARIABLE LABELS E24_WashOut "Wash out rate".
VARIABLE LEVEL E24_WashOut(Scale).
FORMATS E25_Brevity(F4.1).
VARIABLE LABELS E25_Brevity "Brevity".
VARIABLE LEVEL E25_Brevity(Scale).
FORMATS E26_AUC(F6.0).
VARIABLE LABELS E26_AUC "Area under the perfusion curve".
VARIABLE LEVEL E26_AUC(Scale).
FORMATS E27_RegionArea(F4.1).
VARIABLE LABELS E27_RegionArea "Region area".
VARIABLE LEVEL E27_RegionArea(Scale).
FORMATS E28_NoPixels(F4.0).
VARIABLE LABELS E28_NoPixels "Number of pixels".
VARIABLE LEVEL E28_NoPixels(Scale).
FORMATS E29_D1(F6.0).
VARIABLE LABELS E29_D1 "D1".
```

```
VARIABLE LEVEL E29_D1(Scale).
FORMATS E30_D2(F6.0).
VARIABLE LABELS E30_D2 "D2".
VARIABLE LEVEL E30_D2(Scale).
FORMATS E31_D3(F6.0).
VARIABLE LABELS E31_D3 "D3".
VARIABLE LEVEL E31_D3(Scale).
FORMATS E32_D4(F6.0).
VARIABLE LABELS E32_D4 "D4".
VARIABLE LEVEL E32_D4(Scale).
FORMATS E33_D5(F6.0).
VARIABLE LABELS E33_D5 "D5".
VARIABLE LEVEL E33_D5(Scale).
FORMATS E34_D6(F6.0).
VARIABLE LABELS E34_D6 "D6".
VARIABLE LEVEL E34_D6(Scale).
FORMATS E35_D7(F6.0).
VARIABLE LABELS E35_D7 "D7".
VARIABLE LEVEL E35_D7(Scale).
FORMATS E36_D8(F6.0).
VARIABLE LABELS E36_D8 "D8".
VARIABLE LEVEL E36_D8(Scale).
FORMATS E37_D9(F6.0).
VARIABLE LABELS E37_D9 "D9".
VARIABLE LEVEL E37_D9(Scale).
FORMATS E38_D10(F6.0).
VARIABLE LABELS E38_D10 "D10".
VARIABLE LEVEL E38_D10(Scale).
FORMATS E39_DReference(F4.0).
VARIABLE LABELS E39_DReference "DReference".
VARIABLE LEVEL E39_DReference(Scale).
FORMATS E40_TICType(F4.0).
VARIABLE LABELS E40_TICType "Time-intensity curve type".
VARIABLE LEVEL E40_TICType(Nominal).
FORMATS WeeksSurgerytoMRILast(F4.1).
VARIABLE LABELS WeeksSurgerytoMRILast "Surgery to follow-up MRI
(weeks)".
VARIABLE LEVEL WeeksSurgerytoMRILast(Scale).
FORMATS FUpLastMRIE03_FistulaNo(F4.0).
VARIABLE LABELS FUpLastMRIE03_FistulaNo "Number of fistula on MRI at
follow-up".
VALUE LABELS FUpLastMRIE03_FistulaNo 0 "None" 1 "Single unbranched"
2 "Single branched" 10 "Multiple" .
VARIABLE LEVEL FUpLastMRIE03_FistulaNo(Ordinal).
FORMATS FUpLastMRIE04_FistulaParks(F4.0).
VARIABLE LABELS FUpLastMRIE04_FistulaParks "Park's Classification on
MRI at follow-up".
VALUE LABELS FUpLastMRIE04_FistulaParks 0 "NA" 10 "Subcutaneous" 11
"Inter-sphincteric" 12 "Trans-sphincteric" 13 "Supra-sphincteric" 14
"Extra-sphincteric" .
VARIABLE LEVEL FUpLastMRIE04_FistulaParks(Ordinal).
FORMATS FUpLastMRIE05_FistulaLevel(F4.0).
VARIABLE LABELS FUpLastMRIE05_FistulaLevel "Level of fistula on MRI
at follow-up".
VALUE LABELS FUpLastMRIE05_FistulaLevel 0 "NA" 10 "Low" 11 "High" .
VARIABLE LEVEL FUpLastMRIE05_FistulaLevel(Ordinal).
FORMATS FUpLastMRIE06_SecondaryTracts(F4.0).
```

```
VARIABLE LABELS FUpLastMRIE06_SecondaryTracts "Secondary tracts on
MRI at follow-up".
VALUE LABELS FUpLastMRIE06_SecondaryTracts 0 "NA" 1 "None" 10
"Infralevator" 11 "Supralevator" .
VARIABLE LEVEL FUpLastMRIE06_SecondaryTracts(Ordinal).
FORMATS FUpLastMRIE07_FistulaHorseshoe(F4.0).
VARIABLE LABELS FUpLastMRIE07_FistulaHorseshoe "Horseshoe extension
on MRI at follow-up".
VALUE LABELS FUpLastMRIE07_FistulaHorseshoe 0 "NA" 1 "No" 10 "Yes" .
VARIABLE LEVEL FUpLastMRIE07_FistulaHorseshoe(Ordinal).
FORMATS FUpLastMRIE08_Collections(F4.0).
VARIABLE LABELS FUpLastMRIE08_Collections "Collections on MRI at
follow-up".
VALUE LABELS FUpLastMRIE08_Collections 0 "NA" 1 "No" 10 "Yes" .
VARIABLE LEVEL FUpLastMRIE08_Collections(Ordinal).
FORMATS FUpLastMRIE09_RectalInvolvement(F4.0).
VARIABLE LABELS FUpLastMRIE09_RectalInvolvement "Rectal involvement
on MRI at follow-up".
VALUE LABELS FUpLastMRIE09_RectalInvolvement 0 "NA" 1 "Normal" 10
"Thickened" .
VARIABLE LEVEL FUpLastMRIE09_RectalInvolvement(Ordinal).
FORMATS FUpLastMRIE10_FistulaHyperintensityT2(F4.0).
VARIABLE LABELS FUpLastMRIE10_FistulaHyperintensityT2
"Hyperintensity on MRI at follow-up".
VALUE LABELS FUpLastMRIE10_FistulaHyperintensityT2 0 "NA" 1 "Absent"
10 "Mild" 11 "Pronounced" .
VARIABLE LEVEL FUpLastMRIE10_FistulaHyperintensityT2(Ordinal).
FORMATS FUpLastMRIE17_MRIScoreTotal(F4.0).
VARIABLE LABELS FUpLastMRIE17_MRIScoreTotal "MRI score at follow-
up".
VARIABLE LEVEL FUpLastMRIE17_MRIScoreTotal(Scale).
FORMATS MRIScore_Change(F4.0).
VARIABLE LABELS MRIScore_Change "MRI score change from baseline at
follow-up".
VARIABLE LEVEL MRIScore_Change(Scale).
FORMATS ResultsPseudoSubgroupsParticipantID(F4.0).
VARIABLE LABELS ResultsPseudoSubgroupsParticipantID "Participant
ID".
VARIABLE LEVEL ResultsPseudoSubgroupsParticipantID(Nominal).
FORMATS Study_Outcomes(F4.0).
VARIABLE LABELS Study_Outcomes "Outcomes Study".
VALUE LABELS Study_Outcomes 0 "No" 1 "Yes" .
VARIABLE LEVEL Study_Outcomes(Nominal).
FORMATS Study_Immuno(F4.0).
VARIABLE LABELS Study_Immuno "Immunopathology study".
VALUE LABELS Study_Immuno 0 "No" 1 "Yes" .
VARIABLE LEVEL Study_Immuno(Nominal).
FORMATS Study_DCEMRI_Main(F4.0).
VARIABLE LABELS Study_DCEMRI_Main "DCE-MRI study (main)".
VALUE LABELS Study_DCEMRI_Main 0 "No" 1 "Yes" .
VARIABLE LEVEL Study_DCEMRI_Main(Nominal).
FORMATS Study_DCEMRI_Pilot(F4.0).
VARIABLE LABELS Study_DCEMRI_Pilot "DCE-MRI study (pilot)".
VALUE LABELS Study_DCEMRI_Pilot 0 "No" 1 "Yes" .
VARIABLE LEVEL Study_DCEMRI_Pilot(Nominal).
FORMATS Study_DCEMRI_All(F4.0).
VARIABLE LABELS Study_DCEMRI_All "DCE-MRI study".
```

```
VALUE LABELS Study_DCEMRI_All 0 "No" 1 "Yes" .
VARIABLE LEVEL Study_DCEMRI_All(Nominal).
FORMATS S01_TypeBy3(F4.0).
VARIABLE LABELS S01_TypeBy3 "Fistula type".
VALUE LABELS S01_TypeBy3 0 "No fistula" 1 "Hidradenitis suppurativa
only" 2 "Idiopathic" 3 "Intermediate" 10 "Crohn's" .
VARIABLE LEVEL S01_TypeBy3(Ordinal).
FORMATS S02_TypeBy2(F4.0).
VARIABLE LABELS S02_TypeBy2 "Fistula type (binary)".
VALUE LABELS S02_TypeBy2 0 "No fistula" 1 "Hidradenitis suppurativa
only" 2 "Idiopathic" 10 "Crohn's" .
VARIABLE LEVEL S02_TypeBy2(Ordinal).
FORMATS S03_PrevRxSurgGE2(F4.0).
VARIABLE LABELS S03_PrevRxSurgGE2 "Previous operations >=2".
VALUE LABELS S03_PrevRxSurgGE2 1 "No" 10 "Yes" .
VARIABLE LEVEL S03_PrevRxSurgGE2(Ordinal).
FORMATS S04_PrevRxSurgGE3(F4.0).
VARIABLE LABELS S04_PrevRxSurgGE3 "Previous operations >=3".
VALUE LABELS S04_PrevRxSurgGE3 1 "No" 10 "Yes" .
VARIABLE LEVEL S04_PrevRxSurgGE3(Ordinal).
FORMATS S05_PrevRxSurgGE4(F4.0).
VARIABLE LABELS S05_PrevRxSurgGE4 "Previous operations >=4".
VALUE LABELS S05_PrevRxSurgGE4 1 "No" 10 "Yes" .
VARIABLE LEVEL S05_PrevRxSurgGE4(Ordinal).
FORMATS S06_PrevRxCure(F4.0).
VARIABLE LABELS S06_PrevRxCure "Previous curative treatment".
VALUE LABELS S06_PrevRxCure 1 "No" 10 "Yes" .
VARIABLE LEVEL S06_PrevRxCure(Ordinal).
FORMATS S07_PrevRxAntiTNF(F4.0).
VARIABLE LABELS S07_PrevRxAntiTNF "Previous anti-TNF".
VALUE LABELS S07_PrevRxAntiTNF 1 "No" 10 "Yes" .
VARIABLE LEVEL S07_PrevRxAntiTNF(Ordinal).
FORMATS S08_PrevRxAntiTNFRecent(F4.0).
VARIABLE LABELS S08_PrevRxAntiTNFRecent "Previous anti-TNF within
last year".
VALUE LABELS S08_PrevRxAntiTNFRecent 1 "No" 10 "Yes" .
VARIABLE LEVEL S08_PrevRxAntiTNFRecent(Ordinal).
FORMATS S09_CurrentSeton(F4.0).
VARIABLE LABELS S09_CurrentSeton "Seton in situ at recruitment".
VALUE LABELS S09_CurrentSeton 1 "No" 10 "Yes" .
VARIABLE LEVEL S09_CurrentSeton(Ordinal).
FORMATS S10_CrohnsDiagnosed(F4.0).
VARIABLE LABELS S10_CrohnsDiagnosed "Crohn's diagnosed since
recruitment".
VALUE LABELS S10_CrohnsDiagnosed 1 "No" 10 "Yes" .
VARIABLE LEVEL S10_CrohnsDiagnosed(Ordinal).
FORMATS S11_HS(F4.0).
VARIABLE LABELS S11_HS "Hidradenitis suppurativa".
VALUE LABELS S11_HS 1 "No" 10 "Yes" .
VARIABLE LEVEL S11_HS(Ordinal).
FORMATS S12_RxSatisfactory(F4.0).
VARIABLE LABELS S12_RxSatisfactory "Treatment outcome".
VALUE LABELS S12_RxSatisfactory 1 "Unsatisfactory" 10 "Satisfactory"
.
VARIABLE LEVEL S12_RxSatisfactory(Ordinal).
FORMATS S13_RxSatisfactory_FUp1(F4.0).
```

```
VARIABLE LABELS S13_RxSatisfactory_FUp1 "Treatment outcome at
follow-up 1".
VALUE LABELS S13_RxSatisfactory_FUp1 1 "Unsatisfactory" 10
"Satisfactory" .
VARIABLE LEVEL S13_RxSatisfactory_FUp1(Ordinal).
FORMATS S14_RxSatisfactory_FUp2(F4.0).
VARIABLE LABELS S14_RxSatisfactory_FUp2 "Treatment outcome at
follow-up 2".
VALUE LABELS S14_RxSatisfactory_FUp2 1 "Unsatisfactory" 10
"Satisfactory" .
VARIABLE LEVEL S14_RxSatisfactory_FUp2(Ordinal).
MISSING VALUES MaxOfG06_CDColonoscopy(0).
MISSING VALUES MaxOfG07_CDBariumFT(0).
MISSING VALUES MaxOfG08_CDMRIAbdo(0).

*Correct values.
IF ParticipantID = 65  LastEQ5DValueSetsEQ5D_Health_UK = -0.034.
IF ParticipantID = 65  EQ5D_Change = -0.034 + 0.002.
EXECUTE.

*Compute new dichotomous variables.
COMPUTE S15_RxIntent =  (F09_RxSurg > 11)*9+1.
COMPUTE Study_OutcomesFistula = S01_TypeBy3 >1 AND Study_Outcomes.
COMPUTE CrohnsOnImaging = MaxOfG06_CDColonoscopy = 11 OR
MaxOfG07_CDBariumFT = 11 OR MaxOfG08_CDMRIAbdo = 11.
COMPUTE RecurrentDisease = B11_PrevRxSurg > 11 OR ( F09_RxSurg >11
AND LastOfG16_RxResponse < 10).
COMPUTE SetonUnresponsive =  (B11_PrevRxSurg = 11 AND
B12_PrevRxResponse < 4) OR ( F09_RxSurg = 11 AND
LastOfG16_RxResponse < 4).
COMPUTE ComplexAnatomy =  F03_FistulaParks > 12 OR (F03_FistulaParks
= 12 AND (F05_FistulaSecondaryTracts > 9 OR F07_FistulaCollections >
9)).
COMPUTE CrohnsExcludedOnImaging = MIN( MaxOfG06_CDColonoscopy,
MaxOfG07_CDBariumFT, MaxOfG08_CDMRIAbdo).
EXECUTE.
IF MISSING(CrohnsExcludedOnImaging) CrohnsExcludedOnImaging = 0.
E F09_RxSurg F09_RxSurgXECUTE.

*Recode S12_RxSatisfactory to S16_RxSatisfactory.
COMPUTE S16_RxSatisfactory = ((S15_RxIntent = 1 AND
LastOfG16_RxResponse > 3) OR (S15_RxIntent = 10 AND
LastOfG16_RxResponse > 9))*9+1.
EXECUTE.
FORMATS S16_RxSatisfactory(F4.0).
VARIABLE LABELS S16_RxSatisfactory "Treatment outcome".
VALUE LABELS S16_RxSatisfactory 1 "Unsatisfactory" 10 "Satisfactory"
.
VARIABLE LEVEL S16_RxSatisfactory(Ordinal).

*Reassign Fistula Type.
*Caution. This saves original data in new variables then overwrites
existing data.
 * COMPUTE OLD_S01_TypeBy3 = S01_TypeBy3.
 * EXECUTE.
 * COMPUTE OLD_S02_TypeBy2 = S02_TypeBy2.
 * EXECUTE.
```

```
IF  S01_TypeBy3 >1 S01_TypeBy3 =  (RecurrentDisease OR
SetonUnresponsive OR ComplexAnatomy) + 2.
EXECUTE.
IF CrohnsOnImaging S01_TypeBy3 = 10.
EXECUTE.
IF MISSING(S01_TypeBy3) S01_TypeBy3 = OLD_S01_TypeBy3.
EXECUTE.
COMPUTE S02_TypeBy2 = S01_TypeBy3.
EXECUTE.
IF S02_TypeBy2 = 3 S02_TypeBy2 = 2.
EXECUTE.
COMPUTE Study_DCEMRI_All_Acute = Study_DCEMRI_All AND
B13_FistulaDuration <=12.
EXECUTE.
RECODE E40_TICType (3,4,5 = 4)(else=copy) INTO E41_TICType2.
EXECUTE.
COMPUTE ChronicFistula =  B13_FistulaDuration >= 12.
EXECUTE.

*Calculate St James' grade.
IF  BaseMRIE04_FistulaParks = 11 BaseMRIE42_StJames = (1 + (
BaseMRIE06_SecondaryTracts > 1 OR  BaseMRIE08_Collections > 1)).
IF  BaseMRIE04_FistulaParks = 12 BaseMRIE42_StJames = (3 +  (
BaseMRIE06_SecondaryTracts > 1 OR  BaseMRIE08_Collections > 1)).
IF  BaseMRIE04_FistulaParks > 12 BaseMRIE42_StJames = (5).
EXECUTE.

COMPUTE F11_FistulaIntersphincteric =  F03_FistulaParks > 11.
EXECUTE.

FORMATS Study_OutcomesFistula(F4.0).
VARIABLE LABELS Study_OutcomesFistula "Outcomes study (Fistula)".
VALUE LABELS Study_OutcomesFistula 0 "No" 1 "Yes" .
VARIABLE LEVEL Study_OutcomesFistula(Nominal).
FORMATS CrohnsOnImaging(F4.0).
VARIABLE LABELS CrohnsOnImaging "Imaging evidence of Crohn's".
VALUE LABELS CrohnsOnImaging 0 "No" 1 "Yes" .
VARIABLE LEVEL CrohnsOnImaging(Nominal).
FORMATS RecurrentDisease(F4.0).
VARIABLE LABELS RecurrentDisease "Recurrent disease".
VALUE LABELS RecurrentDisease 0 "No" 1 "Yes" .
VARIABLE LEVEL RecurrentDisease(Nominal).
FORMATS SetonUnresponsive(F4.0).
VARIABLE LABELS SetonUnresponsive "Inadequate response to seton".
VALUE LABELS SetonUnresponsive 0 "No" 1 "Yes" .
VARIABLE LEVEL SetonUnresponsive(Nominal).
FORMATS ComplexAnatomy(F4.0).
VARIABLE LABELS ComplexAnatomy "Complex transphincteric fistula or
worse".
VALUE LABELS ComplexAnatomy 0 "No" 1 "Yes" .
VARIABLE LEVEL ComplexAnatomy(Nominal).
FORMATS CrohnsExcludedOnImaging(F4.0).
VARIABLE LABELS CrohnsExcludedOnImaging "Imaging exclusion of
Crohn's".
VALUE LABELS CrohnsExcludedOnImaging 0 "None" 1 "No IBD" 2 "UC" 3
"Declined" 10 "Indeterminate Colitis" 11 "Crohn's" .
```

```
VARIABLE LEVEL CrohnsExcludedOnImaging(Nominal).
FORMATS S15_RxIntent(F4.0).
VARIABLE LABELS S15_RxIntent "Treatment intent".
VALUE LABELS S15_RxIntent 1 "Symptom control" 10 "Cure" .
VARIABLE LEVEL S15_RxIntent(Ordinal).
FORMATS E41_TICType2(F4.0).
VARIABLE LABELS E41_TICType2 "Time-intensity curve type".
VARIABLE LEVEL E41_TICType2(Nominal).
FORMATS ChronicFistula(F4.0).
VARIABLE LABELS ChronicFistula "Chronic Fistula".
VALUE LABELS ChronicFistula 0 "No" 1 "Yes" .
VARIABLE LEVEL ChronicFistula(Ordinal).
FORMATS BaseMRIE42_StJames(F4.0).
VARIABLE LABELS BaseMRIE42_StJames "St James' Grade at Baseline
MRI".
VARIABLE LEVEL BaseMRIE42_StJames(Ordinal).
FORMATS StJamesHigh(F4.0).
VARIABLE LABELS StJamesHigh "St James' Grade 3-5".
VALUE LABELS StJamesHigh 0 "No" 1 "Yes" .
VARIABLE LEVEL StJamesHigh(Ordinal).
FORMATS F11_FistulaIntersphincteric(F4.0).
VARIABLE LABELS F11_FistulaIntersphincteric "Intersphincteric at
Surgery".
VALUE LABELS F11_FistulaIntersphincteric 0 "No" 1 "Yes" .
VARIABLE LEVEL F11_FistulaIntersphincteric(Ordinal).

* FILTER CASES.
FILTER off.
SHOW filter.

*INSPECT DATA.
*1 Find unlikely values with frequency tables and histograms and
define as missing variables.
FREQUENCIES VARIABLES=ParticipantID to S14_RxSatisfactory_FUp2.
FREQUENCIES VARIABLES=B02_Age B13_FistulaDuration
MaxOfG09_CDCalprotectin WeeksSurgery
    G21_WeeksFollowUp G22_WeeksMedsStart BasePDAIC08_PDAI
FUp1PDAIC08_PDAI FUp2PDAIC08_PDAI
    FUpLastPDAIC08_PDAI PDAI_Change BaseEQ5DValueSetsEQ5D_Health_UK
FUp1EQ5DValueSetsEQ5D_Health_UK
    FUp2EQ5DValueSetsEQ5D_Health_UK LastEQ5DValueSetsEQ5D_Health_UK
EQ5D_Change BaseEQ5DD08_EQVAS
    FUp1EQ5DD08_EQVAS FUp2EQ5DD08_EQVAS FUpLastEQ5DD08_EQVAS
EQVAS_Change WeeksMRIBase
    E11_MRIScoreFistulaNo E12_MRIScoreLocation E13_MRIScoreExtension
E14_MRIScoreCollections
    E15_MRIScoreRectum E16_MRIScoreHyperintensity
BaseMRIE17_MRIScoreTotal E18_SliceNo E19_MaxEnhance
    E20_MaxRelEnhance E21_T0 E22_TPeak E23_WashIn E24_WashOut
E25_Brevity E26_AUC E27_RegionArea
    E28_NoPixels E29_D1 E30_D2 E31_D3 E32_D4 E33_D5 E34_D6 E35_D7
E36_D8 E37_D9 E38_D10 E39_DReference
    FUpLastMRIE17_MRIScoreTotal MRIScore_Change
WeeksSurgerytoMRILast
  /FORMAT=NOTABLE
  /HISTOGRAM
  /ORDER=ANALYSIS.
```

```
*2 Check total number of cases and total number of variables.
*3 Check meaning of variables and values - use FREQUENCIES to check
the variable and value labels, coding (higher values represent more
positive answers), user missing values, and that frequencies make
sense.
*4 Check missing values per variable with DESCRIPTIVES and delete or
exclude variables with high amounts of missing data.
DESCRIPTIVES VARIABLES=ParticipantID to S14_RxSatisfactory_FUp2
/STATISTICS=MEAN STDDEV MIN MAX.

*5 Check normality of data.
EXAMINE VARIABLES=B02_Age B10_PrevRxSurgNo B13_FistulaDuration
MaxOfG09_CDCalprotectin WeeksSurgery G21_WeeksFollowUp
G22_WeeksMedsStart
  /PLOT HISTOGRAM NPPLOT
  /STATISTICS NONE
  /CINTERVAL 95
  /MISSING LISTWISE
  /NOTOTAL.
EXAMINE VARIABLES=BasePDAIC03_PDAIDischarge BasePDAIC04_PDAIPain
BasePDAIC05_PDAISexual BasePDAIC06_PDAIDiseaseType
BasePDAIC07_PDAIInduration BasePDAIC08_PDAI
FUp1PDAIC03_PDAIDischarge FUp1PDAIC04_PDAIPain
FUp1PDAIC05_PDAISexual FUp1PDAIC06_PDAIDiseaseType
FUp1PDAIC07_PDAIInduration FUp1PDAIC08_PDAI
FUp2PDAIC03_PDAIDischarge
FUp2PDAIC04_PDAIPain FUp2PDAIC05_PDAISexual
FUp2PDAIC06_PDAIDiseaseType FUp2PDAIC07_PDAIInduration
FUp2PDAIC08_PDAI FUpLastPDAIC03_PDAIDischarge
FUpLastPDAIC04_PDAIPain
FUpLastPDAIC05_PDAISexual FUpLastPDAIC06_PDAIDiseaseType
FUpLastPDAIC07_PDAIInduration FUpLastPDAIC08_PDAI PDAI_Change
  /PLOT HISTOGRAM NPPLOT
  /STATISTICS NONE
  /CINTERVAL 95
  /MISSING LISTWISE
  /NOTOTAL.
EXAMINE VARIABLES=BaseEQ5DValueSetsEQ5D_Health_UK
FUp1EQ5DValueSetsEQ5D_Health_UK FUp2EQ5DValueSetsEQ5D_Health_UK
LastEQ5DValueSetsEQ5D_Health_UK EQ5D_Change BaseEQ5DD08_EQVAS
FUp1EQ5DD08_EQVAS FUp2EQ5DD08_EQVAS FUpLastEQ5DD08_EQVAS
EQVAS_Change
  /PLOT HISTOGRAM NPPLOT
  /STATISTICS NONE
  /CINTERVAL 95
  /MISSING LISTWISE
  /NOTOTAL.
EXAMINE VARIABLES=WeeksMRIBase E11_MRIScoreFistulaNo
E12_MRIScoreLocation E13_MRIScoreExtension E14_MRIScoreCollections
E15_MRIScoreRectum E16_MRIScoreHyperintensity
BaseMRIE17_MRIScoreTotal
  /PLOT HISTOGRAM NPPLOT
  /STATISTICS NONE
  /CINTERVAL 95
  /MISSING LISTWISE
  /NOTOTAL.
```

```
EXAMINE VARIABLES=E19_MaxEnhance E20_MaxRelEnhance E22_TPeak
E23_WashIn E24_WashOut E25_Brevity E26_AUC
  /PLOT HISTOGRAM NPPLOT
  /STATISTICS NONE
  /CINTERVAL 95
  /MISSING LISTWISE
  /NOTOTAL.
EXAMINE VARIABLES=WeeksSurgerytoMRILast FUpLastMRIE17_MRIScoreTotal
MRIScore_Change
  /PLOT HISTOGRAM NPPLOT
  /STATISTICS NONE
  /CINTERVAL 95
  /MISSING LISTWISE
  /NOTOTAL.
```

Clinical Phenotyping

```
* OPEN DATA.
CD '/Users/james/Dropbox/Fistula Studies/Analysis/2015-10 Clinical'.

* FILTER CASES.
FILTER by Study_OutcomesFistula.
SHOW filter.

* ANALYSE DATA.
* Patient characteristics.
CTABLES
  /VLABELS VARIABLES=B03_Gender B02_Age B04_EthnicOrigin
B13_FistulaDuration B08_PrevRxMed S03_PrevRxSurgGE2
    S06_PrevRxCure S09_CurrentSeton B16_Smoking S02_TypeBy2
    DISPLAY=LABEL
  /TABLE B03_Gender [C][COUNT F40.0, COLPCT.TOTALN PCT40.0] +
B02_Age [S][MEAN, STDDEV] + B04_EthnicOrigin [COUNT F40.0,
COLPCT.TOTALN PCT40.0] +
    B13_FistulaDuration [S][MEDIAN, PTILE 25, PTILE 75] +
B08_PrevRxMed [C][COUNT F40.0, COLPCT.TOTALN
    PCT40.0] + B10_PrevRxSurgNo [MEDIAN, PTILE 25, PTILE 75] +
S06_PrevRxCure [C][COUNT
    F40.0, COLPCT.TOTALN PCT40.0] + S09_CurrentSeton [C][COUNT
F40.0, COLPCT.TOTALN PCT40.0] +
    B16_Smoking [C][COUNT F40.0, COLPCT.TOTALN PCT40.0] BY
S02_TypeBy2 [C]
  /SLABELS POSITION=ROW
  /CATEGORIES VARIABLES=B03_Gender [1, 10, OTHERNM] EMPTY=INCLUDE
TOTAL=YES POSITION=BEFORE
  /CATEGORIES VARIABLES=B04_EthnicOrigin [10, HSUBTOTAL='White', 18,
19, 20, 21, HSUBTOTAL='Asian', 16, 17, 15, HSUBTOTAL='Black', 11,
12, 13, 14, 22, 23, 24, HSUBTOTAL='Other', OTHERNM, MISSING]
EMPTY=INCLUDE POSITION=AFTER
  /CATEGORIES VARIABLES=B08_PrevRxMed [1, 10, 11, 12, 13, 14,
OTHERNM] EMPTY=INCLUDE
  /CATEGORIES VARIABLES=S06_PrevRxCure [1, 10, OTHERNM]
EMPTY=INCLUDE
  /CATEGORIES VARIABLES=S09_CurrentSeton [1, 10, OTHERNM]
EMPTY=INCLUDE
```

```
  /CATEGORIES VARIABLES=B16_Smoking [1, 10, 11, OTHERNM]
EMPTY=INCLUDE
  /CATEGORIES VARIABLES=S02_TypeBy2 ORDER=A KEY=VALUE EMPTY=EXCLUDE
TOTAL=YES POSITION=AFTER.

* Chron's characteristics.
CTABLES
  /VLABELS VARIABLES=B07_PrevIBD S10_CrohnsDiagnosed B08_PrevRxMed
B09_PrevRxAntiTNF
    MaxOfG04_CDAbdoFistula MaxOfG05_CDAbdoSurgery S02_TypeBy2
    DISPLAY=LABEL
  /TABLE B07_PrevIBD [C] + S10_CrohnsDiagnosed [C] + B08_PrevRxMed
[C] + B09_PrevRxAntiTNF [C] +
    MaxOfG04_CDAbdoFistula [C] + MaxOfG05_CDAbdoSurgery [C] BY
S02_TypeBy2 [C][COUNT F40.0,
    COLPCT.TOTALN PCT40.0]
  /SLABELS POSITION=ROW
  /CATEGORIES VARIABLES=B07_PrevIBD ORDER=A KEY=VALUE EMPTY=INCLUDE
TOTAL=YES POSITION=BEFORE
  /CATEGORIES VARIABLES=S10_CrohnsDiagnosed B08_PrevRxMed
B09_PrevRxAntiTNF MaxOfG04_CDAbdoFistula
    MaxOfG05_CDAbdoSurgery ORDER=A KEY=VALUE
    EMPTY=INCLUDE
  /CATEGORIES VARIABLES=S02_TypeBy2 [10] EMPTY=EXCLUDE.

* Crhon's diagnosis.
CTABLES
  /VLABELS VARIABLES=CrohnsOnImaging MaxOfG10_CDHistoDiagnosis
MaxOfG11_CDHistoGranulomas S02_TypeBy2 DISPLAY=LABEL
  /TABLE CrohnsOnImaging [C] > MaxOfG10_CDHistoDiagnosis [C] >
MaxOfG11_CDHistoGranulomas [C] BY S02_TypeBy2 [C][COUNT F40.0]
  /SLABELS POSITION=ROW
  /CATEGORIES VARIABLES=CrohnsOnImaging MaxOfG10_CDHistoDiagnosis
MaxOfG11_CDHistoGranulomas ORDER=A KEY=VALUE MISSING=INCLUDE
EMPTY=INCLUDE
  /CATEGORIES VARIABLES=S02_TypeBy2 MISSING=INCLUDE EMPTY=INCLUDE.

* Complex disease.
CTABLES
  /VLABELS VARIABLES=RecurrentDisease SetonUnresponsive
ComplexAnatomy S02_TypeBy2 DISPLAY=LABEL
  /TABLE RecurrentDisease > SetonUnresponsive > ComplexAnatomy BY
S02_TypeBy2 [C][COUNT F40.0]
  /SLABELS POSITION=ROW
  /CATEGORIES VARIABLES=RecurrentDisease SetonUnresponsive
ComplexAnatomy ORDER=A KEY=VALUE
    EMPTY=INCLUDE
  /CATEGORIES VARIABLES=S02_TypeBy2 EMPTY=INCLUDE.

* Crohn's exclusion.
CTABLES
  /VLABELS VARIABLES=MaxOfG03_CDClinical CrohnsExcludedOnImaging
MaxOfG10_CDHistoDiagnosis S02_TypeBy2 DISPLAY=LABEL
  /TABLE MaxOfG03_CDClinical [C] > CrohnsExcludedOnImaging [C] >
MaxOfG10_CDHistoDiagnosis [C] BY S02_TypeBy2 [C][COUNT F40.0]
  /SLABELS VISIBLE=NO
```

```
  /CATEGORIES VARIABLES=MaxOfG03_CDClinical CrohnsExcludedOnImaging
MaxOfG10_CDHistoDiagnosis S02_TypeBy2 ORDER=A KEY=VALUE
EMPTY=EXCLUDE MISSING=EXCLUDE.

* Surgical findings.
CTABLES
  /VLABELS VARIABLES=B15_CurrentSeton F02_FistulaNo F03_FistulaParks
F04_FistulaLevel F05_FistulaSecondaryTracts F06_FistulaHorseshoe
F07_FistulaCollections F08_FistulaRectalInvolvement F09_RxSurg
S02_TypeBy2
    DISPLAY=LABEL
  /TABLE B15_CurrentSeton [C][COUNT F40.0, COLPCT.COUNT PCT40.0] +
F02_FistulaNo [C][COUNT F40.0, COLPCT.COUNT PCT40.0] +
F03_FistulaParks [C][COUNT F40.0, COLPCT.COUNT PCT40.0] +
F04_FistulaLevel [C][COUNT F40.0, COLPCT.COUNT PCT40.0] +
F05_FistulaSecondaryTracts [C][COUNT F40.0, COLPCT.COUNT PCT40.0] +
F06_FistulaHorseshoe [C][COUNT F40.0, COLPCT.COUNT PCT40.0] +
F07_FistulaCollections [C][COUNT F40.0, COLPCT.COUNT PCT40.0] +
F08_FistulaRectalInvolvement [C][COUNT F40.0, COLPCT.COUNT PCT40.0]
+
F09_RxSurg [C][COUNT F40.0, COLPCT.COUNT PCT40.0] BY S02_TypeBy2 [C]
  /CATEGORIES VARIABLES=B15_CurrentSeton F02_FistulaNo
F03_FistulaParks F04_FistulaLevel F05_FistulaSecondaryTracts
F06_FistulaHorseshoe
F07_FistulaCollections F08_FistulaRectalInvolvement F09_RxSurg
ORDER=A KEY=VALUE EMPTY=INCLUDE TOTAL=YES POSITION=AFTER
  /CATEGORIES VARIABLES=S02_TypeBy2 ORDER=A KEY=VALUE EMPTY=EXCLUDE
TOTAL=YES LABEL='All' POSITION=AFTER.

* Weeks to surgery.
CTABLES
  /VLABELS VARIABLES=WeeksSurgery S02_TypeBy2 DISPLAY=LABEL
  /TABLE WeeksSurgery [MEDIAN, PTILE 25, PTILE 75] BY S02_TypeBy2
[C]
  /CATEGORIES VARIABLES=S02_TypeBy2 ORDER=A KEY=VALUE EMPTY=EXCLUDE
TOTAL=YES LABEL='All'
    POSITION=AFTER.

* Define Multiple Response Sets.
MRSETS
  /MCGROUP NAME=$FistulaMicroSet LABEL='Fistula microbiology'
VARIABLES=G18_FistulaMicro G19_FistulaMicro2
  /DISPLAY NAME=[$FistulaMicroSet].
FREQUENCIES VARIABLES=G18_FistulaMicro
  /ORDER=ANALYSIS.

* Micro.
CTABLES
  /VLABELS VARIABLES=$FistulaMicroSet S02_TypeBy2 DISPLAY=LABEL
  /TABLE $FistulaMicroSet [C] BY S02_TypeBy2 [C][COUNT F40.0,
COLPCT.COUNT PCT40.0]
  /CATEGORIES VARIABLES=$FistulaMicroSet ORDER=A KEY=VALUE
EMPTY=EXCLUDE MISSING=EXCLUDE TOTAL=YES
  /CATEGORIES VARIABLES=S02_TypeBy2 ORDER=A KEY=VALUE EMPTY=EXCLUDE
TOTAL=YES LABEL='All' POSITION=AFTER.

* Weeks Follow-up.
```

```
CTABLES
  /VLABELS VARIABLES=G21_WeeksFollowUp S02_TypeBy2 DISPLAY=LABEL
  /TABLE G21_WeeksFollowUp [MEDIAN, PTILE 25, PTILE 75] BY
S02_TypeBy2 [C]
  /CATEGORIES VARIABLES=S02_TypeBy2 ORDER=A KEY=VALUE EMPTY=EXCLUDE
TOTAL=YES LABEL='All' POSITION=AFTER.

* Outcome by treatment intent.
CTABLES
  /VLABELS VARIABLES=S15_RxIntent LastOfG16_RxResponse S02_TypeBy2
DISPLAY=LABEL
  /TABLE S15_RxIntent [C] > LastOfG16_RxResponse [C] BY S02_TypeBy2
[C][COUNT F40.0, COLPCT.COUNT PCT40.0]
  /CATEGORIES VARIABLES=S15_RxIntent ORDER=A KEY=VALUE EMPTY=INCLUDE
  /CATEGORIES VARIABLES=LastOfG16_RxResponse ORDER=A KEY=VALUE
EMPTY=EXCLUDE TOTAL=YES
  /CATEGORIES VARIABLES=S02_TypeBy2 ORDER=A KEY=VALUE EMPTY=EXCLUDE
TOTAL=YES LABEL='All' POSITION=AFTER.

* Outcome.
CTABLES
  /VLABELS VARIABLES=S16_RxSatisfactory S02_TypeBy2 DISPLAY=LABEL
  /TABLE S16_RxSatisfactory [COUNT F40.0, COLPCT.COUNT PCT40.0] BY
S02_TypeBy2
  /CATEGORIES VARIABLES=S16_RxSatisfactory ORDER=A KEY=VALUE
EMPTY=EXCLUDE
  /CATEGORIES VARIABLES=S02_TypeBy2 ORDER=A KEY=VALUE EMPTY=EXCLUDE
TOTAL=YES LABEL='All' POSITION=AFTER
  /SIGTEST TYPE=CHISQUARE ALPHA=0.05 INCLUDEMRSETS=YES
CATEGORIES=ALLVISIBLE.

* Fisher Exact Tests for Operative Findings.
CROSSTABS
  /TABLES=F02_FistulaNo F03_FistulaParks F04_FistulaLevel
F05_FistulaSecondaryTracts
    F06_FistulaHorseshoe F07_FistulaCollections
F08_FistulaRectalInvolvement BY S02_TypeBy2
  /FORMAT=AVALUE TABLES
  /STATISTICS=CHISQ
  /CELLS=COUNT
  /COUNT ROUND CELL
  /METHOD=EXACT TIMER(5).
```

Perineal Disease Activity Index

```
* OPEN DATA.
CD '/Users/james/Dropbox/Fistula Studies/Analysis/2016-01 Symptoms'.

* FILTER CASES.
FILTER by Study_OutcomesFistula.
SHOW filter.

* ANALYSE DATA.
* Show n.
CTABLES
```

```
  /VLABELS VARIABLES=C03_PDAIDischarge C04_PDAIPain C05_PDAISexual
C06_PDAIDiseaseType C07_PDAIInduration C08_PDAI C02_Timepoint
    DISPLAY=LABEL
  /TABLE C03_PDAIDischarge [COUNT F40.0, MISSING] + C04_PDAIPain
[COUNT F40.0, MISSING] + C05_PDAISexual [COUNT F40.0, MISSING]
 + C06_PDAIDiseaseType [COUNT F40.0, MISSING] + C07_PDAIInduration
[COUNT F40.0, MISSING] + C08_PDAI [COUNT F40.0, MISSING] BY
C02_Timepoint
  /CATEGORIES VARIABLES=C02_Timepoint ORDER=A KEY=VALUE
EMPTY=INCLUDE.

* Check distributions.
FREQUENCIES VARIABLES=C03_PDAIDischarge C04_PDAIPain C05_PDAISexual
C06_PDAIDiseaseType C07_PDAIInduration C08_PDAI
  /FORMAT=NOTABLE
  /HISTOGRAM
  /ORDER=ANALYSIS.

* PDAI at baseline, by Type.
CTABLES
  /VLABELS VARIABLES=C03_PDAIDischarge C04_PDAIPain C05_PDAISexual
C06_PDAIDiseaseType C07_PDAIInduration C08_PDAI C02_Timepoint
S02_TypeBy2
    DISPLAY=LABEL
  /TABLE C03_PDAIDischarge [S][MEAN, STDDEV] + C04_PDAIPain
[S][MEAN, STDDEV] + C05_PDAISexual [S][MEAN, STDDEV]
 + C06_PDAIDiseaseType [S][MEAN, STDDEV] + C07_PDAIInduration
[S][MEAN, STDDEV] + C08_PDAI [S][MEAN, STDDEV] BY C02_Timepoint [C]
> S02_TypeBy2 [C]
  /CATEGORIES VARIABLES=C02_Timepoint [1] EMPTY=INCLUDE
  /CATEGORIES VARIABLES=S02_TypeBy2 [0, 1, 2, 10] EMPTY=EXCLUDE
TOTAL=YES POSITION=AFTER.

FILTER FilterBaseline.
SHOW Filter.

T-TEST GROUPS=S02_TypeBy2(2 10)
  /MISSING=ANALYSIS
  /VARIABLES=C08_PDAI
  /CRITERIA=CI(.95).

* Barchart PDAI at baseline by type..
GGRAPH
  /GRAPHDATASET NAME="graphdataset" VARIABLES=S02_TypeBy2
MEANCI(C08_PDAI, 95)[name="MEAN_C08_PDAI" LOW="MEAN_C08_PDAI_LOW"
HIGH="MEAN_C08_PDAI_HIGH"] MISSING=LISTWISE REPORTMISSING=NO
  /GRAPHSPEC SOURCE=INLINE.
BEGIN GPL
  SOURCE: s=userSource(id("graphdataset"))
  DATA: S02_TypeBy2=col(source(s), name("S02_TypeBy2"),
notIn("0", "1"), unit.category())
  DATA: MEAN_C08_PDAI=col(source(s), name("MEAN_C08_PDAI"))
  DATA: LOW=col(source(s), name("MEAN_C08_PDAI_LOW"))
  DATA: HIGH=col(source(s), name("MEAN_C08_PDAI_HIGH"))
  GUIDE: axis(dim(2), label("Mean PDAI"))
  SCALE: cat(dim(1), include("2", "10"))
  SCALE: linear(dim(2), include(0))
```

```
  ELEMENT: interval(position(S02_TypeBy2*MEAN_C08_PDAI),
shape.interior(shape.square))
  ELEMENT:
interval(position(region.spread.range(S02_TypeBy2*(LOW+HIGH))),
shape.interior(shape.ibeam))
END GPL.

FILTER by Study_OutcomesFistula.
SHOW filter.

* Longitudinal analysis.

* PDAI by Type and Timepoint.
CTABLES
  /VLABELS VARIABLES=C03_PDAIDischarge C04_PDAIPain C05_PDAISexual
C06_PDAIDiseaseType C07_PDAIInduration C08_PDAI S02_TypeBy2
C02_Timepoint
    DISPLAY=LABEL
  /TABLE C03_PDAIDischarge [MEAN, STDDEV] + C04_PDAIPain [MEAN,
STDDEV] + C05_PDAISexual [MEAN, STDDEV] + C06_PDAIDiseaseType [MEAN,
STDDEV] + C07_PDAIInduration [MEAN, STDDEV] + C08_PDAI [MEAN,
STDDEV] BY S02_TypeBy2 > C02_Timepoint
  /CATEGORIES VARIABLES=S02_TypeBy2 ORDER=A KEY=VALUE EMPTY=EXCLUDE
TOTAL=YES LABEL='All' POSITION=AFTER
  /CATEGORIES VARIABLES=C02_Timepoint ORDER=A KEY=VALUE
EMPTY=INCLUDE.

* PDAI by Type and timepoint.
GGRAPH
  /GRAPHDATASET NAME="graphdataset" VARIABLES=C02_Timepoint
MEANCI(C08_PDAI, 95)[name="MEAN_C08_PDAI" LOW="MEAN_C08_PDAI_LOW"
HIGH="MEAN_C08_PDAI_HIGH"] S02_TypeBy2 MISSING=LISTWISE
REPORTMISSING=NO
  /GRAPHSPEC SOURCE=INLINE.
BEGIN GPL
  SOURCE: s=userSource(id("graphdataset"))
  DATA: C02_Timepoint=col(source(s), name("C02_Timepoint"),
unit.category())
  DATA: MEAN_C08_PDAI=col(source(s), name("MEAN_C08_PDAI"))
  DATA: S02_TypeBy2=col(source(s), name("S02_TypeBy2"),
notIn("0", "1"), unit.category())
  DATA: LOW=col(source(s), name("MEAN_C08_PDAI_LOW"))
  DATA: HIGH=col(source(s), name("MEAN_C08_PDAI_HIGH"))
  GUIDE: axis(dim(2), label("Mean PDAI"))
  GUIDE: legend(aesthetic(aesthetic.color.interior), label(""))
  SCALE: cat(dim(1), include("1", "10", "11"))
  SCALE: linear(dim(2), include(0))
  SCALE: cat(aesthetic(aesthetic.color.interior), include("2",
"10"))
  ELEMENT: line(position(C02_Timepoint*MEAN_C08_PDAI),
color.interior(S02_TypeBy2), missing.wings())
  ELEMENT:
interval(position(region.spread.range(C02_Timepoint*(LOW+HIGH))),
shape.interior(shape.ibeam), color.interior(S02_TypeBy2))
END GPL.

* PDAI by Type and Timepoint and treatment outcome.
```

```
CTABLES
  /VLABELS VARIABLES=C03_PDAIDischarge C04_PDAIPain C05_PDAISexual
C06_PDAIDiseaseType C07_PDAIInduration C08_PDAI S02_TypeBy2
C02_Timepoint S16_RxSatisfactory
    DISPLAY=LABEL
  /TABLE S16_RxSatisfactory > C03_PDAIDischarge [MEAN, STDDEV] +
S16_RxSatisfactory > C04_PDAIPain [MEAN, STDDEV] +
S16_RxSatisfactory > C05_PDAISexual [MEAN, STDDEV] +
S16_RxSatisfactory > C06_PDAIDiseaseType [MEAN, STDDEV] +
S16_RxSatisfactory > C07_PDAIInduration [MEAN, STDDEV] +
S16_RxSatisfactory > C08_PDAI [MEAN, STDDEV]
BY S02_TypeBy2 > C02_Timepoint
  /CATEGORIES VARIABLES=S16_RxSatisfactory ORDER=A KEY=VALUE
  /CATEGORIES VARIABLES=S02_TypeBy2 ORDER=A KEY=VALUE EMPTY=EXCLUDE
TOTAL=YES LABEL='All' POSITION=AFTER
  /CATEGORIES VARIABLES=C02_Timepoint ORDER=A KEY=VALUE
EMPTY=INCLUDE.

* PDAI by treatment outcome and timepoint.
GGRAPH
  /GRAPHDATASET NAME="graphdataset" VARIABLES=C02_Timepoint
MEANCI(C08_PDAI, 95)[name="MEAN_C08_PDAI" LOW="MEAN_C08_PDAI_LOW"
HIGH="MEAN_C08_PDAI_HIGH"] S16_RxSatisfactory MISSING=LISTWISE
REPORTMISSING=NO
  /GRAPHSPEC SOURCE=INLINE.
BEGIN GPL
  SOURCE: s=userSource(id("graphdataset"))
  DATA: C02_Timepoint=col(source(s), name("C02_Timepoint"),
unit.category())
  DATA: MEAN_C08_PDAI=col(source(s), name("MEAN_C08_PDAI"))
  DATA: S16_RxSatisfactory=col(source(s),
name("S16_RxSatisfactory"), unit.category())
  DATA: LOW=col(source(s), name("MEAN_C08_PDAI_LOW"))
  DATA: HIGH=col(source(s), name("MEAN_C08_PDAI_HIGH"))
  GUIDE: axis(dim(2), label("Mean PDAI"))
  GUIDE: legend(aesthetic(aesthetic.color.interior), label(""))
  GUIDE: text.footnote(label("Error Bars: 95% CI"))
  SCALE: cat(dim(1), include("1", "10", "11"))
  SCALE: linear(dim(2), include(0))
  SCALE: cat(aesthetic(aesthetic.color.interior), include("1",
"10"))
  ELEMENT: line(position(C02_Timepoint*MEAN_C08_PDAI),
color.interior(S16_RxSatisfactory), missing.wings())
  ELEMENT:
interval(position(region.spread.range(C02_Timepoint*(LOW+HIGH))),
shape.interior(shape.ibeam), color.interior(S16_RxSatisfactory))
END GPL.
```

EQ-5D-5L

```
* OPEN DATA.
CD '/Users/james/Dropbox/Fistula Studies/Analysis/2016-01 Symptoms'.

* FILTER CASES.
FILTER by Study_OutcomesFistula.
```

```
SHOW filter.

* ANALYSE DATA.
* Baseline analysis.
* Show n.
CTABLES
  /VLABELS VARIABLES=D03_EQMobility D04_EQSelfCare D05_EQActivities
D06_EQPain D07_EQAnxiety D08_EQVAS EQ5D_Health_UK D02_Timepoint
    DISPLAY=LABEL
  /TABLE D03_EQMobility [COUNT F40.0, TOTALS[COUNT F40.0, MISSING]]
+ D04_EQSelfCare [COUNT F40.0, TOTALS[COUNT F40.0, MISSING]] +
D05_EQActivities [COUNT F40.0, TOTALS[COUNT F40.0, MISSING]] +
D06_EQPain [COUNT F40.0, TOTALS[COUNT F40.0, MISSING]] +
D07_EQAnxiety [COUNT F40.0, TOTALS[COUNT F40.0, MISSING]] +
D08_EQVAS [COUNT F40.0, MISSING] + EQ5D_Health_UK [COUNT F40.0,
MISSING] BY D02_Timepoint
  /CATEGORIES VARIABLES=D03_EQMobility D04_EQSelfCare
D05_EQActivities D06_EQPain D07_EQAnxiety ORDER=A KEY=VALUE
EMPTY=INCLUDE TOTAL=YES POSITION=AFTER
  /CATEGORIES VARIABLES=D02_Timepoint [1] EMPTY=EXCLUDE.

* Show distributions.
FREQUENCIES VARIABLES=D03_EQMobility D04_EQSelfCare D05_EQActivities
D06_EQPain D07_EQAnxiety D08_EQVAS EQ5D_Health_UK
  /FORMAT=NOTABLE
  /HISTOGRAM
  /ORDER=ANALYSIS.

* EQ-5D at baseline, by Type.
CTABLES
  /VLABELS VARIABLES=D03_EQMobility D04_EQSelfCare D05_EQActivities
D06_EQPain D07_EQAnxiety D02_Timepoint S02_TypeBy2
    DISPLAY=LABEL
  /TABLE D03_EQMobility [C] + D04_EQSelfCare [C] + D05_EQActivities
[C] + D06_EQPain [C] + D07_EQAnxiety [C] BY D02_Timepoint [C] >
S02_TypeBy2 [C][COLPCT.COUNT PCT40.0]
  /CATEGORIES VARIABLES=D03_EQMobility D04_EQSelfCare
D05_EQActivities D06_EQPain D07_EQAnxiety ORDER=A KEY=VALUE
EMPTY=INCLUDE
  /CATEGORIES VARIABLES=D02_Timepoint [1] EMPTY=EXCLUDE
  /CATEGORIES VARIABLES=S02_TypeBy2 ORDER=A KEY=VALUE EMPTY=EXCLUDE
TOTAL=YES POSITION=AFTER.

* EAQ VAS and index at baseline.
CTABLES
  /VLABELS VARIABLES=D08_EQVAS EQ5D_Health_UK D02_Timepoint
S02_TypeBy2 DISPLAY=LABEL
  /TABLE D08_EQVAS [S][MEAN, STDDEV] + EQ5D_Health_UK [S][MEAN,
STDDEV] BY D02_Timepoint [C] > S02_TypeBy2 [C]
  /CATEGORIES VARIABLES=D02_Timepoint [1] EMPTY=INCLUDE
  /CATEGORIES VARIABLES=S02_TypeBy2 ORDER=A KEY=VALUE EMPTY=EXCLUDE
TOTAL=YES POSITION=AFTER.

FILTER FilterBaseline.
SHOW Filter.

* T-Test EQ VAS and index.
```

```
T-TEST GROUPS=S02_TypeBy2(2 10)
  /MISSING=ANALYSIS
  /VARIABLES=D08_EQVAS EQ5D_Health_UK
  /CRITERIA=CI(.95).

* Barchart EQ VAS at baseline.
GGRAPH
  /GRAPHDATASET NAME="graphdataset" VARIABLES=S02_TypeBy2
MEANCI(D08_EQVAS, 95)[name="MEAN_D08_EQVAS" LOW="MEAN_D08_EQVAS_LOW"
HIGH="MEAN_D08_EQVAS_HIGH"] MISSING=LISTWISE REPORTMISSING=NO
  /GRAPHSPEC SOURCE=INLINE.
BEGIN GPL
  SOURCE: s=userSource(id("graphdataset"))
  DATA: S02_TypeBy2=col(source(s), name("S02_TypeBy2"),
notIn("0", "1"), unit.category())
  DATA: MEAN_D08_EQVAS=col(source(s), name("MEAN_D08_EQVAS"))
  DATA: LOW=col(source(s), name("MEAN_D08_EQVAS_LOW"))
  DATA: HIGH=col(source(s), name("MEAN_D08_EQVAS_HIGH"))
  GUIDE: axis(dim(2), label("Mean EQ VAS"))
  SCALE: cat(dim(1), include("2", "10"))
  SCALE: linear(dim(2), include(0))
  ELEMENT: interval(position(S02_TypeBy2*MEAN_D08_EQVAS),
shape.interior(shape.square))
  ELEMENT:
interval(position(region.spread.range(S02_TypeBy2*(LOW+HIGH))),
shape.interior(shape.ibeam))
END GPL.

* Barchart EQ index at baseline.
GGRAPH
  /GRAPHDATASET NAME="graphdataset" VARIABLES=S02_TypeBy2
MEANCI(EQ5D_Health_UK, 95)[name="MEAN_EQ5D_Health_UK"
LOW="MEAN_EQ5D_Health_UK_LOW" HIGH="MEAN_EQ5D_Health_UK_HIGH"]
MISSING=LISTWISE REPORTMISSING=NO
  /GRAPHSPEC SOURCE=INLINE.
BEGIN GPL
  SOURCE: s=userSource(id("graphdataset"))
  DATA: S02_TypeBy2=col(source(s), name("S02_TypeBy2"),
notIn("0", "1"), unit.category())
  DATA: MEAN_EQ5D_Health_UK=col(source(s),
name("MEAN_EQ5D_Health_UK"))
  DATA: LOW=col(source(s), name("MEAN_EQ5D_Health_UK_LOW"))
  DATA: HIGH=col(source(s), name("MEAN_EQ5D_Health_UK_HIGH"))
  GUIDE: axis(dim(2), label("Mean EQ index"))
  GUIDE: text.footnote(label("Error Bars: 95% CI"))
  SCALE: cat(dim(1), include("2", "10"))
  SCALE: linear(dim(2), include(0))
  ELEMENT: interval(position(S02_TypeBy2*MEAN_EQ5D_Health_UK),
shape.interior(shape.square))
  ELEMENT:
interval(position(region.spread.range(S02_TypeBy2*(LOW+HIGH))),
shape.interior(shape.ibeam))
END GPL.

FILTER by Study_OutcomesFistula.
SHOW filter.
```

```
* Longitudinal analysis.
* Show n.
CTABLES
  /VLABELS VARIABLES=D03_EQMobility D04_EQSelfCare D05_EQActivities
D06_EQPain D07_EQAnxiety D08_EQVAS EQ5D_Health_UK D02_Timepoint
    DISPLAY=LABEL
  /TABLE D03_EQMobility [COUNT F40.0, TOTALS[COUNT F40.0, MISSING]]
+ D04_EQSelfCare [COUNT F40.0, TOTALS[COUNT F40.0, MISSING]] +
D05_EQActivities [COUNT F40.0, TOTALS[COUNT F40.0, MISSING]] +
D06_EQPain [COUNT F40.0, TOTALS[COUNT F40.0, MISSING]] +
D07_EQAnxiety [COUNT F40.0, TOTALS[COUNT F40.0, MISSING]] +
D08_EQVAS [COUNT F40.0, MISSING] + EQ5D_Health_UK [COUNT F40.0,
MISSING] BY D02_Timepoint
  /CATEGORIES VARIABLES=D03_EQMobility D04_EQSelfCare
D05_EQActivities D06_EQPain D07_EQAnxiety ORDER=A KEY=VALUE
EMPTY=INCLUDE TOTAL=YES POSITION=AFTER
  /CATEGORIES VARIABLES=D02_Timepoint EMPTY=EXCLUDE.

* EQ-5D, by Type.
CTABLES
  /VLABELS VARIABLES=D03_EQMobility D04_EQSelfCare D05_EQActivities
D06_EQPain D07_EQAnxiety D02_Timepoint S02_TypeBy2
    DISPLAY=LABEL
  /TABLE D03_EQMobility [C] + D04_EQSelfCare [C] + D05_EQActivities
[C] + D06_EQPain [C] + D07_EQAnxiety [C] BY S02_TypeBy2 [C] >
D02_Timepoint [C][COLPCT.COUNT PCT40.0]
  /CATEGORIES VARIABLES=D03_EQMobility D04_EQSelfCare
D05_EQActivities D06_EQPain D07_EQAnxiety ORDER=A KEY=VALUE
EMPTY=INCLUDE
  /CATEGORIES VARIABLES=D02_Timepoint EMPTY=EXCLUDE
  /CATEGORIES VARIABLES=S02_TypeBy2 ORDER=A KEY=VALUE EMPTY=EXCLUDE
TOTAL=YES POSITION=AFTER.

* EQ-5D, by Type and Outcome.
CTABLES
  /VLABELS VARIABLES=D03_EQMobility D04_EQSelfCare D05_EQActivities
D06_EQPain D07_EQAnxiety D02_Timepoint S02_TypeBy2
S16_RxSatisfactory
    DISPLAY=LABEL
  /TABLE S16_RxSatisfactory [C] > D03_EQMobility [C] +
S16_RxSatisfactory [C] > D04_EQSelfCare [C] + S16_RxSatisfactory [C]
> D05_EQActivities [C] +
S16_RxSatisfactory [C] > D06_EQPain [C] + S16_RxSatisfactory [C] >
D07_EQAnxiety [C] BY S02_TypeBy2 [C] > D02_Timepoint
[C][COLPCT.COUNT PCT40.0]
  /CATEGORIES VARIABLES=D03_EQMobility D04_EQSelfCare
D05_EQActivities D06_EQPain D07_EQAnxiety ORDER=A KEY=VALUE
EMPTY=INCLUDE
  /CATEGORIES VARIABLES=D02_Timepoint EMPTY=EXCLUDE
  /CATEGORIES VARIABLES=S02_TypeBy2 ORDER=A KEY=VALUE EMPTY=EXCLUDE
TOTAL=YES POSITION=AFTER.

* EQ-VAS and EQ-Index by Type.
CTABLES
  /VLABELS VARIABLES=D08_EQVAS EQ5D_Health_UK D02_Timepoint
S02_TypeBy2 DISPLAY=LABEL
```

```
  /TABLE D08_EQVAS [S][MEAN, STDDEV] + EQ5D_Health_UK [S][MEAN,
STDDEV] BY S02_TypeBy2 [C] > D02_Timepoint [C]
  /CATEGORIES VARIABLES=D02_Timepoint EMPTY=INCLUDE
  /CATEGORIES VARIABLES=S02_TypeBy2 ORDER=A KEY=VALUE EMPTY=EXCLUDE
TOTAL=YES POSITION=AFTER.

* Line chart EQ VAS by type.
GGRAPH
  /GRAPHDATASET NAME="graphdataset" VARIABLES=D02_Timepoint
MEANCI(EQ5D_Health_UK, 95)[name="MEAN_EQ5D_Health_UK"
LOW="MEAN_EQ5D_Health_UK_LOW" HIGH="MEAN_EQ5D_Health_UK_HIGH"]
S02_TypeBy2 MISSING=LISTWISE REPORTMISSING=NO
  /GRAPHSPEC SOURCE=INLINE.
BEGIN GPL
  SOURCE: s=userSource(id("graphdataset"))
  DATA: D02_Timepoint=col(source(s), name("D02_Timepoint"),
unit.category())
  DATA: MEAN_EQ5D_Health_UK=col(source(s),
name("MEAN_EQ5D_Health_UK"))
  DATA: S02_TypeBy2=col(source(s), name("S02_TypeBy2"),
notIn("0", "1"), unit.category())
  DATA: LOW=col(source(s), name("MEAN_EQ5D_Health_UK_LOW"))
  DATA: HIGH=col(source(s), name("MEAN_EQ5D_Health_UK_HIGH"))
  GUIDE: axis(dim(2), label("Mean EQ index"))
  GUIDE: legend(aesthetic(aesthetic.color.interior), label(""))
  SCALE: cat(dim(1), include("1", "10", "11"))
  SCALE: linear(dim(2), include(0))
  SCALE: cat(aesthetic(aesthetic.color.interior), include("2",
"10"))
  ELEMENT: line(position(D02_Timepoint*MEAN_EQ5D_Health_UK),
color.interior(S02_TypeBy2), missing.wings())
  ELEMENT:
interval(position(region.spread.range(D02_Timepoint*(LOW+HIGH))),
shape.interior(shape.ibeam), color.interior(S02_TypeBy2))
END GPL.

* Line chart EQ index by type.
GGRAPH
  /GRAPHDATASET NAME="graphdataset" VARIABLES=D02_Timepoint
MEANCI(D08_EQVAS, 95)[name="MEAN_D08_EQVAS" LOW="MEAN_D08_EQVAS_LOW"
HIGH="MEAN_D08_EQVAS_HIGH"] S02_TypeBy2 MISSING=LISTWISE
REPORTMISSING=NO
  /GRAPHSPEC SOURCE=INLINE.
BEGIN GPL
  SOURCE: s=userSource(id("graphdataset"))
  DATA: D02_Timepoint=col(source(s), name("D02_Timepoint"),
unit.category())
  DATA: MEAN_D08_EQVAS=col(source(s), name("MEAN_D08_EQVAS"))
  DATA: S02_TypeBy2=col(source(s), name("S02_TypeBy2"),
notIn("0", "1"), unit.category())
  DATA: LOW=col(source(s), name("MEAN_D08_EQVAS_LOW"))
  DATA: HIGH=col(source(s), name("MEAN_D08_EQVAS_HIGH"))
  GUIDE: axis(dim(2), label("Mean EQ VAS"))
  GUIDE: legend(aesthetic(aesthetic.color.interior), label(""))
  SCALE: cat(dim(1), include("1", "10", "11"))
  SCALE: linear(dim(2), include(0))
```

```
  SCALE: cat(aesthetic(aesthetic.color.interior), include("2",
"10"))
  ELEMENT: line(position(D02_Timepoint*MEAN_D08_EQVAS),
color.interior(S02_TypeBy2), missing.wings())
  ELEMENT:
interval(position(region.spread.range(D02_Timepoint*(LOW+HIGH))),
shape.interior(shape.ibeam), color.interior(S02_TypeBy2))
END GPL.

* EQ-VAS and EQ-Index by Type and treatment outcome.
CTABLES
  /VLABELS VARIABLES=D08_EQVAS EQ5D_Health_UK D02_Timepoint
S02_TypeBy2 S16_RxSatisfactory DISPLAY=LABEL
  /TABLE S16_RxSatisfactory > D08_EQVAS [S][MEAN, STDDEV] +
S16_RxSatisfactory > EQ5D_Health_UK [S][MEAN, STDDEV] BY S02_TypeBy2
[C] > D02_Timepoint [C]
  /CATEGORIES VARIABLES=D02_Timepoint EMPTY=INCLUDE
  /CATEGORIES VARIABLES=S16_RxSatisfactory ORDER=A KEY=VALUE
  /CATEGORIES VARIABLES=S02_TypeBy2 ORDER=A KEY=VALUE EMPTY=EXCLUDE
TOTAL=YES POSITION=AFTER.

* Line chart EQ VAS by treatment outcome.
GGRAPH
  /GRAPHDATASET NAME="graphdataset" VARIABLES=D02_Timepoint
MEANCI(D08_EQVAS, 95)[name="MEAN_D08_EQVAS" LOW="MEAN_D08_EQVAS_LOW"
HIGH="MEAN_D08_EQVAS_HIGH"] S16_RxSatisfactory MISSING=LISTWISE
REPORTMISSING=NO
  /GRAPHSPEC SOURCE=INLINE.
BEGIN GPL
  SOURCE: s=userSource(id("graphdataset"))
  DATA: D02_Timepoint=col(source(s), name("D02_Timepoint"),
unit.category())
  DATA: MEAN_D08_EQVAS=col(source(s), name("MEAN_D08_EQVAS"))
  DATA: S16_RxSatisfactory=col(source(s),
name("S16_RxSatisfactory"), unit.category())
  DATA: LOW=col(source(s), name("MEAN_D08_EQVAS_LOW"))
  DATA: HIGH=col(source(s), name("MEAN_D08_EQVAS_HIGH"))
  GUIDE: axis(dim(2), label("Mean EQ VAS"))
  GUIDE: legend(aesthetic(aesthetic.color.interior), label(""))
  SCALE: cat(dim(1), include("1", "10", "11"))
  SCALE: linear(dim(2), include(0))
  SCALE: cat(aesthetic(aesthetic.color.interior), include("1",
"10"))
  ELEMENT: line(position(D02_Timepoint*MEAN_D08_EQVAS),
color.interior(S16_RxSatisfactory), missing.wings())
  ELEMENT:
interval(position(region.spread.range(D02_Timepoint*(LOW+HIGH))),
shape.interior(shape.ibeam), color.interior(S16_RxSatisfactory))
END GPL.

* Line chart EQ index by treatment outcome.
GGRAPH
  /GRAPHDATASET NAME="graphdataset" VARIABLES=D02_Timepoint
MEANCI(EQ5D_Health_UK, 95)[name="MEAN_EQ5D_Health_UK"
LOW="MEAN_EQ5D_Health_UK_LOW" HIGH="MEAN_EQ5D_Health_UK_HIGH"]
S16_RxSatisfactory MISSING=LISTWISE REPORTMISSING=NO
  /GRAPHSPEC SOURCE=INLINE.
```

```
BEGIN GPL
  SOURCE: s=userSource(id("graphdataset"))
  DATA: D02_Timepoint=col(source(s), name("D02_Timepoint"),
unit.category())
  DATA: MEAN_EQ5D_Health_UK=col(source(s),
name("MEAN_EQ5D_Health_UK"))
  DATA: S16_RxSatisfactory=col(source(s),
name("S16_RxSatisfactory"), unit.category())
  DATA: LOW=col(source(s), name("MEAN_EQ5D_Health_UK_LOW"))
  DATA: HIGH=col(source(s), name("MEAN_EQ5D_Health_UK_HIGH"))
  GUIDE: axis(dim(2), label("Mean EQ index"))
  GUIDE: legend(aesthetic(aesthetic.color.interior), label(""))
  SCALE: cat(dim(1), include("1", "10", "11"))
  SCALE: linear(dim(2), include(0))
  SCALE: cat(aesthetic(aesthetic.color.interior), include("1",
"10"))
  ELEMENT: line(position(D02_Timepoint*MEAN_EQ5D_Health_UK),
color.interior(S16_RxSatisfactory), missing.wings())
  ELEMENT:
interval(position(region.spread.range(D02_Timepoint*(LOW+HIGH))),
shape.interior(shape.ibeam), color.interior(S16_RxSatisfactory))
END GPL.
```

Cytokine and Phosphoprotein Phenotyping

```
* OPEN AND PREPARE DATA.
CD '/Users/james/Dropbox/Fistula Studies/Analysis/2015-10 Lab'.

* FILTER CASES.
FILTER by Study_ImmunoExHS.
SHOW filter.

* CYTOKINES.
* Show n.
CTABLES
  /VLABELS VARIABLES=H01_EGF Biopsy S02_TypeBy2 DISPLAY=LABEL
  /TABLE H01_EGF [S][VALIDN F40.0] > Biopsy [C] BY S02_TypeBy2 [C]
  /CATEGORIES VARIABLES=Biopsy ORDER=A KEY=VALUE EMPTY=INCLUDE
TOTAL=YES LABEL='All' POSITION=AFTER
  /CATEGORIES VARIABLES=S02_TypeBy2 [0, 2, 10] EMPTY=INCLUDE
TOTAL=YES LABEL='All' POSITION=AFTER.

* NON-PARAMETRIC TESTS.
FILTER by FilterFistula.
SHOW Filter.

* Medians and IQRs.
CTABLES
  /VLABELS VARIABLES=H01_EGF H02_Eotaxin S02_TypeBy2 DISPLAY=LABEL
  /TABLE H01_EGF [MEDIAN, PTILE 25, PTILE 75] + H02_Eotaxin [MEDIAN,
PTILE 25, PTILE 75] + H03_GCSF [MEDIAN, PTILE 25, PTILE 75] +
H04_GMCSF [MEDIAN, PTILE 25, PTILE 75] + H05_IFNa2 [MEDIAN, PTILE
25, PTILE 75] + H06_IFNg [MEDIAN, PTILE 25, PTILE 75] +
H07_IL10 [MEDIAN, PTILE 25, PTILE 75] + H08_IL12p40 [MEDIAN, PTILE
25, PTILE 75] + H09_IL12p70 [MEDIAN, PTILE 25, PTILE 75] +
```

```
H10_IL13 [MEDIAN, PTILE 25, PTILE 75] + H11_IL15 [MEDIAN, PTILE 25,
PTILE 75] + H12_IL17A [MEDIAN, PTILE 25, PTILE 75] +
H13_IL1RA [MEDIAN, PTILE 25, PTILE 75] + H14_IL1a [MEDIAN, PTILE 25,
PTILE 75] + H15_IL1b [MEDIAN, PTILE 25, PTILE 75] +
H16_IL2 [MEDIAN, PTILE 25, PTILE 75] + H17_IL3 [MEDIAN, PTILE 25,
PTILE 75] + H18_IL4 [MEDIAN, PTILE 25, PTILE 75] +
H19_IL5 [MEDIAN, PTILE 25, PTILE 75] + H20_IL6 [MEDIAN, PTILE 25,
PTILE 75] + H21_IL7 [MEDIAN, PTILE 25, PTILE 75] +
H22_IL8 [MEDIAN, PTILE 25, PTILE 75] + H23_IP10 [MEDIAN, PTILE 25,
PTILE 75] + H24_MCP1 [MEDIAN, PTILE 25, PTILE 75] +
H25_MIP1a [MEDIAN, PTILE 25, PTILE 75] + H26_MIP1b [MEDIAN, PTILE
25, PTILE 75] + H27_RANTES [MEDIAN, PTILE 25, PTILE 75] +
H28_TNFa [MEDIAN, PTILE 25, PTILE 75] + H29_TNFb [MEDIAN, PTILE 25,
PTILE 75] + H30_VEGF [MEDIAN, PTILE 25, PTILE 75]
 BY S02_TypeBy2
  /CATEGORIES VARIABLES=S02_TypeBy2 ORDER=A KEY=VALUE EMPTY=EXCLUDE
TOTAL=YES LABEL='All' POSITION=AFTER.

* Nonparametric Tests: Independent Samples.
NPTESTS
  /INDEPENDENT TEST (H01_EGF H02_Eotaxin H03_GCSF H04_GMCSF
H05_IFNa2 H06_IFNg H07_IL10 H08_IL12p40 H09_IL12p70
H10_IL13 H11_IL15 H12_IL17A H13_IL1RA H14_IL1a H15_IL1b H16_IL2
H17_IL3 H18_IL4 H19_IL5 H20_IL6 H21_IL7 H22_IL8
H23_IP10 H24_MCP1 H25_MIP1a H26_MIP1b H27_RANTES H28_TNFa H29_TNFb
H30_VEGF) GROUP (S02_TypeBy2) MANN_WHITNEY HODGES_LEHMANN
  /MISSING SCOPE=ANALYSIS USERMISSING=EXCLUDE
  /CRITERIA ALPHA=0.01  CILEVEL=99.

* Granulation.
FILTER by FilterGranulation.
SHOW Filter.

* Medians and IQRs.
CTABLES
  /VLABELS VARIABLES=H01_EGF H02_Eotaxin S02_TypeBy2 DISPLAY=LABEL
  /TABLE H01_EGF [MEDIAN, PTILE 25, PTILE 75] + H02_Eotaxin [MEDIAN,
PTILE 25, PTILE 75] + H03_GCSF [MEDIAN, PTILE 25, PTILE 75] +
H04_GMCSF [MEDIAN, PTILE 25, PTILE 75] + H05_IFNa2 [MEDIAN, PTILE
25, PTILE 75] + H06_IFNg [MEDIAN, PTILE 25, PTILE 75] +
H07_IL10 [MEDIAN, PTILE 25, PTILE 75] + H08_IL12p40 [MEDIAN, PTILE
25, PTILE 75] + H09_IL12p70 [MEDIAN, PTILE 25, PTILE 75] +
H10_IL13 [MEDIAN, PTILE 25, PTILE 75] + H11_IL15 [MEDIAN, PTILE 25,
PTILE 75] + H12_IL17A [MEDIAN, PTILE 25, PTILE 75] +
H13_IL1RA [MEDIAN, PTILE 25, PTILE 75] + H14_IL1a [MEDIAN, PTILE 25,
PTILE 75] + H15_IL1b [MEDIAN, PTILE 25, PTILE 75] +
H16_IL2 [MEDIAN, PTILE 25, PTILE 75] + H17_IL3 [MEDIAN F40.2, PTILE
25, PTILE 75] + H18_IL4 [MEDIAN, PTILE 25, PTILE 75] +
H19_IL5 [MEDIAN, PTILE 25, PTILE 75] + H20_IL6 [MEDIAN, PTILE 25,
PTILE 75] + H21_IL7 [MEDIAN, PTILE 25, PTILE 75] +
H22_IL8 [MEDIAN, PTILE 25, PTILE 75] + H23_IP10 [MEDIAN, PTILE 25,
PTILE 75] + H24_MCP1 [MEDIAN, PTILE 25, PTILE 75] +
H25_MIP1a [MEDIAN, PTILE 25, PTILE 75] + H26_MIP1b [MEDIAN, PTILE
25, PTILE 75] + H27_RANTES [MEDIAN, PTILE 25, PTILE 75] +
H28_TNFa [MEDIAN, PTILE 25, PTILE 75] + H29_TNFb [MEDIAN, PTILE 25,
PTILE 75] + H30_VEGF [MEDIAN, PTILE 25, PTILE 75]
 BY S02_TypeBy2
```

```
  /CATEGORIES VARIABLES=S02_TypeBy2 ORDER=A KEY=VALUE EMPTY=EXCLUDE
TOTAL=YES LABEL='All' POSITION=AFTER.

* Nonparametric Tests: Independent Samples.
NPTESTS
  /INDEPENDENT TEST (H01_EGF H02_Eotaxin H03_GCSF H04_GMCSF
H05_IFNa2 H06_IFNg H07_IL10 H08_IL12p40 H09_IL12p70
H10_IL13 H11_IL15 H12_IL17A H13_IL1RA H14_IL1a H15_IL1b H16_IL2
H17_IL3 H18_IL4 H19_IL5 H20_IL6 H21_IL7 H22_IL8
H23_IP10 H24_MCP1 H25_MIP1a H26_MIP1b H27_RANTES H28_TNFa H29_TNFb
H30_VEGF) GROUP (S02_TypeBy2) MANN_WHITNEY HODGES_LEHMANN
  /MISSING SCOPE=ANALYSIS USERMISSING=EXCLUDE
  /CRITERIA ALPHA=0.01  CILEVEL=99.

* Mucosa.
FILTER by FilterMucosa.
SHOW Filter.

* Medians and IQRs.
CTABLES
  /VLABELS VARIABLES=H01_EGF H02_Eotaxin S02_TypeBy2 DISPLAY=LABEL
  /TABLE H01_EGF [MEDIAN, PTILE 25, PTILE 75] + H02_Eotaxin [MEDIAN,
PTILE 25, PTILE 75] + H03_GCSF [MEDIAN, PTILE 25, PTILE 75] +
H04_GMCSF [MEDIAN, PTILE 25, PTILE 75] + H05_IFNa2 [MEDIAN, PTILE
25, PTILE 75] + H06_IFNg [MEDIAN, PTILE 25, PTILE 75] +
H07_IL10 [MEDIAN, PTILE 25, PTILE 75] + H08_IL12p40 [MEDIAN, PTILE
25, PTILE 75] + H09_IL12p70 [MEDIAN, PTILE 25, PTILE 75] +
H10_IL13 [MEDIAN, PTILE 25, PTILE 75] + H11_IL15 [MEDIAN, PTILE 25,
PTILE 75] + H12_IL17A [MEDIAN, PTILE 25, PTILE 75] +
H13_IL1RA [MEDIAN, PTILE 25, PTILE 75] + H14_IL1a [MEDIAN, PTILE 25,
PTILE 75] + H15_IL1b [MEDIAN, PTILE 25, PTILE 75] +
H16_IL2 [MEDIAN, PTILE 25, PTILE 75] + H17_IL3 [MEDIAN, PTILE 25,
PTILE 75] + H18_IL4 [MEDIAN, PTILE 25, PTILE 75] +
H19_IL5 [MEDIAN, PTILE 25, PTILE 75] + H20_IL6 [MEDIAN, PTILE 25,
PTILE 75] + H21_IL7 [MEDIAN, PTILE 25, PTILE 75] +
H22_IL8 [MEDIAN, PTILE 25, PTILE 75] + H23_IP10 [MEDIAN, PTILE 25,
PTILE 75] + H24_MCP1 [MEDIAN, PTILE 25, PTILE 75] +
H25_MIP1a [MEDIAN, PTILE 25, PTILE 75] + H26_MIP1b [MEDIAN, PTILE
25, PTILE 75] + H27_RANTES [MEDIAN, PTILE 25, PTILE 75] +
H28_TNFa [MEDIAN, PTILE 25, PTILE 75] + H29_TNFb [MEDIAN, PTILE 25,
PTILE 75] + H30_VEGF [MEDIAN, PTILE 25, PTILE 75]
 BY S02_TypeBy2
  /CATEGORIES VARIABLES=S02_TypeBy2 ORDER=A KEY=VALUE EMPTY=EXCLUDE
TOTAL=YES LABEL='All' POSITION=AFTER.

* Nonparametric Tests: Independent Samples.
NPTESTS
  /INDEPENDENT TEST (H01_EGF H02_Eotaxin H03_GCSF H04_GMCSF
H05_IFNa2 H06_IFNg H07_IL10 H08_IL12p40 H09_IL12p70
H10_IL13 H11_IL15 H12_IL17A H13_IL1RA H14_IL1a H15_IL1b H16_IL2
H17_IL3 H18_IL4 H19_IL5 H20_IL6 H21_IL7 H22_IL8
H23_IP10 H24_MCP1 H25_MIP1a H26_MIP1b H27_RANTES H28_TNFa H29_TNFb
H30_VEGF) GROUP (S02_TypeBy2) MANN_WHITNEY HODGES_LEHMANN
  /MISSING SCOPE=ANALYSIS USERMISSING=EXCLUDE
  /CRITERIA ALPHA=0.01  CILEVEL=99.

* Rectum.
```

```
FILTER by FilterRectum.
SHOW Filter.

* Medians and IQRs.
CTABLES
  /VLABELS VARIABLES=H01_EGF H02_Eotaxin S02_TypeBy2 DISPLAY=LABEL
  /TABLE H01_EGF [MEDIAN, PTILE 25, PTILE 75] + H02_Eotaxin [MEDIAN,
PTILE 25, PTILE 75] + H03_GCSF [MEDIAN, PTILE 25, PTILE 75] +
H04_GMCSF [MEDIAN, PTILE 25, PTILE 75] + H05_IFNa2 [MEDIAN, PTILE
25, PTILE 75] + H06_IFNg [MEDIAN, PTILE 25, PTILE 75] +
H07_IL10 [MEDIAN, PTILE 25, PTILE 75] + H08_IL12p40 [MEDIAN, PTILE
25, PTILE 75] + H09_IL12p70 [MEDIAN, PTILE 25, PTILE 75] +
H10_IL13 [MEDIAN, PTILE 25, PTILE 75] + H11_IL15 [MEDIAN, PTILE 25,
PTILE 75] + H12_IL17A [MEDIAN, PTILE 25, PTILE 75] +
H13_IL1RA [MEDIAN, PTILE 25, PTILE 75] + H14_IL1a [MEDIAN, PTILE 25,
PTILE 75] + H15_IL1b [MEDIAN, PTILE 25, PTILE 75] +
H16_IL2 [MEDIAN, PTILE 25, PTILE 75] + H17_IL3 [MEDIAN F40.3, PTILE
25, PTILE 75] + H18_IL4 [MEDIAN, PTILE 25, PTILE 75] +
H19_IL5 [MEDIAN, PTILE 25, PTILE 75] + H20_IL6 [MEDIAN, PTILE 25,
PTILE 75] + H21_IL7 [MEDIAN, PTILE 25, PTILE 75] +
H22_IL8 [MEDIAN, PTILE 25, PTILE 75] + H23_IP10 [MEDIAN, PTILE 25,
PTILE 75] + H24_MCP1 [MEDIAN, PTILE 25, PTILE 75] +
H25_MIP1a [MEDIAN, PTILE 25, PTILE 75] + H26_MIP1b [MEDIAN, PTILE
25, PTILE 75] + H27_RANTES [MEDIAN, PTILE 25, PTILE 75] +
H28_TNFa [MEDIAN, PTILE 25, PTILE 75] + H29_TNFb [MEDIAN, PTILE 25,
PTILE 75] + H30_VEGF [MEDIAN, PTILE 25, PTILE 75]
 BY S02_TypeBy2
  /CATEGORIES VARIABLES=S02_TypeBy2 ORDER=A KEY=VALUE EMPTY=EXCLUDE
TOTAL=YES LABEL='All' POSITION=AFTER.

* Nonparametric Tests: Independent Samples.
NPTESTS
  /INDEPENDENT TEST (H01_EGF H02_Eotaxin H03_GCSF H04_GMCSF
H05_IFNa2 H06_IFNg H07_IL10 H08_IL12p40 H09_IL12p70
H10_IL13 H11_IL15 H12_IL17A H13_IL1RA H14_IL1a H15_IL1b H16_IL2
H17_IL3 H18_IL4 H19_IL5 H20_IL6 H21_IL7 H22_IL8
H23_IP10 H24_MCP1 H25_MIP1a H26_MIP1b H27_RANTES H28_TNFa H29_TNFb
H30_VEGF) GROUP (S02_TypeBy2) MANN_WHITNEY HODGES_LEHMANN
  /MISSING SCOPE=ANALYSIS USERMISSING=EXCLUDE
  /CRITERIA ALPHA=0.01  CILEVEL=99.

* ControlsVCrohns.
FILTER by FilterControlsVCrohns.
SHOW Filter.

* Medians and IQRs.
CTABLES
  /VLABELS VARIABLES=H01_EGF H02_Eotaxin S02_TypeBy2 DISPLAY=LABEL
  /TABLE H01_EGF [MEDIAN, PTILE 25, PTILE 75] + H02_Eotaxin [MEDIAN,
PTILE 25, PTILE 75] + H03_GCSF [MEDIAN, PTILE 25, PTILE 75] +
H04_GMCSF [MEDIAN, PTILE 25, PTILE 75] + H05_IFNa2 [MEDIAN, PTILE
25, PTILE 75] + H06_IFNg [MEDIAN, PTILE 25, PTILE 75] +
H07_IL10 [MEDIAN, PTILE 25, PTILE 75] + H08_IL12p40 [MEDIAN, PTILE
25, PTILE 75] + H09_IL12p70 [MEDIAN, PTILE 25, PTILE 75] +
H10_IL13 [MEDIAN, PTILE 25, PTILE 75] + H11_IL15 [MEDIAN, PTILE 25,
PTILE 75] + H12_IL17A [MEDIAN, PTILE 25, PTILE 75] +
```

```
H13_IL1RA [MEDIAN, PTILE 25, PTILE 75] + H14_IL1a [MEDIAN, PTILE 25,
PTILE 75] + H15_IL1b [MEDIAN, PTILE 25, PTILE 75] +
H16_IL2 [MEDIAN, PTILE 25, PTILE 75] + H17_IL3 [MEDIAN F40.3, PTILE
25, PTILE 75] + H18_IL4 [MEDIAN, PTILE 25, PTILE 75] +
H19_IL5 [MEDIAN, PTILE 25, PTILE 75] + H20_IL6 [MEDIAN, PTILE 25,
PTILE 75] + H21_IL7 [MEDIAN, PTILE 25, PTILE 75] +
H22_IL8 [MEDIAN, PTILE 25, PTILE 75] + H23_IP10 [MEDIAN, PTILE 25,
PTILE 75] + H24_MCP1 [MEDIAN, PTILE 25, PTILE 75] +
H25_MIP1a [MEDIAN, PTILE 25, PTILE 75] + H26_MIP1b [MEDIAN, PTILE
25, PTILE 75] + H27_RANTES [MEDIAN, PTILE 25, PTILE 75] +
H28_TNFa [MEDIAN, PTILE 25, PTILE 75] + H29_TNFb [MEDIAN, PTILE 25,
PTILE 75] + H30_VEGF [MEDIAN, PTILE 25, PTILE 75]
 BY S02_TypeBy2
  /CATEGORIES VARIABLES=S02_TypeBy2 ORDER=A KEY=VALUE EMPTY=EXCLUDE
TOTAL=YES LABEL='All' POSITION=AFTER.

* Nonparametric Tests: Independent Samples.
NPTESTS
  /INDEPENDENT TEST (H01_EGF H02_Eotaxin H03_GCSF H04_GMCSF
H05_IFNa2 H06_IFNg H07_IL10 H08_IL12p40 H09_IL12p70
H10_IL13 H11_IL15 H12_IL17A H13_IL1RA H14_IL1a H15_IL1b H16_IL2
H17_IL3 H18_IL4 H19_IL5 H20_IL6 H21_IL7 H22_IL8
H23_IP10 H24_MCP1 H25_MIP1a H26_MIP1b H27_RANTES H28_TNFa H29_TNFb
H30_VEGF) GROUP (S02_TypeBy2) MANN_WHITNEY HODGES_LEHMANN
  /MISSING SCOPE=ANALYSIS USERMISSING=EXCLUDE
  /CRITERIA ALPHA=0.01  CILEVEL=99.

* ControlsVFistulae.
FILTER by FilterControls.
SHOW Filter.

* Medians and IQRs.
CTABLES
  /VLABELS VARIABLES=H01_EGF H02_Eotaxin S15_TypeBy1 DISPLAY=LABEL
  /TABLE H01_EGF [MEDIAN, PTILE 25, PTILE 75] + H02_Eotaxin [MEDIAN,
PTILE 25, PTILE 75] + H03_GCSF [MEDIAN, PTILE 25, PTILE 75] +
H04_GMCSF [MEDIAN, PTILE 25, PTILE 75] + H05_IFNa2 [MEDIAN, PTILE
25, PTILE 75] + H06_IFNg [MEDIAN, PTILE 25, PTILE 75] +
H07_IL10 [MEDIAN, PTILE 25, PTILE 75] + H08_IL12p40 [MEDIAN, PTILE
25, PTILE 75] + H09_IL12p70 [MEDIAN, PTILE 25, PTILE 75] +
H10_IL13 [MEDIAN, PTILE 25, PTILE 75] + H11_IL15 [MEDIAN, PTILE 25,
PTILE 75] + H12_IL17A [MEDIAN, PTILE 25, PTILE 75] +
H13_IL1RA [MEDIAN, PTILE 25, PTILE 75] + H14_IL1a [MEDIAN, PTILE 25,
PTILE 75] + H15_IL1b [MEDIAN, PTILE 25, PTILE 75] +
H16_IL2 [MEDIAN, PTILE 25, PTILE 75] + H17_IL3 [MEDIAN F40.3, PTILE
25, PTILE 75] + H18_IL4 [MEDIAN, PTILE 25, PTILE 75] +
H19_IL5 [MEDIAN, PTILE 25, PTILE 75] + H20_IL6 [MEDIAN, PTILE 25,
PTILE 75] + H21_IL7 [MEDIAN, PTILE 25, PTILE 75] +
H22_IL8 [MEDIAN, PTILE 25, PTILE 75] + H23_IP10 [MEDIAN, PTILE 25,
PTILE 75] + H24_MCP1 [MEDIAN, PTILE 25, PTILE 75] +
H25_MIP1a [MEDIAN, PTILE 25, PTILE 75] + H26_MIP1b [MEDIAN, PTILE
25, PTILE 75] + H27_RANTES [MEDIAN, PTILE 25, PTILE 75] +
H28_TNFa [MEDIAN, PTILE 25, PTILE 75] + H29_TNFb [MEDIAN, PTILE 25,
PTILE 75] + H30_VEGF [MEDIAN, PTILE 25, PTILE 75]
 BY S15_TypeBy1
  /CATEGORIES VARIABLES=S15_TypeBy1 ORDER=A KEY=VALUE EMPTY=EXCLUDE
TOTAL=YES LABEL='All' POSITION=AFTER.
```

```
* Nonparametric Tests: Independent Samples.
NPTESTS
  /INDEPENDENT TEST (H01_EGF H02_Eotaxin H03_GCSF H04_GMCSF
H05_IFNa2 H06_IFNg H07_IL10 H08_IL12p40 H09_IL12p70
H10_IL13 H11_IL15 H12_IL17A H13_IL1RA H14_IL1a H15_IL1b H16_IL2
H17_IL3 H18_IL4 H19_IL5 H20_IL6 H21_IL7 H22_IL8
H23_IP10 H24_MCP1 H25_MIP1a H26_MIP1b H27_RANTES H28_TNFa H29_TNFb
H30_VEGF) GROUP (S15_TypeBy1) MANN_WHITNEY HODGES_LEHMANN
  /MISSING SCOPE=ANALYSIS USERMISSING=EXCLUDE
  /CRITERIA ALPHA=0.01  CILEVEL=99.

FILTER by Study_ImmunoExHS.
SHOW filter.

* Medians across all specimens.
CTABLES
  /VLABELS VARIABLES=H01_EGF Biopsy S02_TypeBy2 DISPLAY=LABEL
  /TABLE H01_EGF [MEDIAN] + H02_Eotaxin [MEDIAN] + H03_GCSF [MEDIAN]
+
H04_GMCSF [MEDIAN] + H05_IFNa2 [MEDIAN] + H06_IFNg [MEDIAN] +
H07_IL10 [MEDIAN] + H08_IL12p40 [MEDIAN] + H09_IL12p70 [MEDIAN] +
H10_IL13 [MEDIAN] + H11_IL15 [MEDIAN] + H12_IL17A [MEDIAN] +
H13_IL1RA [MEDIAN] + H14_IL1a [MEDIAN] + H15_IL1b [MEDIAN] +
H16_IL2 [MEDIAN] + H17_IL3 [MEDIAN F40.3] + H18_IL4 [MEDIAN] +
H19_IL5 [MEDIAN] + H20_IL6 [MEDIAN] + H21_IL7 [MEDIAN] +
H22_IL8 [MEDIAN] + H23_IP10 [MEDIAN] + H24_MCP1 [MEDIAN] +
H25_MIP1a [MEDIAN] + H26_MIP1b [MEDIAN] + H27_RANTES [MEDIAN] +
H28_TNFa [MEDIAN] + H29_TNFb [MEDIAN] + H30_VEGF [MEDIAN] BY Biopsy
> S02_TypeBy2
  /CATEGORIES VARIABLES=Biopsy [1,2,3,4] EMPTY=INCLUDE
  /CATEGORIES VARIABLES=S02_TypeBy2 [0, 2, 10] EMPTY=INCLUDE.

* Table to compare cytokine concentration medians with Tozer et al.
CTABLES
  /VLABELS VARIABLES=H16_IL2 H18_IL4 H20_IL6 H23_IP10 H28_TNFa
H06_IFNg H12_IL17A S01_TypeBy3 Biopsy
    DISPLAY=LABEL
  /TABLE H16_IL2 [MEDIAN F40.2, PTILE 25 F40.2, PTILE 75 F40.2] +
H18_IL4 [MEDIAN F40.2, PTILE 25 F40.2, PTILE 75 F40.2] + H20_IL6
[MEDIAN F40.2, PTILE 25 F40.2, PTILE 75 F40.2] +
  H23_IP10 [MEDIAN F40.2, PTILE 25 F40.2, PTILE 75 F40.2] + H28_TNFa
[MEDIAN F40.2, PTILE 25 F40.2, PTILE 75 F40.2] + H06_IFNg [MEDIAN
F40.2, PTILE 25 F40.2, PTILE 75 F40.2] +
  H12_IL17A [MEDIAN F40.2, PTILE 25 F40.2, PTILE 75 F40.2] BY
S01_TypeBy3 > Biopsy
  /SLABELS POSITION=ROW
  /CATEGORIES VARIABLES=S01_TypeBy3 [0, HSUBTOTAL='Normal', 2, 3,
HSUBTOTAL='Idiopathic', 10] EMPTY=INCLUDE POSITION=AFTER
  /CATEGORIES VARIABLES=Biopsy [1, 4] EMPTY=INCLUDE.

* IL-1RA/ IL-1 Ratio
FILTER by Study_ImmunoExHS.
SHOW filter.

* Medians and IQRs.
CTABLES
```

```
  /VLABELS VARIABLES=H31_IL1RA_IL1_Ratio Biopsy S02_TypeBy2
DISPLAY=LABEL
  /TABLE H31_IL1RA_IL1_Ratio [MEDIAN, PTILE 25, PTILE 75] > Biopsy
BY S02_TypeBy2
  /CATEGORIES VARIABLES=Biopsy [1, 2, 3, 4] EMPTY=INCLUDE
  /CATEGORIES VARIABLES=S02_TypeBy2 [2, 10] EMPTY=INCLUDE TOTAL=YES
LABEL='All' POSITION=AFTER.

FILTER by FilterFistula.
SHOW Filter.

* Nonparametric Tests: Independent Samples.
NPTESTS
  /INDEPENDENT TEST (H31_IL1RA_IL1_Ratio) GROUP (S02_TypeBy2)
MANN_WHITNEY HODGES_LEHMANN
  /MISSING SCOPE=ANALYSIS USERMISSING=EXCLUDE
  /CRITERIA ALPHA=0.01  CILEVEL=99.

FILTER by FilterGranulation.
SHOW Filter.

* Nonparametric Tests: Independent Samples.
NPTESTS
  /INDEPENDENT TEST (H31_IL1RA_IL1_Ratio) GROUP (S02_TypeBy2)
MANN_WHITNEY HODGES_LEHMANN
  /MISSING SCOPE=ANALYSIS USERMISSING=EXCLUDE
  /CRITERIA ALPHA=0.01  CILEVEL=99.

FILTER by FilterMucosa.
SHOW Filter.

* Nonparametric Tests: Independent Samples.
NPTESTS
  /INDEPENDENT TEST (H31_IL1RA_IL1_Ratio) GROUP (S02_TypeBy2)
MANN_WHITNEY HODGES_LEHMANN
  /MISSING SCOPE=ANALYSIS USERMISSING=EXCLUDE
  /CRITERIA ALPHA=0.01  CILEVEL=99.

FILTER by FilterRectum.
SHOW Filter.

* Nonparametric Tests: Independent Samples.
NPTESTS
  /INDEPENDENT TEST (H31_IL1RA_IL1_Ratio) GROUP (S02_TypeBy2)
MANN_WHITNEY HODGES_LEHMANN
  /MISSING SCOPE=ANALYSIS USERMISSING=EXCLUDE
  /CRITERIA ALPHA=0.01  CILEVEL=99.

* ControlsVCrohns.
FILTER by FilterControlsVCrohns.
SHOW Filter.

* Medians and IQRs.
CTABLES
  /VLABELS VARIABLES=H31_IL1RA_IL1_Ratio Biopsy S02_TypeBy2
DISPLAY=LABEL
```

```
  /TABLE H31_IL1RA_IL1_Ratio [MEDIAN, PTILE 25, PTILE 75] > Biopsy
BY S02_TypeBy2
  /CATEGORIES VARIABLES=Biopsy [1, 2, 3, 4] EMPTY=INCLUDE
  /CATEGORIES VARIABLES=S02_TypeBy2 [0, 10] EMPTY=EXCLUDE.

* Nonparametric Tests: Independent Samples.
NPTESTS
  /INDEPENDENT TEST (H31_IL1RA_IL1_Ratio) GROUP (S02_TypeBy2)
MANN_WHITNEY HODGES_LEHMANN
  /MISSING SCOPE=ANALYSIS USERMISSING=EXCLUDE
  /CRITERIA ALPHA=0.01  CILEVEL=99.

FILTER by Study_ImmunoExHS.
SHOW filter.

* IL-1RA/IL-1β Ratio.
GGRAPH
  /GRAPHDATASET NAME="graphdataset" VARIABLES=Biopsy
H31_IL1RA_IL1_Ratio S02_TypeBy2 MISSING=LISTWISE REPORTMISSING=NO
  /GRAPHSPEC SOURCE=INLINE.
BEGIN GPL
  SOURCE: s=userSource(id("graphdataset"))
  DATA: Biopsy=col(source(s), name("Biopsy"),
notIn("5", "6"), unit.category())
  DATA: H31_IL1RA_IL1_Ratio=col(source(s),
name("H31_IL1RA_IL1_Ratio"))
  DATA: S02_TypeBy2=col(source(s), name("S02_TypeBy2"),
notIn("1"), unit.category())
  DATA: id=col(source(s), name("$CASENUM"), unit.category())
  COORD: rect(dim(1,2), cluster(3,0))
  GUIDE: axis(dim(2), label("IL-1RA/IL-1β Ratio"))
  GUIDE: legend(aesthetic(aesthetic.color), label(""))
  SCALE: cat(dim(3), include("1", "2", "3", "4"))
  SCALE: linear(dim(2), include(0))
  SCALE: cat(aesthetic(aesthetic.color), sort.values("2", "10",
"0"))
  SCALE: cat(dim(1), sort.values("2", "10", "0"))
  ELEMENT:
schema(position(bin.quantile.letter(S02_TypeBy2*H31_IL1RA_IL1_Ratio*
Biopsy)), color(S02_TypeBy2), label(id))
END GPL.

FREQUENCIES VARIABLES=H31_IL1RA_IL1_Ratio
  /ORDER=ANALYSIS.

* IL-12p70.
GGRAPH
  /GRAPHDATASET NAME="graphdataset" VARIABLES=Biopsy H09_IL12p70
S02_TypeBy2 MISSING=LISTWISE REPORTMISSING=NO
  /GRAPHSPEC SOURCE=INLINE.
BEGIN GPL
  SOURCE: s=userSource(id("graphdataset"))
  DATA: Biopsy=col(source(s), name("Biopsy"),
notIn("5", "6"), unit.category())
  DATA: H09_IL12p70=col(source(s), name("H09_IL12p70"))
  DATA: S02_TypeBy2=col(source(s), name("S02_TypeBy2"),
notIn("1"), unit.category())
```

```
  DATA: id=col(source(s), name("$CASENUM"), unit.category())
  COORD: rect(dim(1,2), cluster(3,0))
  GUIDE: axis(dim(2), label("IL-12p70"))
  GUIDE: legend(aesthetic(aesthetic.color), label(""))
  SCALE: cat(dim(3), include("1", "2", "3", "4"))
  SCALE: linear(dim(2), include(0))
  SCALE: cat(aesthetic(aesthetic.color), sort.values("2", "10",
"0"))
  SCALE: cat(dim(1), sort.values("2", "10", "0"))
  ELEMENT:
schema(position(bin.quantile.letter(S02_TypeBy2*H09_IL12p70*Biopsy))
, color(S02_TypeBy2), label(id))
END GPL.

FREQUENCIES VARIABLES=H09_IL12p70
  /ORDER=ANALYSIS.

* PHOSPHOPROTEINS.
* Show n.
CTABLES
  /VLABELS VARIABLES= I01_EGFR_ErbB1 S02_TypeBy2 DISPLAY=LABEL
  /TABLE I01_EGFR_ErbB1 [S][VALIDN F40.0] > Biopsy [C] BY
S02_TypeBy2 [C]
  /CATEGORIES VARIABLES=Biopsy ORDER=A KEY=VALUE EMPTY=INCLUDE
TOTAL=YES LABEL='All' POSITION=AFTER
  /CATEGORIES VARIABLES=S02_TypeBy2 [0, 2, 10] EMPTY=INCLUDE
TOTAL=YES LABEL='All' POSITION=AFTER.

* NON-PARAMETRIC TESTS.
FILTER by FilterFistula.
SHOW Filter.

* Medians and IQRs.
CTABLES
  /VLABELS VARIABLES=I01_EGFR_ErbB1 H02_Eotaxin S02_TypeBy2
DISPLAY=LABEL
  /TABLE I01_EGFR_ErbB1[MEDIAN, PTILE 25, PTILE 75] +
I02_HER2_ErbB2[MEDIAN, PTILE 25, PTILE 75] +
I03_HER3_ErbB3[MEDIAN, PTILE 25, PTILE 75] + I04_FGFR1[MEDIAN, PTILE
25, PTILE 75] + I05_FGFR3[MEDIAN, PTILE 25, PTILE 75] +
I06_FGFR4[MEDIAN, PTILE 25, PTILE 75] + I07_InsR[MEDIAN, PTILE 25,
PTILE 75] + I08_IGF_IR[MEDIAN, PTILE 25, PTILE 75] +
I09_TrkA_NTRK1[MEDIAN, PTILE 25, PTILE 75] + I10_TrkB_NTRK2[MEDIAN,
PTILE 25, PTILE 75] + I11_Met_HGFR[MEDIAN, PTILE 25, PTILE 75] +
I12_Ron_MST1R[MEDIAN, PTILE 25, PTILE 75] + I13_Ret[MEDIAN, PTILE
25, PTILE 75] +
I14_ALK[MEDIAN, PTILE 25, PTILE 75] + I15_PDGFR[MEDIAN, PTILE 25,
PTILE 75] + I16_c_Kit_SCFR[MEDIAN, PTILE 25, PTILE 75] +
I17_FLT3_Flk2[MEDIAN, PTILE 25, PTILE 75] +
I18_M_CSFR_CSF_1R[MEDIAN, PTILE 25, PTILE 75] +
I19_EphA1[MEDIAN, PTILE 25, PTILE 75] + I20_EphA2[MEDIAN, PTILE 25,
PTILE 75] + I21_EphA3[MEDIAN, PTILE 25, PTILE 75] +
I22_EphB1[MEDIAN, PTILE 25, PTILE 75] + I23_EphB3[MEDIAN, PTILE 25,
PTILE 75] + I24_EphB4[MEDIAN, PTILE 25, PTILE 75] +
I25_Tyro3_Dtk[MEDIAN F40.3, PTILE 25 F40.3, PTILE 75 F40.3] +
I26_Axl[MEDIAN, PTILE 25, PTILE 75] + I27_Tie2_TEK[MEDIAN, PTILE 25,
```

```
PTILE 75] + I28_VEGFR2_KDR[MEDIAN, PTILE 25, PTILE 75] +
I29_Akt_PKB_Rac@Thr308[MEDIAN, PTILE 25, PTILE 75] +
I30_Akt_PKB_Rac@Ser473[MEDIAN, PTILE 25, PTILE 75] +
I31_p44_42_MAPK[MEDIAN, PTILE 25, PTILE 75] +
I32_S6_Ribosomal_Protein[MEDIAN, PTILE 25, PTILE 75] +
I33_c_Abl[MEDIAN, PTILE 25, PTILE 75] +
I34_IRS_1[MEDIAN, PTILE 25, PTILE 75] + I35_Zap_70[MEDIAN, PTILE 25,
PTILE 75] + I36_Src[MEDIAN, PTILE 25, PTILE 75] + I37_Lck[MEDIAN,
PTILE 25, PTILE 75] + I38_Stat1[MEDIAN, PTILE 25, PTILE 75] +
I39_Stat3 [MEDIAN, PTILE 25, PTILE 75]
BY S02_TypeBy2
  /CATEGORIES VARIABLES=S02_TypeBy2 ORDER=A KEY=VALUE EMPTY=EXCLUDE
TOTAL=YES LABEL='All' POSITION=AFTER.

* Nonparametric Tests: Independent Samples.
NPTESTS
  /INDEPENDENT TEST (I01_EGFR_ErbB1 I02_HER2_ErbB2
I03_HER3_ErbB3 I04_FGFR1 I05_FGFR3 I06_FGFR4 I07_InsR I08_IGF_IR
I09_TrkA_NTRK1 I10_TrkB_NTRK2 I11_Met_HGFR I12_Ron_MST1R I13_Ret
I14_ALK I15_PDGFR I16_c_Kit_SCFR I17_FLT3_Flk2 I18_M_CSFR_CSF_1R
I19_EphA1 I20_EphA2 I21_EphA3 I22_EphB1 I23_EphB3 I24_EphB4
I25_Tyro3_Dtk I26_Axl I27_Tie2_TEK I28_VEGFR2_KDR
I29_Akt_PKB_Rac@Thr308
I30_Akt_PKB_Rac@Ser473 I31_p44_42_MAPK I32_S6_Ribosomal_Protein
I33_c_Abl
I34_IRS_1 I35_Zap_70 I36_Src I37_Lck I38_Stat1 I39_Stat3) GROUP
(S02_TypeBy2) MANN_WHITNEY HODGES_LEHMANN
  /MISSING SCOPE=ANALYSIS USERMISSING=EXCLUDE
  /CRITERIA ALPHA=0.01  CILEVEL=99.

FILTER by FilterGranulation.
SHOW Filter.

* Medians and IQRs.
CTABLES
  /VLABELS VARIABLES=I01_EGFR_ErbB1 H02_Eotaxin S02_TypeBy2
DISPLAY=LABEL
  /TABLE I01_EGFR_ErbB1[MEDIAN, PTILE 25, PTILE 75] +
I02_HER2_ErbB2[MEDIAN, PTILE 25, PTILE 75] +
I03_HER3_ErbB3[MEDIAN, PTILE 25, PTILE 75] + I04_FGFR1[MEDIAN, PTILE
25, PTILE 75] + I05_FGFR3[MEDIAN, PTILE 25, PTILE 75] +
I06_FGFR4[MEDIAN, PTILE 25, PTILE 75] + I07_InsR[MEDIAN, PTILE 25,
PTILE 75] + I08_IGF_IR[MEDIAN, PTILE 25, PTILE 75] +
I09_TrkA_NTRK1[MEDIAN, PTILE 25, PTILE 75] + I10_TrkB_NTRK2[MEDIAN,
PTILE 25, PTILE 75] + I11_Met_HGFR[MEDIAN, PTILE 25, PTILE 75] +
I12_Ron_MST1R[MEDIAN, PTILE 25, PTILE 75] + I13_Ret[MEDIAN, PTILE
25, PTILE 75] +
I14_ALK[MEDIAN, PTILE 25, PTILE 75] + I15_PDGFR[MEDIAN, PTILE 25,
PTILE 75] + I16_c_Kit_SCFR[MEDIAN, PTILE 25, PTILE 75] +
I17_FLT3_Flk2[MEDIAN, PTILE 25, PTILE 75] +
I18_M_CSFR_CSF_1R[MEDIAN, PTILE 25, PTILE 75] +
I19_EphA1[MEDIAN, PTILE 25, PTILE 75] + I20_EphA2[MEDIAN, PTILE 25,
PTILE 75] + I21_EphA3[MEDIAN, PTILE 25, PTILE 75] +
I22_EphB1[MEDIAN, PTILE 25, PTILE 75] + I23_EphB3[MEDIAN, PTILE 25,
PTILE 75] + I24_EphB4[MEDIAN, PTILE 25, PTILE 75] +
I25_Tyro3_Dtk[MEDIAN, PTILE 25, PTILE 75] + I26_Axl[MEDIAN, PTILE
25, PTILE 75] + I27_Tie2_TEK[MEDIAN, PTILE 25, PTILE 75] +
```

```
I28_VEGFR2_KDR[MEDIAN, PTILE 25, PTILE 75] +
I29_Akt_PKB_Rac@Thr308[MEDIAN, PTILE 25, PTILE 75] +
I30_Akt_PKB_Rac@Ser473[MEDIAN, PTILE 25, PTILE 75] +
I31_p44_42_MAPK[MEDIAN, PTILE 25, PTILE 75] +
I32_S6_Ribosomal_Protein[MEDIAN, PTILE 25, PTILE 75] +
I33_c_Abl[MEDIAN, PTILE 25, PTILE 75] +
I34_IRS_1[MEDIAN, PTILE 25, PTILE 75] + I35_Zap_70[MEDIAN, PTILE 25,
PTILE 75] + I36_Src[MEDIAN, PTILE 25, PTILE 75] + I37_Lck[MEDIAN,
PTILE 25, PTILE 75] + I38_Stat1[MEDIAN, PTILE 25, PTILE 75] +
I39_Stat3 [MEDIAN, PTILE 25, PTILE 75]
BY S02_TypeBy2
  /CATEGORIES VARIABLES=S02_TypeBy2 ORDER=A KEY=VALUE EMPTY=EXCLUDE
TOTAL=YES LABEL='All' POSITION=AFTER.

* Nonparametric Tests: Independent Samples.
NPTESTS
  /INDEPENDENT TEST (I01_EGFR_ErbB1 I02_HER2_ErbB2
I03_HER3_ErbB3 I04_FGFR1 I05_FGFR3 I06_FGFR4 I07_InsR I08_IGF_IR
I09_TrkA_NTRK1 I10_TrkB_NTRK2 I11_Met_HGFR I12_Ron_MST1R I13_Ret
I14_ALK I15_PDGFR I16_c_Kit_SCFR I17_FLT3_Flk2 I18_M_CSFR_CSF_1R
I19_EphA1 I20_EphA2 I21_EphA3 I22_EphB1 I23_EphB3 I24_EphB4
I25_Tyro3_Dtk I26_Axl I27_Tie2_TEK I28_VEGFR2_KDR
I29_Akt_PKB_Rac@Thr308
I30_Akt_PKB_Rac@Ser473 I31_p44_42_MAPK I32_S6_Ribosomal_Protein
I33_c_Abl
I34_IRS_1 I35_Zap_70 I36_Src I37_Lck I38_Stat1 I39_Stat3) GROUP
(S02_TypeBy2) MANN_WHITNEY HODGES_LEHMANN
  /MISSING SCOPE=ANALYSIS USERMISSING=EXCLUDE
  /CRITERIA ALPHA=0.01  CILEVEL=99.

FILTER by FilterMucosa.
SHOW Filter.

* Medians and IQRs.
CTABLES
  /VLABELS VARIABLES=I01_EGFR_ErbB1 H02_Eotaxin S02_TypeBy2
DISPLAY=LABEL
  /TABLE I01_EGFR_ErbB1[MEDIAN, PTILE 25, PTILE 75] +
I02_HER2_ErbB2[MEDIAN, PTILE 25, PTILE 75] +
I03_HER3_ErbB3[MEDIAN, PTILE 25, PTILE 75] + I04_FGFR1[MEDIAN, PTILE
25, PTILE 75] + I05_FGFR3[MEDIAN, PTILE 25, PTILE 75] +
I06_FGFR4[MEDIAN, PTILE 25, PTILE 75] + I07_InsR[MEDIAN, PTILE 25,
PTILE 75] + I08_IGF_IR[MEDIAN, PTILE 25, PTILE 75] +
I09_TrkA_NTRK1[MEDIAN, PTILE 25, PTILE 75] + I10_TrkB_NTRK2[MEDIAN,
PTILE 25, PTILE 75] + I11_Met_HGFR[MEDIAN, PTILE 25, PTILE 75] +
I12_Ron_MST1R[MEDIAN, PTILE 25, PTILE 75] + I13_Ret[MEDIAN, PTILE
25, PTILE 75] +
I14_ALK[MEDIAN, PTILE 25, PTILE 75] + I15_PDGFR[MEDIAN, PTILE 25,
PTILE 75] + I16_c_Kit_SCFR[MEDIAN, PTILE 25, PTILE 75] +
I17_FLT3_Flk2[MEDIAN, PTILE 25, PTILE 75] +
I18_M_CSFR_CSF_1R[MEDIAN, PTILE 25, PTILE 75] +
I19_EphA1[MEDIAN, PTILE 25, PTILE 75] + I20_EphA2[MEDIAN, PTILE 25,
PTILE 75] + I21_EphA3[MEDIAN, PTILE 25, PTILE 75] +
I22_EphB1[MEDIAN, PTILE 25, PTILE 75] + I23_EphB3[MEDIAN F40.3,
PTILE 25, PTILE 75] + I24_EphB4[MEDIAN, PTILE 25, PTILE 75] +
I25_Tyro3_Dtk[MEDIAN, PTILE 25, PTILE 75] + I26_Axl[MEDIAN, PTILE
25, PTILE 75] + I27_Tie2_TEK[MEDIAN, PTILE 25, PTILE 75] +
```

```
I28_VEGFR2_KDR[MEDIAN, PTILE 25, PTILE 75] +
I29_Akt_PKB_Rac@Thr308[MEDIAN, PTILE 25, PTILE 75] +
I30_Akt_PKB_Rac@Ser473[MEDIAN, PTILE 25, PTILE 75] +
I31_p44_42_MAPK[MEDIAN, PTILE 25, PTILE 75] +
I32_S6_Ribosomal_Protein[MEDIAN, PTILE 25, PTILE 75] +
I33_c_Abl[MEDIAN, PTILE 25, PTILE 75] +
I34_IRS_1[MEDIAN, PTILE 25, PTILE 75] + I35_Zap_70[MEDIAN, PTILE 25,
PTILE 75] + I36_Src[MEDIAN, PTILE 25, PTILE 75] + I37_Lck[MEDIAN,
PTILE 25, PTILE 75] + I38_Stat1[MEDIAN, PTILE 25, PTILE 75] +
I39_Stat3 [MEDIAN, PTILE 25, PTILE 75]
BY S02_TypeBy2
  /CATEGORIES VARIABLES=S02_TypeBy2 ORDER=A KEY=VALUE EMPTY=EXCLUDE
TOTAL=YES LABEL='All' POSITION=AFTER.

* Nonparametric Tests: Independent Samples.
NPTESTS
  /INDEPENDENT TEST (I01_EGFR_ErbB1 I02_HER2_ErbB2
I03_HER3_ErbB3 I04_FGFR1 I05_FGFR3 I06_FGFR4 I07_InsR I08_IGF_IR
I09_TrkA_NTRK1 I10_TrkB_NTRK2 I11_Met_HGFR I12_Ron_MST1R I13_Ret
I14_ALK I15_PDGFR I16_c_Kit_SCFR I17_FLT3_Flk2 I18_M_CSFR_CSF_1R
I19_EphA1 I20_EphA2 I21_EphA3 I22_EphB1 I23_EphB3 I24_EphB4
I25_Tyro3_Dtk I26_Axl I27_Tie2_TEK I28_VEGFR2_KDR
I29_Akt_PKB_Rac@Thr308
I30_Akt_PKB_Rac@Ser473 I31_p44_42_MAPK I32_S6_Ribosomal_Protein
I33_c_Abl
I34_IRS_1 I35_Zap_70 I36_Src I37_Lck I38_Stat1 I39_Stat3) GROUP
(S02_TypeBy2) MANN_WHITNEY HODGES_LEHMANN
  /MISSING SCOPE=ANALYSIS USERMISSING=EXCLUDE
  /CRITERIA ALPHA=0.01  CILEVEL=99.

FILTER by FilterRectum.
SHOW Filter.

* Medians and IQRs.
CTABLES
  /VLABELS VARIABLES=I01_EGFR_ErbB1 H02_Eotaxin S02_TypeBy2
DISPLAY=LABEL
  /TABLE I01_EGFR_ErbB1[MEDIAN, PTILE 25, PTILE 75] +
I02_HER2_ErbB2[MEDIAN, PTILE 25, PTILE 75] +
I03_HER3_ErbB3[MEDIAN, PTILE 25, PTILE 75] + I04_FGFR1[MEDIAN, PTILE
25, PTILE 75] + I05_FGFR3[MEDIAN, PTILE 25, PTILE 75] +
I06_FGFR4[MEDIAN, PTILE 25, PTILE 75] + I07_InsR[MEDIAN, PTILE 25,
PTILE 75] + I08_IGF_IR[MEDIAN, PTILE 25, PTILE 75] +
I09_TrkA_NTRK1[MEDIAN, PTILE 25, PTILE 75] + I10_TrkB_NTRK2[MEDIAN,
PTILE 25, PTILE 75] + I11_Met_HGFR[MEDIAN, PTILE 25, PTILE 75] +
I12_Ron_MST1R[MEDIAN, PTILE 25, PTILE 75] + I13_Ret[MEDIAN, PTILE
25, PTILE 75] +
I14_ALK[MEDIAN, PTILE 25, PTILE 75] + I15_PDGFR[MEDIAN, PTILE 25,
PTILE 75] + I16_c_Kit_SCFR[MEDIAN, PTILE 25, PTILE 75] +
I17_FLT3_Flk2[MEDIAN, PTILE 25, PTILE 75] +
I18_M_CSFR_CSF_1R[MEDIAN, PTILE 25, PTILE 75] +
I19_EphA1[MEDIAN, PTILE 25, PTILE 75] + I20_EphA2[MEDIAN, PTILE 25,
PTILE 75] + I21_EphA3[MEDIAN, PTILE 25, PTILE 75] +
I22_EphB1[MEDIAN, PTILE 25, PTILE 75] + I23_EphB3[MEDIAN, PTILE 25,
PTILE 75] + I24_EphB4[MEDIAN, PTILE 25, PTILE 75] +
I25_Tyro3_Dtk[MEDIAN, PTILE 25, PTILE 75] + I26_Axl[MEDIAN, PTILE
25, PTILE 75] + I27_Tie2_TEK[MEDIAN, PTILE 25, PTILE 75] +
```

```
I28_VEGFR2_KDR[MEDIAN, PTILE 25, PTILE 75] +
I29_Akt_PKB_Rac@Thr308[MEDIAN, PTILE 25, PTILE 75] +
I30_Akt_PKB_Rac@Ser473[MEDIAN, PTILE 25, PTILE 75] +
I31_p44_42_MAPK[MEDIAN, PTILE 25, PTILE 75] +
I32_S6_Ribosomal_Protein[MEDIAN, PTILE 25, PTILE 75] +
I33_c_Abl[MEDIAN, PTILE 25, PTILE 75] +
I34_IRS_1[MEDIAN, PTILE 25, PTILE 75] + I35_Zap_70[MEDIAN, PTILE 25,
PTILE 75] + I36_Src[MEDIAN, PTILE 25, PTILE 75] + I37_Lck[MEDIAN,
PTILE 25, PTILE 75] + I38_Stat1[MEDIAN, PTILE 25, PTILE 75] +
I39_Stat3 [MEDIAN, PTILE 25, PTILE 75]
BY S02_TypeBy2
  /CATEGORIES VARIABLES=S02_TypeBy2 ORDER=A KEY=VALUE EMPTY=EXCLUDE
TOTAL=YES LABEL='All' POSITION=AFTER.

* Nonparametric Tests: Independent Samples.
NPTESTS
  /INDEPENDENT TEST (I01_EGFR_ErbB1 I02_HER2_ErbB2
I03_HER3_ErbB3 I04_FGFR1 I05_FGFR3 I06_FGFR4 I07_InsR I08_IGF_IR
I09_TrkA_NTRK1 I10_TrkB_NTRK2 I11_Met_HGFR I12_Ron_MST1R I13_Ret
I14_ALK I15_PDGFR I16_c_Kit_SCFR I17_FLT3_Flk2 I18_M_CSFR_CSF_1R
I19_EphA1 I20_EphA2 I21_EphA3 I22_EphB1 I23_EphB3 I24_EphB4
I25_Tyro3_Dtk I26_Axl I27_Tie2_TEK I28_VEGFR2_KDR
I29_Akt_PKB_Rac@Thr308
I30_Akt_PKB_Rac@Ser473 I31_p44_42_MAPK I32_S6_Ribosomal_Protein
I33_c_Abl
I34_IRS_1 I35_Zap_70 I36_Src I37_Lck I38_Stat1 I39_Stat3) GROUP
(S02_TypeBy2) MANN_WHITNEY HODGES_LEHMANN
  /MISSING SCOPE=ANALYSIS USERMISSING=EXCLUDE
  /CRITERIA ALPHA=0.01  CILEVEL=99.

FILTER by FilterControlsVCrohns.
SHOW Filter.

* Medians and IQRs.
CTABLES
  /VLABELS VARIABLES=I01_EGFR_ErbB1 H02_Eotaxin S02_TypeBy2
DISPLAY=LABEL
  /TABLE I01_EGFR_ErbB1[MEDIAN, PTILE 25, PTILE 75] +
I02_HER2_ErbB2[MEDIAN, PTILE 25, PTILE 75] +
I03_HER3_ErbB3[MEDIAN, PTILE 25, PTILE 75] + I04_FGFR1[MEDIAN, PTILE
25, PTILE 75] + I05_FGFR3[MEDIAN, PTILE 25, PTILE 75] +
I06_FGFR4[MEDIAN, PTILE 25, PTILE 75] + I07_InsR[MEDIAN, PTILE 25,
PTILE 75] + I08_IGF_IR[MEDIAN, PTILE 25, PTILE 75] +
I09_TrkA_NTRK1[MEDIAN, PTILE 25, PTILE 75] + I10_TrkB_NTRK2[MEDIAN,
PTILE 25, PTILE 75] + I11_Met_HGFR[MEDIAN, PTILE 25, PTILE 75] +
I12_Ron_MST1R[MEDIAN, PTILE 25, PTILE 75] + I13_Ret[MEDIAN, PTILE
25, PTILE 75] +
I14_ALK[MEDIAN, PTILE 25, PTILE 75] + I15_PDGFR[MEDIAN, PTILE 25,
PTILE 75] + I16_c_Kit_SCFR[MEDIAN, PTILE 25, PTILE 75] +
I17_FLT3_Flk2[MEDIAN, PTILE 25, PTILE 75] +
I18_M_CSFR_CSF_1R[MEDIAN, PTILE 25, PTILE 75] +
I19_EphA1[MEDIAN, PTILE 25, PTILE 75] + I20_EphA2[MEDIAN, PTILE 25,
PTILE 75] + I21_EphA3[MEDIAN, PTILE 25, PTILE 75] +
I22_EphB1[MEDIAN, PTILE 25, PTILE 75] + I23_EphB3[MEDIAN, PTILE 25,
PTILE 75] + I24_EphB4[MEDIAN, PTILE 25, PTILE 75] +
I25_Tyro3_Dtk[MEDIAN, PTILE 25, PTILE 75] + I26_Axl[MEDIAN, PTILE
25, PTILE 75] + I27_Tie2_TEK[MEDIAN, PTILE 25, PTILE 75] +
```

```
I28_VEGFR2_KDR[MEDIAN, PTILE 25, PTILE 75] +
I29_Akt_PKB_Rac@Thr308[MEDIAN, PTILE 25, PTILE 75] +
I30_Akt_PKB_Rac@Ser473[MEDIAN, PTILE 25, PTILE 75] +
I31_p44_42_MAPK[MEDIAN, PTILE 25, PTILE 75] +
I32_S6_Ribosomal_Protein[MEDIAN, PTILE 25, PTILE 75] +
I33_c_Abl[MEDIAN, PTILE 25, PTILE 75] +
I34_IRS_1[MEDIAN, PTILE 25, PTILE 75] + I35_Zap_70[MEDIAN, PTILE 25,
PTILE 75] + I36_Src[MEDIAN, PTILE 25, PTILE 75] + I37_Lck[MEDIAN,
PTILE 25, PTILE 75] + I38_Stat1[MEDIAN, PTILE 25, PTILE 75] +
I39_Stat3 [MEDIAN, PTILE 25, PTILE 75]
BY S02_TypeBy2
  /CATEGORIES VARIABLES=S02_TypeBy2 ORDER=A KEY=VALUE EMPTY=EXCLUDE
TOTAL=YES LABEL='All' POSITION=AFTER.

* Nonparametric Tests: Independent Samples.
NPTESTS
  /INDEPENDENT TEST (I01_EGFR_ErbB1 I02_HER2_ErbB2
I03_HER3_ErbB3 I04_FGFR1 I05_FGFR3 I06_FGFR4 I07_InsR I08_IGF_IR
I09_TrkA_NTRK1 I10_TrkB_NTRK2 I11_Met_HGFR I12_Ron_MST1R I13_Ret
I14_ALK I15_PDGFR I16_c_Kit_SCFR I17_FLT3_Flk2 I18_M_CSFR_CSF_1R
I19_EphA1 I20_EphA2 I21_EphA3 I22_EphB1 I23_EphB3 I24_EphB4
I25_Tyro3_Dtk I26_Axl I27_Tie2_TEK I28_VEGFR2_KDR
I29_Akt_PKB_Rac@Thr308
I30_Akt_PKB_Rac@Ser473 I31_p44_42_MAPK I32_S6_Ribosomal_Protein
I33_c_Abl
I34_IRS_1 I35_Zap_70 I36_Src I37_Lck I38_Stat1 I39_Stat3) GROUP
(S02_TypeBy2) MANN_WHITNEY HODGES_LEHMANN
  /MISSING SCOPE=ANALYSIS USERMISSING=EXCLUDE
  /CRITERIA ALPHA=0.01  CILEVEL=99.

FILTER by Study_ImmunoExHS.
SHOW filter.

* Medians across all specimens.
CTABLES
  /VLABELS VARIABLES=I01_EGFR_ErbB1 Biopsy S02_TypeBy2 DISPLAY=LABEL
  /TABLE I01_EGFR_ErbB1 [MEDIAN] + I02_HER2_ErbB2 [MEDIAN] +
I03_HER3_ErbB3 [MEDIAN] + I04_FGFR1 [MEDIAN] + I05_FGFR3 [MEDIAN] +
I06_FGFR4 [MEDIAN] + I07_InsR [MEDIAN] + I08_IGF_IR [MEDIAN] +
I09_TrkA_NTRK1 [MEDIAN] + I10_TrkB_NTRK2 [MEDIAN] + I11_Met_HGFR
[MEDIAN] + I12_Ron_MST1R [MEDIAN] + I13_Ret [MEDIAN] +
I14_ALK [MEDIAN] + I15_PDGFR [MEDIAN] + I16_c_Kit_SCFR [MEDIAN] +
I17_FLT3_Flk2 [MEDIAN] + I18_M_CSFR_CSF_1R [MEDIAN] +
I19_EphA1 [MEDIAN] + I20_EphA2 [MEDIAN] + I21_EphA3 [MEDIAN] +
I22_EphB1 [MEDIAN] + I23_EphB3 [MEDIAN] + I24_EphB4 [MEDIAN] +
I25_Tyro3_Dtk [MEDIAN] + I26_Axl [MEDIAN] + I27_Tie2_TEK [MEDIAN] +
I28_VEGFR2_KDR [MEDIAN] + I29_Akt_PKB_Rac@Thr308 [MEDIAN] +
I30_Akt_PKB_Rac@Ser473 [MEDIAN] + I31_p44_42_MAPK [MEDIAN] +
I32_S6_Ribosomal_Protein [MEDIAN] + I33_c_Abl [MEDIAN] +
I34_IRS_1 [MEDIAN] + I35_Zap_70 [MEDIAN] + I36_Src [MEDIAN] +
I37_Lck [MEDIAN] + I38_Stat1 [MEDIAN] + I39_Stat3 [MEDIAN]
BY Biopsy > S02_TypeBy2
  /CATEGORIES VARIABLES=Biopsy [1,2,3,4] EMPTY=INCLUDE
  /CATEGORIES VARIABLES=S02_TypeBy2 [0, 2, 10] EMPTY=INCLUDE.

* Controls.
* Negative controls.
```

```
GGRAPH
  /GRAPHDATASET NAME="graphdataset" VARIABLES=Biopsy I00_ControlNeg
MISSING=LISTWISE REPORTMISSING=NO
  /GRAPHSPEC SOURCE=INLINE.
 BEGIN GPL
   SOURCE: s=userSource(id("graphdataset"))
   DATA: Biopsy=col(source(s), name("Biopsy"),
 notIn("5", "6"), unit.category())
   DATA: I00_ControlNeg=col(source(s), name("I00_ControlNeg"))
   DATA: id=col(source(s), name("$CASENUM"), unit.category())
   GUIDE: axis(dim(2), label("Pixel intensity %"))
   GUIDE: text.title(label("Negative control spots"))
   SCALE: cat(dim(1), include("1", "2", "3", "4"))
   SCALE: linear(dim(2), include(0))
   ELEMENT:
schema(position(bin.quantile.letter(Biopsy*I00_ControlNeg)),
label(id))
 END GPL.

* Positive controls.
GGRAPH
  /GRAPHDATASET NAME="graphdataset" VARIABLES=Biopsy I99_ControlPos
MISSING=LISTWISE REPORTMISSING=NO
  /GRAPHSPEC SOURCE=INLINE.
BEGIN GPL
  SOURCE: s=userSource(id("graphdataset"))
  DATA: Biopsy=col(source(s), name("Biopsy"),
notIn("5", "6"), unit.category())
  DATA: I99_ControlPos=col(source(s), name("I99_ControlPos"))
  DATA: id=col(source(s), name("$CASENUM"), unit.category())
  GUIDE: axis(dim(2), label("Pixel intensity %"))
  GUIDE: text.title(label("Positive control spots"))
  SCALE: cat(dim(1), include("1", "2", "3", "4"))
  SCALE: linear(dim(2), include(0))
  ELEMENT:
schema(position(bin.quantile.letter(Biopsy*I99_ControlPos)),
label(id))
END GPL.

* Negative Control Samples.
GGRAPH
  /GRAPHDATASET NAME="graphdataset" VARIABLES=MEDIAN(I01_EGFR_ErbB1)
MEDIAN(I02_HER2_ErbB2)
MEDIAN(I03_HER3_ErbB3) MEDIAN(I04_FGFR1) MEDIAN(I05_FGFR3)
MEDIAN(I06_FGFR4) MEDIAN(I07_InsR) MEDIAN(I08_IGF_IR)
MEDIAN(I09_TrkA_NTRK1) MEDIAN(I10_TrkB_NTRK2) MEDIAN(I11_Met_HGFR)
MEDIAN(I12_Ron_MST1R) MEDIAN(I13_Ret)
MEDIAN(I14_ALK) MEDIAN(I15_PDGFR) MEDIAN(I16_c_Kit_SCFR)
MEDIAN(I17_FLT3_Flk2) MEDIAN(I18_M_CSFR_CSF_1R)
MEDIAN(I19_EphA1) MEDIAN(I20_EphA2) MEDIAN(I21_EphA3)
MEDIAN(I22_EphB1) MEDIAN(I23_EphB3) MEDIAN(I24_EphB4)
MEDIAN(I25_Tyro3_Dtk) MEDIAN(I26_Axl) MEDIAN(I27_Tie2_TEK)
MEDIAN(I28_VEGFR2_KDR) MEDIAN(I29_Akt_PKB_Rac@Thr308)
MEDIAN(I30_Akt_PKB_Rac@Ser473) MEDIAN(I31_p44_42_MAPK)
MEDIAN(I32_S6_Ribosomal_Protein) MEDIAN(I33_c_Abl)
MEDIAN(I34_IRS_1) MEDIAN(I35_Zap_70) MEDIAN(I36_Src) MEDIAN(I37_Lck)
MEDIAN(I38_Stat1) MEDIAN(I39_Stat3)
```

```
    Biopsy MISSING=LISTWISE REPORTMISSING=NO
    TRANSFORM=VARSTOCASES(SUMMARY="#SUMMARY" INDEX="#INDEX")
  /GRAPHSPEC SOURCE=INLINE.
BEGIN GPL
  SOURCE: s=userSource(id("graphdataset"))
  DATA: SUMMARY=col(source(s), name("#SUMMARY"))
  DATA: INDEX=col(source(s), name("#INDEX"), unit.category())
  DATA: Biopsy=col(source(s), name("Biopsy"),
notIn("1", "2", "3", "4"), unit.category())
  COORD: rect(dim(1,2), cluster(3,0))
  GUIDE: axis(dim(2), label("Median pixel intensity, %"))
  GUIDE: legend(aesthetic(aesthetic.color.interior), label(""))
  GUIDE: text.title(label("Negative control samples"))
  SCALE: cat(dim(3), include("0", "1"))
  SCALE: linear(dim(2), include(0))
  SCALE: cat(aesthetic(aesthetic.color.interior), include("5", "6"))
  SCALE: cat(dim(1), include("5", "6"))
  ELEMENT: interval(position(Biopsy*SUMMARY*INDEX),
color.interior(Biopsy), shape.interior(shape.line))
END GPL.
```

Dynamic Contrast-Enhanced MRI

```
* OPEN DATA.
CD '/Users/james/Dropbox/Fistula Studies/Analysis/2015-10 Clinical'.

* FILTER CASES.
FILTER by Study_DCEMRI_All.
SHOW filter.

* ANALYSE DATA.
* Table to show patient characteristics.
CTABLES
  /VLABELS VARIABLES=B03_Gender B02_Age B04_EthnicOrigin
B13_FistulaDuration B08_PrevRxMed S03_PrevRxSurgGE2
    S06_PrevRxCure S09_CurrentSeton B16_Smoking  BasePDAIC08_PDAI
S02_TypeBy2
    DISPLAY=LABEL
  /TABLE B03_Gender [C][COUNT F40.0, COLPCT.TOTALN PCT40.0] +
B02_Age [S][MEAN, STDDEV] + B04_EthnicOrigin [COUNT F40.0,
COLPCT.TOTALN PCT40.0] +
    B13_FistulaDuration [S][MEDIAN, PTILE 25, PTILE 75] +
B08_PrevRxMed [C][COUNT F40.0, COLPCT.TOTALN
    PCT40.0] + B10_PrevRxSurgNo [MEDIAN, PTILE 25, PTILE 75] +
S06_PrevRxCure [C][COUNT
    F40.0, COLPCT.TOTALN PCT40.0] + S09_CurrentSeton [C][COUNT
F40.0, COLPCT.TOTALN PCT40.0] +
    B16_Smoking [C][COUNT F40.0, COLPCT.TOTALN PCT40.0] +
BasePDAIC08_PDAI [S][MEAN, STDDEV F40.1] BY S02_TypeBy2 [C]
  /SLABELS POSITION=ROW
  /CATEGORIES VARIABLES=B03_Gender [1, 10, OTHERNM] EMPTY=INCLUDE
TOTAL=YES POSITION=BEFORE
  /CATEGORIES VARIABLES=B04_EthnicOrigin [10, HSUBTOTAL='White', 18,
19, 20, 21, HSUBTOTAL='Asian', 16, 17, 15, HSUBTOTAL='Black', 11,
```

```
12, 13, 14, 22, 23, 24, HSUBTOTAL='Other', OTHERNM, MISSING]
EMPTY=INCLUDE POSITION=AFTER
  /CATEGORIES VARIABLES=B08_PrevRxMed [1, 10, 11, 12, 13, 14,
OTHERNM] EMPTY=INCLUDE
  /CATEGORIES VARIABLES=S06_PrevRxCure [1, 10, OTHERNM]
EMPTY=INCLUDE
  /CATEGORIES VARIABLES=S09_CurrentSeton [1, 10, OTHERNM]
EMPTY=INCLUDE
  /CATEGORIES VARIABLES=B16_Smoking [1, 10, 11, OTHERNM]
EMPTY=INCLUDE
  /CATEGORIES VARIABLES=S02_TypeBy2 ORDER=A KEY=VALUE EMPTY=EXCLUDE
TOTAL=YES POSITION=AFTER.

* Follow-up.
CTABLES
  /VLABELS VARIABLES=G21_WeeksFollowUp S02_TypeBy2 DISPLAY=LABEL
  /TABLE G21_WeeksFollowUp [MEDIAN, PTILE 25, PTILE 75] BY
S02_TypeBy2
  /CATEGORIES VARIABLES=S02_TypeBy2 ORDER=A KEY=VALUE EMPTY=INCLUDE
TOTAL=YES LABEL='All' POSITION=AFTER.

* Conventional MRI.
CTABLES
  /VLABELS VARIABLES=BaseMRIE03_FistulaNo BaseMRIE04_FistulaParks
BaseMRIE05_FistulaLevel BaseMRIE06_SecondaryTracts
BaseMRIE07_FistulaHorseshoe
BaseMRIE08_Collections BaseMRIE09_RectalInvolvement
BaseMRIE10_FistulaHyperintensityT2 BaseMRIE42_StJames S02_TypeBy2
    DISPLAY=LABEL
  /TABLE BaseMRIE03_FistulaNo [C] + BaseMRIE04_FistulaParks [C] +
BaseMRIE05_FistulaLevel [C] + BaseMRIE06_SecondaryTracts [C] +
BaseMRIE07_FistulaHorseshoe [C] +
BaseMRIE08_Collections [C] + BaseMRIE09_RectalInvolvement [C] +
BaseMRIE10_FistulaHyperintensityT2 [C] + BaseMRIE42_StJames [C] BY
S02_TypeBy2 [C][COUNT F40.0, COLPCT.COUNT PCT40.0]
  /CATEGORIES VARIABLES=BaseMRIE03_FistulaNo BaseMRIE04_FistulaParks
BaseMRIE05_FistulaLevel BaseMRIE06_SecondaryTracts
BaseMRIE07_FistulaHorseshoe
BaseMRIE08_Collections BaseMRIE09_RectalInvolvement
BaseMRIE10_FistulaHyperintensityT2 BaseMRIE42_StJames ORDER=A
KEY=VALUE EMPTY=INCLUDE
  /CATEGORIES VARIABLES=S02_TypeBy2 ORDER=A KEY=VALUE EMPTY=EXCLUDE
TOTAL=YES LABEL='All' POSITION=AFTER.

* Conventional MRI.
CTABLES
  /VLABELS VARIABLES=BaseMRIE17_MRIScoreTotal S02_TypeBy2
DISPLAY=LABEL
  /TABLE BaseMRIE17_MRIScoreTotal [MEAN F40.1, STDDEV F40.1] BY
S02_TypeBy2 [C]
  /CATEGORIES VARIABLES=S02_TypeBy2 ORDER=A KEY=VALUE EMPTY=EXCLUDE
TOTAL=YES LABEL='All' POSITION=AFTER.

* DCE-MRI Parametric.
CTABLES
  /VLABELS VARIABLES=E19_MaxEnhance E20_MaxRelEnhance E23_WashIn
E24_WashOut E26_AUC S02_TypeBy2 DISPLAY=LABEL
```

```
  /TABLE E19_MaxEnhance [MEAN, STDDEV] + E20_MaxRelEnhance [MEAN,
STDDEV] + E23_WashIn [MEAN, STDDEV] + E24_WashOut [MEAN, STDDEV] +
E26_AUC [MEAN, STDDEV] BY S02_TypeBy2 [C]
  /CATEGORIES VARIABLES=S02_TypeBy2 ORDER=A KEY=VALUE EMPTY=EXCLUDE
TOTAL=YES LABEL='All' POSITION=AFTER.

T-TEST GROUPS=S02_TypeBy2(2 10)
  /MISSING=ANALYSIS
  /VARIABLES=E19_MaxEnhance E20_MaxRelEnhance E23_WashIn E24_WashOut
E26_AUC
  /CRITERIA=CI(.95).

T-TEST GROUPS= ChronicFistula(0 1)
  /MISSING=ANALYSIS
  /VARIABLES=E19_MaxEnhance E20_MaxRelEnhance E23_WashIn E24_WashOut
E26_AUC
  /CRITERIA=CI(.95).

T-TEST GROUPS=S16_RxSatisfactory(10 1)
  /MISSING=ANALYSIS
  /VARIABLES=E19_MaxEnhance E20_MaxRelEnhance E23_WashIn E24_WashOut
E26_AUC
  /CRITERIA=CI(.95).

T-TEST GROUPS=StJamesHigh(0 1)
  /MISSING=ANALYSIS
  /VARIABLES=E19_MaxEnhance E20_MaxRelEnhance E23_WashIn E24_WashOut
E26_AUC
  /CRITERIA=CI(.95).

FILTER by Study_DCEMRI_All_Acute.
SHOW filter.

T-TEST GROUPS=S02_TypeBy2(2 10)
  /MISSING=ANALYSIS
  /VARIABLES=E19_MaxEnhance E20_MaxRelEnhance E23_WashIn E24_WashOut
E26_AUC
  /CRITERIA=CI(.95).

FILTER by Study_DCEMRI_All.
SHOW filter.

* Mean ME by Parks.
GGRAPH
  /GRAPHDATASET NAME="graphdataset" VARIABLES=StJamesHigh
MEANCI(E19_MaxEnhance, 95)[name="MEAN_E19_MaxEnhance"
LOW="MEAN_E19_MaxEnhance_LOW" HIGH="MEAN_E19_MaxEnhance_HIGH"]
MISSING=LISTWISE REPORTMISSING=NO
  /GRAPHSPEC SOURCE=INLINE.
BEGIN GPL
  SOURCE: s=userSource(id("graphdataset"))
  DATA: StJamesHigh=col(source(s), name("StJamesHigh"),
unit.category())
  DATA: MEAN_E19_MaxEnhance=col(source(s),
name("MEAN_E19_MaxEnhance"))
  DATA: LOW=col(source(s), name("MEAN_E19_MaxEnhance_LOW"))
  DATA: HIGH=col(source(s), name("MEAN_E19_MaxEnhance_HIGH"))
```

```
  GUIDE: axis(dim(1), label("St James' Grade 3-5"))
  GUIDE: axis(dim(2), label("Mean max enhancement"))
  SCALE: cat(dim(1), include("0", "1"))
  SCALE: linear(dim(2), include(0))
  ELEMENT: point(position(StJamesHigh*MEAN_E19_MaxEnhance))
  ELEMENT:
interval(position(region.spread.range(StJamesHigh*(LOW+HIGH))),
shape.interior(shape.ibeam))
END GPL.

* Mean MRE by Parks.
GGRAPH
  /GRAPHDATASET NAME="graphdataset" VARIABLES=StJamesHigh
MEANCI(E20_MaxRelEnhance, 95)[name="MEAN_E20_MaxRelEnhance"
LOW="MEAN_E20_MaxRelEnhance_LOW" HIGH="MEAN_E20_MaxRelEnhance_HIGH"]
MISSING=LISTWISE REPORTMISSING=NO
  /GRAPHSPEC SOURCE=INLINE.
BEGIN GPL
  SOURCE: s=userSource(id("graphdataset"))
  DATA: StJamesHigh=col(source(s), name("StJamesHigh"),
unit.category())
  DATA: MEAN_E20_MaxRelEnhance=col(source(s),
name("MEAN_E20_MaxRelEnhance"))
  DATA: LOW=col(source(s), name("MEAN_E20_MaxRelEnhance_LOW"))
  DATA: HIGH=col(source(s), name("MEAN_E20_MaxRelEnhance_HIGH"))
  GUIDE: axis(dim(2), label("Mean max relative enhancement"))
  SCALE: cat(dim(1), include("0", "1"))
  SCALE: linear(dim(2), include(0))
  ELEMENT: point(position(StJamesHigh*MEAN_E20_MaxRelEnhance))
  ELEMENT:
interval(position(region.spread.range(StJamesHigh*(LOW+HIGH))),
shape.interior(shape.ibeam))
END GPL.

* Mean AUC by Parks.
GGRAPH
  /GRAPHDATASET NAME="graphdataset" VARIABLES=StJamesHigh
MEANCI(E26_AUC, 95)[name="MEAN_E26_AUC" LOW="MEAN_E26_AUC_LOW"
HIGH="MEAN_E26_AUC_HIGH"] MISSING=LISTWISE REPORTMISSING=NO
  /GRAPHSPEC SOURCE=INLINE.
BEGIN GPL
  SOURCE: s=userSource(id("graphdataset"))
  DATA: StJamesHigh=col(source(s), name("StJamesHigh"),
unit.category())
  DATA: MEAN_E26_AUC=col(source(s), name("MEAN_E26_AUC"))
  DATA: LOW=col(source(s), name("MEAN_E26_AUC_LOW"))
  DATA: HIGH=col(source(s), name("MEAN_E26_AUC_HIGH"))
  GUIDE: axis(dim(2), label("Mean area under TIC"))
  SCALE: cat(dim(1), include("0", "1"))
  SCALE: linear(dim(2), include(0))
  ELEMENT: point(position(StJamesHigh*MEAN_E26_AUC))
  ELEMENT:
interval(position(region.spread.range(StJamesHigh*(LOW+HIGH))),
shape.interior(shape.ibeam))
END GPL.

* DCE-MRI TIC analysis.
```

```
CTABLES
  /VLABELS VARIABLES=E40_TICType S02_TypeBy2 DISPLAY=LABEL
  /TABLE E40_TICType [C][COUNT F40.0, COLPCT.COUNT PCT40.0] BY
S02_TypeBy2 [C]
  /CATEGORIES VARIABLES=E40_TICType ORDER=A KEY=VALUE EMPTY=EXCLUDE
  /CATEGORIES VARIABLES=S02_TypeBy2 ORDER=A KEY=VALUE EMPTY=EXCLUDE
TOTAL=YES LABEL='All' POSITION=AFTER.

CROSSTABS
  /TABLES=E40_TICType BY S02_TypeBy2
  /FORMAT=AVALUE TABLES
  /STATISTICS=CHISQ
  /CELLS=COUNT
  /COUNT ROUND CELL
  /METHOD=EXACT TIMER(5).

CROSSTABS
  /TABLES=ChronicFistula S16_RxSatisfactory StJamesHigh BY
E41_TICType2
  /FORMAT=AVALUE TABLES
  /STATISTICS=CHISQ
  /CELLS=COUNT
  /COUNT ROUND CELL
  /METHOD=EXACT TIMER(5).
```

APPENDIX 5 LABORATORY PROTOCOL

Collection of Specimens

1. Collect biopsy specimens after patient is positioned, prepped and draped and before the surgery begins.
2. Use a sterile curette to obtain the granulation tissue.
3. Use scissors or endoscopic biopsy forceps to acquire the remaining specimens.
4. Wash with sterile saline in-between samplings.
5. The specimens required are:
   F: Fistula tract
   G: Granulation tissue from within the fistula tract
   M: Mucosa adjacent to internal opening
   R: Rectal mucosa
6. Store each specimen in a separate plain sterile pot filled with 10 ml saline. Keep on ice if not going to lab immediately.
7. Label with participant ID and specimen letter.
8. Complete the specimen form.
9. Transport in specimen bag to the lab.

Preparation of Specimens

10. If specimens cannot be processed immediately, then decant off saline and cover each with 10 ml PBS and store on ice overnight.
11. Examine specimens in a sterile petri dish under the microscope and trim off extraneous tissue (e.g. fat, blood clot) using instruments sterilised in alcohol and aseptic technique.
12. Where possible, divide specimens into equal 2-3 mm^3 samples.

Snap Freezing of Fresh Samples

13. Work at room temperature in tissue culture lab.
14. Place samples in cryotube.
15. Snap freeze on dry ice for 5 min.
16. Transfer to -80°C freezer.
17. Complete the specimen log.

Tissue Culture

18. Work under the extractor hood at room temperature.
19. Place samples into a 24-well culture plate and label.
20. Cover each sample with 300 µl culture medium (500ml Lonza HL-1, 10 ml / 5000 units penicillin and streptokinase, 1.6 ml Gentamicin 10 mg/ml, 5 ml L-Glutamine) using a filtered pipette.
21. Incubate at 37°C for 24 hours.

Tissue Culture: Snap Freezing Samples

22. Work under the extractor hood at room temperature.
23. Remove samples from incubator.
24. Pipette supernatant into mini Eppendorf tubes. (If necessary, first pipette supernatant and tissue component into a cryotube, centrifuge at 12,000 rpm for 5 min.)
25. Place tissue components into cryotubes.
26. Snap freeze the samples on dry ice for 5 min.
27. Transfer to -80°C freezer.
28. Complete the specimen log.

Phosphoarray: Preparing Cell Lysates

29. Work on ice in open laboratory. Keep reagents on ice.
30. Collect 8 (or 16) samples, label and record.
31. Prepare lysis buffer as follows (NB double volumes for 16 samples):
    Pipette 1000 µl of RIPA Buffer (Sigma R0278-50ML) into an Eppendorf tube. Add an extra 100 µl for each sample that is large.
    Add 10 µl of Phosphatase Inhibitor Cocktail 2 (Sigma P5726-1ML).
    Add 10 µl of Protease Inhibitor in DMSO (Sigma P8340-1ML; thaw at hand temperature, or room temperature for 10 minutes and then vortex; refreeze entire vial at -20°C after use).
    Vortex.
32. Add 100 µl of lysis buffer to each sample.
33. Use ultrasonic cell disruptor to lyse cells:
    Administer 2-3 watts for a few seconds. Don't touch the bottom of the tube, this will cause a hole.
    Allow to cool on ice.
    Repeat at least once.
34. Pre-chill centrifuge to 4°C.
35. Incubate on ice for 10 mins, vortexing every 1 minute.
36. Centrifuge at 13,300 rpm for 5 min at 4°C.
37. Pipette off each sample lysate supernatant into Eppendorf tubes, labelled 1-8.
38. Use immediately or store in -80°C freezer.
39. Discard cell pellet.

Phosphoarray: Bradford Assay

40. Work on ice in open laboratory. Keep reagents on ice.
41. Prepare standard samples by serial dilution as follows:
    Label mini Eppendorf tubes A-H.
    Add 40 µl distilled water to each tube.
    Add 40 µl Bovine Gamma Globulin (2 mg/ml) (Bio-Rad #500-0209) into tube A. Vortex.
    Then take 40 µl from tube A and add to tube B. Vortex.
    Repeat serially to G. Leave H untouched.
    Tubes A-G now have concentrations of Bovine Gamma Globulin from 1 mg/ml to 0.016 mg/ml.
42. Prepare 1 in 100 solutions of each sample lysate as follows:
    Label mini Eppendorf tubes 1-8.
    Add 99 µl distilled water to each tube.

Add 1 µl of each sample lysate to each tube.
Vortex.

43. Add 10 µl of each sample in duplicate to a 96-well plate as follows:

	Standard 1	Standard 2	PA01 3	PA01 4	PA02 5	PA02 6	7	8	9	10	Dilutions 11	Dilutions 12
A	A	A	Sample	Sample	Sample	Sample						
B	B	B	Sample	Sample	Sample	Sample						
C	C	C	Sample	Sample	Sample	Sample						
D	D	D	Sample	Sample	Sample	Sample						
E	E	E	Sample	Sample	Sample	Sample						
F	F	F	Sample	Sample	Sample	Sample						
G	G	G	Sample	Sample	Sample	Sample						
H	H	H	Sample	Sample	Sample	Sample						

44. Pipette 50 µl of (1X) QuickStart Bradford Dye Reagent (Bio-Rad #500-0205) into each occupied well using a multipipetter.
45. If any wells of lysate samples appear outside the standard range then prepare a stronger or weaker concentration (i.e. 1 in 50 or 1 in 200) and pipette into adjacent wells.
46. Use ELx800 plate reader and Gen5 2.00.18 software (BioTek Instruments Ltd., Winooski VT) to record the optical densities at 595 nm.
47. Samples in the 96-well plate can be discarded and plate cleaned with distilled water.
48. Store lysates in -80°C freezer.
49. Use Excel 2010 (Microsoft, Redmond WA) spreadsheet to calculate what volume lysate is needed to achieve 150 µg of protein for each sample as follows:
    Calculate the mean optical density for each duplicate sample.
    Calculate the slope and intercept for a linear best fit line through the standard sample plot (excluding points at the extremes where linearity is poor).
    Calculate the protein concentrations for each lysate sample using the standard samples as a reference and slope and intercept equation.
    Calculate the volume of sample lysate needed to achieve 150 µg of protein for each sample.
    Calculate the volume of Array Diluent Buffer needed to achieve a final volume of 200 µl.

Phosphoarray: Assay Procedure Part 1

50. Work at room temperature in open laboratory. Keep reagents on ice.
51. Thaw lysates at room temperature then keep on ice.
52. Use PathScan® RTK Signalling Antibody Array Kit (Chemiluminescent Readout) (Cell Signalling Technology #7982). 1 slide for 8 samples or 2 slides for 16 samples.
53. Bring glass slides and blocking buffer to room temperature before use.
54. Assemble cassette. Marker needs to be in top right corner when assembled cassette is placed flat on bench.
55. Add 150 µl Array Blocking Buffer to each well using multipipetter.
56. Cover with sealing tape and incubate on rocker for 15 min at room temperature.
57. Prepare diluted sample lysates as follows:
    Meanwhile, label Eppendorf tubes 1-8.
    Add calculated volume of Array Diluent Buffer to each tube (as per Bradford Assay calculations).
    Add calculated volume of each sample lysate to each tube (as per Bradford Assay calculations).
    Vortex.
58. Decant the cassette wells by gently flicking out the liquid into a sink.
59. Add 150 µl of each diluted sample lysate to each corresponding well and cover with sealing tape.
60. Incubate overnight on rocker at 4°C.

61. Return unused lysate to -80°C freezer.

Phosphoarray: Assay Procedure Part 2

62. Work at room temperature in open laboratory. Keep reagents on ice (NB double for 2 slides).
63. Prepare (1X) Array Wash Buffer as follows (NB double for 2 slides):
    Add 30ml of distilled water to a Falcon Tube.
    Add 1.5ml of (20X) Array Wash Buffer.
    Vortex.
64. Take cassette off the rocker and decant the wells.
65. Add 200 µl (1X) Array Wash Buffer to each well using multipipetter.
66. Cover and incubate on rocker for 5 min at room temperature.
67. Repeat steps 64 to 66 a further 3 times.
68. Prepare (1X) Detection Antibody Cocktail as follows (NB double for 2 slides):
    Add 1215 µl of Array Diluent Buffer to an Eppendorf tube.
    Add 135 µl of (10X) Detection Antibody Cocktail.
    Vortex.
69. Take cassette off the rocker and decant the wells.
70. Add 150 µl of (1X) Detection Antibody Cocktail to each well.
71. Cover and incubate on rocker for 1 hour at room temperature.
72. Take cassette off the rocker and decant the wells.
73. Add 200 µl of (1X) Array Wash Buffer to each well.
74. Cover and incubate on rocker for 5 min at room temperature.
75. Repeat steps 72 to 73 a further 3 times.
76. Prepare (1X) HRP-linked Streptavidin as follows (NB double for 2 slides):
    Add 1215 µl Array Diluent Buffer to an Eppendorf tube.
    Add 135 µl (10X) HRP-linked Streptavidin.
    Vortex.
77. Take cassette off the rocker and decant the wells.
78. Add 150 µl of (1X) HRP-linked Streptavidin to each well.
79. Cover and incubate on rocker for 30 min at room temperature.
80. Take cassette off the rocker and decant the wells.
81. Add 200 µl of (1X) Array Wash Buffer to each well using multipipetter.
82. Cover and incubate on rocker for 5 min at room temperature.
83. Repeat steps 80 to 82 a further 3 times.
84. Take cassette off the rocker and decant the wells.
85. Dismantle cassette by pulling the bottom of the metal clips away from the centre of the slide, then peeling the slide and gasket apart.
86. Place the slide face up in a plastic dish (e.g. pipette tip box cover). When using two slides keep left and right positions consistent to prevent confusion.
87. Wash briefly with 10ml (1X) Array Wash Buffer.
88. Prepare (1X) LumiGLO/Peroxide reagent immediately before use as follows:
    Add 9 ml of distilled water to an Eppendorf tube.
    Add 500 µl of (20X) LumiGLO.
    Add 500 µl of (20X) Peroxide.
    Vortex.
89. Decant Array Wash Buffer and cover slide with (1X) LumiGLO/Peroxide reagent.
90. Transfer slide to sheet protector and sandwich inside it, ensuring that it is still covered by (1X) LumiGLO/Peroxide reagent (add a small amount on top of the slide). When folding the top sheet over, take care not to trap air bubbles.
91. Immediately capture the image using.

Phosphoarray: Chemiluminescent Film Image Capture

92. Work in a dark room at room temperature.
93. Lay film on top of the slide(s) for varying exposures between 20-50 seconds.
94. Develop the film using the automated film developer.
95. Label the film with the date, experiment number, array numbers, and exposure time

Phosphoarray: Lightbox and Digital Camera Image Digitisation

96. Use a lightbox and digital camera rig set up as below.

Height setting on camera rig: 51.5 cm (this allows autofocus at the nearest distance to the film)

97. Illuminate with the fluorescent backlight only.
98. Use a Nikon D70 digital camera with the following settings:

Dimensions	3040 x 2014
Bit depth	48
Flash	No
Exposure time	1/10 s
Aperture	Various from f22 to f16
Max. aperture	4.44
Focal length	70.00 mm
Focal length (EQ35mm)	105 mm
ISO	200
Digital zoom ratio	1.00
Exposure bias	-1/3
Metering mode	Spot
Exposure mode	Manual exposure
White balance	Manual
Exposure program	Manual
Orientation	Normal
Sharpness	Normal
Contrast	Normal
Saturation	Normal
Gain control	None
Scene capture type	Standard
Light source	Cool white fluorescent (W 3800–4500K)
Software	Ver.1.02
DPI	300.00
Sensing method	One-chip colour area sensor
Custom image processing	Normal process

Lens 18.00 - 70.00 mm f/3.5 - 4.5
Image Quality RAW

99. Centre the image take multiple images at different exposures. Keep the speed at 1/10s and adjust the aperture from f22 to f12. Retain the image where the histogram is as far to the right as possible without it being cropped (image blowout).

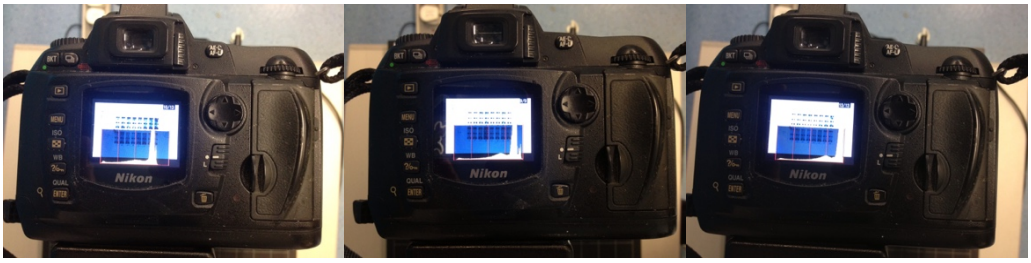

100. Download the photos into Zoner Photo Studio v17 (Zoner Inc., Kennesaw GA).
101. Check that the blowout indicator does not encroach onto the slide. In the example below, blue highlights areas of blowout, a warning symbol on the histogram indicates image blowout, and the selected exposure is shown in the red box.

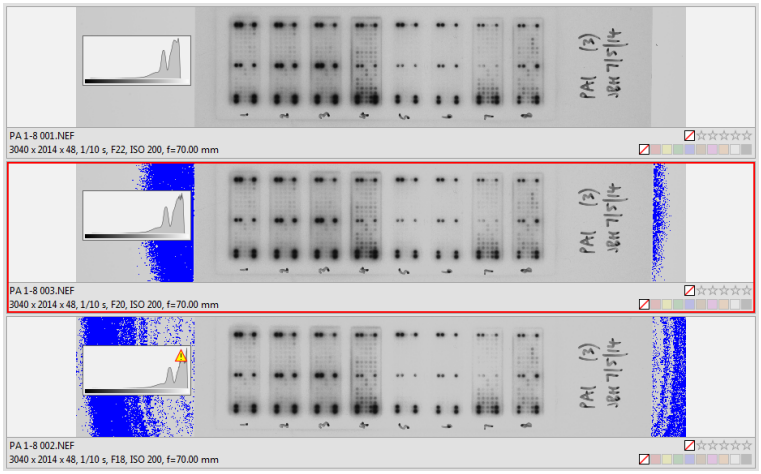

102. Export the RAW image to TIFF using the following settings:
8-bit grayscale
No compression

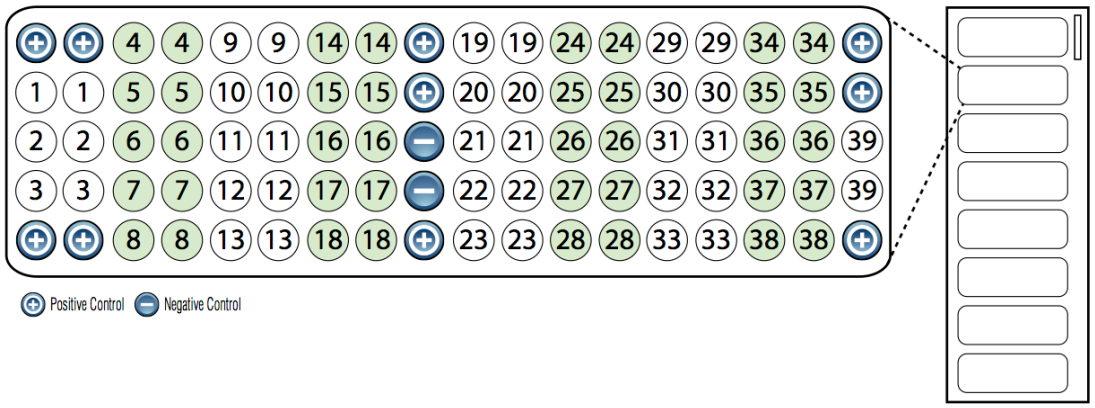

Receptor Tyrosine Kinases

	Target	Phosphorylation Site	Family
1	EGFR/ErbB1	pan-Tyr	EGFR
2	HER2/ErbB2	pan-Tyr	EGFR
3	HER3/ErbB3	pan-Tyr	EGFR
4	FGFR1	pan-Tyr	FGFR
5	FGFR3	pan-Tyr	FGFR
6	FGFR4	pan-Tyr	FGFR
7	InsR	pan-Tyr	Insulin R
8	IGF-IR	pan-Tyr	Insulin R
9	TrkA/NTRK1	pan-Tyr	NGFR
10	TrkB/NTRK2	pan-Tyr	NGFR
11	Met/HGFR	pan-Tyr	HGFR
12	Ron/MST1R	pan-Tyr	HGFR
13	Ret	pan-Tyr	Ret
14	ALK	pan-Tyr	LTK
15	PDGFR	pan-Tyr	PDGFR
16	c-Kit/SCFR	pan-Tyr	PDGFR
17	FLT3/Flk2	pan-Tyr	PDGFR
18	M-CSFR/CSF-1R	pan-Tyr	PDGFR
19	EphA1	pan-Tyr	EphR
20	EphA2	pan-Tyr	EphR
21	EphA3	pan-Tyr	EphR
22	EphB1	pan-Tyr	EphR
23	EphB3	pan-Tyr	EphR
24	EphB4	pan-Tyr	EphR
25	Tyro3/Dtk	pan-Tyr	Axl
26	Axl	pan-Tyr	Axl
27	Tie2/TEK	pan-Tyr	Tie
28	VEGFR2/KDR	pan-Tyr	VEGFR

Signaling Nodes

	Target	Phosphorylation Site	Family
29	Akt/PKB/Rac	Thr308	Akt
30	Akt/PKB/Rac	Ser473	Akt
31	p44/42 MAPK (ERK1/2)	Thr202/Tyr204	MAPK
32	S6 Ribosomal Protein	Ser235/236	RSK
33	c-Abl	pan-Tyr	Abl
34	IRS-1	pan-Tyr	IRS
35	Zap-70	pan-Tyr	Zap-70
36	Src	pan-Tyr	Src
37	Lck	pan-Tyr	Src
38	Stat1	Tyr701	Stat
39	Stat3	Tyr705	Stat

Phosphoarray: Image and Data Analysis

103. Use ImageQuant TL 2005 (GE Healthcare Life Sciences, Pittsburg PA) for each array as follows:
    Open the image and check orientation.
    Draw grid over array spots (adjust spot shape and size to fit the array).
    Label each cell according to target map and key (see above).
    Select a rectangle on the edge of the slide as the background.
    Select all the positive controls and normalise their mean value to 100% (exclude any spots that look like they haven't produced a strong full signal)
    Export data table as CSV file.
104. Duplicate the arx file and open to use the previous settings and labels.
105. Import the CSV file into the database for analysis.

Cytokine Multiplex: MAGPIX Cleaning, Calibration and Verification

106. If there have been recent problems with the system, clean the probe tip as follows:
    Turn off MAGPIX machine (Luminex Corporation, Austin, TX) and open maintenance hatch.
    Unscrew and remove probe tip.
    Flush through with distilled water using syringe.
    Submerge in distilled water in Falcon tube and immerse in sonicator for 10 minutes.
    Flush through the probe again with distilled water.
    Replace probe tip back into machine.
    Tighten screw connector until it clicks.
    Turn MAGPIX back on.
107. Clean the reagent wells as follows:
    Eject the tray and remove the reagent wells.
    Clean out any residue with distilled water, soak if necessary, then dry.
108. Check drive fluid (left-hand chamber) as follows:
    Check level.
    Check the vent in the cap is not crusted over.
109. Check the waste chamber (right-hand chamber, orange connector) as follows:
    Empty if full, taking care not to wet the sensor filter.
    Swap for spare chamber if sensor wet.
110. Calibrate the probe height as folllows:
    Ensure reagent wells are clean and dry.
    Install a clean and dry 8-well strip.
    Put 2 calibration discs in a centre well of the 96-well plate that will be used.
    Use the xPONENT software (Luminex Corporation, Austin, TX) to select the test well and run the calibration program.
111. If there have been recent problems with the system:
    Disconnect and remove the drive fluid chamber
    Add 25 ml of 1M NaOH solution to a bottle.
    Add 225 ml of distilled water.
    Mix then pour into a clean chamber and connect to the drive fluid port.
    Use a custom maintenance program to prime the system 4 times.
112. Clean the system as follows:
    Select the Enhanced Start-up Routine program.
    Add the relevant reagents to the reagent wells (half-filled) as indicated by the program.
    Run.
113. If there have been recent problems with the system:
    Repeat the Enhanced Start-up Routine.

Watch the probe whilst it is at the Clean step. It will pause for a few minutes, and then will drop down. At this point turn the power off.
Leave the system to soak like this for 1 hour, or overnight if experiencing continuing problems.
Turn the MAGPIX back on and allow it to reset.
Replace and reconnect the drive fluid chamber with drive fluid in it.
Use a custom maintenance program to prime the system 4 times.

114. Flush the system as follows:
Select the Daily Fluidics Prep program.
Check the relevant reagents are in the correct reagent wells as indicated by the program.
Run the program 4 times.
115. Calibrate and verify the system as follows:
Use the MAGPIX Calibration Kit (Luminex Corporation, Austin, TX, #MPX-PVER-K25) and MAGPIX Performance Verification Kit (Luminex Corporation, Austin, TX, #MPX-CAL-K25) kits.
Vortex the beads well.
Check the calibration and verification lot numbers on the box correspond with what is specified in the program. If not available, load the correct lxl file from the kit's included CD, using the Lot Management screen.
Add 6 drops of the beads to the correct test wells as indicated by the program (vortex again just before using each vial).
116. Shutdown the system.

Cytokine Multiplex: Protocol and Batch Setup

117. Create a new protocol with the following settings (only required once) as follows:
Name: HCYTMAG-60K-PX30
Analysis: quantitative
Standards: 6
Controls: 2
Curve: Fit all standards
118. Enter settings for the beads (only required once) as follows:
Select the correct beads according to their region for the 30 targets.
Add the target name to the label.
Units: pg/ml (for majority at least)
Bead count: 50
Fit: Logistic 5P
119. Enter standard and control details (required for each different kit batch number)
120. Create a new batch from the protocol.
121. Select the sample wells, in singlet, and label.

Cytokine Multiplex: Plate Setup and Incubation

122. Remove the 30-plex Milliplex MAP Kit (EMD Millipore, Billerica, MA, #HCYTMAG-60K-PX30) from the fridge 1 hour before use to allow to warm to room temperature. Work at room temperature on the open bench.
123. Retrieve the samples from the freezer and thaw at room temperature.
124. Centrifuge the samples at 7,000 rpm for 5 min.
125. Prepare 1X Wash Buffer as follows:
Pour 30ml 10X Wash Buffer into a bottle.

Add 270 ml distilled water.
Mix.[**]

126. Reconstitute the Standard and Controls 1 and 2 as follows:
Tap the vials on the table to encourage powder to settle.
Open rubber stopper from glass vial slowly and half-way only.
Add in 250 µl of distilled water.
Leave to sit for 10 minutes.
Vortex.[††]

127. Prepare the Standards as follows:
Label 6 Eppendorf tubes 2,000, 400, 80, 16, 3.2 and 0 pg/ml.
Add 200 µl of Assay Buffer to each tube.
Add 50 µl of the 10,000 pg/ml reconstituted standard to the 2,000 pg/ml tube.
Vortex.
Repeat the 1 in 5 serial dilution with the remaining tubes in descending order of concentration until 3.2 pg/ml (i.e. do not add to the 0 pg/ml background).

128. Prepare the Antibody-Immobilized Beads as follows:
Sonicate the Bead Bottle and the RANTES bottle for 30 seconds.
Vortex for 1 minute.
Add 70 µl of RANTES to the Bead Bottle.
Vortex.

129. Wash the plate as follows:
Add 200 µl of 1X Wash Buffer to each well of the plate using a multipipette.
Place on plate shaker for 10 minutes at 500 rpm.
Decant by tapping out smartly onto paper towels.

130. Lay out the plate as follows:

	1	2	3	4	5	6	7	8	9	10	11	12
A	0 Standard	400 Standard	QC-2 Control	Sample	Sample	Sample	Sample	Sample	Sample	Sample	Sample	Sample
B	0 Standard	400 Standard	QC-2 Control	Sample	Sample	Sample	Sample	Sample	Sample	Sample	Sample	Sample
C	3.2 Standard	2,000 Standard	Sample	Sample	Sample	Sample	Sample	Sample	Sample	Sample	Sample	Sample
D	3.2 Standard	2,000 Standard	Sample	Sample	Sample	Sample	Sample	Sample	Sample	Sample	Sample	Sample
E	16 Standard	10,000 Standard	Sample	Sample	Sample	Sample	Sample	Sample	Sample	Sample	Sample	Sample
F	16 Standard	10,000 Standard	Sample	Sample	Sample	Sample	Sample	Sample	Sample	Sample	Sample	Sample
G	80 Standard	QC-1 Control	Sample	Sample	Sample	Sample	Sample	Sample	Sample	Sample	Sample	Sample
H	80 Standard	QC-1 Control	Sample	Sample	Sample	Sample	Sample	Sample	Sample	Sample	Sample	Sample

Add 25 µl of Standards or Controls to the corresponding standard/control wells.
Add 25 µl of Culture Medium (as in step 20) to each standard/control wells.
Add 25 µl of Assay Buffer to the sample wells using a multipipette.
Add 25 µl of each Sample to the sample wells.
Vortex the Beads.
Add 25 µl of Beads to all the wells using a multipipette (reverse pipette in the reagent tray each

[**] After use store 1X Wash Buffer at 2-8°C for 1 month.
[††] After use store Standard and Controls at -20°C for 1 month (discard the diluted standards).

time to keep the beads in suspension).
Cover plate with sealing tape and foil.

131. Incubate the plate on a plate shaker at 500 rpm overnight (16-18h) at 4°C.

Cytokine Multiplex: MAGPIX System Initialization

132. Reset the probe height as in step 110.
133. Select the system initialization program, add the correct reagents to the reagent wells and run.

Cytokine Multiplex: Antibody Detection and Plate Reading

134. Allow plate to warm to room temperature on the plate shaker at 500 rpm for 30 minutes.
135. Decant wells as follows:
Place plate on hand-held magnet
Leave for 1 minute to allow beads to settle (rest foil cover over to protect from light).
KEEP MAGNET AND PLATE TOGETHER.
Decant the wells into sink with a swift motion.
Return to bench and separate plate and magnet.
136. Wash as follows:
Add 200 µl Wash Buffer to each well using a multipipette.
Place on plate shaker at 500 rpm for 1 minute (rest foil cover on top).
137. Decant wells with hand-held magnet as before.
138. Repeat wash and decant steps 136 to 137.
139. Add 25 µl Detection Antibodies to each well using a multipipette.
140. Cover plate with sealing tape and foil.
141. Incubate at room temperature on a plate shaker at 500 rpm for 1 hour.
142. DO NOT DECANT.
143. Add 25 µl Streptavidin-Phycoerythrin to each well using a multipipette.
144. Cover plate with sealing tape and foil.
145. Incubate at room temperature on a plate shaker at 500 rpm for 30 minutes.
146. Decant wells with hand-held magnet as before.
147. Wash as follows:
Add 200 µl Wash Buffer to each well using a multipipette.
Place on plate shaker at 500 rpm for 1 minute (rest foil cover on top).
148. Decant wells with hand-held magnet as before.
149. Repeat wash and decant steps 147 to 148.
150. Add 100 µl Drive Fluid to each well using a multipipette.‡‡
151. Incubate at room temperature on a plate shaker at 500 rpm for 10 minutes.

---

‡‡ If required, the plate can be stored at 4°C (preferably on a plate shaker at 500 rpm) for up to 48 hours. Storage for up to 1 week can still yield results but variability is likely to be higher.

Cytokine Multiplex: Plate Reading

152. Place the plate onto the tray.
153. Add the appropriate reagents for the Post-Batch Routine.
154. Select the correct pending batch and run.

Cytokine Multiplex: Results Analysis

155. Open the batch.
156. With each of the 30 analytes, review the % recovery of the standards. If it is <70% or >130%, review the plot to judge if it is skewing the curve. If it is, invalidate the point and re-analyse to see if the curve fit is better and the % recovery values are closer to 100%. Then review the % recovery of the controls to see if they are within the 70-130% range. If not, then the curve fit is poor.
157. Then review the test results. If concentrations appear outside the standard curve 3.2-10,000 pg/ml, the absolute values need to be treated with caution. Also to be borne in mind are the minimum detectable concentrations for each analyte (listed in the protocol book). Analytes that are giving low values would require a more sensitive assay for more accurate quantification. Analytes that are giving high values require a dilution factor.

APPENDIX 6 MILLIPLEX MAP HUMAN CYTOKINE/CHEMOKINE MAGNETIC BEAD PANEL ASSAY SENSITIVITIES

Table 37 Assay sensitivities for Milliplex MAP Human Cytokine/Chemokine Magnetic Bead Panel. Min DC, minimum detectable concentration; SD, standard deviation; CV, coefficient of variation.

Cytokine	Min DC, pg/ml	Min DC + 2SD, pg/ml	Intra-assay CV, %	Inter-assay CV, %
EGF	2.8	4.6	2.3	5.8
Eotaxin	4.0	6.8	7.2	10.8
G-CSF	1.8	3.3	1.8	15.5
GM-CSF	7.5	15	3.1	10.1
IFN-α2	2.9	4.8	2.4	13.3
IFN-γ	0.8	1.1	1.6	12
IL-10	1.1	1.6	1.6	16.8
IL-12P40	7.4	12.7	2.8	12.4
IL-12P70	0.6	1	2.2	16.7
IL-13	1.3	1.9	2.2	9.2
IL-15	1.2	1.7	2.7	8.1
IL-17	0.7	1.2	2.2	7.9
IL-1RA	8.3	17.1	2.1	10.7
IL-1α	9.4	12.6	3.3	12.8
IL-1β	0.8	1	2.3	6.7
IL-2	1.0	1.6	2.1	6.3
IL-3	0.7	1	3.4	6.1
IL-4	4.5	7.1	2.9	14.2
IL-5	0.5	0.7	2.6	10.8
IL-6	0.9	1.3	2.0	18.3
IL-7	1.4	2.4	1.7	16.1
IL-8	0.4	0.7	1.9	3.5
IP-10	8.6	14	2.6	15.3
MCP-1	1.9	3.4	1.5	7.9
MIP-1α	2.9	6.2	1.9	14.5
MIP-1β	3.0	4.8	2.4	8.8
TNF-α	0.7	1.1	2.6	13
TNF-β	1.5	1.9	1.6	11.4
RANTES	1.2	1.9	1.9	5
VEGF	26.3	47.9	3.7	10.4

APPENDIX 7 MAGPIX PERFORMANCE VERIFICATION

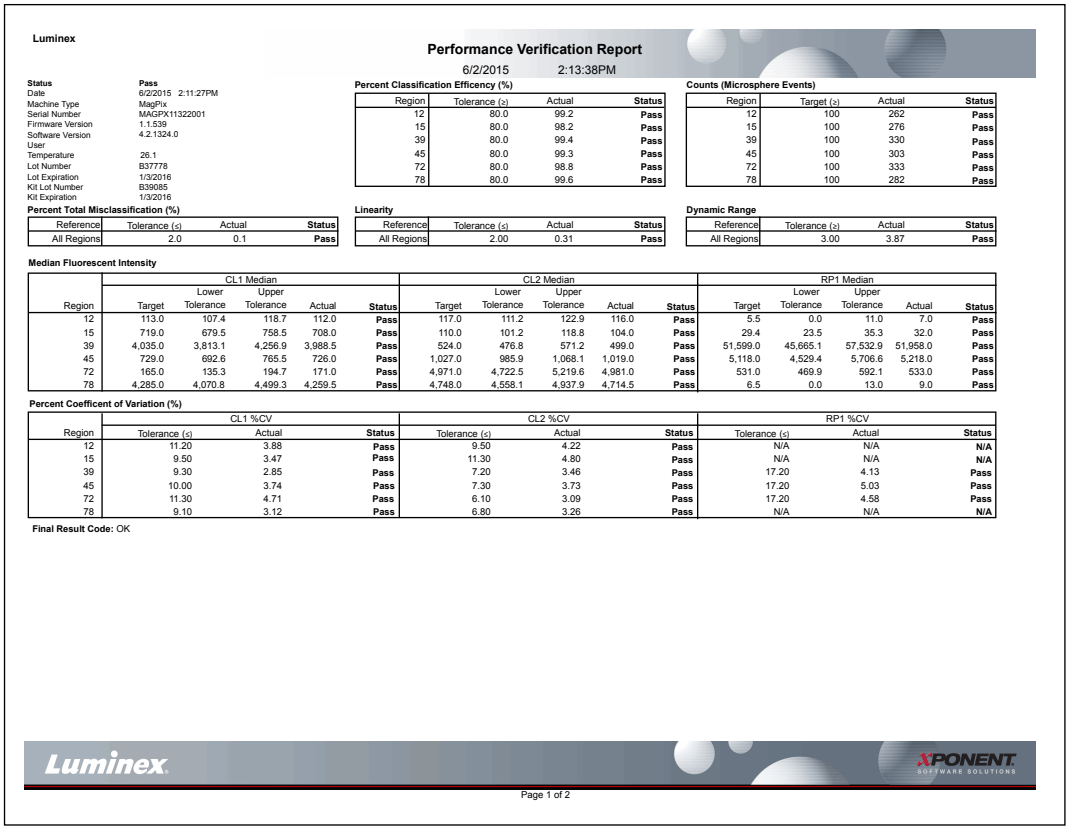

Luminex

Performance Verification Report

6/2/2015 2:13:38PM

Status	Pass
Date	6/2/2015 2:11:27PM
Machine Type	MagPix
Serial Number	MAGPX11322001
Firmware Version	1.1.539
Software Version	4.2.1324.0
User	
Temperature	26.1
Lot Number	B37778
Lot Expiration	1/3/2016
Kit Lot Number	B39085
Kit Expiration	1/3/2016

Percent Classification Efficency (%)

Region	Tolerance (≥)	Actual	Status
12	80.0	99.2	Pass
15	80.0	98.2	Pass
39	80.0	99.4	Pass
45	80.0	99.3	Pass
72	80.0	98.8	Pass
78	80.0	99.6	Pass

Counts (Microsphere Events)

Region	Target (≥)	Actual	Status
12	100	262	Pass
15	100	276	Pass
39	100	330	Pass
45	100	303	Pass
72	100	333	Pass
78	100	282	Pass

Percent Total Misclassification (%)

Reference	Tolerance (≤)	Actual	Status
All Regions	2.0	0.1	Pass

Linearity

Reference	Tolerance (≤)	Actual	Status
All Regions	2.00	0.31	Pass

Dynamic Range

Reference	Tolerance (≥)	Actual	Status
All Regions	3.00	3.87	Pass

Median Fluorescent Intensity

	CL1 Median					CL2 Median					RP1 Median				
Region	Target	Lower Tolerance	Upper Tolerance	Actual	Status	Target	Lower Tolerance	Upper Tolerance	Actual	Status	Target	Lower Tolerance	Upper Tolerance	Actual	Status
12	113.0	107.4	118.7	112.0	Pass	117.0	111.2	122.9	116.0	Pass	5.5	0.0	11.0	7.0	Pass
15	719.0	679.5	758.5	708.0	Pass	110.0	101.2	118.8	104.0	Pass	29.4	23.5	35.3	32.0	Pass
39	4,035.0	3,813.1	4,256.9	3,988.5	Pass	524.0	476.8	571.2	499.0	Pass	51,599.0	45,665.1	57,532.9	51,958.0	Pass
45	729.0	692.6	765.5	726.0	Pass	1,027.0	985.9	1,068.1	1,019.0	Pass	5,118.0	4,529.4	5,706.6	5,218.0	Pass
72	165.0	135.3	194.7	171.0	Pass	4,971.0	4,722.5	5,219.6	4,981.0	Pass	531.0	469.9	592.1	533.0	Pass
78	4,285.0	4,070.8	4,499.3	4,259.5	Pass	4,748.0	4,558.1	4,937.9	4,714.5	Pass	6.5	0.0	13.0	9.0	Pass

Percent Coefficent of Variation (%)

	CL1 %CV			CL2 %CV			RP1 %CV		
Region	Tolerance (≤)	Actual	Status	Tolerance (≤)	Actual	Status	Tolerance (≤)	Actual	Status
12	11.20	3.88	Pass	9.50	4.22	Pass	N/A	N/A	N/A
15	9.50	3.47	Pass	11.30	4.80	Pass	N/A	N/A	N/A
39	9.30	2.85	Pass	7.20	3.46	Pass	17.20	4.13	Pass
45	10.00	3.74	Pass	7.30	3.73	Pass	17.20	5.03	Pass
72	11.30	4.71	Pass	6.10	3.09	Pass	17.20	4.58	Pass
78	9.10	3.12	Pass	6.80	3.26	Pass	N/A	N/A	N/A

Final Result Code: OK

Luminex XPONENT SOFTWARE SOLUTIONS

Page 1 of 2

Luminex

Performance Verification Report

6/2/2015 2:13:39PM

Status	**Pass**
Date	6/2/2015 2:12:41PM
Machine Type	MagPix
Serial Number	MAGPX11322001
Firmware Version	1.1.539
Software Version	4.2.1324.0
User	
Temperature	26.10
Fluid 1 Lot Number	B37750
Fluid 1 Lot Expiration	1/3/2016
Fluid 2 Lot Number	B37751
Fluid 2 Lot Expiration	1/3/2016
Kit Lot Number	B39085
Kit Expiration	1/3/2016

Final Result Code: OK

Counts (Microsphere Events)

Reference	Tolerance (≥)	Actual	Status
FLUID1	1,000	2,087	Pass
FLUID2	1,000	1,916	Pass

Percent Total Carryover (%)

Reference	Tolerance % (≤)	Actual	Status
Total	4.00	0.19	Pass

Luminex

Performance Verification Report

6/22/2015 2:49:18PM

Status	**Pass**
Date	6/22/2015 2:44:17PM
Machine Type	MagPix
Serial Number	MAGPX11322001
Firmware Version	1.1.539
Software Version	4.2.1324.0
User	
Temperature	26.1
Lot Number	B40661
Lot Expiration	6/20/2016
Kit Lot Number	B42348
Kit Expiration	4/10/2016

Percent Classification Efficency (%)

Region	Tolerance (≥)	Actual	Status
12	80.0	100.0	Pass
15	80.0	97.8	Pass
39	80.0	99.7	Pass
45	80.0	99.7	Pass
72	80.0	100.0	Pass
78	80.0	99.3	Pass

Counts (Microsphere Events)

Region	Target (≥)	Actual	Status
12	100	253	Pass
15	100	231	Pass
39	100	324	Pass
45	100	330	Pass
72	100	295	Pass
78	100	270	Pass

Percent Total Misclassification (%)

Reference	Tolerance (≤)	Actual	Status
All Regions	2.0	1.5	Pass

Linearity

Reference	Tolerance (≤)	Actual	Status
All Regions	2.00	0.24	Pass

Dynamic Range

Reference	Tolerance (≥)	Actual	Status
All Regions	3.00	3.95	Pass

Median Fluorescent Intensity

	CL1 Median					CL2 Median					RP1 Median				
Region	Target	Lower Tolerance	Upper Tolerance	Actual	Status	Target	Lower Tolerance	Upper Tolerance	Actual	Status	Target	Lower Tolerance	Upper Tolerance	Actual	Status
12	112.0	106.4	117.6	110.0	Pass	114.0	108.3	119.7	113.0	Pass	4.6	0.0	9.2	6.0	Pass
15	684.0	646.4	721.6	676.0	Pass	106.0	97.5	114.5	103.0	Pass	28.3	22.6	34.0	30.0	Pass
39	3,997.0	3,777.2	4,216.8	3,980.5	Pass	541.0	492.3	589.7	529.0	Pass	51,974.0	45,997.0	57,951.0	53,115.5	Pass
45	690.0	655.5	724.5	687.0	Pass	960.0	921.6	998.4	958.5	Pass	5,355.0	4,739.2	5,970.8	5,426.0	Pass
72	156.0	127.9	184.1	161.0	Pass	4,997.0	4,747.2	5,246.9	5,026.0	Pass	553.0	489.4	616.6	558.0	Pass
78	3,969.0	3,770.6	4,167.5	3,938.0	Pass	4,751.0	4,561.0	4,941.0	4,731.5	Pass	7.2	0.0	14.4	9.0	Pass

Percent Coefficent of Variation (%)

	CL1 %CV			CL2 %CV			RP1 %CV		
Region	Tolerance (≤)	Actual	Status	Tolerance (≤)	Actual	Status	Tolerance (≤)	Actual	Status
12	11.20	3.49	Pass	9.50	3.90	Pass	N/A	N/A	N/A
15	9.50	3.19	Pass	11.30	3.90	Pass	N/A	N/A	N/A
39	9.30	2.90	Pass	7.20	3.32	Pass	17.20	5.12	Pass
45	10.00	2.74	Pass	7.30	2.82	Pass	17.20	4.20	Pass
72	11.30	4.41	Pass	6.10	2.96	Pass	17.20	4.49	Pass
78	9.10	2.84	Pass	6.80	2.56	Pass	N/A	N/A	N/A

Final Result Code: OK

Luminex

Performance Verification Report

6/22/2015 2:49:18PM

Status	**Pass**
Date	6/22/2015 2:45:32PM
Machine Type	MagPix
Serial Number	MAGPX11322001
Firmware Version	1.1.539
Software Version	4.2.1324.0
User	
Temperature	26.20
Fluid 1 Lot Number	B39601
Fluid 1 Lot Expiration	4/10/2016
Fluid 2 Lot Number	B39602
Fluid 2 Lot Expiration	4/15/2016
Kit Lot Number	B42348
Kit Expiration	4/10/2016

Final Result Code: OK

Counts (Microsphere Events)

Reference	Tolerance (≥)	Actual	Status
FLUID1	1,000	1,966	Pass
FLUID2	1,000	1,736	Pass

Percent Total Carryover (%)

Reference	Tolerance % (≤)	Actual	Status
Total	4.00	0.46	Pass

Luminex

Performance Verification Report

6/23/2015 11:19:31AM

Status	**Pass**
Date	6/23/2015 10:51:50AM
Machine Type	MagPix
Serial Number	MAGPX11322001
Firmware Version	1.1.539
Software Version	4.2.1324.0
User	\
Temperature	25.4
Lot Number	B40661
Lot Expiration	6/20/2016
Kit Lot Number	B42348
Kit Expiration	4/10/2016

Percent Classification Efficency (%)

Region	Tolerance (≥)	Actual	Status
12	80.0	99.6	Pass
15	80.0	96.2	Pass
39	80.0	100.0	Pass
45	80.0	96.3	Pass
72	80.0	99.6	Pass
78	80.0	100.0	Pass

Counts (Microsphere Events)

Region	Target (≥)	Actual	Status
12	100	223	Pass
15	100	213	Pass
39	100	251	Pass
45	100	269	Pass
72	100	266	Pass
78	100	238	Pass

Percent Total Misclassification (%)

Reference	Tolerance (≤)	Actual	Status
All Regions	2.0	1.8	Pass

Linearity

Reference	Tolerance (≤)	Actual	Status
All Regions	2.00	0.08	Pass

Dynamic Range

Reference	Tolerance (≥)	Actual	Status
All Regions	3.00	4.02	Pass

Median Fluorescent Intensity

	CL1 Median					CL2 Median					RP1 Median				
		Lower	Upper				Lower	Upper				Lower	Upper		
Region	Target	Tolerance	Tolerance	Actual	Status	Target	Tolerance	Tolerance	Actual	Status	Target	Tolerance	Tolerance	Actual	Status
12	112.0	106.4	117.6	111.0	Pass	114.0	108.3	119.7	114.0	Pass	4.6	0.0	9.2	5.0	Pass
15	684.0	646.4	721.6	674.0	Pass	106.0	97.5	114.5	103.0	Pass	28.3	22.6	34.0	29.0	Pass
39	3,997.0	3,777.2	4,216.8	3,994.0	Pass	541.0	492.3	589.7	530.0	Pass	51,974.0	45,997.0	57,951.0	52,665.0	Pass
45	690.0	655.5	724.5	684.0	Pass	960.0	921.6	998.4	959.0	Pass	5,355.0	4,739.2	5,970.8	5,390.0	Pass
72	156.0	127.9	184.1	163.0	Pass	4,997.0	4,747.2	5,246.9	5,038.0	Pass	553.0	489.4	616.6	559.0	Pass
78	3,969.0	3,770.6	4,167.5	3,936.5	Pass	4,751.0	4,561.0	4,941.0	4,765.0	Pass	7.2	0.0	14.4	8.0	Pass

Percent Coefficent of Variation (%)

	CL1 %CV			CL2 %CV			RP1 %CV		
Region	Tolerance (≤)	Actual	Status	Tolerance (≤)	Actual	Status	Tolerance (≤)	Actual	Status
12	11.20	3.35	Pass	9.50	3.32	Pass	N/A	N/A	N/A
15	9.50	3.17	Pass	11.30	4.09	Pass	N/A	N/A	N/A
39	9.30	2.84	Pass	7.20	3.52	Pass	17.20	4.71	Pass
45	10.00	3.49	Pass	7.30	3.49	Pass	17.20	5.48	Pass
72	11.30	4.08	Pass	6.10	2.78	Pass	17.20	4.38	Pass
78	9.10	3.20	Pass	6.80	3.09	Pass	N/A	N/A	N/A

Final Result Code: OK

Luminex

Performance Verification Report

6/23/2015 11:19:32AM

Status	**Pass**
Date	6/23/2015 10:53:05AM
Machine Type	MagPix
Serial Number	MAGPX11322001
Firmware Version	1.1.539
Software Version	4.2.1324.0
User	\
Temperature	25.50
Fluid 1 Lot Number	B39601
Fluid 1 Lot Expiration	4/10/2016
Fluid 2 Lot Number	B39602
Fluid 2 Lot Expiration	4/15/2016
Kit Lot Number	B42348
Kit Expiration	4/10/2016

Final Result Code: OK

Counts (Microsphere Events)

Reference	Tolerance (≥)	Actual	Status
FLUID1	1,000	1,701	Pass
FLUID2	1,000	1,624	Pass

Percent Total Carryover (%)

Reference	Tolerance % (≤)	Actual	Status
Total	4.00	0.47	Pass

Luminex

Performance Verification Report

6/24/2015 10:40:37AM

Status	**Pass**
Date	6/24/2015 10:32:37AM
Machine Type	MagPix
Serial Number	MAGPX11322001
Firmware Version	1.1.539
Software Version	4.2.1324.0
User	\
Temperature	25.6
Lot Number	B40661
Lot Expiration	6/20/2016
Kit Lot Number	B42348
Kit Expiration	4/10/2016

Percent Classification Efficency (%)

Region	Tolerance (≥)	Actual	Status
12	80.0	99.2	Pass
15	80.0	98.6	Pass
39	80.0	98.6	Pass
45	80.0	100.0	Pass
72	80.0	99.2	Pass
78	80.0	99.2	Pass

Counts (Microsphere Events)

Region	Target (≥)	Actual	Status
12	100	241	Pass
15	100	208	Pass
39	100	290	Pass
45	100	274	Pass
72	100	264	Pass
78	100	241	Pass

Percent Total Misclassification (%)

Reference	Tolerance (≤)	Actual	Status
All Regions	2.0	0.2	Pass

Linearity

Reference	Tolerance (≤)	Actual	Status
All Regions	2.00	0.09	Pass

Dynamic Range

Reference	Tolerance (≥)	Actual	Status
All Regions	3.00	4.02	Pass

Median Fluorescent Intensity

	CL1 Median					CL2 Median					RP1 Median				
Region	Target	Lower Tolerance	Upper Tolerance	Actual	Status	Target	Lower Tolerance	Upper Tolerance	Actual	Status	Target	Lower Tolerance	Upper Tolerance	Actual	Status
12	112.0	106.4	117.6	110.0	Pass	114.0	108.3	119.7	113.0	Pass	4.6	0.0	9.2	5.0	Pass
15	684.0	646.4	721.6	677.0	Pass	106.0	97.5	114.5	103.0	Pass	28.3	22.6	34.0	29.0	Pass
39	3,997.0	3,777.2	4,216.8	3,976.5	Pass	541.0	492.3	589.7	530.0	Pass	51,974.0	45,997.0	57,951.0	52,596.0	Pass
45	690.0	655.5	724.5	687.0	Pass	960.0	921.6	998.4	960.0	Pass	5,355.0	4,739.2	5,970.8	5,395.5	Pass
72	156.0	127.9	184.1	161.0	Pass	4,997.0	4,747.2	5,246.9	5,021.0	Pass	553.0	489.4	616.6	557.0	Pass
78	3,969.0	3,770.6	4,167.5	3,933.0	Pass	4,751.0	4,561.0	4,941.0	4,739.0	Pass	7.2	0.0	14.4	9.0	Pass

Percent Coefficent of Variation (%)

	CL1 %CV			CL2 %CV			RP1 %CV		
Region	Tolerance (≤)	Actual	Status	Tolerance (≤)	Actual	Status	Tolerance (≤)	Actual	Status
12	11.20	3.54	Pass	9.50	3.17	Pass	N/A	N/A	N/A
15	9.50	3.14	Pass	11.30	4.30	Pass	N/A	N/A	N/A
39	9.30	2.90	Pass	7.20	3.36	Pass	17.20	5.08	Pass
45	10.00	2.82	Pass	7.30	2.80	Pass	17.20	4.31	Pass
72	11.30	3.97	Pass	6.10	2.74	Pass	17.20	4.18	Pass
78	9.10	3.03	Pass	6.80	3.01	Pass	N/A	N/A	N/A

Final Result Code: OK

Luminex

Performance Verification Report

6/24/2015 10:40:37AM

Status	**Pass**
Date	6/24/2015 10:33:51AM
Machine Type	MagPix
Serial Number	MAGPX11322001
Firmware Version	1.1.539
Software Version	4.2.1324.0
User	\
Temperature	25.70
Fluid 1 Lot Number	B39601
Fluid 1 Lot Expiration	4/10/2016
Fluid 2 Lot Number	B39602
Fluid 2 Lot Expiration	4/15/2016
Kit Lot Number	B42348
Kit Expiration	4/10/2016

Final Result Code: OK

Counts (Microsphere Events)

Reference	Tolerance (≥)	Actual	Status
FLUID1	1,000	1,756	Pass
FLUID2	1,000	1,630	Pass

Percent Total Carryover (%)

Reference	Tolerance % (≤)	Actual	Status
Total	4.00	0.40	Pass

Luminex

Performance Verification Report

10/1/2015 1:10:53PM

Status	**Pass**
Date	9/3/2015 4:09:58PM
Machine Type	MagPix
Serial Number	MAGPX11322001
Firmware Version	1.1.539
Software Version	4.2.1324.0
User	
Temperature	26.2
Lot Number	B40661
Lot Expiration	6/20/2016
Kit Lot Number	B42348
Kit Expiration	4/10/2016

Percent Classification Efficency (%)

Region	Tolerance (≥)	Actual	Status
12	80.0	98.3	Pass
15	80.0	98.8	Pass
39	80.0	99.7	Pass
45	80.0	98.8	Pass
72	80.0	99.7	Pass
78	80.0	98.8	Pass

Counts (Microsphere Events)

Region	Target (≥)	Actual	Status
12	100	236	Pass
15	100	258	Pass
39	100	326	Pass
45	100	337	Pass
72	100	298	Pass
78	100	256	Pass

Percent Total Misclassification (%)

Reference	Tolerance (≤)	Actual	Status
All Regions	2.0	0.2	Pass

Linearity

Reference	Tolerance (≤)	Actual	Status
All Regions	2.00	0.19	Pass

Dynamic Range

Reference	Tolerance (≥)	Actual	Status
All Regions	3.00	3.94	Pass

Median Fluorescent Intensity

	CL1 Median					CL2 Median					RP1 Median				
Region	Target	Lower Tolerance	Upper Tolerance	Actual	Status	Target	Lower Tolerance	Upper Tolerance	Actual	Status	Target	Lower Tolerance	Upper Tolerance	Actual	Status
12	112.0	106.4	117.6	110.0	Pass	114.0	108.3	119.7	113.0	Pass	4.6	0.0	9.2	6.0	Pass
15	684.0	646.4	721.6	675.0	Pass	106.0	97.5	114.5	103.0	Pass	28.3	22.6	34.0	30.0	Pass
39	3,997.0	3,777.2	4,216.8	3,983.5	Pass	541.0	492.3	589.7	531.0	Pass	51,974.0	45,997.0	57,951.0	52,643.0	Pass
45	690.0	655.5	724.5	682.0	Pass	960.0	921.6	998.4	956.0	Pass	5,355.0	4,739.2	5,970.8	5,393.0	Pass
72	156.0	127.9	184.1	160.0	Pass	4,997.0	4,747.2	5,246.9	5,024.5	Pass	553.0	489.4	616.6	561.5	Pass
78	3,969.0	3,770.6	4,167.5	3,933.5	Pass	4,751.0	4,561.0	4,941.0	4,767.5	Pass	7.2	0.0	14.4	10.0	Pass

Percent Coefficent of Variation (%)

	CL1 %CV			CL2 %CV			RP1 %CV		
Region	Tolerance (≤)	Actual	Status	Tolerance (≤)	Actual	Status	Tolerance (≤)	Actual	Status
12	11.20	3.99	Pass	9.50	4.17	Pass	N/A	N/A	N/A
15	9.50	3.36	Pass	11.30	4.48	Pass	N/A	N/A	N/A
39	9.30	2.91	Pass	7.20	3.46	Pass	17.20	5.12	Pass
45	10.00	2.98	Pass	7.30	2.90	Pass	17.20	4.54	Pass
72	11.30	4.29	Pass	6.10	2.86	Pass	17.20	4.40	Pass
78	9.10	3.07	Pass	6.80	2.94	Pass	N/A	N/A	N/A

Final Result Code: OK

Luminex

Performance Verification Report

10/1/2015 1:10:53PM

Status	**Pass**
Date	9/3/2015 4:11:13PM
Machine Type	MagPix
Serial Number	MAGPX11322001
Firmware Version	1.1.539
Software Version	4.2.1324.0
User	
Temperature	26.20
Fluid 1 Lot Number	B39601
Fluid 1 Lot Expiration	4/10/2016
Fluid 2 Lot Number	B39602
Fluid 2 Lot Expiration	4/15/2016
Kit Lot Number	B42348
Kit Expiration	4/10/2016

Final Result Code: OK

Counts (Microsphere Events)

Reference	Tolerance (≥)	Actual	Status
FLUID1	1,000	2,143	**Pass**
FLUID2	1,000	1,927	**Pass**

Percent Total Carryover (%)

Reference	Tolerance % (≤)	Actual	Status
Total	4.00	0.19	**Pass**

APPENDIX 8 SUPPLEMENTARY TABLES

Perineal Disease Activity Index

Table 38 PDAI by treatment outcome at baseline (t0), follow-up 1 (t1) and follow-up 2 (t2). Range for each domain 0 to 4. Range for PDAI 0 to 24. Mean (standard deviation) shown.

	Treatment outcome	Idiopathic			Crohn's Disease			All		
		t0	t1	t2	t0	t1	t2	t0	t1	t2
Discharge	Unsatisfactory	1.25 (0.86)	1.33 (1.18)	2.00 (1.04)	1.67 (1.15)	1.67 (1.53)	1.50 (2.12)	1.32 (0.89)	1.39 (1.20)	1.94 (1.12)
	Satisfactory	1.45 (1.02)	1.11 (1.13)	0.92 (1.10)	1.91 (1.14)	1.73 (1.10)	1.10 (1.20)	1.58 (1.06)	1.28 (1.15)	0.97 (1.11)
Pain/ restriction	Unsatisfactory	1.19 (1.11)	1.20 (1.21)	1.43 (1.09)	1.67 (0.58)	2.33 (1.53)	2.00 (2.83)	1.26 (1.05)	1.39 (1.29)	1.50 (1.26)
	Satisfactory	1.03 (1.12)	0.63 (0.97)	0.52 (0.73)	1.45 (1.44)	1.45 (1.44)	1.22 (1.09)	1.15 (1.21)	0.87 (1.17)	0.72 (0.89)
Sexual function	Unsatisfactory	0.81 (1.28)	0.60 (1.24)	1.07 (1.33)	0.67 (1.15)	0.33 (0.58)	2.00 (2.83)	0.79 (1.23)	0.56 (1.15)	1.19 (1.47)
	Satisfactory	0.45 (1.24)	0.59 (1.31)	0.48 (1.20)	0.36 (1.21)	1.00 (1.48)	0.67 (1.00)	0.42 (1.22)	0.71 (1.35)	0.53 (1.14)
Type	Unsatisfactory	2.00 (0.00)	1.27 (0.96)	1.71 (0.73)	2.00 (0.00)	1.67 (0.58)	2.50 (0.71)	2.00 (0.00)	1.33 (0.91)	1.81 (0.75)
	Satisfactory	2.03 (0.19)	1.18 (0.94)	1.13 (0.99)	2.00 (0.89)	1.91 (0.70)	2.00 (0.94)	2.03 (0.48)	1.38 (0.94)	1.38 (1.04)
Induration	Unsatisfactory	0.50 (0.63)	0.73 (0.80)	1.71 (1.44)	3.33 (0.58)	0.67 (1.15)	2.50 (0.71)	0.95 (1.22)	0.72 (0.83)	1.81 (1.38)
	Satisfactory	0.66 (0.81)	0.39 (0.74)	0.42 (0.72)	2.00 (1.26)	1.00 (1.34)	1.11 (1.17)	1.03 (1.12)	0.56 (0.97)	0.61 (0.90)
PDAI	Unsatisfactory	5.75 (2.27)	5.13 (3.94)	7.93 (3.65)	9.33 (2.08)	6.67 (1.53)	10.50 (9.19)	6.32 (2.56)	5.39 (3.66)	8.25 (4.23)
	Satisfactory	5.62 (3.08)	4.00 (3.70)	3.43 (3.26)	7.73 (4.38)	7.09 (4.28)	6.22 (3.67)	6.20 (3.55)	4.89 (4.07)	4.22 (3.55)

EQ-5D-5L

Table 39 EQ-5D-5L dimensions by treatment outcome at baseline (t0), follow-up 1 (t1) and follow-up 2 (t2). Percentages for levels 1 to 5 shown (level 1 = no problems).

EQ-5D-5L Dimension	Treatment outcome	EQ Level	Idiopathic			Crohn's Disease			All		
			t0	t1	t2	t0	t1	t2	t0	t1	t2
Mobility	Unsatisfactory	1	50%	53%	43%	100%	33%	50%	58%	50%	44%
		2	38%	7%	14%	0%	33%	50%	32%	11%	19%
		3	13%	33%	29%	0%	33%	0%	11%	33%	25%
		4	0%	7%	14%	0%	0%	0%	0%	6%	13%
		5	0%	0%	0%	0%	0%	0%	0%	0%	0%
	Satisfactory	1	76%	77%	78%	45%	45%	56%	68%	68%	72%
		2	10%	4%	9%	27%	9%	11%	15%	5%	9%
		3	0%	4%	9%	27%	36%	22%	8%	14%	13%
		4	10%	12%	4%	0%	9%	11%	8%	11%	6%
		5	3%	4%	0%	0%	0%	0%	3%	3%	0%
Self-care	Unsatisfactory	1	94%	73%	86%	67%	67%	100%	89%	72%	88%
		2	6%	20%	0%	33%	0%	0%	11%	17%	0%
		3	0%	7%	7%	0%	33%	0%	0%	11%	6%
		4	0%	0%	7%	0%	0%	0%	0%	0%	6%
		5	0%	0%	0%	0%	0%	0%	0%	0%	0%
	Satisfactory	1	86%	85%	91%	100%	73%	67%	90%	81%	84%
		2	3%	8%	4%	0%	27%	22%	3%	14%	9%
		3	10%	8%	0%	0%	0%	11%	8%	5%	3%
		4	0%	0%	4%	0%	0%	0%	0%	0%	3%
		5	0%	0%	0%	0%	0%	0%	0%	0%	0%
Usual activities	Unsatisfactory	1	56%	40%	43%	67%	100%	50%	58%	50%	44%
		2	31%	13%	7%	0%	0%	50%	26%	11%	13%
		3	0%	27%	29%	33%	0%	0%	5%	22%	25%
		4	6%	7%	21%	0%	0%	0%	5%	6%	19%
		5	6%	13%	0%	0%	0%	0%	5%	11%	0%
	Satisfactory	1	79%	81%	91%	36%	36%	44%	68%	68%	78%
		2	7%	0%	0%	18%	9%	0%	10%	3%	0%
		3	0%	4%	4%	36%	36%	22%	10%	14%	9%
		4	7%	15%	0%	0%	18%	22%	5%	16%	6%
		5	7%	0%	4%	9%	0%	11%	8%	0%	6%
Pain/ discomfort	Unsatisfactory	1	25%	27%	29%	67%	0%	50%	32%	22%	31%
		2	38%	27%	7%	0%	67%	0%	32%	33%	6%
		3	31%	27%	14%	33%	33%	0%	32%	28%	13%
		4	6%	20%	43%	0%	0%	50%	5%	17%	44%
		5	0%	0%	7%	0%	0%	0%	0%	0%	6%
	Satisfactory	1	38%	65%	30%	18%	18%	33%	33%	51%	31%
		2	34%	12%	30%	45%	55%	11%	38%	24%	25%
		3	24%	12%	22%	18%	27%	44%	23%	16%	28%
		4	0%	12%	17%	18%	0%	11%	5%	8%	16%
		5	3%	0%	0%	0%	0%	0%	3%	0%	0%

EQ-5D-5L Dimension	Treatment outcome	EQ Level	Idiopathic			Crohn's Disease			All		
			t0	t1	t2	t0	t1	t2	t0	t1	t2
Anxiety/ depression	Unsatisfactory	1	63%	60%	43%	67%	33%	50%	63%	56%	44%
		2	25%	7%	14%	33%	67%	0%	26%	17%	13%
		3	6%	20%	7%	0%	0%	50%	5%	17%	13%
		4	6%	13%	29%	0%	0%	0%	5%	11%	25%
		5	0%	0%	7%	0%	0%	0%	0%	0%	6%
	Satisfactory	1	62%	77%	87%	45%	45%	44%	58%	68%	75%
		2	28%	8%	9%	36%	9%	0%	30%	8%	6%
		3	3%	12%	4%	9%	27%	56%	5%	16%	19%
		4	3%	4%	0%	9%	9%	0%	5%	5%	0%
		5	3%	0%	0%	0%	9%	0%	3%	3%	0%

Table 40 EQ VAS and index by treatment outcome at baseline (t0), follow-up 1 (t1) and follow-up 2 (t2). Mane (standard deviation) shown.

	Treatment Outcome	Idiopathic			Crohn's disease			All		
		t0	t1	t2	t0	t1	t2	t0	t1	t2
EQ VAS	Unsatis-factory	71.4 (14.8)	62.0 (19.2)	51.9 (18.0)	70.0 (10.0)	68.3 (14.4)	65.0 (21.2)	71.2 (13.9)	63.1 (18.2)	53.6 (18.2)
	Satis-factory	70.9 (24.3)	74.1 (20.1)	78.0 (20.5)	61.5 (22.2)	59.1 (19.6)	61.7 (10.3)	68.3 (23.9)	69.6 (20.8)	73.4 (19.5)
EQ index	Unsatis-factory	0.723 (0.184)	0.633 (0.286)	0.491 (0.249)	0.851 (0.165)	0.704 (0.135)	0.675 (0.228)	0.743 (0.183)	0.645 (0.265)	0.514 (0.247)
	Satis-factory	0.739 (0.299)	0.808 (0.287)	0.784 (0.217)	0.677 (0.217)	0.656 (0.267)	0.655 (0.280)	0.722 (0.277)	0.763 (0.286)	0.748 (0.239)

Table 41 Fistula tract median cytokine concentrations. Median difference and 99% confidence intervals estimated using Hodges-Lehman method; hypotheses tested using Mann-Whitney U (significance level 0.01). IQR, interquartile range; CI, confidence interval.

	Median concentration (IQR), pg/ml			Median difference (99% CI), pg/ml	*p*
	Idiopathic	Crohn's disease	All		
EGF	14.7 (7.2–27.9)	17.4 (7.4–32.2)	15.1 (7.2–30.7)	0.2 (-19.9–21.6)	0.880
Eotaxin	13.2 (4.9–18.8)	10.7 (7.4–19.3)	12.4 (4.9–19.3)	0.0 (-10.5–8.0)	0.907
G-CSF	950.6 (56.9–6727.4)	4693.6 (34.1–22402.3)	967.5 (38.7–22402.3)	0.0 (-1406.9–21451.8)	0.647
GM-CSF	14 (6.2–93.5)	30 (5.6–219)	14.6 (5.6–129.4)	9.1 (-21.0–212.7)	0.423
IFN-α2	19.7 (8.9–28.2)	16.8 (6.2–30.3)	19.1 (8.3–29.8)	0.0 (-15.7–21.4)	0.991
IFN-γ	4 (1.6–7.3)	5.7 (1.1–10.9)	4.1 (1.4–8)	1.1 (-3.1–8.4)	0.430
IL-10	24.7 (6.9–156.9)	29.2 (10.2–141.7)	25.3 (6.9–156.9)	0.4 (-87.9–129.9)	0.908
IL-12p40	12.4 (4.9–17.2)	8.8 (5.2–27.7)	11.9 (4.9–17.5)	1.0 (-9.2–15.7)	0.843
IL-12p70	3.7 (1.6–5.4)	2.5 (1.2–11.5)	3.7 (1.4–5.9)	0.7 (-2.9–8.6)	0.676
IL-13	3.9 (1.6–5.2)	5.2 (0.5–7.3)	4 (0.9–5.6)	0.5 (-3.2–5.1)	0.531
IL-15	3.7 (2.3–5.5)	4.3 (1.2–5.7)	3.7 (2–5.6)	0.0 (-2.9–3.4)	0.954
IL-17A	4.1 (2–6.3)	4.3 (1–12.7)	4.2 (1.8–7.2)	1.4 (-3.4–11.1)	0.486
IL-1RA	31.8 (10.9–299.4)	244.5 (40.5–275)	45.1 (11.2–299.4)	36.3 (-160.1–260.1)	0.223
IL-1α	10.5 (3.1–35.9)	24 (7.5–30.5)	11.3 (3.1–34)	2.8 (-22.4–26.5)	0.618
IL-1β	4.4 (1.3–30.7)	4.3 (1–56.2)	4.3 (1.1–39.2)	0.1 (-17.6–55.2)	0.871
IL-2	1.9 (1.2–2.7)	2.3 (1–3.4)	1.9 (1.1–2.8)	0.3 (-1.2–2.1)	0.493
IL-3	1.1 (0–1.7)	0.3 (0–1.7)	1.1 (0–1.7)	0.0 (-1.3–0.6)	0.765
IL-4	9.9 (5.1–12.8)	9.1 (5.8–17.9)	9.6 (5.1–14.1)	0.9 (-6.3–10.4)	0.772
IL-5	1.1 (0.7–2)	2 (0.8–2.6)	1.2 (0.7–2.2)	0.2 (-1.0–1.7)	0.633
IL-6	324.6 (83.4–1976.6)	576.5 (29.3–2302.7)	370 (80.8–1989.7)	27.4 (-746.6–2298.1)	0.816
IL-7	11 (5.4–14.7)	9.5 (7.2–14)	11 (5.5–14.4)	0.2 (-6.8–8.7)	0.880
IL-8	8063.7 (2622.3–10888.1)	7996.7 (297.2–12641.4)	8030.2 (1907–10965)	-8.0 (-7038.2–7703.9)	0.991
IP-10	16 (6.7–28.4)	22.8 (17.2–80.2)	17.1 (6.9–29.7)	9.9 (-8.5–78.5)	0.117
MCP-1	540.7 (221.4–959.5)	709.8 (234.7–1052.2)	609.9 (221.4–979)	136.4 (-551.9–1033.2)	0.570
MIP-1α	16.3 (2.7–86.6)	15.6 (6.2–173.5)	15.9 (2.7–100.8)	4.3 (-22.0–168.4)	0.450
MIP-1β	9.9 (5.4–30.5)	14.9 (11.1–52.1)	11 (5.4–32.7)	7.8 (-8.6–49.4)	0.186
RANTES	324.4 (112.1–1048.7)	529.6 (85.9–884.3)	345.9 (96.8–1048.7)	28.9 (-629.8–668.2)	0.790
TNF-α	8.4 (3.2–21.1)	9.7 (4.1–29.8)	8.7 (3.2–25)	2.3 (-9.6–25.9)	0.423
TNF-β	1.8 (0.9–2.4)	2.5 (0.7–4.5)	1.8 (0.9–2.7)	0.6 (-1.2–2.7)	0.358
VEGF	82.2 (38.3–119.7)	107.1 (48.2–161.5)	82.2 (38.3–133.1)	16.8 (-63.4–102.2)	0.593

Table 42 Granulation tissue median cytokine concentrations. Median difference and 99% confidence intervals estimated using Hodges-Lehman method; hypotheses tested using Mann-Whitney U (significance level 0.01). IQR, interquartile range; CI, confidence interval.

	Median concentration (IQR), pg/ml			Median difference (99% CI), pg/ml	*p*
	Idiopathic	Crohn's disease	All		
EGF	34.8 (17.5–66.9)	28.7 (14.6–37.8)	29.5 (17.5–66.9)	-6.3 (-51.7–20.3)	0.499
Eotaxin	14.6 (6–20.3)	11 (7.8–19.3)	14.1 (6–20.3)	-1.7 (-11.8–7.4)	0.661
G-CSF	22402.3 (4777.9–22402.3)	22402.3 (22402.3–22402.3)	22402.3 (5081.8–22402.3)	0.0 (0.0–17624.4)	0.589
GM-CSF	69.3 (27.3–194.4)	128.5 (23.8–202.6)	80.6 (23.8–202.6)	7.2 (-150.4–158.0)	0.893
IFN-α2	28.2 (22–35.4)	22.1 (17.8–26.7)	25.8 (19.9–35.4)	-5.6 (-17.6–5.8)	0.142
IFN-γ	12.3 (6.1–18.4)	28.9 (17.1–171.9)	15.2 (7.1–27.3)	17.1 (-1.7–249.5)	0.021
IL-10	321.5 (139.6–599.9)	155.2 (52.3–512.7)	313.6 (138.7–599.9)	-87.3 (-502.6–448.7)	0.343
IL-12p40	24 (20–34.1)	21.7 (17.9–27.9)	24 (19.2–31.2)	-3.4 (-16.4–5.0)	0.248
IL-12p70	5.7 (4.4–9.6)	8.1 (5–8.5)	5.7 (4.7–9.6)	1.0 (-2.9–4.9)	0.457
IL-13	6 (4.9–7.6)	6 (4.7–7.3)	6 (4.7–7.4)	-0.4 (-3.8–1.8)	0.661
IL-15	8.8 (6.3–11.6)	7.9 (6.9–11.1)	8.8 (6.9–11.6)	-0.8 (-4.6–3.4)	0.686
IL-17A	13.3 (8–28.8)	18.4 (11.8–47.1)	15.1 (9.7–30.2)	4.2 (-12.1–34.1)	0.543
IL-1RA	741 (220.9–2233)	541.7 (429.1–597.8)	548.5 (246.7–1512.1)	-82.5 (-2372.1–387.9)	0.919
IL-1α	140.5 (46–549.6)	51 (30.4–141.1)	123.5 (35.6–488.2)	-64.5 (-543.7–63.8)	0.221
IL-1β	302.2 (73.2–977.2)	263.3 (62.9–748.7)	295.1 (70.5–955.5)	-52.1 (-872.3–460.7)	0.478
IL-2	2.8 (2–3.5)	2.5 (2–2.7)	2.7 (2–3.4)	-0.4 (-1.5–0.6)	0.208
IL-3	0 (0–1.2)	0.9 (0–1.2)	0.04 (0–1.2)	0.0 (-0.4–1.1)	0.636
IL-4	12.1 (10.1–15.9)	11.1 (9.1–13.4)	12 (9.8–15.9)	-1.4 (-6.0–3.1)	0.343
IL-5	2.5 (1.6–2.9)	2.3 (1.3–4.3)	2.3 (1.5–3)	-0.1 (-1.5–10.2)	0.813
IL-6	646.4 (325–1473.2)	1010.2 (523.4–4302.8)	708.7 (325–1954.8)	455.8 (-642.7–4122.4)	0.343
IL-7	13.4 (11.1–15.5)	10.3 (8.2–13.8)	13.1 (9.5–15.5)	-2.3 (-6.9–2.8)	0.234
IL-8	8281.7 (6444.4–9474.4)	7863.6 (4323.6–9001.2)	8206.2 (6247.9–9474.4)	-884.7 (-4689.6–2359.2)	0.436
IP-10	30.3 (19.8–36.9)	116 (40.5–163.4)	32 (19.9–48.4)	73.7 (-4.7–140.7)	0.026
MCP-1	744.1 (380–1485.4)	678.6 (349.8–954.1)	711.4 (356.2–1353.3)	-137.5 (-851.7–472.1)	0.499
MIP-1α	61.6 (36–134.2)	43.8 (25.5–60.7)	59.6 (33–123.2)	-23.5 (-112.7–16.8)	0.115
MIP-1β	34.6 (27.8–48.4)	32.5 (24–52.6)	33.5 (24–48.6)	-3.8 (-24.7–18.0)	0.840
RANTES	801.4 (431.1–1590.1)	814.5 (213.2–887.6)	808 (400.5–1358.4)	-214.0 (-1624.1–420.1)	0.293
TNF-α	28.3 (13.3–50.4)	16.5 (10.4–36.3)	26.4 (12.5–39.6)	-7.0 (-42.0–11.7)	0.457
TNF-β	3.2 (2.1–3.8)	2.8 (2.4–3.9)	3.1 (2.3–3.8)	0.0 (-1.5–1.3)	0.973
VEGF	124.4 (86.1–181.2)	104.5 (86.1–138.9)	121.4 (86.1–173.5)	-16.3 (-80.6–37.0)	0.417

Table 43 Internal opening median cytokine concentrations. Median difference and 99% confidence intervals estimated using Hodges-Lehman method; hypotheses tested using Mann-Whitney U (significance level 0.01). IQR, interquartile range; CI, confidence interval.

	Median concentration (IQR), pg/ml			Median difference (99% CI), pg/ml	*p*
	Idiopathic	Crohn's disease	All		
EGF	20.5 (15.5–29.1)	28.2 (19.5–35.6)	21 (16.7–30.6)	7.3 (-4.3–17.4)	0.086
Eotaxin	18 (13.5–22.3)	21.1 (19.9–29.1)	19.4 (14.6–23.2)	5.3 (-1.1–12.1)	0.043
G-CSF	7214.2 (702.2–22402.3)	22402.3 (3738.8–22402.3)	15547 (1011.9–22402.3)	0.0 (-140.1–20526.7)	0.215
GM-CSF	34.5 (19.5–123.6)	203.6 (50.6–861.7)	39.8 (23.2–220.3)	47.1 (-17.8–820.8)	0.046
IFN-α2	37.4 (23.5–54.7)	41.1 (34.5–67)	39.5 (25.9–56.2)	9.5 (-14.1–34.2)	0.190
IFN-γ	7.4 (4–10.9)	12.6 (8.6–26.5)	8.2 (4.3–13)	6.1 (-0.7–17.5)	0.022
IL-10	55.6 (21.6–176.3)	67.7 (62.9–191.1)	63.8 (28.1–183.7)	15.0 (-91.3–85.2)	0.531
IL-12p40	19.2 (9.5–31.2)	29.1 (22.5–43.7)	22.2 (10.6–32.8)	13.0 (-1.9–34.2)	0.026
IL-12p70	7.4 (4.6–12.7)	28.3 (7.4–50.1)	8 (5–15.3)	19.7 (0.2–40.4)	**0.008**
IL-13	8 (3.9–10.5)	7.5 (7.4–9.8)	7.8 (4.5–10.3)	1.0 (-2.9–4.9)	0.601
IL-15	5 (2.9–6.7)	7.8 (5.5–10.9)	5.6 (3.3–7)	3.1 (-0.1–5.9)	0.015
IL-17A	4.1 (2.4–7.4)	7.4 (5.1–10.7)	4.9 (2.8–7.9)	3.0 (-0.9–7.6)	0.037
IL-1RA	516.1 (89.4–883)	128.3 (63.5–423.8)	433.4 (78.2–860.5)	-167.2 (-698.0–185.6)	0.246
IL-1α	24.3 (7.3–46.5)	17.4 (10.1–40)	23.1 (7.5–46.4)	-0.8 (-31.7–27.2)	0.926
IL-1β	20.2 (8.3–88.5)	58.3 (10.7–180.9)	25.1 (8.7–96)	21.6 (-17.0–163.2)	0.171
IL-2	3.7 (2.1–4.9)	5.7 (4.4–9.2)	3.9 (2.4–5.3)	2.7 (-0.2–6.5)	0.013
IL-3	1.2 (0–1.7)	1.1 (0–3)	1.2 (0–1.7)	0.2 (-1.1–2.0)	0.527
IL-4	17.3 (12–25.8)	22.7 (19.1–27.7)	19.2 (12.3–26.3)	4.0 (-5.4–12.8)	0.241
IL-5	2.1 (1.3–3.7)	3.2 (1.7–3.9)	2.5 (1.4–3.9)	0.5 (-1.3–2.2)	0.390
IL-6	6362.3 (520.6–9061.3)	6181.2 (2616.5–8509.3)	6181.2 (585.9–9014.4)	270.0 (-3759.2–5723.9)	0.642
IL-7	18.5 (14–21.8)	21 (18.2–28)	18.9 (14.1–24)	3.5 (-3.5–10.8)	0.186
IL-8	10811.1 (7768.9–13415.3)	11902.6 (10892.9–13208.8)	11149.9 (8415.8–13403.7)	1441.2 (-2499.2–5565.9)	0.318
IP-10	26.6 (17–71.2)	33.4 (26.5–104.2)	27.6 (18.5–71.4)	7.9 (-33.7–34.0)	0.236
MCP-1	1296.8 (566–4265.5)	3390.3 (1300.9–6525.9)	1553.8 (599.4–4721.7)	1064.6 (-935.6–3978.4)	0.137
MIP-1α	66.6 (18.7–177.2)	93.9 (28.7–302.4)	66.6 (21.6–184.8)	13.1 (-88.6–160.8)	0.501
MIP-1β	23.4 (10–52.7)	36.8 (16.9–123)	23.4 (11.7–58.8)	9.5 (-22.2–90.9)	0.296
RANTES	169.3 (96.3–648)	233.8 (221.9–281.4)	222.7 (97.2–593.3)	50.0 (-426.2–184.3)	0.593
TNF-α	30.9 (20.7–46.1)	25 (15.1–57.3)	29.3 (19.5–46.8)	-2.0 (-21.6–30.3)	0.763
TNF-β	3.2 (1.8–4)	5.2 (3.6–5.7)	3.2 (1.9–4.3)	1.9 (-0.2–3.4)	0.022
VEGF	173.5 (118.3–333.6)	284.3 (149–380.7)	176.6 (130.7–358.7)	74.3 (-108.6–232.9)	0.307

Table 44 Rectal mucosa median cytokine concentrations. Median difference and 99% confidence intervals estimated using Hodges-Lehman method; hypotheses tested using Mann-Whitney U (significance level 0.01). IQR, interquartile range; CI, confidence interval.

	Median concentration (IQR), pg/ml			Median difference (99% CI), pg/ml	*p*
	Idiopathic	Crohn's disease	All		
EGF	22.7 (19.7–32.5)	20.8 (13–27.4)	22.6 (18.4–29.7)	-4.5 (-15.8–5.6)	0.204
Eotaxin	17.2 (13.7–25.4)	14.2 (10.5–19.3)	17 (13.4–24.3)	-4.2 (-14.4–4.3)	0.156
G-CSF	3139.5 (931.2–4321.6)	1605.1 (640.7–4377.7)	2941.2 (850.5–4327.8)	-184.6 (-2876.9–1611.1)	0.757
GM-CSF	31.2 (15.7–66.6)	30.2 (19.2–86.4)	30.8 (16.9–74.8)	6.7 (-35.6–80.4)	0.601
IFN-α2	49.7 (27.5–66)	39 (34.5–67.7)	45.6 (28.1–66.8)	-5.4 (-31.5–20.6)	0.601
IFN-γ	8.4 (6–14.4)	9 (5.3–28.8)	8.8 (6–15.9)	1.6 (-5.7–20.4)	0.651
IL-10	13.5 (7.8–30.5)	7.2 (5.4–12.3)	12.6 (6.5–27.1)	-5.7 (-23.4–4.0)	0.117
IL-12p40	37.2 (26.6–51.3)	28.7 (20.2–48)	36.9 (25.4–51.3)	-8.2 (-28.2–14.9)	0.315
IL-12p70	18.1 (12–24.4)	15.9 (13–20.8)	17.4 (12–24.4)	-1.5 (-12.4–9.8)	0.725
IL-13	6.9 (3.9–8.6)	4 (3.8–4.4)	5.5 (3.9–8.5)	-1.6 (-5.4–1.0)	0.111
IL-15	6.8 (5.2–9.2)	7.6 (5–9.7)	7 (5.1–9.5)	-0.1 (-3.8–3.6)	0.924
IL-17A	5.5 (3.9–8)	4 (2.8–6.4)	5.3 (3.5–7.7)	-1.0 (-4.1–2.7)	0.282
IL-1RA	72 (50.2–140.4)	84.9 (38.5–115.2)	75.5 (49–136.4)	-2.8 (-84.8–60.6)	0.943
IL-1α	11.4 (6.6–27.5)	13.7 (12.4–35.6)	12.4 (6.7–27.5)	3.5 (-8.6–23.2)	0.327
IL-1β	20.6 (9.6–51.5)	15.5 (9.7–35.7)	20.5 (9.6–44.2)	-3.5 (-35.2–19.2)	0.601
IL-2	8.4 (5.6–10.9)	5.8 (5.4–7)	7.5 (5.5–10.7)	-1.7 (-5.5–2.7)	0.250
IL-3	0 (0–1.5)	0 (0–1.5)	0.04 (0–1.5)	0.0 (-1.3–0.1)	0.924
IL-4	18.9 (12.5–24)	14.9 (13.4–20.7)	18.7 (12.6–23.4)	-3.6 (-13.9–4.7)	0.293
IL-5	2.7 (2–4.2)	1.9 (1.7–2.4)	2.6 (1.7–3.9)	-0.9 (-2.5–0.2)	0.026
IL-6	638.3 (176.5–2351.3)	427 (161.7–1314.6)	627.8 (172.5–2089.7)	-137.4 (-1469.0–1143.6)	0.536
IL-7	19.9 (14.8–27.4)	17.8 (14–21.5)	19.2 (14.8–26.2)	-3.3 (-12.2–4.6)	0.293
IL-8	6002.3 (3675.4–8800.5)	4415.4 (1344–8885.9)	5967.9 (3135.8–8843.2)	-1194.0 (-5482.3–3315.9)	0.431
IP-10	30.5 (17.3–42.4)	29 (19.1–106.3)	30.2 (18.2–46.2)	5.2 (-16.5–90.2)	0.601
MCP-1	1089.2 (556.9–1696.6)	741.4 (535.4–1250)	1017.3 (546.1–1693.4)	-241.7 (-1069.0–468.5)	0.377
MIP-1α	43 (17.5–142.3)	31.4 (3.6–40.3)	37.5 (16.2–118.2)	-19.6 (-104.0–22.1)	0.171
MIP-1β	26.9 (14.9–48.7)	17.9 (14.5–31.9)	26.7 (14.7–47.8)	-2.8 (-24.0–16.0)	0.617
RANTES	94.9 (61.5–130.7)	84.9 (45.3–101)	91 (61.1–127.3)	-22.5 (-88.3–28.4)	0.231
TNF-α	18.6 (12.3–28.4)	12.6 (11–16.5)	17.7 (11.6–27.8)	-4.7 (-16.8–5.7)	0.250
TNF-β	3.8 (2.6–5.9)	3.4 (2.5–4.4)	3.8 (2.6–5.5)	-0.4 (-2.5–1.4)	0.489
VEGF	225.8 (153–413.2)	159.4 (143.8–205.6)	220.5 (151–353.5)	-66.2 (-254.9–46.5)	0.129

Table 45 IL-1RA/IL-1 ratio. Median difference and 99% confidence intervals estimated using Hodges-Lehman method; hypotheses tested using Mann-Whitney U (significance level 0.01). IQR, interquartile range; CI, confidence interval.

	Median IL-1RA/IL-1 ratio (IQR)				Median difference (99% CI), pg/ml	*p*
	Healthy Controls	Idiopathic	Crohn's disease	All		
Fistula Tract		7.6 (2.7–16.3)	9.4 (4.9–25.8)	7.8 (2.7–16.8)	2.8 (-8.8–24.7)	0.437
Granulation Tissue		2.3 (1–4.8)	2.6 (0.7–7.2)	2.5 (1–6.1)	0.3 (-3.3–6.7)	0.787
Internal Opening		19.0 (4.3–51.2)	3.3 (1.8–7.6)	12.9 (3.3–38.6)	-15.0 (-50.5–-0.4)	**0.008**
Rectal Mucosa		3.6 (1.5–6.5)	3.7 (2.2–7)	3.6 (1.7–6.7)	0.1 (-3.6–3.5)	0.831
Rectal Mucosa	5.3 (2.2–5.9)		3.7 (2.2–7)		-1.1 (-4.6–13.9)	0.955

Table 46 Comparison with healthy controls. Rectal mucosa median cytokine concentrations. Median difference and 99% confidence intervals estimated using Hodges-Lehman method; hypotheses tested using Mann-Whitney U (significance level 0.01). IQR, interquartile range; CI, confidence interval.

	Median concentration (IQR), pg/ml		Median difference (99% CI), pg/ml	*p*
	Healthy Controls	Crohn's disease		
EGF	20.7 (18.9–22.5)	20.8 (13–27.4)	-0.6 (-14.9–9.7)	0.955
Eotaxin	20.9 (17.6–21.8)	14.2 (10.5–19.3)	-4.8 (-20.8–5.0)	0.145
G-CSF	2638.8 (2361.9–3843.8)	1605.1 (640.7–4377.7)	-388.9 (-3203.1–2748.5)	0.864
GM-CSF	32.1 (13.7–44)	30.2 (19.2–86.4)	12.6 (-27.9–1868.6)	0.607
IFN-α2	40.5 (36–50)	39 (34.5–67.7)	-1.0 (-33.5–38.4)	0.864
IFN-γ	11.6 (8.2–12)	9 (5.3–28.8)	0.6 (-9.6–120.4)	1.000
IL-10	17.5 (10.3–23.7)	7.2 (5.4–12.3)	-7.1 (-39.9–178.9)	0.181
IL-12p40	33.3 (28.7–36.8)	28.7 (20.2–48)	-3.7 (-28.6–35.0)	0.607
IL-12p70	16.2 (14.1–25.7)	15.9 (13–20.8)	-0.3 (-13.3–18.6)	0.955
IL-13	5.9 (3.6–8.1)	4 (3.8–4.4)	-1.2 (-7.1–3.6)	0.456
IL-15	5.9 (5.5–7.6)	7.6 (5–9.7)	0.5 (-4.1–5.4)	0.864
IL-17A	4.1 (3.3–4.5)	4 (2.8–6.4)	0.5 (-2.3–31.7)	0.776
IL-1RA	79.6 (68.8–156.2)	84.9 (38.5–115.2)	-27.6 (-583.6–93.0)	0.776
IL-1α	10.8 (8.2–20.2)	13.7 (12.4–35.6)	5.2 (-13.9–35.4)	0.388
IL-1β	22.7 (11.9–74.7)	15.5 (9.7–35.7)	-5.2 (-107.2–31.0)	0.456
IL-2	6.6 (5.7–7.1)	5.8 (5.4–7)	-0.2 (-4.0–8.7)	0.776
IL-3	0.32 (0.3–0.3)	0.04 (0–1.5)	-0.3 (-0.3–1.2)	0.328
IL-4	22.2 (17.2–27.4)	14.9 (13.4–20.7)	-6.4 (-19.4–4.5)	0.066
IL-5	2.8 (1.9–5.5)	1.9 (1.7–2.4)	-0.8 (-4.2–0.6)	0.066
IL-6	580.6 (496.9–1689.3)	427 (161.7–1314.6)	-153.7 (-1591.0–6498.5)	0.776
IL-7	21.1 (16.5–22)	17.8 (14–21.5)	-3.0 (-15.2–6.7)	0.456
IL-8	6442.8 (5055.5–13929.7)	4415.4 (1344–8885.9)	-3420.9 (-12587.9–5579.4)	0.272
IP-10	23.9 (21.4–27.7)	29 (19.1–106.3)	5.0 (-13.5–498.9)	0.607
MCP-1	1642.1 (650.4–2045.4)	741.4 (535.4–1250)	-646.4 (-3452.8–716.3)	0.272
MIP-1α	58.2 (25.5–80.5)	31.4 (3.6–40.3)	-22.9 (-79.1–103.7)	0.456
MIP-1β	22.5 (21.2–38.2)	17.9 (14.5–31.9)	-4.6 (-23.7–48.6)	0.607
RANTES	49 (38.1–60.3)	84.9 (45.3–101)	26.0 (-29.0–100.6)	0.224
TNF-α	20.2 (13.9–35.6)	12.6 (11–16.5)	-6.1 (-32.3–21.8)	0.145
TNF-β	3.8 (2.7–5.4)	3.4 (2.5–4.4)	-0.2 (-2.9–2.6)	0.689
VEGF	230.7 (168.6–251)	159.4 (143.8–205.6)	-54.9 (-438.7–177.4)	0.328

Phosphoproteins

Table 47 Control spots. Median (IQR) pixel intensities of the negative and positive control spots.

	Fistula Tract	Granulation Tissue	Internal Opening	Rectal Mucosa
Negative control spots	19 (12.8–28.1)	19 (10.4–30.3)	16.2 (9.9–28.9)	17.4 (11.4–30.1)
Positive control spots	100 (100-100)	100 (100-100)	100 (100-100)	100 (100-100)

Table 48 Fistula tract median phosphoprotein pixel intensities. Median difference and 99% confidence intervals estimated using Hodges-Lehman method; hypotheses tested using Mann-Whitney U (significance level 0.01). IQR, interquartile range; CI, confidence interval.

	Median pixel intensity (IQR), %			Median difference (99% CI), %	*p*
	Idiopathic	Crohn's disease	All		
EGFR/ErbB1	26.7 (15.6–42.3)	41.1 (27.4–48.5)	28.6 (16.2–45.1)	12.1 (-4.4–28.8)	0.057
HER2/ErbB2	18.1 (9–28.1)	26.6 (15–41.7)	19.3 (12.2–33.2)	7.0 (-8.1–24.1)	0.216
HER3/ErbB3	37.4 (19.1–48.6)	49.4 (34.5–59.9)	39.1 (22.6–51.4)	15.1 (-1.4–33.9)	0.021
FGFR1	24.1 (13.2–37.3)	29.7 (21.7–41.6)	25.5 (14.9–37.3)	5.6 (-8.4–19.4)	0.266
FGFR3	21.8 (14.4–35.1)	22.6 (21.5–33.2)	22.4 (15.8–33.7)	3.5 (-9.2–14.5)	0.291
FGFR4	27.4 (17.3–47.9)	30.1 (21.2–48.7)	28.1 (17.4–47.9)	4.2 (-13.4–22.2)	0.466
InsR	10.4 (4.2–19.4)	16.3 (10.1–20.7)	11.9 (6.4–19.4)	4.8 (-4.2–12.8)	0.144
IGF-IR	7.3 (2.5–17.3)	10.5 (4.1–17.6)	7.4 (3–17.3)	2.8 (-5.0–10.7)	0.332
TrkA/NTRK1	8.2 (0.9–16.8)	6.7 (1.9–18.7)	7.8 (1.7–17.7)	0.4 (-7.7–9.5)	0.855
TrkB/NTRK2	10 (3–21.8)	6.5 (4.8–23.8)	9.6 (3.2–23.2)	-0.2 (-9.2–7.5)	0.878
Met/HGFR	1.4 (0–5.8)	1.3 (0–3.8)	1.4 (0–5.6)	0.0 (-3.2–2.6)	0.564
Ron/MST1R	4.3 (0.2–11)	2.3 (0.7–7.3)	3.8 (0.2–11)	-0.1 (-6.4–4.3)	0.802
Ret	1.6 (0–6)	0.1 (0–1.1)	1.1 (0–5.5)	-0.8 (-4.6–0.1)	0.104
ALK	1 (0–6.1)	0.1 (0–3.1)	0.5 (0–5.3)	0.0 (-4.2–0.1)	0.392
PDGFR	5.3 (0.3–12.9)	2.4 (0.1–15.7)	4.5 (0.1–13.4)	0.0 (-6.4–6.6)	0.855
c-Kit/SCFR	10.7 (3.8–19.2)	15.1 (8.1–23.8)	11.1 (4.7–20.9)	4.9 (-4.4–14.9)	0.111
FLT3/Flk2	3.8 (0.4–8.7)	4 (1.7–6.9)	3.8 (0.7–7.1)	0.2 (-5.0–4.4)	0.795
M-CSFR/CSF-1R	6.4 (0.9–13.4)	5.8 (1.2–12.8)	5.9 (1.1–13.4)	0.1 (-7.1–6.3)	0.833
EphA1	1.5 (0–11.8)	1.2 (0.4–8)	1.3 (0–10.9)	0.0 (-6.2–2.2)	0.992
EphA2	3.3 (0.4–15.6)	4.1 (1.6–12.9)	3.5 (0.4–15.6)	0.0 (-8.4–5.7)	0.810
EphA3	3.8 (0.4–12.4)	3.1 (0.5–11.5)	3.4 (0.4–12.4)	0.0 (-6.7–4.9)	0.962
EphB1	2.8 (0.1–8.9)	1.2 (0.1–7.1)	2.2 (0.1–8.7)	-0.1 (-6.2–4.2)	0.700
EphB3	0.2 (0–3.7)	0 (0–1.5)	0.1 (0–2.8)	0.0 (-1.9–0.2)	0.303
EphB4	2.3 (0–8.2)	2.5 (0–11.5)	2.3 (0–9)	0.0 (-3.2–6.7)	0.582
Tyro3/Dtk	0 (0–3.3)	0.1 (0–3)	0.015 (0–3.2)	0.0 (-1.1–2.1)	0.647
Axl	0.3 (0–4.3)	1.4 (0–3.9)	0.4 (0–4.1)	0.0 (-1.2–2.6)	0.843
Tie2/TEK	9.2 (3.8–17.8)	13.1 (7.1–28.1)	9.6 (4.2–21.6)	5.0 (-4.7–16.9)	0.144
VEGFR2/KDR	0.7 (0–7.3)	0.9 (0–6.7)	0.7 (0–7.3)	0.0 (-3.8–4.4)	0.852
Akt/PKB/Rac @Thr308	9.2 (1.2–18.3)	12.8 (0.1–28.9)	9.2 (0.5–22.9)	0.1 (-11.4–22.0)	0.863
Akt/PKB/Rac @Ser473	0.6 (0–6.2)	1.2 (0–10.4)	0.8 (0–9.1)	0.0 (-2.1–8.3)	0.832
p44/42 MAPK (ERK1/2)	4.6 (0.5–21.6)	3.6 (0–11.5)	4.6 (0.3–21.3)	-0.7 (-15.4–4.9)	0.386
S6 Ribosomal Protein	1.3 (0–9.6)	0.2 (0–11.5)	1 (0–9.6)	0.0 (-4.5–4.6)	0.742
c-Abl	0.2 (0–8)	0 (0–6.8)	0.2 (0–8)	0.0 (-4.0–1.8)	0.428
IRS-1	13.1 (3.5–29.9)	13.3 (3.1–43.7)	13.1 (3.5–30.8)	0.8 (-12.3–26.7)	0.722
Zap-70	9.1 (1.1–15.4)	9.1 (0.1–20.6)	9.1 (1.1–15.7)	0.1 (-8.8–12.1)	0.773
Src	17.4 (5.2–24.8)	13.9 (2.2–29.5)	16.6 (4.6–24.8)	0.1 (-12.5–14.3)	0.946
Lck	4.7 (0.1–13.5)	4.2 (0–20.2)	4.7 (0.1–13.5)	0.0 (-5.9–12.9)	0.893
Stat1	16.6 (7.8–36.9)	37 (12.3–51.6)	19.7 (7.8–37.4)	13.1 (-8.5–32.6)	0.134
Stat3	48.7 (31.8–71.1)	57.7 (44.2–72.3)	50.4 (34.1–71.1)	6.7 (-16.9–29.2)	0.431

Table 49 Granulation tissue median phosphoprotein pixel intensities. Median difference and 99% confidence intervals estimated using Hodges-Lehman method; hypotheses tested using Mann-Whitney U (significance level 0.01). IQR, interquartile range; CI, confidence interval.

	Median pixel intensity (IQR), %			Median difference (99% CI), %	*p*
	Idiopathic	Crohn's disease	All		
EGFR/ErbB1	26 (18.2–38.6)	37.3 (23.6–46.9)	28 (18.2–42.2)	7.0 (-9.0–22.8)	0.283
HER2/ErbB2	17.1 (14.3–29.6)	24.2 (12.2–31.4)	17.6 (14–30.7)	1.8 (-9.5–14.8)	0.650
HER3/ErbB3	37.5 (24–49.3)	41 (30.8–63)	38.9 (25.3–51.2)	7.7 (-10.8–25.4)	0.248
FGFR1	23.1 (12.6–34.3)	22.5 (17.2–35.8)	22.8 (14.3–35)	1.7 (-13.9–13.9)	0.810
FGFR3	33.8 (15.8–45.2)	26.6 (18.1–52.8)	32.4 (16.6–46.3)	4.8 (-16.5–25.1)	0.437
FGFR4	23 (16.3–46.3)	28.6 (20.3–38.5)	23.6 (17.5–45.7)	4.3 (-12.9–17.7)	0.334
InsR	9.3 (5.8–15.8)	19.4 (10.1–23.3)	11.7 (6.6–19.8)	5.3 (-3.9–13.7)	0.099
IGF-IR	7 (3.1–16.2)	13.1 (4.3–18.3)	10.7 (3.3–17.2)	3.5 (-5.5–13.0)	0.248
TrkA/NTRK1	5.6 (1.5–18.3)	10.4 (6.3–11.7)	8.5 (1.8–17.1)	1.6 (-10.0–8.9)	0.769
TrkB/NTRK2	6.9 (1.4–19)	7.2 (1.7–13.4)	7 (1.5–17.2)	-0.5 (-11.8–7.0)	0.852
Met/HGFR	0.8 (0–5.4)	2.2 (0–4.6)	1.3 (0–4.8)	0.0 (-3.0–3.8)	0.769
Ron/MST1R	2.9 (0.1–11.3)	8.2 (0–13.7)	4 (0.1–11.9)	1.6 (-4.4–8.6)	0.538
Ret	1 (0–6.8)	2.9 (0–6.2)	2.2 (0–6.5)	0.2 (-3.1–4.0)	0.689
ALK	0.1 (0–4.8)	0.2 (0–0.9)	0.2 (0–3.7)	0.0 (-3.2–0.6)	0.831
PDGFR	1.7 (0.4–12.7)	6.2 (2–10.4)	4.3 (0.4–11.3)	1.1 (-6.2–6.2)	0.574
c-Kit/SCFR	8.9 (5.1–20.7)	14.8 (9.5–21.7)	10.1 (5.8–20.9)	4.1 (-7.5–13.7)	0.216
FLT3/Flk2	3.3 (0.2–10.3)	6.3 (1.9–12.2)	3.5 (0.2–10.9)	1.5 (-4.6–6.4)	0.487
M-CSFR/CSF-1R	5 (0.7–14.4)	7.8 (0.2–14.7)	6.4 (0.6–14.6)	0.2 (-7.4–8.6)	0.689
EphA1	2 (0.1–11.8)	5.1 (0–6.8)	2.1 (0.1–10.9)	-0.1 (-7.9–5.1)	0.574
EphA2	4 (1–13.5)	4 (0.7–9)	4 (0.9–13.3)	-0.3 (-11.3–4.5)	0.630
EphA3	3.5 (0.4–9.9)	6 (0.4–9)	4.3 (0.4–9.4)	0.0 (-7.1–6.0)	0.979
EphB1	4.2 (0.2–9.4)	3.6 (0.4–10.4)	3.9 (0.3–9.9)	0.0 (-6.3–6.2)	0.915
EphB3	0.2 (0–4.6)	0.6 (0–5.5)	0.2 (0–5)	0.0 (-1.6–2.5)	0.979
EphB4	1.5 (0–10.6)	0 (0–3.9)	0.9 (0–8.4)	-0.9 (-10.0–0.1)	0.138
Tyro3/Dtk	0.7 (0–3.6)	0 (0–2.5)	0.3 (0–3.1)	0.0 (-2.5–1.4)	0.391
Axl	0.9 (0–4.8)	0 (0–3.4)	0.8 (0–4.2)	0.0 (-3.8–2.0)	0.422
Tie2/TEK	13.5 (3–22.3)	10.6 (3.9–14.6)	12.4 (3.5–20.6)	-2.1 (-14.1–8.2)	0.538
VEGFR2/KDR	3.6 (0–9.5)	2.1 (0–7.1)	3.6 (0–7.4)	-0.1 (-6.3–3.5)	0.437
Akt/PKB/Rac @Thr308	8.4 (0.5–19.8)	5.8 (0.1–16.3)	8.3 (0.1–19.3)	-1.6 (-14.0–9.4)	0.630
Akt/PKB/Rac @Ser473	0.7 (0–8.7)	0 (0–4.5)	0.5 (0–8.1)	0.0 (-6.9–0.6)	0.283
p44/42 MAPK (ERK1/2)	0.4 (0–9.7)	0 (0–3.9)	0.3 (0–8.9)	0.0 (-7.5–2.1)	0.334
S6 Ribosomal Protein	2.6 (0.1–8.3)	0.2 (0–6.7)	2.5 (0–8)	-0.1 (-7.2–2.6)	0.348
c-Abl	0.9 (0–7.4)	0.1 (0–4.9)	0.8 (0–7.4)	-0.2 (-7.2–2.9)	0.308
IRS-1	20.9 (4–28)	16.4 (5.8–22.4)	18.3 (4.7–27.1)	-3.9 (-18.4–11.3)	0.391
Zap-70	13 (1.5–19.2)	7 (0–14.2)	10.2 (1.1–17)	-2.6 (-13.9–6.6)	0.295
Src	18.2 (4.9–27.2)	10.1 (0–20.2)	17.6 (3.1–23.4)	-3.8 (-16.9–7.8)	0.283
Lck	9.3 (0.7–15.3)	4.5 (0–15.3)	6.4 (0.5–15.3)	-0.7 (-11.6–5.9)	0.574
Stat1	27.8 (6.1–37.2)	40.6 (16.3–63.5)	28.6 (10.2–40.5)	12.5 (-10.4–41.5)	0.153
Stat3	62.7 (42–75.6)	64.7 (41.1–83)	63.7 (41.6–76.5)	-0.1 (-24.8–24.6)	1.000

Table 50 Internal opening median phosphoprotein pixel intensities. Median difference and 99% confidence intervals estimated using Hodges-Lehman method; hypotheses tested using Mann-Whitney U (significance level 0.01). IQR, interquartile range; CI, confidence interval.

	Median pixel intensity (IQR), %			Median difference (99% CI), %	*p*
	Idiopathic	Crohn's disease	All		
EGFR/ErbB1	35 (22.1–50.8)	43.8 (27–46.5)	37.1 (22.5–49.8)	4.7 (-13.8–22.0)	0.584
HER2/ErbB2	23.4 (12.7–37.3)	22.4 (19.3–33.1)	23.3 (13.7–34.6)	-0.1 (-13.4–13.4)	0.984
HER3/ErbB3	50.7 (32–64.5)	47.2 (38.1–56.5)	47.8 (32.8–61.7)	-0.7 (-17.2–21.6)	0.876
FGFR1	28.6 (19.7–43.8)	36.3 (15.3–44.7)	31.5 (18.3–43.8)	1.5 (-15.5–20.1)	0.830
FGFR3	43.5 (22.7–64.6)	36.3 (23.9–59.3)	41 (23.4–60)	-1.0 (-23.9–20.1)	0.860
FGFR4	33.2 (18.6–53)	33.2 (22.5–41.5)	33.2 (20.9–51)	0.0 (-18.2–17.5)	1.000
InsR	17.8 (8.4–31.8)	20.2 (11.9–25.4)	18.3 (10.3–27.6)	0.4 (-13.6–12.2)	0.876
IGF-IR	13.6 (5.3–27.7)	16.1 (10.3–20.7)	14 (7.8–26.8)	0.5 (-13.6–11.2)	0.891
TrkA/NTRK1	12.6 (4.3–25.6)	12.2 (3.2–16.7)	12.2 (4.3–23.2)	-2.5 (-15.2–9.1)	0.544
TrkB/NTRK2	12.7 (3.7–26.7)	9.1 (4.1–17.7)	12.1 (3.7–24.2)	-2.7 (-15.4–6.7)	0.481
Met/HGFR	0.8 (0–7)	0 (0–5.9)	0.6 (0–7)	0.0 (-4.8–0.7)	0.347
Ron/MST1R	5.7 (0.4–17.2)	3.7 (0.4–10.2)	5.1 (0.4–16.1)	-1.0 (-11.8–4.2)	0.563
Ret	1.5 (0–10.1)	0.4 (0–6.7)	0.8 (0–9.4)	0.0 (-7.8–0.8)	0.545
ALK	0.1 (0–3.4)	0 (0–4.8)	0.1 (0–3.4)	0.0 (-2.2–0.4)	0.425
PDGFR	4.5 (0–14.9)	1.2 (0–8.5)	3.3 (0–12.6)	-0.8 (-9.4–2.5)	0.352
c-Kit/SCFR	14 (4.4–27.1)	9.3 (6.2–18.5)	12.7 (5.3–26.6)	-1.6 (-17.2–7.7)	0.799
FLT3/Flk2	4.8 (0.4–16.4)	2.2 (0–9.7)	3.9 (0.2–15.8)	-1.6 (-12.9–2.2)	0.188
M-CSFR/CSF-1R	11.3 (2.7–20.8)	6.7 (2.5–12.1)	8.3 (2.7–19.4)	-2.7 (-14.7–4.9)	0.434
EphA1	3.3 (0.1–11.9)	0.3 (0–3.8)	1.4 (0.1–10.1)	-1.0 (-9.4–0.2)	0.120
EphA2	5 (0.4–16.1)	0.8 (0.2–7.3)	4 (0.4–15.5)	-2.7 (-15.1–0.7)	0.139
EphA3	11.1 (0.8–18.9)	3 (0–7.9)	7.7 (0.4–15.9)	-5.8 (-14.9–0.2)	0.031
EphB1	3.2 (0.2–15.1)	1.1 (0–5.1)	2 (0.1–12.7)	-1.1 (-12.1–0.8)	0.163
EphB3	0.1 (0–8.4)	0 (0–1.3)	0.01 (0–5.7)	0.0 (-4.0–0.0)	0.113
EphB4	6.9 (0.4–15.9)	0.1 (0–1.9)	3.8 (0–14.4)	-4.9 (-15.1–0.0)	0.018
Tyro3/Dtk	0.9 (0–6.6)	0 (0–0.8)	0.1 (0–5.2)	-0.7 (-6.3–0.0)	0.082
Axl	1.3 (0–8.1)	0 (0–2.2)	0.8 (0–5.9)	-0.5 (-5.9–0.0)	0.054
Tie2/TEK	22.8 (13.9–32)	17.1 (9.4–23.1)	20.6 (13.4–28)	-6.2 (-19.4–4.0)	0.108
VEGFR2/KDR	8.2 (0–16.5)	0.9 (0–3.9)	5.2 (0–14.7)	-6.1 (-14.9–0.4)	0.059
Akt/PKB/Rac @Thr308	37.4 (14.6–48.2)	11.9 (1.6–37.8)	31.9 (10.7–44.1)	-14.5 (-36.5–4.7)	0.088
Akt/PKB/Rac @Ser473	4.2 (0.1–16.1)	0 (0–9.1)	3.1 (0–12.7)	-1.4 (-11.4–0.0)	0.044
p44/42 MAPK (ERK1/2)	12.2 (5–31.1)	3.9 (0.1–21.3)	10.1 (3.8–31.1)	-5.0 (-22.4–4.3)	0.108
S6 Ribosomal Protein	14.5 (2.3–33)	1 (0–6.7)	11.8 (0.6–29.6)	-11.4 (-29.6–0.0)	0.014
c-Abl	5.6 (0–18.8)	0 (0–4.7)	3.7 (0–18)	-3.1 (-17.3–0.0)	0.028
IRS-1	26.1 (10.3–43.6)	7.3 (1–29)	23.3 (7.9–41.2)	-13.3 (-33.2–2.2)	0.055
Zap-70	11.5 (1.7–22.9)	0.1 (0–17.1)	10.3 (0.2–21.4)	-8.4 (-19.5–0.0)	0.026
Src	35.1 (19.6–44.9)	7.5 (0.4–25.7)	31.4 (5.9–43.4)	-19.2 (-36.3–1.3)	0.031
Lck	10.9 (2.1–27.6)	0.8 (0–13.6)	10.4 (0.1–19.5)	-6.7 (-16.8–0.9)	0.062
Stat1	49.3 (28.3–64.5)	33.9 (22.2–44.6)	43.7 (22.6–58.6)	-11.3 (-32.7–14.1)	0.225
Stat3	74 (51–87.7)	59.8 (39.5–70.2)	68.8 (47.8–87.1)	-15.1 (-33.2–10.8)	0.108

Table 51 Rectal mucosa median phosphoprotein pixel intensities. Median difference and 99% confidence intervals estimated using Hodges-Lehman method; hypotheses tested using Mann-Whitney U (significance level 0.01). IQR, interquartile range; CI, confidence interval.

	Median pixel intensity (IQR), %			Median difference (99% CI), %	*p*
	Idiopathic	Crohn's disease	All		
EGFR/ErbB1	48.2 (21.3–62.4)	45.4 (33.1–59.6)	48.2 (24.3–62.4)	1.6 (-18.2–25.4)	0.821
HER2/ErbB2	37.3 (22.7–61.3)	36.3 (27.7–56.2)	37.3 (24.3–60.3)	1.4 (-20.7–24.2)	0.792
HER3/ErbB3	63.2 (40.1–80.5)	75 (61.5–78.1)	64.9 (42.1–79)	9.7 (-10.2–32.5)	0.300
FGFR1	40.9 (28.3–58.7)	43.7 (32.6–55.5)	41.5 (28.4–58.7)	3.1 (-15.7–20.8)	0.638
FGFR3	60.1 (35.4–70.9)	68.4 (51.1–73.1)	60.2 (40.6–70.9)	8.4 (-10.6–30.9)	0.187
FGFR4	42.7 (23.7–67.9)	46.4 (36.8–55.7)	44.8 (27.1–67.1)	4.8 (-19.8–24.7)	0.611
InsR	35.9 (18.2–50.4)	42.6 (35–48.4)	38.6 (18.8–50)	7.8 (-10.5–27.8)	0.283
IGF-IR	29 (14.6–44.6)	42.1 (32.5–49.6)	31.7 (16.1–47.7)	12.3 (-5.0–30.3)	0.077
TrkA/NTRK1	22.6 (13–40.8)	28.9 (21.3–41.1)	27.2 (13.6–40.8)	4.2 (-13.1–19.8)	0.498
TrkB/NTRK2	17 (7.7–38.6)	17.9 (8.5–25.9)	17.1 (7.7–34.4)	0.0 (-17.9–12.8)	1.000
Met/HGFR	7.7 (0–22.7)	8.2 (0.1–16.4)	7.7 (0–22.5)	0.0 (-11.4–10.6)	0.902
Ron/MST1R	15.2 (4.4–32.3)	21.7 (7.7–32)	16.6 (4.6–32.1)	3.1 (-11.7–18.9)	0.572
Ret	0.5 (0–8.1)	1.9 (0–15.3)	0.5 (0–9.3)	0.0 (-1.5–11.1)	0.531
ALK	0.5 (0–8.4)	0.1 (0–2.6)	0.3 (0–7.1)	0.0 (-5.5–0.2)	0.464
PDGFR	5.5 (0–21.5)	6.8 (2.8–14.2)	5.5 (0–20.2)	0.0 (-10.9–7.6)	1.000
c-Kit/SCFR	30.6 (18.2–43.1)	33.8 (20.8–40.5)	30.6 (18.2–42.9)	3.1 (-12.9–18.4)	0.658
FLT3/Flk2	6.9 (0.3–15.5)	4.8 (0.7–16.9)	5.7 (0.3–16.8)	0.0 (-8.0–8.3)	0.917
M-CSFR/CSF-1R	20.6 (5.3–29.4)	15.9 (9.3–38.1)	19.5 (6.3–29.7)	2.3 (-14.0–16.0)	0.735
EphA1	13.7 (0.3–27.1)	10.3 (0–19.5)	12.8 (0.3–26.4)	-1.4 (-17.2–8.6)	0.258
EphA2	10 (0.2–28.9)	7.6 (0–19.8)	7.8 (0.1–24.3)	-0.9 (-16.9–7.7)	0.376
EphA3	10.3 (0.4–28.9)	9.6 (0.4–21)	10.2 (0.4–28.5)	-1.0 (-17.3–9.1)	0.558
EphB1	7.9 (0.6–23.6)	5.9 (0–24.7)	7.1 (0.4–23.6)	0.0 (-11.7–12.4)	0.748
EphB3	0.1 (0–6.2)	0 (0–16.1)	0.1 (0–6.8)	0.0 (-1.5–10.6)	0.937
EphB4	23.2 (6.2–41.3)	17.1 (0.2–31.4)	21.8 (5.5–36.6)	-4.3 (-23.4–14.5)	0.451
Tyro3/Dtk	9.4 (0.2–19.8)	3.7 (0–15.5)	8.9 (0.1–17.7)	-0.4 (-14.2–6.9)	0.422
Axl	10.9 (0.6–18.6)	6.1 (0–18.1)	9.5 (0.6–18.6)	-0.6 (-12.5–9.0)	0.497
Tie2/TEK	41.6 (24.9–57.9)	38.4 (13–54.4)	41.6 (23.1–57.9)	-6.0 (-29.3–17.0)	0.492
VEGFR2/KDR	14.1 (6.5–28.4)	15.5 (0.3–33.6)	14.1 (6.3–28.6)	-0.1 (-14.1–18.9)	0.828
Akt/PKB/Rac @Thr308	41.4 (22.8–58)	34.1 (7.8–53.5)	39.2 (22.3–57.1)	-5.6 (-30.6–18.2)	0.498
Akt/PKB/Rac @Ser473	11.5 (0.6–23.3)	7.2 (0–14.9)	8.5 (0.1–22.9)	-1.0 (-15.9–7.6)	0.363
p44/42 MAPK (ERK1/2)	23.9 (8.7–39.9)	10.7 (0–54.8)	19.8 (6.5–42.6)	-5.9 (-26.7–23.0)	0.309
S6 Ribosomal Protein	24.9 (10–50.5)	23.1 (9–57.7)	24.9 (10–52.9)	0.0 (-22.0–29.0)	1.000
c-Abl	9.5 (1.4–21.4)	5.3 (0–23.5)	9 (0.4–21.4)	-0.2 (-14.0–9.8)	0.591
IRS-1	40.9 (24.5–62.6)	25 (9.1–41.3)	35.6 (16.7–61.9)	-10.7 (-35.5–16.1)	0.207
Zap-70	18.7 (3.5–28.1)	6.8 (0.9–18.7)	12.2 (1.7–26.4)	-3.9 (-19.6–7.3)	0.336
Src	35.7 (15.9–49.6)	23.3 (5.7–38.8)	33.1 (11.1–47.6)	-8.0 (-30.6–14.0)	0.258
Lck	14.4 (0.8–24.2)	5.6 (0.6–17.6)	13.3 (0.8–24.1)	-1.7 (-15.7–9.4)	0.502
Stat1	40.8 (22.8–57)	35.8 (18.7–49.9)	39.7 (20–56.8)	-3.1 (-24.1–22.8)	0.742
Stat3	62.4 (37.1–76.3)	53.6 (36.1–68.3)	59.4 (37.1–75.8)	-4.6 (-26.5–19.7)	0.598

Table 52 Comparison with healthy controls. Rectal mucosa median phosphoprotein pixel intensities. Median difference and 99% confidence intervals estimated using Hodges-Lehman method; hypotheses tested using Mann-Whitney U (significance level 0.01). IQR, interquartile range; CI, confidence interval.

	Median pixel intensity (IQR), %			Median difference (99% CI), %	*p*
	Healthy Controls	Crohn's disease	All		
EGFR/ErbB1	30.5 (27.3–40.6)	45.4 (33.1–59.6)	39.8 (28.3–48.4)	13.3 (-15.2–44.4)	0.213
HER2/ErbB2	59.2 (55.7–64.5)	36.3 (27.7–56.2)	51.9 (33.2–60.8)	-19.2 (-40.0–15.3)	0.125
HER3/ErbB3	81 (79.3–84.4)	75 (61.5–78.1)	77.2 (62.9–81.4)	-6.3 (-29.8–16.6)	0.180
FGFR1	56.8 (47.6–60.7)	43.7 (32.6–55.5)	48.3 (32.6–60.7)	-10.0 (-33.5–18.9)	0.291
FGFR3	71 (59–76.4)	68.4 (51.1–73.1)	69 (52.5–75.5)	-3.4 (-27.5–27.1)	0.682
FGFR4	51.6 (46.6–58.9)	46.4 (36.8–55.7)	49.3 (37.7–56.7)	-4.5 (-26.4–27.1)	0.616
InsR	67.7 (65.5–76.4)	42.6 (35–48.4)	47.1 (38.4–67.6)	-26.3 (-45.0–8.1)	0.032
IGF-IR	58 (48.5–61.9)	42.1 (32.5–49.6)	47.7 (34.7–59.4)	-13.8 (-39.9–19.5)	0.180
TrkA/NTRK1	62.6 (54.4–69.2)	28.9 (21.3–41.1)	35.2 (23–60.1)	-31.3 (-48.0–8.2)	0.013
TrkB/NTRK2	41.2 (34.1–52.6)	17.9 (8.5–25.9)	22.1 (15.8–38)	-22.0 (-40.4–5.2)	0.018
Met/HGFR	16.7 (14.6–23.1)	8.2 (0.1–16.4)	12.6 (1.7–20.2)	-8.3 (-22.9–7.4)	0.125
Ron/MST1R	34.2 (30.2–39.2)	21.7 (7.7–32)	29.1 (11.4–36.6)	-10.5 (-31.7–16.4)	0.102
Ret	9.7 (8.9–13.6)	1.9 (0–15.3)	8.3 (0–14.4)	-5.1 (-13.6–12.2)	0.250
ALK	3.3 (2.3–4)	0.1 (0–2.6)	1.3 (0–3.4)	-2.3 (-4.0–1.1)	0.041
PDGFR	17.5 (14.9–19.3)	6.8 (2.8–14.2)	10.5 (4.8–18.8)	-9.3 (-17.1–6.3)	0.083
c-Kit/SCFR	55.5 (51.4–61.4)	33.8 (20.8–40.5)	37.3 (29.1–54.5)	-20.7 (-40.7–8.2)	0.032
FLT3/Flk2	12.8 (9–14.8)	4.8 (0.7–16.9)	10 (2.7–16.8)	-6.3 (-13.9–8.8)	0.385
M-CSFR/CSF-1R	39.1 (27.9–41.9)	15.9 (9.3–38.1)	23.9 (11.9–41)	-17.5 (-35.0–20.1)	0.102
EphA1	42.2 (38.9–48.9)	10.3 (0–19.5)	17.4 (8.6–38.9)	-30.3 (-48.9–-8.6)	**0.001**
EphA2	27.1 (26.9–29.9)	7.6 (0–19.8)	14.5 (7.4–27)	-19.2 (-28.5–-0.2)	**0.007**
EphA3	32.7 (29.8–33.8)	9.6 (0.4–21)	17.6 (7–32.4)	-20.1 (-33.7–1.3)	0.010
EphB1	46.9 (36.2–50.7)	5.9 (0–24.7)	24.7 (3–46)	-34.7 (-50.7–-8.1)	**<0.001**
EphB3	22.7 (14.5–32.8)	0 (0–16.1)	13.9 (0–21)	-16.6 (-32.8–2.5)	0.018
EphB4	68.3 (57.6–73.9)	17.1 (0.2–31.4)	29.2 (15.4–60.6)	-46.1 (-69.6–-9.0)	**0.001**
Tyro3/Dtk	35.8 (33.1–38.4)	3.7 (0–15.5)	15.5 (0.2–34.1)	-29.2 (-38.4–-2.3)	**0.002**
Axl	36.1 (28–39.1)	6.1 (0–18.1)	16.8 (1.5–36.6)	-26.5 (-39.1–4.1)	0.018
Tie2/TEK	70.6 (50.6–73.8)	38.4 (13–54.4)	50.6 (21.5–73.6)	-26.4 (-67.2–7.5)	0.053
VEGFR2/KDR	81.1 (57.7–84.4)	15.5 (0.3–33.6)	33.6 (6.3–75.5)	-56.3 (-82.2–-11.5)	**<0.001**
Akt/PKB/Rac @Thr308	31.1 (28.7–38.2)	34.1 (7.8–53.5)	31.1 (13.7–44.1)	1.4 (-31.0–38.8)	1.000
Akt/PKB/Rac @Ser473	32.5 (30.4–33.5)	7.2 (0–14.9)	13.1 (0.2–32.8)	-24.7 (-33.5–20.6)	0.032
p44/42 MAPK (ERK1/2)	24.3 (18.5–30.9)	10.7 (0–54.8)	19.1 (0.2–32.7)	-13.6 (-30.9–45.4)	0.494
S6 Ribosomal Protein	62.6 (29.1–67.6)	23.1 (9–57.7)	35.9 (12.2–67.4)	-20.9 (-60.9–27.1)	0.180
c-Abl	30.8 (19.7–33.8)	5.3 (0–23.5)	18.3 (2.7–32.4)	-19.2 (-33.8–22.0)	0.067
IRS-1	73.7 (70.5–81.6)	25 (9.1–41.3)	41.3 (17.3–75)	-48.2 (-73.0–9.5)	0.018
Zap-70	28.1 (24.9–28.8)	6.8 (0.9–18.7)	13.6 (2.8–28.2)	-18.1 (-28.2–28.2)	0.041
Src	29.4 (27.9–33)	23.3 (5.7–38.8)	29.1 (13–34.3)	-8.6 (-30.0–46.2)	0.616
Lck	27.2 (20–29)	5.6 (0.6–17.6)	16.4 (2.2–27.5)	-18.2 (-29.0–39.9)	0.041
Stat1	50.9 (36.3–60.7)	35.8 (18.7–49.9)	41.9 (31.1–53.3)	-15.1 (-43.4–30.6)	0.180
Stat3	40.3 (39.4–42.3)	53.6 (36.1–68.3)	49.1 (39.4–59.7)	13.5 (-31.8–46.4)	0.102

Table 53 DCE-MRI measurements by fistula disease duration. Hypotheses tested using T test (significance level 0.05). SD, standard deviation; CI, confidence interval; TIC, time-intensity curve. NB these measurements have no units.

	< 12 months	≥ 12 months	Mean diff (95% CI)	*p*
Mean max enhancement (SD)	762 (292)	641 (507)	121 (-234–475)	0.486
Mean max relative enhancement (SD)	0.964 (.4121)	0.797 (.4932)	0.167 (-0.226–0.560)	0.387
Mean wash in rate (SD)	80.8 (26.2)	67.9 (59.6)	12.9 (-26.5–52.2)	0.503
Mean wash out rate (SD)	6.0 (6.8)	36.2 (42.6)	-30.2 (-399.5–339.2)	0.499
Mean area under TIC (SD)	13961 (6331)	10511 (12607)	3451 (-5085–11987)	0.410

Table 54 DCE-MRI measurements by treatment outcome. Hypotheses tested using T test (significance level 0.05). SD, standard deviation; CI, confidence interval; TIC, time-intensity curve. NB these measurements have no units.

	Satisfactory	Unsatisfactory	Mean diff (95% CI)	*p*
Mean max enhancement (SD)	649 (124)	870 (508)	-221 (-571–129)	0.193
Mean max relative enhancement (SD)	0.924 (.2020)	1.023 (.5473)	-0.100 (-0.561–0.362)	0.653
Mean wash in rate (SD)	69.3 (21.3)	92.5 (55.2)	-23.3 (-70.0–23.5)	0.307
Mean wash out rate (SD)	23.5 (29.3)	2.9 (4.5)	20.6 (-24.3–65.5)	0.292
Mean area under TIC (SD)	11334 (2800)	16172 (12469)	-4838 (-13387–3711)	0.240

Table 55 DCE-MRI measurements by Parks' classification. Hypotheses tested using T test (significance level 0.05). IS, inter-sphincteric; TS, trans-sphincteric; SS, supra-sphincteric; SD, standard deviation; CI, confidence interval; TIC, time-intensity curve. NB these measurements have no units.
*** *n* = 1**

	IS	TS or SS	Mean diff (95% CI)	*p*
Mean max enhancement (SD)	327 (87)	776 (390)	449 (36–863)	**0.035**
Mean max relative enhancement (SD)	0.465 (0.164)	0.987 (0.437)	0.522 (0.056–0.988)	**0.030**
Mean wash in rate (SD)	38.8 (12.6)	80.6 (44.9)	41.9 (-5.8–89.5)	0.082
Mean wash out rate (SD)	0.2*	15.3 (21.4)	15.2 (-38.4–68.8)	0.524
Mean area under TIC (SD)	3986 (3166)	13859 (9595)	9872 (-343–20087)	0.057

Table 56 Clinical by time-intensity curve type: quick enhancement (type 3–5) versus slow enhancement (type 2). Data compared with Fisher's Exact test.

	Type 3–5	Type 2	*p*
Parks' classification:			
Inter-sphincteric	0	4	
Trans- or supra-sphincteric	3	17	1.000
Fistula disease duration:			
< 12 months	1	11	
≥ 12 months	2	9	0.590
Treatment outcome:			
Satisfactory	1	6	
Unsatisfactory	1	10	1.000